Metabonomic analysis of *Drosophila* mutants using high resolution mass spectrometry

A thesis submitted for the degree of
Doctor of Philosophy at the University of Strathclyde

By

Mohammed Mofareh ALbratty

Strathclyde Institute of Pharmacy and Biomedical Sciences
University of Strathclyde
161 Cathedral Street
Glasgow G4 0RE

2013

Abstract

The availability of fully sequenced genomes of model organisms such as *Drosophila* and their subsequent annotation has afforded opportunities for reverse genetics in a complex model organism. Metabonomics used as an aid to functional genomics can be used to understand the functions of genes in living systems. Thus metabonomics has been employed to study *Drosophila* samples extracted from whole animals at different developmental stages or in response to external stimuli or genetic mutation. With unmatched mass resolution, accuracy, and detection sensitivity, linear ion trap - Fourier Transform Orbitrap Mass Spectrometry (LTQ-Orbitrap-MS) has the potential for high throughput metabonomic analysis. Five different but linked studies are reported in this work. A global metabolic profiling method based on electrospray ionisation mass spectrometry was developed for *Drosophila melanogaster* metabolites. The method involved optimizing the extraction of *Drosophila* metabolites followed by analysis using liquid chromatography coupled with high-resolution mass spectrometry. The effect of extraction conditions and storage were studied, thus 750-800 metabolites were putatively identified in order to obtain the metabolite profiles of *Drosophila* reference strains and mutants. Metabolic studies were carried out to elucidate gene functions using established protocols.

The online resource FlyAtlas.org provides detailed microarray-based expression data for the tissues and life-stages of *Drosophila*. Since downstream genes, such as urate oxidase are tubule-specific, an Orbitrap technology has been used to elucidate tissue specific metabolomes. Additionally, genetic interventions using designed RNA interference were also made and validated by *q*PCR and metabonomics. The method produced a new opportunity for metabonomics use in validating gene expressions.

The xanthine oxidase inhibitor allopurinol was used to phenocopy the rosy mutation which caused the levels of xanthine and hypoxanthine to rise while the levels of uric acid fell. In addition, many unexpected metabolic changes followed this treatment with

effects on the pentose phosphate pathway and tryptophan metabolism being the most marked.

The yellow (*y*) gene was first discovered in *Drosophila*, but occurs in many insect species and in some bacteria. The *y* protein is similar to the major royal jelly proteins produced by bees. Metabolomic profiling was carried out on Oregon R (OR) and *y* *Drosophila* larvae at the third instar. There were numerous metabolic differences between the metabolic profiles of OR and *y*. Phenylalanine, tyrosine and DOPA were all elevated in *y*, as might be expected since the mutation blocks melanin biosynthesis. In addition, there were other metabolic effects including marked effects on to lysine metabolism.

The white mutation of *Drosophila*, which affects ABC transporters, was studied with regards to its effect on pigment biosynthesis in *Drosophila*. In addition to the expected effects on pigments there were interesting male/female differences possibly related to the presence of the *white* gene in the X chromosome. In addition the effect of salt stess on wild type and white flies was studied.

Overall, LTQ-Orbitrap-MS proved suitable for metabonomic analysis of both wild-type and mutant *Drosophila* and had potential in the analysis of metabolomes of single tissues. The possibility of using Orbitrap-based metabonomics in combination with *Drosphila* for drug testing is discussed and is a goal for the future.

Contents

Abstract 2
Contents 4
List of tables 7
List of figures 8
Published and Proposed Contributions from this work 14
Acknowledgement 15
Author's declaration 16
Definitions 17
Part I: Concept and Methodology 19
1. General Introduction: Metabonomic approaches in Drosophila functional genomics 20
1.1 Functional Genomics 21
1.2 Model Organisms 22
1.3 Drosophila melanogaster 23
1.4 Drosophila genetics 25
1.5 Drosophila Malpighian tubule 27
1.6 Drosophila models of human diseases 32
1.7 Inborn errors metabolism (IEMs) 36
1.8 Metabonomics 41
1.9 Metabolome analysis 43
1.10 Analytical tools 43
1.10.1 Mass spectrometry 44
1.10.2 Direct injection mass spectroscopy (DIMS) 46
1.10.3 Separation technology 47
1.10.4 Gas chromatography 49
1.10.5 Liquid chromatography 50
1.11 Data analysis and Databases 54
1.12 Aim of Study 55
2. Experimental 57
2.1 Chemicals 58
2.1.1 Buffered methanol-water (MW) 59
2.1.2 Buffered chloroform-methanol-water (MCW) 59
2.2 Drosophila melanogaster 59
2.3 Fly Larvae 60
2.4 DNA/RNA hydrolysis 61
2.5 Nuclear Protein Isolation 62
2.6 RNA interference (RNAi) 62
2.7 Tissue dissections 65
2.8 Validation by Quantitative PCR for gene knockdown 66
2.9 Allopurinol treatment of flies 68
2.10 Salt diet and survival assay 68

2.11 Salt eating behaviour assay 68
2.12 High-performance liquid chromatography (HPLC) analysis 69
2.12.1 The ZIC-HILIC Column 69
2.12.2 ZIC-pHILIC column 69
2.12.3 Silica column 69
2.13 Mass spectrometry of polar metabolites 70
2.14 Mass spectrometry of lipids 70
2.15 Metabolite identification 70
3. Optimization of the Extraction and Mass Spectrometric Analysis of the *Drosophila* Metabolome. 75
3.1 Optimization of sample extraction: the choice of buffer 76
3.1.1 Sample extraction evaluation 76
3.1.2 Stability and storage of extracts 84
3.1.3 Chromatographic evaluation of HILIC columns for separation of metabolites 87
3.2 Metabolite Coverage 91
3.3 Structure elucidation for phospholipids 108
3.4 Statistical analysis 115
3.5 Method validation 115
Part 2 Case studies 117
4. Chapter four: Validation of the knockdown of Urate Oxidase Using Metabonomics 118
4.1 Making of transgenic fly lines and their validation 119
4.2 Tissue specific knockdown of urate oxidase activity 121
4.3 Conclusion 123
5. Chapter five: Phenocopying the rosy gene 124
5.1 History 125
5.2 Expression sensitivity to *ry* localization 126
5.3 Loss of *ry* results in reduced red eye pigment 129
5.4 The effects of allopurinol treatment on Drosophila 131
5.5 Allopurinol phenocopies rosy, but provides temporal resolution 133
5.7 Pharmacokinetics 136
1.7 Allopurinol impacts on ascorbate metabolism 137
5.5.1 Allopurinol and the kynurenine pathway 140
5.6 How similar are *ry* mutant and phenocopy of rosy 142
5.7 Concluding Remarks 144
6. Chapter six: Study of the Yellow (y) gene using metabonomics 145
6.1 Introduction 146
6.2 Larval and adult metabolomes differ markedly 147
6.3 Metabolic differences between y and wild-type in larval stage 148
6.4 Melanisation 152
6.5 Lysine Metabolism 154
6.6 Impact of *Y* on Histone Methylation 157
6.7 Impact of *Y* on Cuticle Biosynthesis 159
6.8 Other Changes 165

6.9 Concluding Remarks 169
7. Chapter seven: Study of the White gene using metabonomics 170
7.1 Introduction 171
7.2 Where does the regulation of *w* expression occur? 173
7.3 Global metabolomics of *w* and wild-type flies 175
7.4 Eye Development in *Drosophila* a fascinating story 181
7.5 How could lack of *w* impact on the drosopterin pathway? 182
7.6 How could lack of w impact on the xanthomatin pathway? 184
7.7 Mini-white rescues the *w* phenotype 186
7.8 The sensitivity of eye pigmentation to dosage compensation 190
7.9 Mechanisms for Compensating for Salt Stress 201
7.10 Loss of w results in reduced resistance to salt stress 204
7.11 Metabolomic flux response of whole organism to high salt diet 206
7.12 Overall Conclusion and Future Work 218
8. Chapter eight: Summary and future work 219
8.1 *Drosophila melanogaster* used as model for genetic lesions and environmental stimuli 220
8.2 Optimisation of metabonomics studies 221
8.3 Future work 222
9. Appendices 223
10. References 255

List of tables

Table 1-1 Human renal disease loci conserved between fly and human as shown (Dow and Romero, 2010) 35
Table 1-2 Examples of metabolic disorders detected using metabolomics screening approaches to screen newborns (Moolenaar et al., 2003) 39
Table 2-1 Reagents used in the study 58
Table 2-2 Fly stocks used in this study 60
Table 5-1 Metabolic pathways where several metabolites are significantly affected by allopurinol comparing each time point of treatment with untreated flies (batches of 10 male + 10 female flies, n = 4 for each time point). T/C = treatment/control. 133
Table 6-1 List of metabolites and metabolites displaying significant differences between y and OR analysed. Four extracts of 50 *y* and 50 OR larvae were prepared on 3 occasions over a two month time period. "Ratio" is of y: OR signal. 149
Table 6-2 MS^2 data for some of the more usual metabolites extracted from the larvae. Obtained with a CID of 40V. 152
Table 6-3. Methylated lysines and arginine obtained by hydrolysis of histone proteins isolated from *y* and OR. Hydrolysis was carried out on 4 aliquots of the extract. The levels are expressed as a % of the mean peak areas compared against the mean peak area for lysine. 159
Table 6-4. DNA and RNA bases present in DNA/RNA extracted from *y* and OR larvae. 166
Table 6-5 Some stable metabolites which do not vary between OR and *y* larvae for two of the batches. 168
Table 7-1 List of metabolites displaying significant differences between *w* and wt analysed. "Ratio" is of *w*: wt signal (n=4). 179
Table 7-2. The genetic location for usual genes involved in eyes pigmentation on *Drosophila melanogaster* Chromosomes. 193
Table 7-3. Shows the main difference between sexes. Four extracts of 10 *females* and 10 males adult wild type were prepared. "Ratio" is of males/females peak areas. 200

List of figures

Figure 1-1 Trade-off between genetic modelling power and biomedical relevance; adapted from (Dow, 2007)..... 23
Figure 1-2 *Drosophila* life cycle; adapted from(ArtScience, 2011)..... 24
Figure 1-3 The GAL4 system; as shown in (Sun et al., 1995)..... 27
Figure 1-4 Three views of Malpighian tubule A) Genetic analysis for tubule, B) classical morphological analysis, C) different cells are shown in different colours, green for stellate and yellow for principal cells. taken (Dow, 2009)..... 29
Figure 1-5 Summary of major groups of genes enriched in tubule as revealed by microarray approach (Wang et al., 2004)..... 31
Figure 1-6 Classification of 714 drosophila genes related to different human diseases.(Chien et al., 2002) 34
Figure 1-7 Clinical classification of IEMs; taken from (Martins, 1999) 38
Figure 1-8 The numbers presented show only the trend in publications in metabonomics field over the last decade (Hobani, 2012, Oldiges et al., 2007)..... 42
Figure 1-9 shows the parts of LTQ-Orbitrap:(I) heated capillary, (II) multi-pole focusing devices, (III) a gating lens, multi-pole (IV) a, transfer octopole; b, curved RF-only quadrupole (c-trap); c, gate electrode; d, trap electrode; e; ion optics, f; inner spindle-like; g, outer barrel-like..... 46
Figure 1-10 (Right panel) shows the distribution of analytes between the mobile phase and the water-enriched layer absorbed on the surface of HILIC column; (left panel) shows partition mechanism that is mainly based on polarity of analyte and degree of solvation(Corporation, 2010)..... 48
Figure 1-11 Raw data (upper panel) can be processed by chemometric method (lower-left panel) or quantitative method (lower –right panel) 53
Figure 2-1 Germline transformation of *Drosophila* showing it is conducted by injecting embryos from *white*$^{-}$ strains with a P-element shuttle vector containing the gene of interest and a marker *mini-white* gene, along with a 2-3 helper plasmid. The flies from these embryos are crossed with *white*$^{-}$. Progeny of this cross are then screened for red eyes, implying they carry *mini-white* and thus transgenic. The red-eyed adult flies are then back-crossed to *white*$^{-}$ and selected to produce a stably transformed line. 64
Figure 2-2 Malpighian tubule dissection method where the forceps hold fly from its thorax region and with the other hand, the tubule is slowly and gently is pulled very end part of the fly. At this point the Malpighian tubules will start to appear..... 65
Figure 2-3 showing the right *q*PCR product for *lkr* where it was identified using melting curve. 67
Figure 2-4 Workflow of the metabolomic software used in the current study..... 71
Figure 2-5 Typical screenshot of the alignment step in Sieve 72
Figure 2-6 Sample output from Sieve Extractor (SE) Programme..... 73
Figure 3-1 Comparison of two different extraction solvents for metabolic profiling in *Drosophila*, Red: MCW and Green: MW. 77

Figure 3-2 Upper panel shows TIC (conditions as in 2.12.1) for *Drosophila* extracted by MW coloured red against blank (no *Drosophila* present) coloured blue while lower panel shows TIC *Drosophila* extracted by MCW coloured red against blank (no *Drosophila* present) coloured blue. 78
Figure 3-3 Electrospray mass spectra of metabolites (whole m/z range,75-850/whole time range) of : (upper panel) blank (no fly present); (central panel) *Drosophila* extracted by MW; (lower panel) Drosophila extracted by MCW. 79
Figure 3-4 Distribution of 230 different detectable metabolites related to their intensity ratios using the two extraction procedures where ratio is MW/MCW. 81
Figure 3-5 Levels of GSH and glutamate following storage at -80°C for 1 and 8 week periods. Data are shown as mean ±SEM for N=3 independent experiments. Data that differ significantly are marked with asterisks are analyzed by Student's *t*-test two tailed. 86
Figure 3-6 Extracted ion chromatographs of AMP, ADP and ATP on ZICpHILIC (upper panel) and on ZICHILIC (lower panel) extracted from *Drosophila*. 89
Figure 3-7 Extracted ion chromatograms for fumaric, succinic and malic acids on ZICpHILIC (upper panel) and ZICHILIC (lower panel). 90
Figure 3-8 TIC for metabolites extracted from adult Drosophila run in positive mode. The sample was analysed by ZIC –HILIC column as in section 2.12.1. 93
Figure 3-9 TIC for lipids extracted from adult *Drosophila* run in positive mode. The sample was analysed on a silica column as described in section 2.12.3. 95
Figure 3-10 This diagram shows the electrogram of the traces of PE.Upper trace, extracted ion chromatograms of PE m/z 740.5. Lower panel, MS/MS spectra of PE m/z 740.5 showing fragment peak for 599.5 formed as a result of loss of phosphoethanolamine. Chromatograms were generated by using Chromatographic conditions as in 2.12.3. 110
Figure 3-11 This diagram shows the electrogram of the traces of PC. Upper trace, extracted ion chromatograms of PC m/z 730.5; lower panel, MS/MS spectra of PC m/z 730.5 showing fragment peaks for 494.3 formed from $C_{24}H_{49}O_7NP$ and 184 formed from $C_5H_{15}O_4NP^+$. Chromatograms were generated by using Chromatographic conditions as in 2.12.3. 111
Figure 3-12 This diagram shows the electrogram of the traces of lysoPC. Upper trace, extracted ion chromatograms of lysoPC m/z 520.3; lower panel, MS/MS spectra of lysoPC m/z 520.3 showing fragment peaks for 502.3 formed from $C_{26}H_{49}O_6NP$ after loss of water and 184 formed from $C_5H_{15}O_4NP^+$. Chromatograms were generated by using the chromatographic conditions as in 2.12.3. 112
Figure 3-13 This diagram shows the electrogram of the traces of TAG. Upper extracted ion trace, ESI-MS spectra of ammoniated molecular ion at m/z 680.583; lower panel, MS/MS spectra of TAG m/z 680.583. Chromatograms were generated by using the chromatographic conditions as in 2.12.3. 113
Figure 3-14 This diagram shows the electrogram of the traces of lysoPE. Upper trace, extracted ion chromatograms of lysoPE m/z 480.3; lower panel, MS/MS spectra of lysoPE m/z 480.3 showing fragment peaks for 462.3 formed from $C_{23}H_{77}O_6NP$ after loss of water and = 339 formed from $C_{21}H_{39}O_3$. Chromatograms were generated by using the chromatographic conditions as in 2.12.3. 114

Figure 3-15 Work flow for metabolomic approach on *Drosophila* samples. 116
Figure 4-1 The pBac transgenic insertion site on the uro gene obtained from Flybase.org on 15th June, 2012 119
Figure 4-2 Impact of *uro* knockdown on purine catabolism with known *Drosophila* enzymes indicated, and fold changes for metabolites for uro RNAi knockdown versus their parents, with fold changes superimposed 121
Figure 4-3 *uro* RNAi knockdown validated by *q*PCR approach. It shows *uro* gene knockdown expression dissected from tubules compared to parental lines. Approximately 80% lower expression was observed. Data are shown as mean ±SEM for N=4 independent experiments. Data that differ significantly are marked with asterisks are analyzed by Student's *t*-test two tailed 122
Figure 4-4 *Uro* RNAi knockdown validated by metabolomics approach. It shows the impact of uro gene knockdown expression on purine metabolite levels in dissected tubules compared to parental lines. Approximately 70% lower expression. Data are shown as mean ±SEM for N=4 independent experiments. Data that differ significantly are marked with asterisks are analyzed by Student's *t*-test two tailed 123
Figure 5-1 *ry* expression across *Drosophila melanogaster* tissues. Effects on hypo xanthine-allantoin axis in the purine metabolism pathway are presented for *ry* against the tissues. The expression is predominant in abdomen for *ry* in panal (B and c according to statistical significance (n=4; *t*-test; $P \leq 0.001$). Panel A shows the internal tissues in *Drosophila.* 128
Figure 5-2 Diagram of red pigment formation in Drosophila taken from (Summers et al., 1982) 129
Figure 5-3 Impact of *ry* on red pigment (drospterin , pterin and iosxanthopterin). Data are shown as mean ±SEM for N=4 independent experiments. Data that differ significantly are marked with asterisks are analyzed by Student's *t*-test two tailed 130
Figure 5-4 Impact of *ry* (A) and allopurinol (B) on the uric acid pathway, with fold... 136
Figure 5-5 Increase of hypoxanthine and allopurinol levels with time in *Drosophila* treated with allopurinol. Chromatograms were generated by using chromatographic conditions as in 2.12.1. 137
Figure 5-6 Loss of ascorbic acid in *Drosophila* following treatment with allopurinol. Chromatograms were generated by using chromatographic conditions as in 2.12.1. 138
Figure 5-7 Impact of allopurinol on the ascorbic acid pathway: extracted from the KEGG pathway map. 140
Figure 5-8 Comparison the effect of lack of rosy (upper panel) and allopurinol (lower panel) on osmolyte biosynthesis: extracted from the KEGG pathway map where green colouration indicates to enzymetic pathway involved in lipid matabolism. 143
Figure 6-1 Impact of *y* mutation on eumelanin biosynthesis with known *Drosophila* enzymes indicated, and fold changes for metabolites for *y* versus OR (from Table 6-1) shown in arrows. 153
Figure 6-2 Extracted ion trace showing the putatively identified GSH conjugates of DHI 154

Figure 6-3 Impact of *y* mutation on lysine catabolism with known *Drosophila* enzymes indicated, and fold changes for metabolites for *y* versus OR (from Table 6-1) shown in arrows. Note that there are no enzymes present in drosophila capable of synthesizing lysine; as in other higher animals, lysine is an essential amino acid. 156
Figure 6-4 Extracted ion traces for Galactosamine, Glucosamine-1-phosphate, Glucosamine-6-phosphate and Acetylglucosamine-6-phosphate showing their elution order by ZIC-HILIC column. Chromatograms were generated by using Chromatographic conditions as in 2.12.1. 161
Figure 6-5 taken from (Merzendorfer and Zimoch, 2003) showing Impact of *y* mutation on chitin biosynthesis with known *Drosophila* enzymes indicated, and fold changes for metabolites for *y* versus OR (from Table 6-1) shown in arrows. 162
Figure 6-6 Positive ion MS^2 spectrum of Glucosamine-6- phosphate at 35Vgenerated from [M+H] at m/z 260.053 showed product ions at m/z 224 , 206, 144 and 126 which were considered to be $[M+H–2H_2O]^+$, $[M+H–3H_2O]^+$ $[M+H–H_3PO_4 - H_2O]^+$ and $[M+H– H_3PO_4- 2H_2O]^+$ respectively. 163
Figure 6-7 Positive ion MS/MS spectrum of acetylgalactosamine generated from [M+H] at m/z 222.975 showed product ions at m/z 186 and 126 which were considered to be $[M–2H_2O+H]^+$ and $[M–C_2H_8O_4+H]^+$ respectively. 164
Figure 6-8 Extracted ion traces for guanosine (upper panel) and dimethylguanosine (lower panel) in a RNA/DNA hydrolysate giving an indication of the dynamic range available for detection of modified DNA/RNA bases. Chromatograms were generated by using Chromatographic conditions as in 2.12.1. 167
Figure 7-1 Evidence for differential precursors of *w* gene in wild-type according to their avaliblity in the abdomen and heads. All panels showed *white's* substrates are higher in abdomen than head implying that *w* expression was found significantly higher in the abdomen. Data are shown as mean ±SEM for N=4 independent experiments. Data that differ significantly are marked with asterisks are analyzed by Student's *t*-test two tailed. Since the mass of the tissues were different the intensities of the metabolites were normalised relative to protein content determined by the Bradford assay. 174
Figure 7-2 Variation in CDP-Ethanolamine, GPC and CDP-choline in male and female *w* flies. Data are shown as mean ±SEM for N=4 independent experiments. Data that differ significantly are marked with asterisks are analyzed by Student's *t*-test two tailed. 177
Figure 7-3 Phosphotyrosine levels are higher in *w* mutants than wild type in normal conditions. Data are shown as mean ±SEM for N=4 independent experiments. Data that differ significantly are marked with asterisks are analyzed by Student's *t*-test two tailed. 178
Figure 7-4 Proposed red pigment biosynthetic pathways in *Drosophila* wild-type larvae. 182
Figure 7-5 Impact of *w* mutation on drosopterin biosynthesis with known *Drosophila* enzymes indicated, and fold changes for metabolites for *w* versus OR (from Table 7-1) shown in arrows. 184

Figure 7-6 Impact of *w* mutation on xanthomatin biosynthesis with known *Drosophila* enzymes indicated, and fold changes for metabolites for *w* versus OR (from Table 7-1) shown in arrows. 186
Figure 7-7 Impact of *mini-w*$^{+}$ insertion on drosopterin and xanthomatin showing their sensitivity to mini-*w*$^{+}$. Data are shown as mean ±SEM for N=4 independent experiments. Data that differ significantly are marked with asterisks are analyzed by Student's *t*-test two tailed. 187
Figure 7-8 Genomic organisation of w (upper panel); lower panel (right) Showing the characteristic red eye colour of *mini-w*$^{+}$ against white eyed flies (*w1118*) (left) (Data obtained from Flybase.org on 10th June, 2012, (Evans et al., 2008) and (Holtzman et al., 2010) 188
Figure 7-9. Impact of *mini-w*$^{+}$ insertion on uric acid pathway showing *ry* is up regulated 10 times as can be observed from the urate level. Data are shown as mean ±SEM for N=4 independent experiments. Data that differ significantly are marked with asterisks are analyzed by Student's *t*-test two tailed. 189
Figure 7-10. Impact of *mini-w*$^{+}$ insertion on white's substrates showing Guanine ,Tryptophan, Kynurenine , Hydroxykynurenine and Riboflvine were accumulated in *mini-w*$^{+}$ flies confirming that these compounds are sensitive to *w* expression at different levels. Data was statistically assessed by Student's *t*-test (two tailed);n=4. 190
Figure 7-11. Impact of *gender* on red pigment levels showing drosopterin is slightly higher in female flies. Data are shown as mean ±SEM for N=4 independent experiments. Data that differ significantly are marked with asterisks are analyzed by Student's *t*-test two tailed. 194
Figure 7-12. Impact of *gender* on brown pigment showing xanthomatin level is doubled in females, reflecting deficit compensation on the X chromosome. Data are shown as mean ±SEM for N=4 independent experiments. Data that differ significantly are marked with asterisks are analyzed by Student's *t*-test two tailed. 195
Figure 7-13 Chromatograms comparing methylated amino acids in extracts from 10 female (A) and 10 male (B) flies. 197
Figure 7-14 High levels of S-adenosylmethylpropylamine occur in male compared to female *Drosophila* 198
Figure 7-15. Model for universal functions of renal system: tubule (blue), guts (yellow and orange); adapted from (Chintapalli et al., 2012) 202
Figure 7-16. Survival curves showing that the *w* mutants are sensitive to salt stress. .. 205
Figure 7-17 Flies eat salty food. Fly eating behaviour was assayed according to section 2.10. After one day of feeding, almost all the flies, including *w* mutants had abdomens that were coloured blue (lower panel) implying that they eat food even with high concentrations of salt. However, the changes in intercellular pH were monitored by blue colour, which was more pronounced in salt assays. 206
Figure 7-18 Level of phosphotyrosine is more abundant in white mutation flies in both cases (salted and unsalted condition) while in wild type flies under salt condation, phosphotyrosine was accumulated 5 fold than wild type flies fed by normal food Data are shown as mean ±SEM for N=4 independent experiments. Data that differ

significantly are marked with asterisks are analyzed by Student's *t*-test two tailed. 210
Figure 7-19 Peaks obtained for a typical PC lysolipid for WT and *w* cultured on normal growth medium and under salt stress (chromatographic conditions as in section 2.12.3. 213
Figure 7-20 Pathways that are either directly regulated byguanylate cyclase C(GC-C) or modified by cGMP production (adapted from Radeff-Huang, Seasholtz et al. 2004). 216
Figure 7-21. Effect of salt stress on cAMP and cGMP in WT flies. Chromatographic conditions as in 2.12.3. 217
Figure 7-22. Effect of salt stress on cAMP and cGMP in *w.* Chromatographic conditions as in 2.12.3. 217

Published and Proposed Contributions from this work

Al Bratty, M., Hobani, Y., Dow, J.A.T. , and Watson, D.G. (2011) *Metabolomic profiling of the effects of allopurinol on Drosophila melanogaster*. Metabolomics, 7 (4). pp. 542-548. ISSN 1573-3882 (doi:10.1007/s11306-011-0275-6)

Venkateswara R. Chintapalli, Selim Terhzaz, Jing Wang, Mohammed Al Bratty, David G. Watson, Pawel Herzyk, Shireen A. Davies and Julian A. T. Dow (2012). Functional correlates of positional and gender-specific renal asymmetry *in Drosophila*. PLoS ONE 7(4): e32577.

Al Bratty, M., Venkateswara R. Chintapalli., Dow, J.A.T. , Zhang T, and Watson, D.G. (2012) Drosophila melanogaster larvae with the yellow mutation have altered lysine metabolism. FEBS Open Bio. (In press)

Al Bratty, M., Venkateswara R. Chintapalli., Dow, J.A.T. , and Watson, D.G. (2012). Correlation of gene expression with lipid profiling in Drosophila. (In prep)

Al Bratty, M., Venkateswara R. Chintapalli., Dow, J.A.T. , and Watson, D.G. (2012). Metabolic Flux Response to Salt-induced Stress in *Drosophila melanogaster*. (In prep)

Acknowledgement

First of all, I thank Allah for completing this project.
I am very grateful to my supervisor, Dr David G. Watson, who gave me the opportunity to be trained in his lab and guided and supported me by providing a lot of valuable advice.
I definitely want to thank Professor Julian Dow and his students, Yahya Hobani and Venkateswara at Glasgow University, for their help with and collaboration on this project and for providing the samples.

My sincere thanks also go to all of my classmates and co-workers in the laboratory for their cooperation, assistance and helpful discussions.

I want to express my gratitude to my mother and father, and to my wife and children, who have always taken great interest in and cared about my studies.

Finally, I would like to thank the Jazan University representative of the Saudi government for funding my studies at the University of Strathclyde, especially for the PhD project

Author’s declaration

This thesis is the result of the author's original research. It has been composed by the author and has not been previously submitted for examination which has led to the award of a degree. The copyright of this thesis belongs to the author under the terms of the United Kingdom Copyright Acts as qualified by University of Strathclyde Regulation 3.50. Due acknowledgement must always be made of the use of any material contained in, or derived from, this thesis.

Definitions

AMP	adenosine monophosphate
ANOVA	analysis of variance
APCI	atmospheric pressure chemical ionization
API	atmospheric pressure ionization
ATP	adenosine triphosphate
cAMP	cyclic adenosine monophosphate
cDNA	complementary DNA
CE	capillary electrophoresis
CER I	Cytoplasmic Extraction Reagent I
cGMP	cyclic guanosine monophosphate
CID	collision-induced dissociation
CyO	curly of Oster
dNTP	deoxyribonucloetide triphosphate
EDTA	ethylenediamine tetra acetic acid
EI	Electron impact
ESI	Electrospray ionization
EV	electron volt
FC	fold change
FTICR	Fourier transform ion cyclotron resonance
FTIR	Fourier transform infrared spectroscopy
FWHM	full width at half maximum
GAL4	yeast transcription factor
GC-MS	Gas chromatography MS
GMP	guanosine monophosphate
GPCR	G-protein-coupled receptor
G-protein	guanine nucleotide-binding protein
GTP	guanosine-5'-triphosphate
HBS	HEPES buffered saline
IEM	Inborn errors of metabolism
KEGG	Kyoto Encyclopaedia Of Genes And Genomes
LC-MS	Liquid chromatography MS
LTQ	linear ion trap
m/z	mass-to-charge ratio
MALDI	Matrix assisted laser desorption ionization
mg	milligram
$MgCl_2$	Magnesium chloride
min	minutes

ml	millilitre
mM	millimolar
Moco	Molybdenum cofactor
mRNA	messenger ribonucleic acid
MS/MS	mass spectrometry
MS/MS	tandem mass spectrometry
MVA	multivariate (data) analysis
NaCl	sodium chloride
NAD+	Nicotinamide Adenine Dinucleotide
NADH	Nicotinamide Adenine Dinucleotide reduced
NADPH	Nicotinamide adenine dinucleotide phosphate
NaHCO3	Sodium bicarbonate
NER	Nuclear Extraction Reagent
NER-PER	Nuclear and Cytoplasmic Protein Extraction Reagent Kit
NMR	nuclear magnetic resonance
NO	Nitric oxide
NOS	Nitric oxide synthase
O_2-	Superoxide
PBS	phosphate buffered saline
PCA	principal component analysis
PDE	phosphodiesterase
Q-PCR	Quantitative polymerase chain reaction
QqTOF	hybrid quadrupole time-of-flight mass spectrometer
RNAi	RNA interference
ROS	Reactive oxygen species
RT-PCR	Reverse transcriptase polymerase chain reaction
s	second
SDS	sodium dodecyl sulphate
SFC	Supercritical Fluid Chromatography
TOF	Time of flight
TQ	triple quadrupole
Tris	2-amino-2-(hydroxymethyl)-1,3-propanediol
UAS	Upstream activating sequence
UPLC	ultra performance liquid chromatography

Part I: Concept and Methodology

1. General Introduction: Metabonomic approaches in Drosophila functional genomics

1.1 Functional Genomics

The addition of the complete genome sequence of *Drosophila melanogaster* (fruit fly) to GenBank in 2000 opened up an era in fly genetics for new explorations into gene functions. The study of "functional genomics" aims to assign functions to specific genes and their products, which is often coupled with phenotypes associated with gene mutations. Today, the functions of only half of all identified genes are known in fruit flies. The gap between genotype and phenotype can potentially be filled using high-throughput techniques. These methods enable the analysis of a large set of components within a cell, tissue or whole organism, and serve as a systems approach for functional genomics (Oliver et al., 1998)

Microarrays and 2D-gel electrophoresis coupled with mass spectrometry are the most common methods for analyzing and identifying a large number of genes and proteins. Microarrays are used to measure all gene products in a living cell at the mRNA level, referred to as transcriptomics, and this has enabled fly researchers to identify both the transcribed genes and the expression levels in individual samples. Functional genomics can also be applied at the proteomic level using gel electrophoresis coupled with mass spectrometry to separate proteins according to their isoelectric point and molecular weight. Mass spectrometry is then used to identify the separated proteins. Thus, this technology is useful for investigating protein expression and determining post-transcriptional modifications of the proteins in each sample, which can identify whether a protein is active or inactive(Oliver et al., 1998).

Additionally, functional genomics can also help to close the gap between number of genes that are still unidentified and the number of phenotypes that are visibly characterized which is called the "phenotype gap". The gap leads to knowledge discrepancies between what we already know and what we need to know. For example, we need knowledge of the genes that cause diseases. This term was presented in literature in 1996 and has improved from the use of reverse genetic approaches. The

reverse genetic method introduces a mutation at a specific gene, and the resulting phenotype is then observed (Brown and Peters 1996; Dow and Davies 2003). Fortunately for biomedical researchers, many diseases appear to be linked with clear phenotypes that aid disease diagnosis or drug discovery. However, a better understanding and characterization of the correlation between genotype and phenotype on a whole organism is the true goal of all integrative systems of biology studies. Thus, combining fly genetics with fields such as genomics, transcriptomics, proteomics, and newer branches of other "omics" such as metabolomics (A more detailed introduction is provided later in this chapter) may help establish comprehensive knowledge for a wide range of gene functions and reveal their interactive networks. These integrated approaches give scientists the opportunity to map cellular functions and may lead to the control of systems biology in future studies (Kamleh et al., 2008c, Oliver et al., 1998).

1.2 Model Organisms

Although EP George (George EP. Box, 1987) stated "essentially, all models are wrong, but some are useful", the availability of simple model organisms yields an important opportunity to understand small variations in biological systems. It is vital to compare these variations with humans for modeling human genetics and genetic modifications. For this purpose, only a few animal models are well-studied for modeling human health and diseases. These animal models include mouse, fly, worm, arabidopsis, yeast, and bacteria as seen in figure 1-1. Humans are complex biosystems, and the metabolism of this super-organism can be affected by factors such as age, body composition, health status, and external factors such as food and drink (Nicholson et al., 1999).

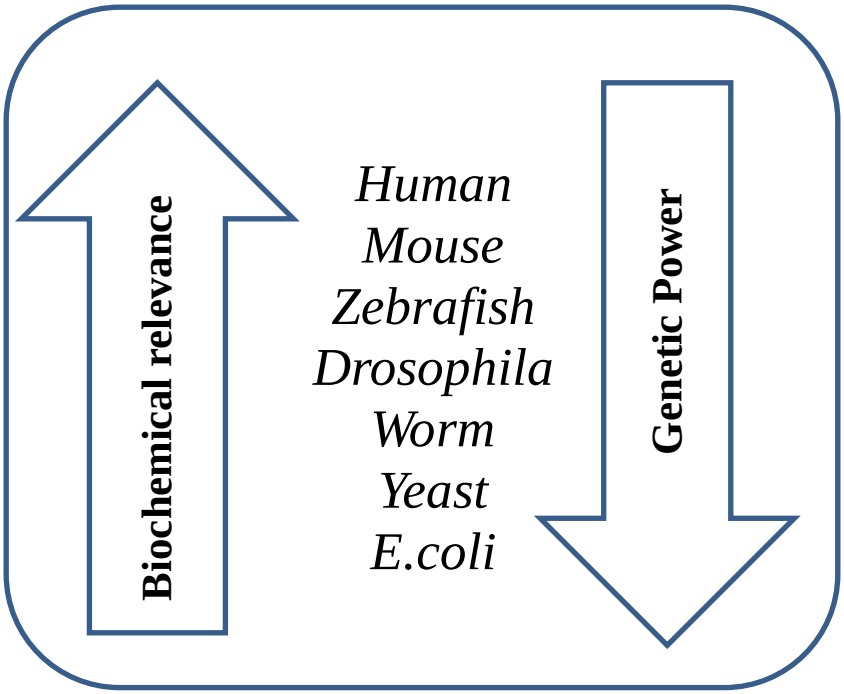

Figure 1-1 Trade-off between genetic modelling power and biomedical relevance; adapted from (Dow, 2007).

1.3 Drosophila melanogaster

Drosophila melanogaster belongs to the Drosophilidae family. There are four stages in the life-cycle of *Drosophila* which include embryonic, larval, pupal and adult stages (Figure 1-2). Research studies have tended to use the fruit fly as an animal model for the past 100 years because of its genetic amenability. Moreover, it offers the following advantages:

- It is about 3-mm long so it is easy to grow in the lab, the maintenance cost is relatively low, and it can multiply quickly.

- The fly genome can be easily manipulated using genetic tools to generate phenotypes similar to those of mammalian cells. Thus, it is possible to make a

transgenic *Drosophila* line within three months for approximately $500, and maintain it for $30 per year.

- The Drosophyila line has four chromosomes carrying 14,000 genes and lacks genetic redundancy. Thus it is considered as a useful model for understanding mammalian cell physiology and biochemistry.

- It has been demonstrated that great homology exists between fruit flies and mammals at the genetic structure and function levels. Therefore, many fly genes can resemble human genes and that may aid drug discovery for a wide range of diseases including cancer, neurological and other serious diseases (a more detailed discussion is in Section 1) (Adams and Sekelsky, 2002, Dow, 2003).

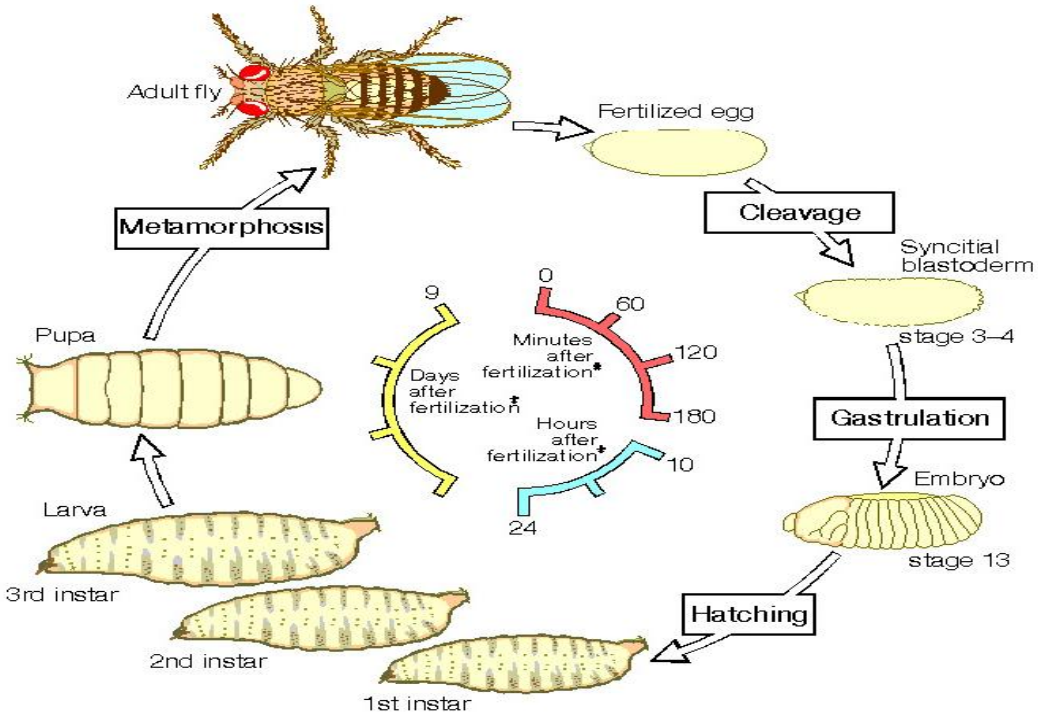

Figure 1-2 *Drosophila* life cycle; adapted from(ArtScience, 2011)

In addition to its usefulness as genetic tool, *Drosophila* has a distinct physiology and their organs are small and relative easy to dissect. Although *Drosophila* has commonly been used for developmental or behavioural studies for many years, they are now being used to study many physiological processes such as circadian cycle, learning and memory, immunity, and renal function (Dudai, 1977, Konopka and Benzer, 1971, Dow, 2009). Due to the increased amount of information from many studies, and owing to over a century of work on *Drosophila*, there are several comprehensive websites that serve as literature and information resources. These websites collect and provide detailed information about fruit flies, including genes, gene homologues to human diseases, gene expression in multiple tissues, and mutants and RNAi stocks for many *Drosophila* genes. These databases such as Flybase, FlyAtlas and Homophila are freely available for use to fly researchers (Chintapalli et al., 2007b, Chien et al., 2002).

In contrast to advantages mentioned above for the fly model, there are some areas, such as heart and bone diseases, that have not benefitted from fly online resources because the fruit fly belongs to the invertebrate family. Thus, there are some limitations when using the fly to model human diseases because it does not possess a four-chambered heart, mammary ducts, or bone calcification as part of its physiology (Bier, 2005).

1.4 Drosophila genetics

The fruit fly is an attractive genetic tool for a wide range of scientific investigation because of its ability to adapt and produce thousands of mutations using either forward or reverse genetic methods. Half of all *Drosophila* genes have been mutated and are stored in stock centres such as Bloomington (Dietzl et al., 2007).

Historically, classical mutations are naturally-occurring due to errors in genomic sequences introduced during meiosis or DNA replication. The most famous fly mutant is *white* which shows characteristic white eyes instead of red eyes in the wild-type. This is due to the aberration in the eye pigmentation pathways which form drosopterin and xanthomatin precursors. Many other classical gene mutations are also associated with

certain phenotypes (Sullivan et al., 1979). A more detailed discussion is provided in chapter two.

Recently, genetic tools have allowed investigators to easily delete, insert, and knock down a gene of choice. A full range of forward and reverse genetic approaches are now possible. There are several genetic methods for producing transgenic lines using chemical or physical mutagenesis with for example, ethyl methane sulphonate (EMS), or ionizing radiation such as gamma rays (St Johnston, 2002) and germline transformation (for UAS/GAL4 system) for reverse genetics. Thus, the mutation sites can be designed, and the resulting phenotypes are also clearly characterized (Ryder and Russell, 2003).

P-elements are naturally occurring transposons found in the fly genome. Other transposon families can be used for molecular interventions to construct and generate transgenic flies. The p-element typically has one gene to encode the transposase enzyme to initiate the transposition process. The size of the transposable element is small, around 2.9-kb, and it can be inserted from plasmids into the germline within the *Drosophila* genome. Because the p-element construct is microinjected into the syncytial blastoderm where it is randomly incorporated into the fly embryo genome, the p-element must be modified to allow its introduction into fly DNA to be easily traced. Therefore, p-element modifications are introduced with markers such as the *mini-white* gene inserted within the p-elements. This enables fly researchers to monitor p-element insertions from one fly generation to another (Sun et al., 1995).

Furthermore, the p-elements can be adapted for enhancer-trapping to map patterns of gene expression in the embryonic or adult fly stage by allowing the identification of spatially or temporally expressed genes. Indeed, only two types of enhancer traps that employed lacZ- or Gal4-reporters have been widely used. The former is the first generation of enhancer trap elements that is coupled to the beta-galactosidase gene. Its expression can be detected by methods such as immunohistochemistry. The

GAL4/UAS system is a second generation enhancer trap based on a yeast transcription factor. In order to be targeted to a specific tissue, it is driven by a specific GAL4 to activate the transgene fused downstream of the UAS (Figure1-3). For example, in the Malpighian tubules, uro-GAL4 are crossed to flies which carry UAS-gene X lines; as part of this thesis double stranded RNA was expressed for Uro to knockdown its expression (Brand and Perrimon, 1993).

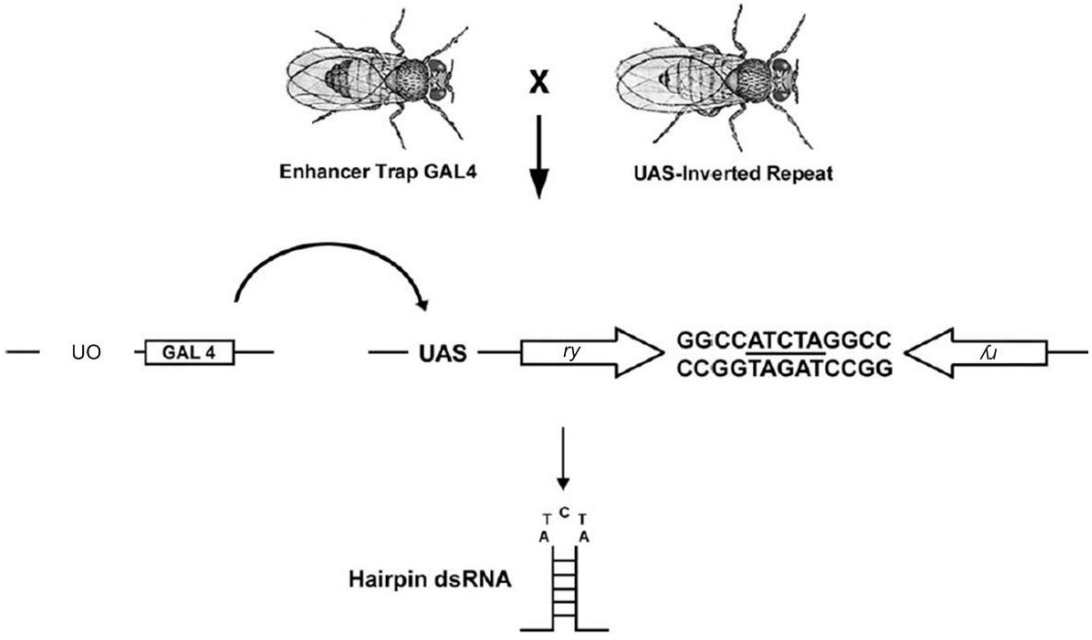

Figure 1-3 The GAL4 system; as shown in (Sun et al., 1995)

1.5 Drosophila Malpighian tubule

The Malpighian tubule is named after Marcelo Malpighi (Dow and Romero, 2010), who was a 17th-century anatomist. It later provided a most interesting research area in Ramsay's lab in the mid-20th century after methods were devised to easily measure fluids secreted by tubules. That study has provided a method for studying the physiology of *Drosophila* tubules. Professor Simone Maddrell pioneered transport

physiological studies using this simple excretory system in *Manduca sexta* (Dow, 2009). Since then, many studies have been published that reported the Malpighian tubule performs not only as a renal system in *Drosophila* but also functions as a liver and as an immune system. Furthermore, many efforts are being made to test its ability to model human renal diseases. Thus, elucidating the morphology and physiology of this structure could aid in understanding human disease relevant to its biological processes (Dow, 2009, Dow and Romero, 2010, McGettigan et al., 2005).

At the morphological level, the Malpighian tubule is a simple cylindrical tube containing approximately 150 cells, 2 mm in length and 35 µm in diameter. It constitutes two pairs: an anterior (left hand) and posterior (right hand). Each pair is linked with a common ureter and opens up into the hindgut. The anterior tubule can be divided into three functional domains: the initial, the transitional, and the main domain. In contrast to the anterior segments, however, the posterior tubule possesses only the main segment and no distinct regions are visible. The contribution to fluid secretion is roughly equal in both pairs of tubules (O'Donnell and Maddrell, 1995).

Moreover, fly tubules consist of two cell types as seen in figure 1-4: the columnar epithelial principal cell and the star-shaped stellate cell. The former arises from ectodermal epithelial buds that have deep basal infoldings, elaborate cytoarchitecture, long apical microvilli and massive mitochondria, while the latter is smaller and thinner with fewer mitochondria, less basal infoldings and elaborate cytoarchitecture thus the star-shaped cells appear to be originated from the recruitment of mesenchymal cells.

The concept of tubule morphology has recently been demonstrated using the transcriptomics approach. The relationship between morphological asymmetry and physiological function in both pairs of fly tubules is important for understanding functional genes in specific tissues, where the generation of potentially toxic ammonia is correlated with only the left-hand tubule. The right-hand tubule is implicated in the excretion of calcium in its phosphate form (Dow et al., 1998).

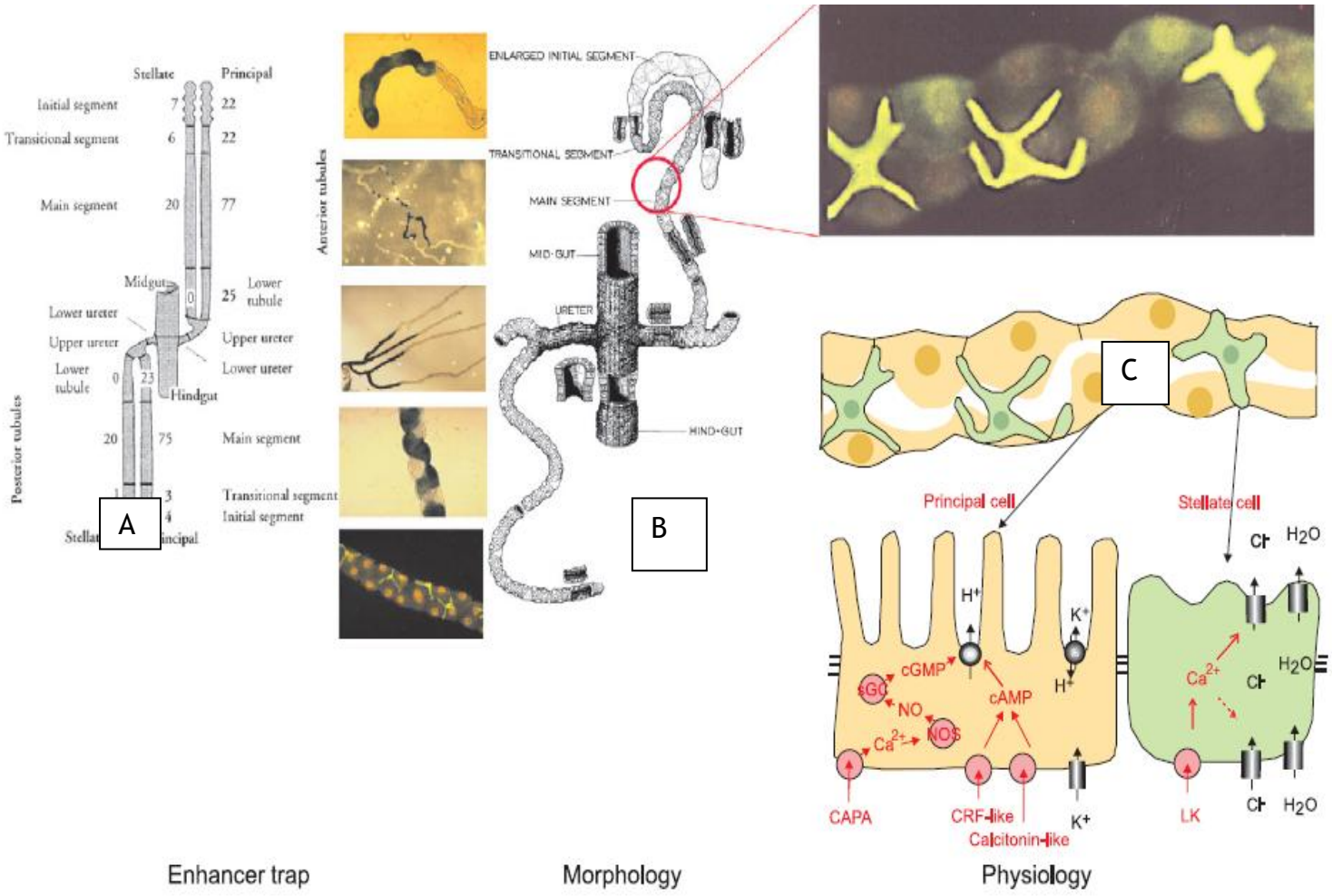

Figure 1-4 Three views of Malpighian tubule A) Genetic analysis for tubule, B) classical morphological analysis, C) different cells are shown in different colours, green for stellate and yellow for principal cells. taken (Dow, 2009)

Over the years, progress has been made at the physiological level to show the importance of this tissue in metabolic activities such as ion absorption, excretion, osmoregulation and water balance. Also, the Malpighian tubules have a vital role in immune response because they are able to up-regulate various anti-microbial genes, such as the diptericin gene, to kill bacteria, which means the tubule is of major importance to as a cell-autonomous immune system (Jules A, 1995). Detoxification enzymes, second messenger cyclic AMP, GMP pathways, and peptide hormones have distinct roles in both types of tubule cells (Imler and Hoffmann, 2000, Coast et al., 1991).

Microarray data analyses were used to draw the genetic framework that is highly-enriched in tubules. Many of the above genes show differences in gene expression between the whole fly and its tubule. So these experiments provided extensive gene expression data for over 300 genes that are related to signaling, transport, and detoxification (Figure 1-5) (Sözen et al., 1997, Wang et al., 2004). More recently, the physiology of tubules was examined in detail using electrophysiological methods. These results indicate that the tubule is a major site for maintaining ion homeostasis, where the alteration in basal secretion rate of K^+ and Na^+ is enhanced by increasing intracellular calcium ions in order to adapt to salt stress (Naikkhwah and O'Donnell, 2011). However, this finding is in agreement with Dow's findings (Wang et al., 2004) in which the principal cells are responsible for active cation transport, while the passive transport of anions and water are carried out only in star-shaped stellate cells. The fluid secretion process is regulated by vacuolar ATPase that is found primarily in principal cells, which in turn increases the activity of alkali metal-proton exchangers that excrete K^+ into the tubule lumen (Dow et al., 1998, Dow, 2009).

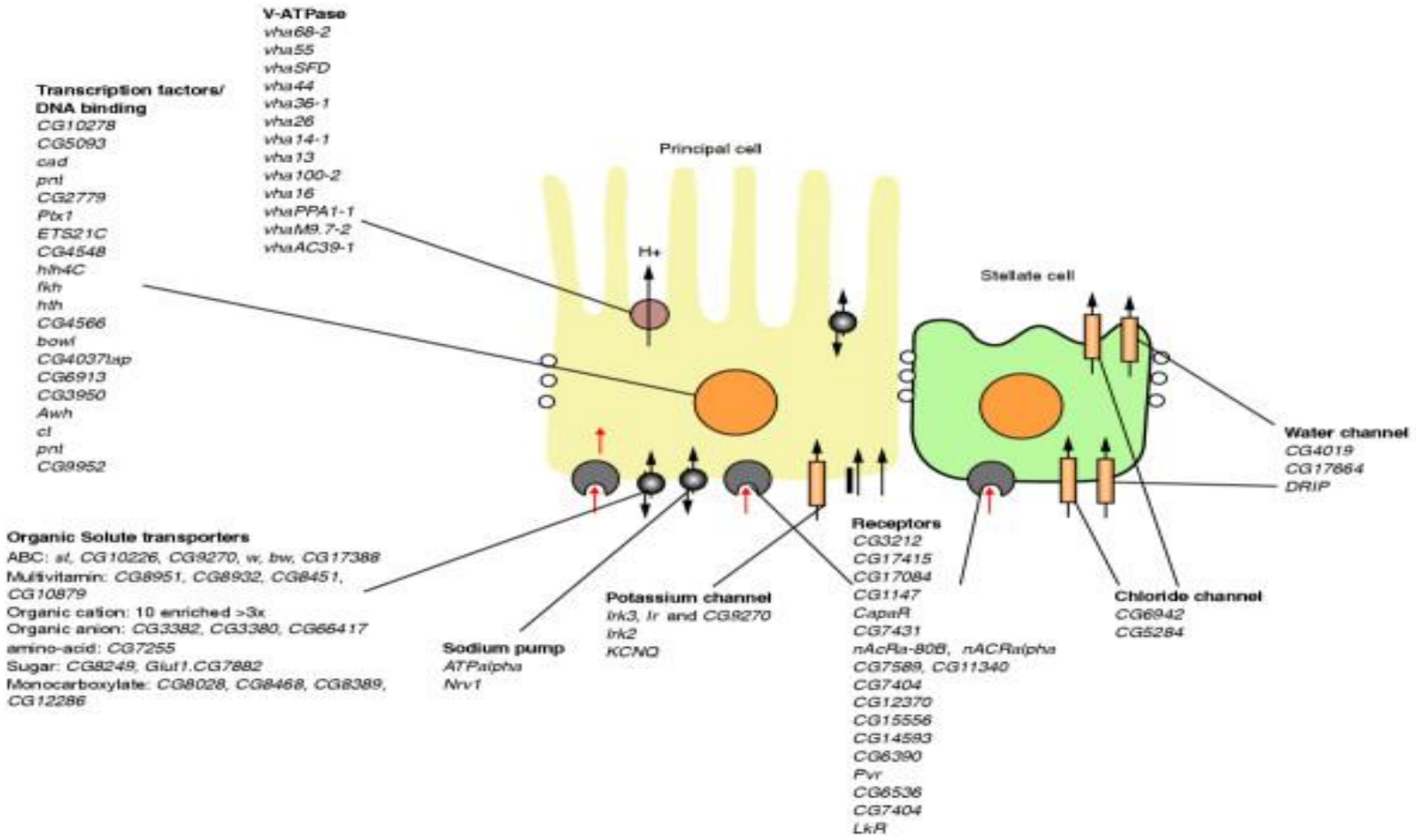

Figure 1-5 Summary of major groups of genes enriched in tubule as revealed by microarray approach (Wang et al., 2004)

Furthermore, the integration of transcriptomics and metabolomics approaches has been recently used to investigate genes that are highly enriched or suppressed in the fly tubule relative to their sidedness and gender (Chintapalli et al., 2012). This study shed light on the need to produce genomic data from isolated tissues rather than the whole fly to understand gene functions within the whole fly context.

The shift from gene identification to gene exploration is being made using tubule as a specific tissue because most renal diseases in *Drosophila* closely resemble human renal diseases also. Malpighian tubules are considered a model for metabolic disorders and inborn errors of metabolism (IEMs), to which particular ethnic populations are susceptible and display symptoms such as citrullinemia. The relationship between IEM diseases and Malpighian tubules can be interpreted in nephrolithiasis terms because this term refers to either minor or major stone aggregation in any part of the kidney in humans or in the fly tubule. Thus, nephrolithiasis is a feature of a wide range of acquired or inherited metabolic disorders. Typically, metabolic diseases are derived from misregulation of metabolites, which could result in disturbed metabolic pathways accompanied by nephrolithiasis. (Dow and Romero, 2010). (Detail in section 1.6).

1.6 Drosophila models of human diseases

Drosophila melanogaster has been evaluated in several studies that covered a wide spectrum of human diseases including cardiovascular, obesity, diabetes, neurological, cancer, and viral infections such as HIV and influenza. This success of the fruit fly as an organismal model when used as a whole fly or as an organotypic model when specific tissues are involved or for human diseases is due to its ease of application and the powerful genetic tools recently developed (Adamson et al., 2011, Bilen and Bonini, 2005, Konig et al., 2010, Lasko, 2002).

Genetic diseases can be classified into four classes: multi-factorial, chromosomal, mitochondrial, and single gene disorders (Goh et al., 2007). Indeed there are several factors such as mutations, particular deficiency in a metabolic pathway, and

environmental factors that cause multifactorial diseases. The best example in this case is diabetes, which is rapidly growing in the developed world and can be linked to obesity, (Goh et al., 2007). Chromosomal diseases can occur because of defects in chromosomal number or structure, as in the case of Down's syndrome, while mitochondrial diseases are caused by changes in mitochondrial DNA. For example, Leber's hereditary optic neuropathy (LHON) affects the retinal ganglion cells and leads to the loss of central vision by disturbing energy pathways. A single gene disorder is derived from a single mutated gene (Ellaway et al., 2002). Single gene diseases can be grouped into subcategories: dominant, recessive, autosomal and X-linked. Single gene disorders can pass the mutated gene across generations, and have major or minor effects on the metabolism of amino acids, organic acids, sugars, lipids, and nucleosides. Therefore, single gene disorders may associate with metabolic disorders in some cases. As mentioned above, genetic diseases are being extensively studied based on the *Drosophila* and human gene homology, or based on disease markers (Houten, 2009, Goh et al., 2007, Ellaway et al., 2002, Martins, 1999).

Online databases such as Homophila support our knowledge of human disease genes. They provide a rich source of information relating to *Drosophila* genes in conjunction with the human genomic sequence. The 714 *Drosophila* genes relating to categories of human disease genes have been added to the literature and can be seen in figure 1-6. The renal disease category is represented in table 1-2. The ability to modulate IEMs in Malpighian tubules and find solutions to human hereditary diseases is emerging rapidly (Chien et al., 2002, Potter et al., 2000, William, 1999, Reiter et al., 2001).

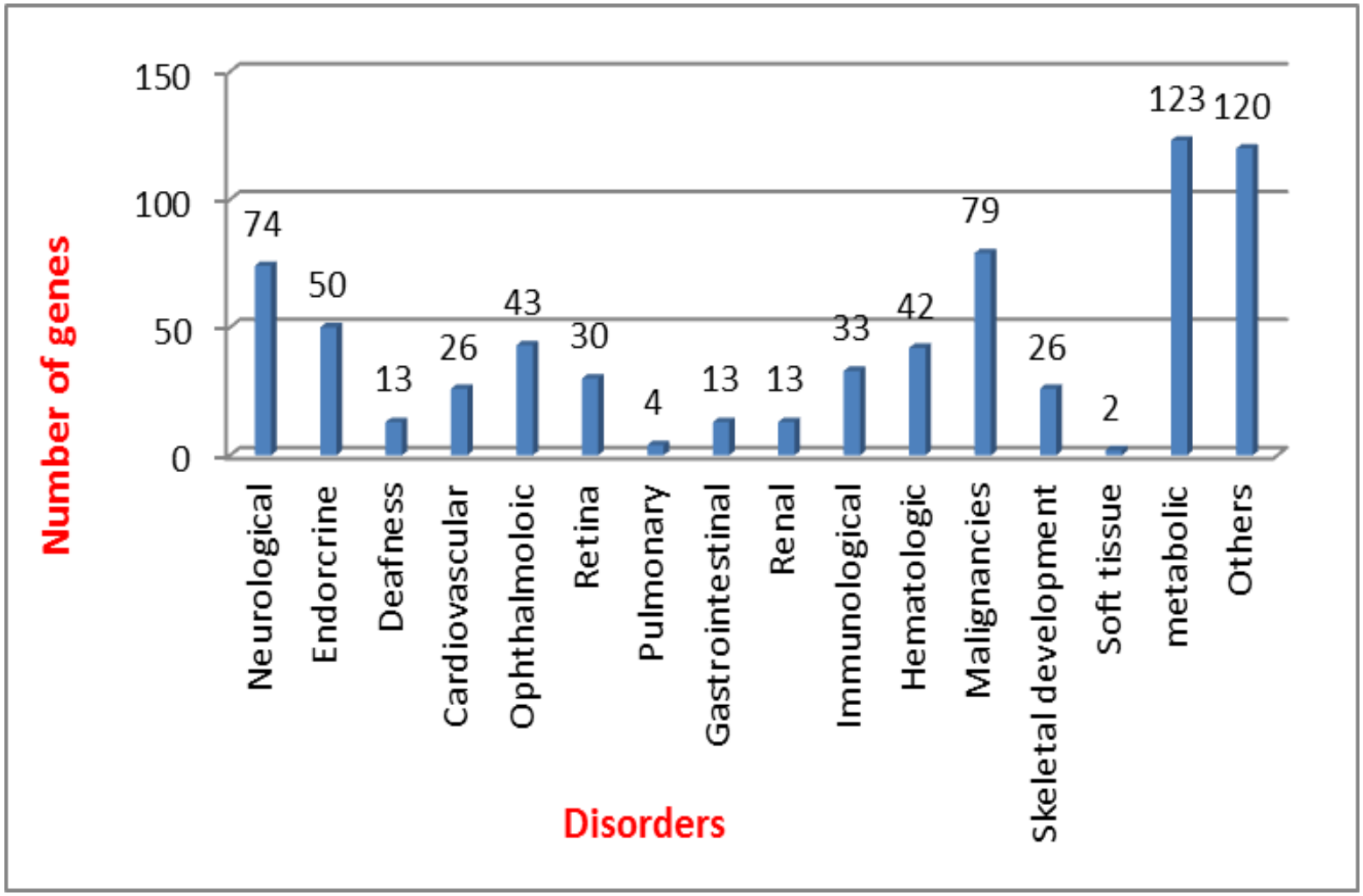

Figure 1-6 Classification of 714 drosophila genes related to different human diseases.(Chien et al., 2002)

Table 1-1 Human renal disease loci conserved between fly and human as shown (Dow and Romero, 2010)

Gene	Affymetrix Signal	Enrichment (Tubule:Fly)	BLAST Score	Human Disease	Notes
CG10226	1055	26	0	Colchicine resistance	MDR1 homolog
CG1315	1934	23	1.00E-123	Citrullinemia	Argininosuccinate synthase
ry	770	19	0	Xanthinuria, type I	Xanthine oxidase
CG31999	2097	16	2.00E-011	Hyperuricemic nephropathy	Uromodulin/fibulin-like
CG31116	1162	11	1.00E-111	Bartter syndrome types 3 and 4	CLCNKA/B homolog
Spat	1682	9.7	3.00E-091	Hyperoxaluria, primary type 1	Serine-pyruvate aminotransferase
CG1140	1729	9.5	2.00E-174	Ketoacidosis: SCOT deficiency	Citric acid synthase
CG9547	1458	7.9	4.00E-171	Glutaricacidemia type I	Glutaryl-CoA deydrogenase
CG6126	2316	7.5	4.00E-056	Hypouricemia, 1	SLC22A12 urate transporter
CG17119	1294	7	7.00E-073	Cystinosis, nephropathic	CTNS cystine transporter
ir	1099	5.5	2.00E-078	Bartter syndrome type 2	Inward-rectifier K^+ channel
Drip	589	5.1	4.00E-037	Diabetes insipidus, nephrogenic, autosomal recessive	AQP2 water channel
CG5284	1335	4	0	Dent disease	CLCK2 chloride channel
vha55	4016	3.7	0	Renal tubular acidosis with deafness	V-ATPase subunit
wal	3073	3.5	3.00E-112	Glutaricaciduria type IIA	Electron transfer flavoprotein, α-polypeptide
CG7834	3035	2.1	1.00E-082	Glutaricaciduria type IIB	Electron transfer flavoprotein, β-polypeptide

1.7 Inborn errors metabolism (IEMs)

The term IEM was established by Sir Archibald Garrod and can be clinically divided into Group I and Group II. Disorders that affect the functional or anatomical system are classified as Group I and have clear symptoms that are easily diagnosed by symptoms or phenotypes. These type of IEMs usually affect a particular functional system such as the coagulation process (Houten, 2009).

On the contrary, Group II diseases are quite complicated and need special attention because their ramifications upon different cells and organs do not specify the affected metabolic pathway. Therefore, wide disease diversity would appear to be represented by either the direct or indirect influence of a metabolic pathway. Indeed, this group can be split into three groups, as seen in Figure 1-7. Anabolic or catabolic metabolism disturbance represents the first group. This disturbance results in an accumulation of complex metabolites in some vital cells/organs such as lysosomes that leads to lysosomal diseases such as Gaucher's disorder. Group two diseases result in chronic intoxication such as cystinuria from the impairment of dibasic amino acids transport. Lastly, the third group results from disturbance in energy production due to deficient glycolysis and gluconeogenesis in metabolic pathways (Martins, 1999).

Clearly, the diversity of IEM diseases has challenged scientists to discover a specific marker for each disease. Thus, most IEM disorders are diagnosed by several metabolites that are found at significantly abnormal levels relative to normal subjects. One example is Xanthinuria type I which results from altered purine catabolism resulting from a mutation in the *xanthine oxidase* gene (*ry*). Mutation in the *ry* gene deletes the xanthine oxidase XO/XDH enzyme and this leads to an accumulation of hypoxanthine and xanthine, and depletion of uric acid and allantoin which are used as disease markers (Kamleh et al., 2008c). Moreover, two IEM disorders share at least one metabolite as a disease marker in some cases, which makes their characterization difficult. One example is citrullinemia II and homocystinuria disease where both can be characterized by measuring methionine.

The newest metabolomics approaches (detailed in Section 1.8) which have high sensitivity and specificity can be used to study metabolic disorders and allow the identification of new IEMs and the further characterization of many well-known IEMs (Tavazzi et al., 2005). Efforts in the last decade were well-documented and are summarized in the table1-3 which presents integrative information for medical and diagnostic purposes (Moolenaar et al., 2003). Metabolomic methods have become important, not only for the identification of metabolic intermediates, but also for their quantification to directly link genes with gene function via metabolites.

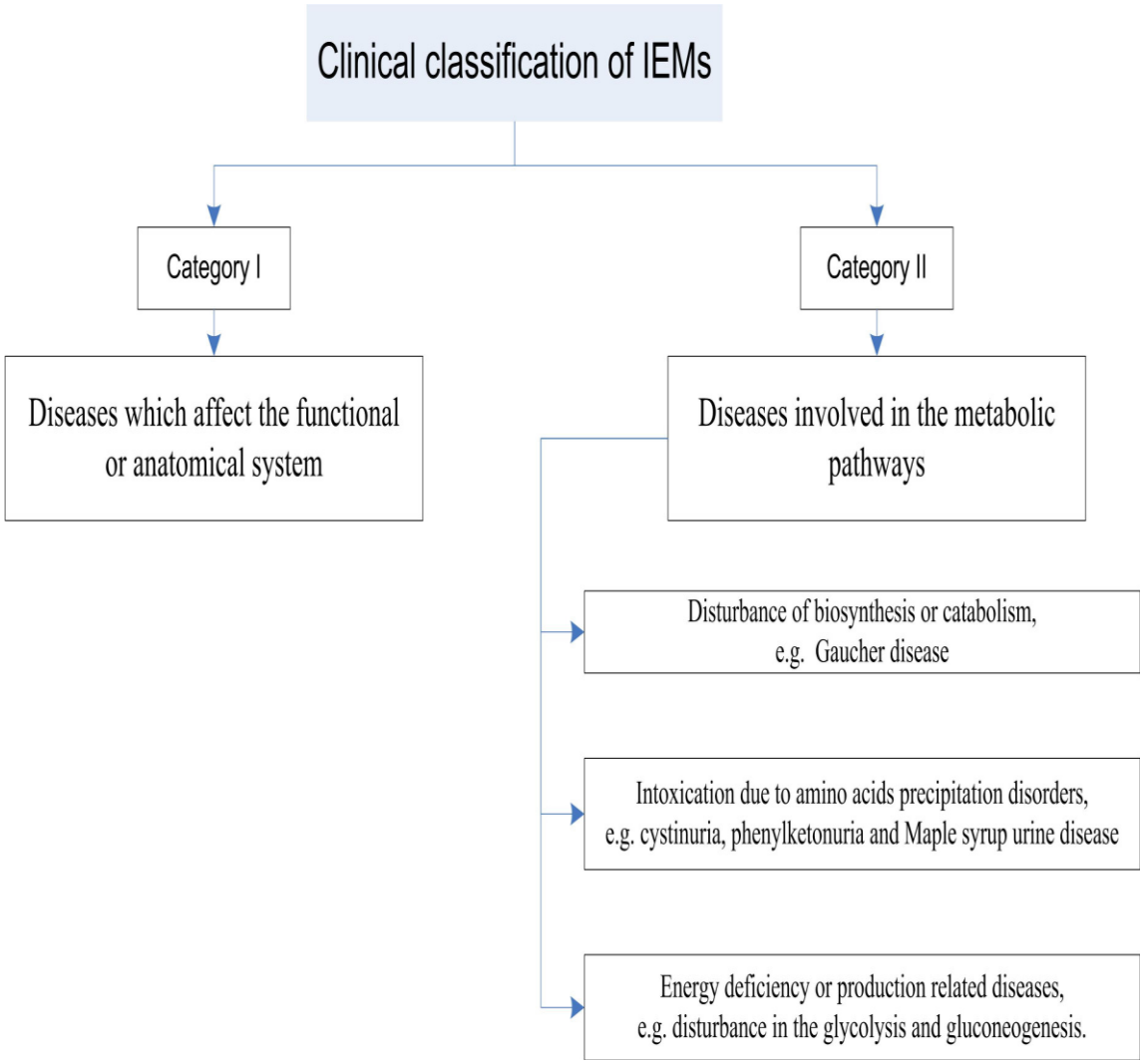

Figure 1-7 Clinical classification of IEMs; taken from (Martins, 1999)

Table 1-2 Examples of metabolic disorders detected using metabolomics screening approaches to screen newborns (Moolenaar et al., 2003)

Metabolic disorders	Abnormal metabolite
Organic acidemias	
Lactic acidemia	Lactic acid, Alanine
Propionic acidemia	Methylcitric acid , Propionylglycine, Tiglyglycine, 3-hydroy-n-valeric acid, 3-hydroxypropionic acid, 2- Methyl-3-hydroxyvaleric acid
Glutaric aciduria type I	Glutarc acid, 3-hydroxyglutaric acid, glutaconic acid
Glutaric aciduria type II	Glutarc acid, Ethlamlonic acid,Adipic acid , Suberic acid , 2- hydroxyglutaric acid
Propionic aciduria	Acetona, 3-hydroxybutyric acid, 3-Hydroxypropionic acid, Acetoacetic acid
Malonic aciduria	Malonic acid
Methylmalonic aciduria	Methylmalonic, Methylcitric acid
Mevalonic aciduria	Mevalonic acid, Mevalonolactone
2- hydroxyglutaric aciduria	2- hydroxyglutaric acid
2- ketoadipic 2- aminoadipic aciduria	2-oxoadipic acid , 2hydroxyadipic acid, 2-aminoadipic acid, 2-oxoadipic acid
2-methyl-3- hydroxybutyryl CoA dehydrogenase deficiency	Tiglyglycine,2-methyl-3hydroxybutyric acid
3-HMG-CoA lyase deficiency	3-hydroxy-3 -methylglutaric acid, 3-methylglutaconi acid , 3- hydroxyisovaleric acid
Multiple carboxylase deficiency	3-hydroxymethylcrotonylglycine, Methylcitric acid, 3-hydroxyisovaleric acid
3-ketothiolase deficiency	2-methyl-3- hydroxybutyric acid, 2-methylacetoacetic acid,Tiglyglycine
Amino acid disorders	
Tyrosinemia	Tyrosine,4-hydroxphenyllactic acid, 4-Hydroxyphenylacetic acid, Succinylacetone,4-Hydroxyphenlpyruvic acid
Lysinuria	lysine
Maple syrup urine disease	Leucine,Isoleucine,Valine,2-Hydroxyisocaproic acid,2-Hydroxy-3-methylvaleric acid, 2-Hydroxyisovaleric acid
phenylketonuria	Phenylalanine, Phenyllactic acid, 2-hydroxphenylacetic acid, phenylpyruvic acid
cystinuria	Cystine, Lysine, Ornithine

homocystinuria	Homocytein, Methionine, Homocystine
Hyperglycemia	Glycine
Hyperphenylalaninemia	Phenylalanine
Iminoglycinuria	Glycine,Proline,Hydroxyproline
Fatty acid oxidation defect	
very long -chain aceyl CoA dehydrogenase deficiency	Teradecenolacarnitine
Multiple acyl CoA dehydrogenase deficiency	Cis-4- decenoic acid
Medium-chain acyl-Co A dehydrogenase deficiency	Octanoylcarnitine, Hexanoylcarnitine,Decanoylcarnintine Hexanoyl-glycine, Suberyl-glycine, Phenylpropinyl -glycine, Cis-4-decenoic acid
Isovaleryl-CoA dehydrogenase deficiency	Iso valeric acid ,Iso- C5 acylcarnitine
Urea cycle defects	
Arginosucccininc aciduria	Arginosuccinic acid, Orotic acid, Orotidine, Uracil
Orinthine transcarbamylase deficiency	Orotic acid, Uridine,Uracil
Citrullinemia	N- Acetylcitrulline, citrulline, Orotic acid , Ortodine, Uracil
Citrullinemia II	Methionine, Phenylalanine, Galactose
Miscellaneous	
3-methylcrotonylglcinuria	3- hydroxyisovaleric acid,3-methylcrotonylglcine
4-hydroxybutyric aciduria adenosine deaminase deficiency	4-hydroxybutyric acid Deoxyadenosine
Alkaptonuria	Homogentisic acid
Aspartylglycosaminuria	N-Aspartylglycosamine
Beta- monnosidosis	Mannosyl(1-4)-Nacetyglucosamine
Canavan Disease	N-Acetylaspartic acid
Congenital adrenal hyperplasia Cystathioni	17- hydroxyprogesterone, adrostenedione, cortisol
cysthathionine Beta - synthase Deficiency	Methionine sulfoxide
Dihydropyrimidinase deficiency	5,6-Dihydro-uracil,5,6-dihydrothymine,Thymine,Uracil
Dihydropyrimidinase dehydrogenase deficiency	Thymine, Uracil
Dimethylglycine dehydrogenase dificiency	N,N-Dimethylglycine, Betaine
Ethylmalonic encephalopathy	Lactic acid., Ethylmalonic acid , C4 and C5 acylcarntitines.
Galactosemia	Galactose, Galactitiol, Galactonic acid
Molybdenume cofactor deficiency	Xanthine,Hypoxanthine,Uric acid, Sulfite
Glycerol Kinase Deficiency	glycerol

Hawkinsinuria	4- Hydroxycyclohexylacetic acid, Hawlinsin
Histidinemia	Histidine, N-acetylhistidine
Isovaleric academia or Isovleric aciduria	Isovalerylglycine, 3-hydroxyisovaleric acid
Krabbe disease	Galactocerebroside
Neuroblastoma	Homovanilic acid, Vanillymandelic acid
Oxoprolinuria	5- oxoproline
Polyol disease	Arbinitol, Ribotol,Arabinose,
Prolinemia type II	Pyrrol-2-Carboxyglycine,Proline
Purine nucleioside phosophorylase deficiency	Inosine, Dexyinosine, Deoxyguanosine, Guanosine
Sarcosinemia	Sarcosine
Trimethylaminuria	Trimethylamine N-oxide, Trimethylamine
UMP synthase deficiency	Orotic acid, Orotidine,Uracil,
Ureidoproprionase deficiency	3-Ureidoproprionic acid, 3- Ureidosiobutryric acid

1.8 Metabonomics

Metabonomics/metabolomics are often used interchangeably referring to the relative new term which has been added to the "omics" group along with genomics, transcriptomics, and proteomics in order to gain a global understanding of biological systems. Like other omics technology, metabolomics is comprised of the words metabolome and omics. Metabolome is derived from the ancient Greek word *metabol* referring to change. Metabolome has been defined as "the complete set of small molecules (metabolites) produced by a cell as a result of metabolism". "Omics" platforms ultimately lead to comprehensive biochemical and molecular characterizations of organ, tissue, or cell type. The concept of metabolomics was presented by Fiehn (Fiehn, 2001): "A comprehensive and quantitative analysis of all metabolites could help researchers understand such (biological) systems since such an analysis reveals the metabolome of the biological system under study". In the last decade, the use of metabolomics with its several neologisms (metabolomics, metabolic profiling, etc.) is rapidly increasing and has been applied in a wide range of scientific fields for the last decade as seen in figure1-8. Metabolomic tools are an essential part of the study of all

small molecules in biological samples due to the massive number, complexity, diversity and dynamic concentration of metabolites (Dettmer et al., 2007). Chromatography (HPLC, UPLC, GC, SFC, and CE) has been used either on-line or off-line in combination with MS, NMR FTIR and Raman spectroscopy in order to separate, determine, identify and quantify metabolites from different biological samples.

The challenge of metabolomics is to deal with the massive amount of data that result from the analytical platform. Scientists have developed strategies, methodologies and metabolomic tools in order to resolve these problems (Nicholson and Wilson, 2003, Fiehn, 2001).

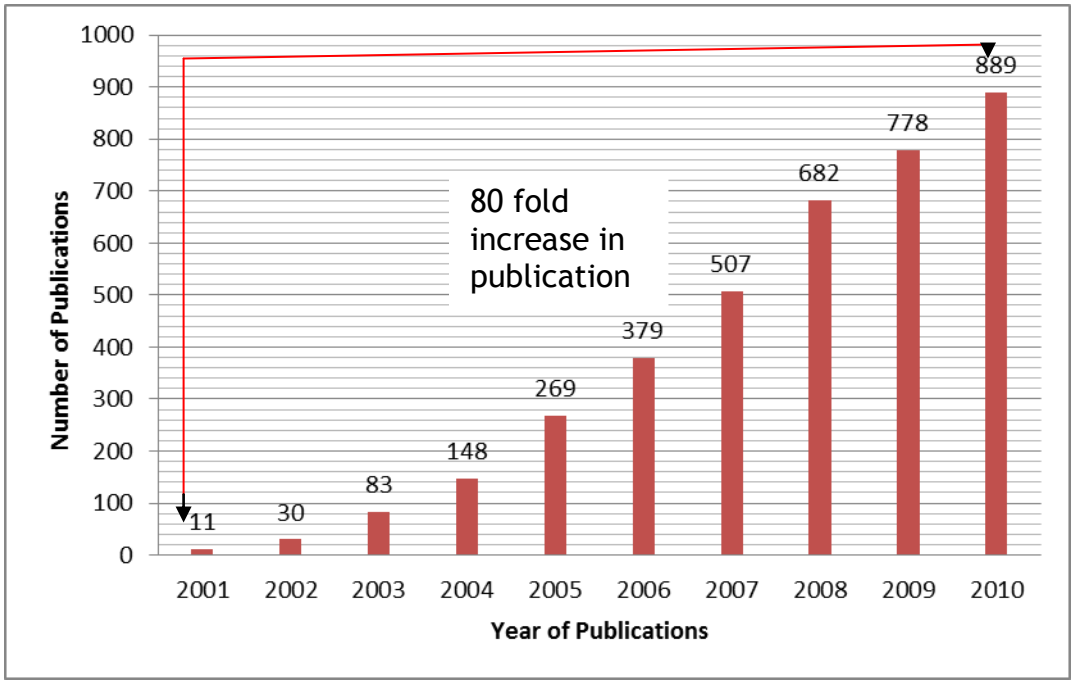

Figure 1-8 The numbers presented show only the trend in publications in metabonomics field over the last decade (Hobani, 2012, Oldiges et al., 2007)

1.9 Metabolome analysis

The comprehensive study of either metabolite amount or isoform changes is facilitated by analytical platforms. These technologies represent the bottleneck in metabolome analysis. Thus, the analytical platform provides a picture of the metabolome at one point in time. Metabolome analysis can be subjected to two types of analysis. The first is target metabolite analysis and the second is untargeted metabolite profiling. Their application depends on the nature of the analytical sample examined. The metabolic profiling approach profiles all metabolites within *ca* 2000 Dalton and can be further classified as metabolic finger-printing and foot-printing. Metabolic finger-printing identifies and quantifies all intercellular metabolites, while metabolic foot-printing characterizes extracellular metabolites. Metabolome target analysis refers to the selected metabolites in the biosample. The biological sample is a complex system contains a large number of metabolites ranging from polar to nonpolar compounds that vary in size and concentrations. Obviously, no single analytical tool is sufficiently comprehensive, selective, and sensitive enough to identify and quantify all metabolites in a biological sample. The goal of measuring metabolites is to obtain as broad a range of information about the metabolism of a system as possible. Thus, the coupling of multiple analytical tools is necessary to provide the best coverage of the metabolome (Dettmer et al., 2007, Oliver et al., 1998).

1.10 Analytical tools

Metabolites are chemical components that can be measured using a standard chemical analysis apparatus. Generally, metabolites include organic, inorganic, and elemental species such as carbohydrates, amino and fatty acids, vitamins, and lipids as well as inorganic anions and cations and all of these vary based on the type of organism studied. Unlike metabolomics, proteomics has only 22 amino acids to consider and transcriptomics has four major nucleotides. Those substances are similar chemically and physically (e.g., thermal stability, polarity, solubility, and molecular weight). Thus, the metabolomics approach necessitates the use of different technologies and methodologies

because metabolites have large variability in their chemical structures. The metabolomics analysis toolbox includes metabolite separation techniques (e.g., gas chromatography, liquid chromatography, and variants including ultra-performance liquid chromatography, capillary electrophoresis), spectroscopy detection techniques (e.g. Fourier transform infrared spectroscopy, Raman spectroscopy, and NMR spectroscopy), and statistical data processing to determine metabolite variations in biological samples (Dettmer et al., 2007, Oliver et al., 1998).

1.10.1 Mass spectrometry

The most commonly used tool in metabolome analysis is mass spectrometry (MS). MS consists of different ionization sources (e.g. ESI, APCI, and MALDI) and different analyzers including quadrupole (Q), ion trap (IT), and time of flight (TOF), Fourier transform ion cyclotron resonance (FT-ICR), and the recently developed Orbitrap technique. The differences between the mass analyzers depend on their mass resolving power, mass accuracy, sensitivity, and capability of generating spectral fragment masses from compound ions. These vary in conception and performance, and each has its own advantages and disadvantages. A combination of the strengths of various ion separation techniques in one mass spectrometer has become possible in recent studies, such as triple-Q, IT-TOF, Q-IT, TOF-TOF, Q-TOF, IT-FT-ICR, or IT-Orbitrap. A scientist can choose between two achievable methods amongst the significantly different ion separation technologies: “in-time” instruments and “in-space” mass spectrometers. “In-space” mass spectrometers can be grouped into two classes: (i) without field scanning instruments (e.g., TOF/MS-MS) and (ii) magnetic or electrostatic field scanning devices (e.g., quadrupole). “In-time” instruments are based on ion trapping where ions are stored for a short duration in ion traps. There are a number of ion traps on the market. Some use an electromagnetic field (e.g., FTICR) or an electrostatic field without a magnetic field (e.g., Orbitrap). MS systems were improved by the addition of soft ionization methods such as photo ionization (APPI) or electrospray (ESI) to become more sophisticated and robust for metabolome analysis. The advantage of using a mass spectrometer is that it can be tailored to the sample type and the metabolic problem.

Nordstrom et al (Nordstrom et al., 2007) compared different MS ionization sources including APCI, MALDI, and ESI for metabolite identification in a complex sample. The researchers suggested that identifying a large number of metabolites from a sample mixture requires multiple ionization sources, although ESI was used for more than 90% of the samples analyzed (Nordstrom et al., 2007). Major improvements in mass detectors make the MS a major instrument in biomedical field because of its ability to detect low levels of compounds. Thus, the new technology, such as LTQ Orbitrap mass spectrometer, has increased the value of metabolic data obtained from a single sample compared to the other mass detectection techniques. The LTQ Orbitrap analyzer operates by combining two analyzers, namely a linear ion trap and a Fourier transform mass spectrometer, the Orbitrap. This development in mass spectroscopy provides accurate mass measurements that are beneficial for detecting the elemental composition of metabolites (Makarov, 2000, Makarov et al., 2006). The following figure 1-9 illustrates the Orbitrap's principal parts and how it works. In the ESI, the analytes are pumped into the source solution via the eluent flow from the LC that is interfaced with a mass spectrometer. The transitional phases can be described by the following steps:

The analyte solution pumped through the electrospray needle to form charged droplets, where they travel between the needle tip and the counter electrode in order to evaporate the solvent before sample introduction into the mass spectrometer. When a high voltage is applied, the evaporated ions will be produced and a spray of negatively or positively charged droplets. Then charged ions produced from the droplets pass through four stages all of which involve differential pumping through the RF-only multipoles into a curved RF-only quadrupole, also called the C-trap. Ions in the C-trap accumulate and their energy is dampened using nitrogen gas. They are then injected by a curved lens system that provides three additional areas of differential pumping before passing into the Orbitrap detector.

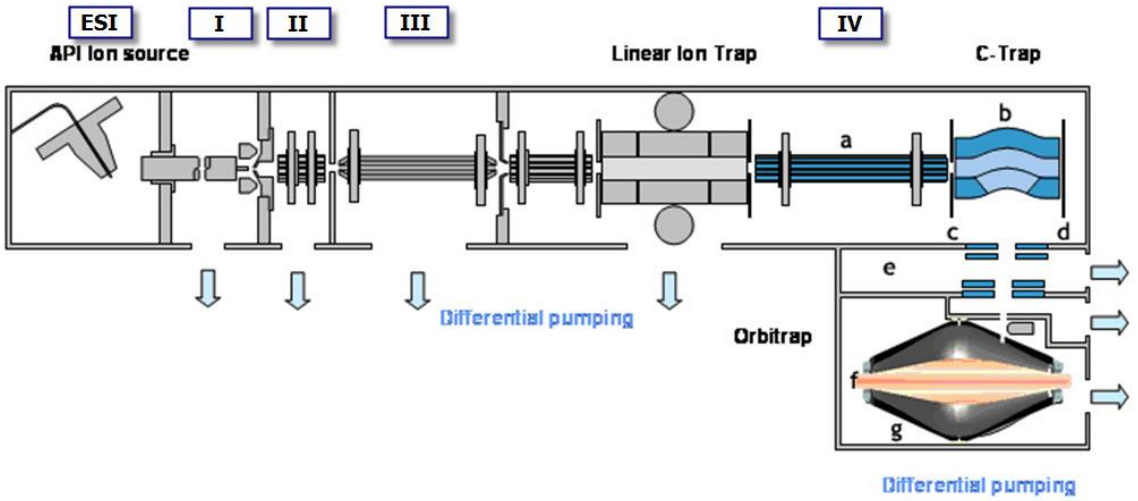

Figure 1-9 shows the parts of LTQ-Orbitrap:(I) heated capillary, (II) multi-pole focusing devices, (III) a gating lens, multi-pole (IV) a, transfer octopole; b, curved RF-only quadrupole (c-trap); c, gate electrode; d, trap electrode; e; ion optics, f; inner spindle-like; g, outer barrel-like.

1.10.2 Direct injection mass spectroscopy (DIMS)

DIMS can be used for metabolome analysis in order to obtain a metabolite spectrum within a few minutes without using any separation techniques. DIMS is sufficient when the metabolite under investigation is well represented in a biochemical or metabolomics dataset. This technique can be used with atmospheric pressure ionization (API) interfaces, especially ESI. The investigation of a metabolite mixture using direct injection MS can be impeded by competitive ionization of the analytes, which may result in low sensitivity. This method requires procedures to avoid ionization suppression that limits detection. The use of high-resolution techniques and high mass accuracy allows reliably assigned molecular structure of detected metabolites. This means that thousands of compounds can be measured and identified simultaneously without separation. DIMS is primarily applied to plants and microbial systems but can also be used for clinical applications (Dettmer et al., 2007).

1.10.3 Separation technology

Chromatography techniques either based on gas or liquid mobile phases play an important role in metabolome analysis because the number of metabolites varies in different biological samples. Chromatography is a physical separation method where metabolites distribute between two phases: the stationary phase and the mobile phase. The nature of the stationary phase or column chemistry will affect chromatography resolution and sensitivity. Silica-based or monolithic based columns are most commonly used for reversed-phase chromatographic analysis of the metabolome. The mobile phase gradient for RP-HPLC of the metabolite mixture requires a slow process and a long gradient. The starting mobile phase is high in water content and the ending solvent has high organic content. The advantage of RP columns for analyzing the metabolome is that non-polar compounds can be analysed easily, but many metabolites such as polar amino acids are not retained in RP chromatography. HILIC columns are an alternative to RP chromatography. These columns can be silica-based with a hydrophilic stationary phase. On the ZIC-HILIC column, that is being used extensively in the metabolomic field, the sulfobetaine zwitterionic functional group coats the silica and so permits polar analytes to separate by partitioning into a hydrophilic environment. Although the distribution of analytes between the mobile phase and the water-enriched layer absorbed on the surface of the zwitterionic column is easily explained by Lewis' theory figure 1-10 (where the interacting forces are based on the basicity and acidity of the solute to control selectivity in HILIC), ion exchange interactions between the analyte of interest and the stationary phase is also possible in some cases. Unlike the RP column, the HILIC mobile phase mode uses organic solvents with volatile buffers or water where the gradient mobile phase starts at a high organic solvent concentration such as 95% acetonitrile. Ammonium acetate and formic acid are suitable buffers that give the ZIC-HILIC phase buffer a pH ranging from 3 to 8. Thus, the choice of separation tool is dictated by the properties of the metabolite (Jandera, 2008).

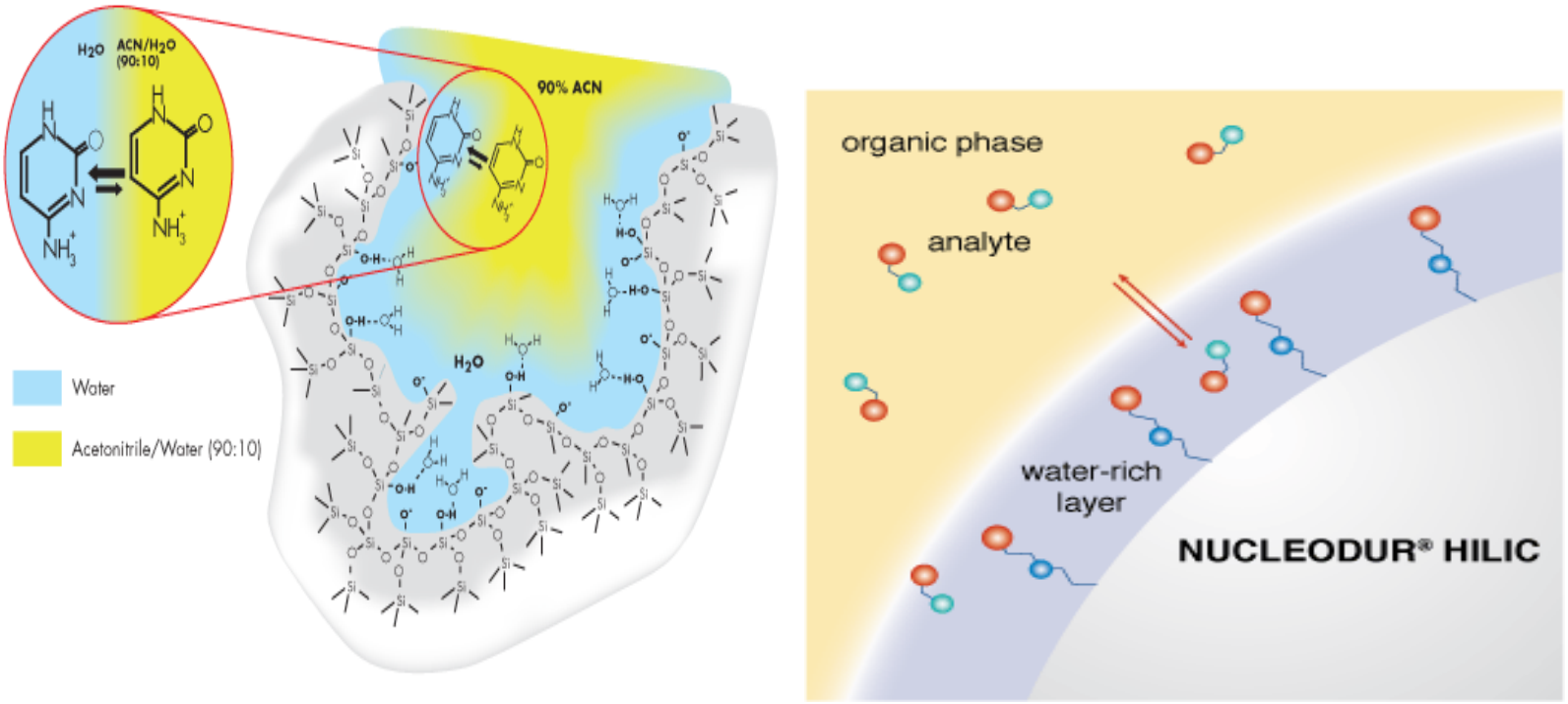

Figure 1-10 (Right panel) shows the distribution of analytes between the mobile phase and the water-enriched layer absorbed on the surface of HILIC column; (left panel) shows partition mechanism that is mainly based on polarity of analyte and degree of solvation**(Corporation, 2010)**

1.10.4 Gas chromatography

Gas chromatography (GC) techniques have been utilized widely in metabolomics research, especially for volatile and heat stable compounds. The eluted compounds are then analyzed by either electron impact EI or chemical ionization Cl. Large metabolites and nonvolatile compounds such as nucleotides cannot be determined by using GC. Some of these metabolites usually require derivatisation by converting carbonyl groups to alkyl oximes, carboxylic acid groups to methyl esters or trimethylsilyl esters (TMS), and hydroxyl groups to TMS ethers in order to increase their heat stability, increase volatility and reduce polarity. A number of detectors can be used with GC to including flame ionization (FID), chemiluminescence (CLD), electron capture (ECD), and thermionic ionization (TID). Linking MS with gas chromatography can offer increased sensitivity and high chromatographic resolution in combination with high specificity. The choice of ion separation methods play an important role in GC-MS sensitivity and time of flight separation offers high sensitivity and high resolution. Nevertheless, the dynamic range for the quadrupoles analyzer is higher than for TOF analysers. Furthermore, many parameters may be optimised to improve sensitivity in GC instruments. A splitless injector is utilized to carry samples into the GC system(Pasikanti et al., 2008). During the analysis process, the typical injection volumes into a GC column are 1 µL or less in the splitless system. Using GCXGC, where the samples is separated on two different columns, with TOF-MS provides rapid data acquisition and decreases the time needed to analyze the sample so that this method results in very narrow peaks (Dettmer et al., 2007, Kamleh et al., 2009a).

Reproducibility is pivotal for GC-MS analyses. The stability of the derivatised sample and the chromatography parameters are vital for GC-MS reproducibility in metabolome analysis. The stability of the analytes is the main source of GC-MS variability, and so an internal standard could be used to resolve this problem and reduce the variation between samples. For example, GC coupled with MS has been used for diagnosing IEMs related

to an organic aciduria, which results from distribution at certain branched-chain amino acids metabolism(Kuhara, 2005, Kamleh et al., 2009a)

1.10.5 Liquid chromatography

Liquid chromatography separation results from the interaction of the solvent from the mobile and stationary phase with the analyte. This approach differs from gas chromatography as sample volatility or thermal stability is not required. Metabolite analysis using liquid chromatography requires the use of a very sensitive detector to detect metabolome which are not volatile.

LC is the most widely applied analytical tool in metabolome analysis when combined with MS. LC/MS is a powerful technology for metabolomics research that separates and identifies metabolites. This approach is becoming increasingly helpful in metabolomics studies. Modern analyzers such as the Orbitrap and ionization techniques such as ESI are used to gain accurate mass measurements and reduce MS signal redundancy. ESI and APCI are suitable for identifying a wide range of metabolites. ESI can be used for polar and ionic metabolites, and APCI may be utilized for analysing less polar and neutral compounds. In addition, the detection of neutral molecules is also possible using the positive ionization mode in ESI through sodium and potassium adduct formations. Therefore, the pH of the mobile phase is a critical requirement for the ESI process. This should be adjusted to a specific range to facilitate the ionisable group either acquiring a proton or losing a proton. For example, the ionization of molecules containing amines, amides, and phosphates require a slightly acidic condition to be protonated in ESI. In contrast, the ionisation of compounds containing sugar phosphates, fatty acids, polar acids such as citrate, and several lipid classes such as phosphatidylinositols require slightly basic or neutral conditions for deprotonation in ESI. Furthermore, a spectrum can be further complicated by the formation of several adducts and multimers that may be observed in positive or negative mode of ESI. Two main theories have been proposed to explain the droplet formation mechanism by ESI, but all of them need further

investigation for validation. The “charged residue model” suggests that each individual droplet will shrink until its surface tension cannot sustain more shrinking or splitting. This mechanism occurs when the solvent is completely evaporated and is most applicable to big molecules or proteins. While the “ion evaporation model” proposed by Dole suggests that the flow of nitrogen gas either off- or on-axis ionization aids solvent evaporation and facilitates nebulisation, and this mechanism applies to small molecules.

Generally, LC/MS can be used to analyse a wide range of metabolites with greater sensitivity than GC-MS without any prior derivatisation. LC-MS capability is expanded by multistage MS-MS or high-energy C-trap dissociation (HCD) on the Orbitrap to enhance the characterisation of the parent ion and to elucidate fragment structure (Kamleh et al., 2009a, Holčapek et al., 2012) .

1.10.6 Data processing

Data processing aims to extract relative information and remove noise in order to facilitate data analysis and data interpretation. This process may start with the acquisition of metabolomic data obtained from various analytical tools, but this section is centred on LC/MS data because it is of particular relevance to this thesis. The resulting data requires pre-processing before multivariate statistical analysis (MVA) to avoid insufficient correction for background ions, retention time shifts, and insufficient amounts of metabolites. Furthermore, four considerations should be kept in mind when dealing with data processing in metabolomic experiments using LC/MS. First, LC/MS covers the whole metabolome in the biological context and contains a large diversity of metabolites in terms of biochemical structures and concentrations. Second, processing the data prior to MVA is a source of errors that can lead to artificial signals produced by peak picking, variable alignment, and chemical noise. Thus, MVA results may be influenced by the pre-processing of the data (Dettmer et al., 2007).

Thirdly, LC/MS generates many MS signals due to adduct and product ions generated from a single metabolite during solvent evaporation process in ESI. Therefore, signal redundancy prohibits proper metabolite identification by increasing the number of

variables that can produce a false positive in MVA results because many MS signals are identified after MVA.

Another matter of concern is that the identification step of acquired signals in metabolomic experiments consumes time and effort. It is usually done by matching databases with the filtered mass spectra. Further experiments such as MS/MS fragmentation are needed to rigorously confirm the results (Werner et al., 2008). Broadly, scientists have developed two methods for extracting information from metabolome data. Chemometric or non-target methods, and quantitative or target methods as shown in figure1-11. Chemometrics is defined as "the application of mathematical, statistical, graphical or symbolic methods to maximize the information which can be extracted from chemical or spectral data". It can be used to distinguish between sample categories under different conditions by reducing the number of dimensions and by simplifying subsequent analysis that results in significant differences in the data. It is useful for identifying phenotypes and drawing conclusions without the need to identify and quantify metabolites. Indeed, the chemometric analysis approach presents two most widely utilized chemometric approaches for pattern recognition. They are principal components analysis (PCA) and the partial least squares discrimination analysis (PLS-DA). PCA allows the clustering tendency to be easily detected by visualization in an unsupervised manner. The chemometric tools for metabolomics data processing must be selected based on the purpose of the study. If the purpose is sample discrimination, and prior information on sample identity is unknown, then unsupervised methods such as PCA are used. Supervised methods such as PLS may be used when the class of some samples is known. Contrary to the chemometric methods, the quantitative methods require the metabolites in a given biological sample to be identified and quantified prior to analysis. These methods can be applied to the data as acquired by NMR or MS via available reference databases to identify their signals (details in the next section). Chemometric approaches may be less applicable to LC-MS data because the number peaks present in a sample run can be > 20000, and because the alignment of chromatograms drifts from run to run (Trygg et al., 2007, Werner et al., 2008).

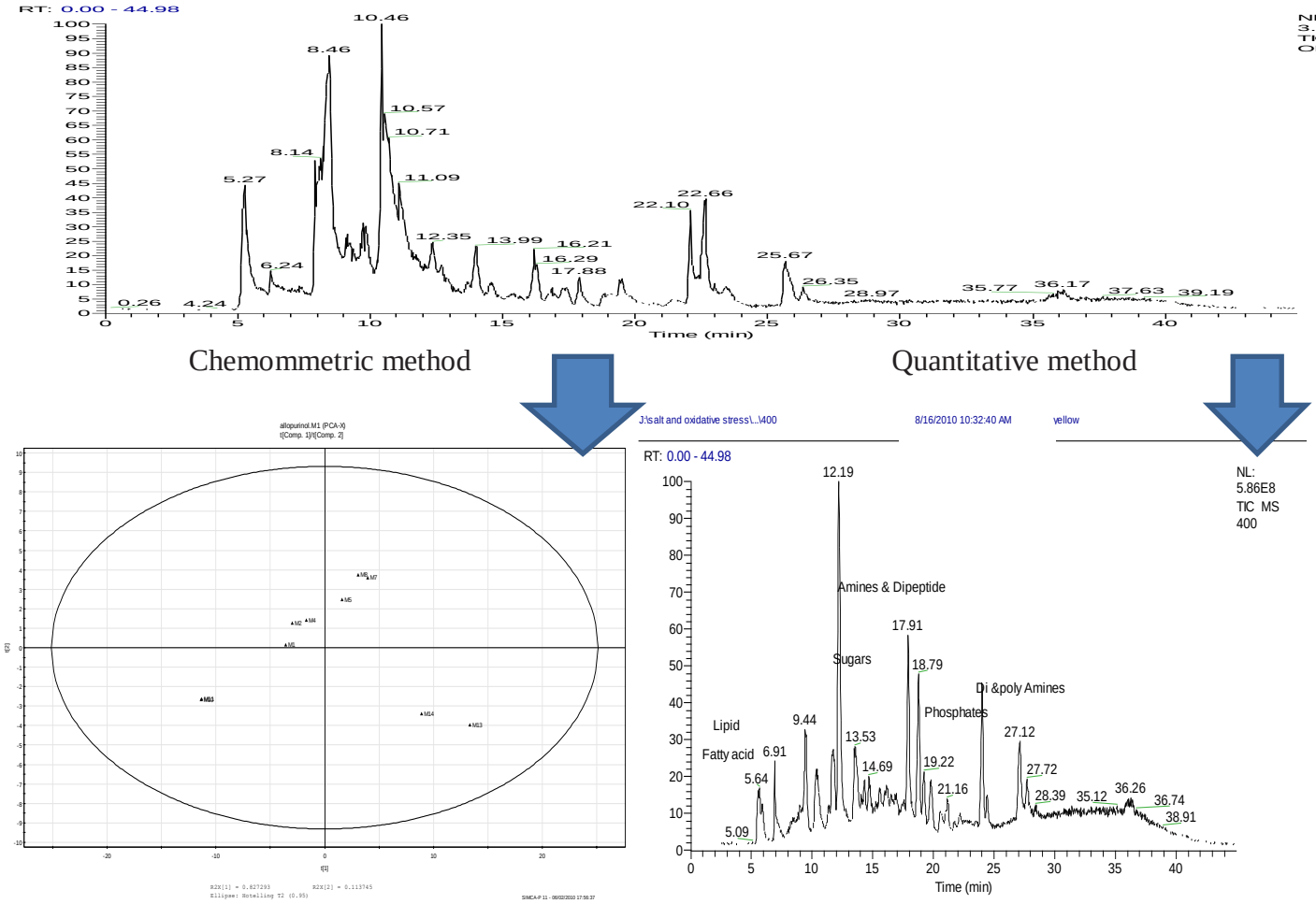

Figure 1-11 Raw data (upper panel) can be processed by chemometric method (lower- left panel) or quantitative method (lower –right panel)

1.11 Data analysis and Databases

Metabolomic approaches generate huge quantities of data. Therefore, these data should be processed using commercial or non-commercial software to plot ion chromatograms across the mass spectrometer full scan range. SIEVE software from Thermo Fisher, which features peak extraction, peak alignment, and peak tabulation according to peak intensity, in which every peak picked is given an ID corresponding to the metabolite, and offers statistical analysis such as p-values that depends on the differences between control and treated samples. This software makes it is easy to reveal the significant difference in peak intensity between two analyzed groups, and visually illustrate and compare the peaks between groups (Katajamaa and Oresic, 2005, America and Cordewener, 2008, Zhu et al., 2009). SIEVE can also connect with the ChemSpider database to aid metabolite identification (detailed in Chapter 2).

There are various non-commercial softwares such MZMatch enables peak extraction, match filtering, normalization and identification. A drawback of MZMatch is that computer programming knowledge is required for its use (Pluskal et al., 2010). MzMine was developed by a Finnish scientist, Matej Oresic for analyzing high-resolution LC-MS datasets (Katajamaa et al., 2006). It provides peak picking, statistical analysis, and visualization tools with database searches.

Searching databases is a major challenge in metabolomics research because of the large volume of data generated by different research groups that must be safely transmitted and stored (Katajamaa and Oresic, 2007). A database can be utilized to identify unknown metabolites and provide a comprehensive understanding of the acquired data. This step requires queries by atomic composition or by molecular mass, both of which are based on the instrument used and the method of analysis. For example, there is high reproducibility between instruments in case of GC/MS experiments, while metabolome data acquired from LC/MS instruments may vary between similar instruments. Consequently, there are four types of databases compatible with LC/MS instruments and which provide rich metabolite data on their exact mass, chemical formula, structure, and possible adducts. Despite this limitation, all can present information on fragmentation.

(a) the MassBank metabolome database features a spectral browser, peak search function that displays 10,000 spectral data obtained using LC/MS, GC/MS, and CE/MS. (b) The LipidMaps structure database represents eight classes of lipid metabolites containing 30,000 entries facilitating their prediction based on mass tolerance, head group, and precursor ions of MS data. (c) Metlin is a metabolite database containing over 50,000 structures. These entries are linked to outside resources such as the Kyoto Encyclopedia of Genes and Genomes (KEGG) to help researchers understand the molecular interactions and reaction networks. Metlin also provides MS/MS data obtained by Q-TOF MS using either positive or negative mode ionization operated at four different collision energies (0, 10, 20 and 40 v). (d) The HMDB contains spectra data for 7,900 metabolites extracted from human biofluids. It is designed to provide literature-derived data, mass and NMR spectra, quantitative chemical data, and clinical and biological data about human metabolites by linking to seven databases, such as MetaCyc. The exploitation of these databases to identify unknown metabolites is required for metabolomic approaches to give biological relevance to the data generated. Indeed, some of the databases reported above combine several general chemical databases, such as PubChem, that contains synthetic and natural compounds. Therefore, it is important to keep up with all databases for ongoing work (Werner et al., 2008, Dettmer et al., 2007).

1.12 Aim of Study

The aim of this study will be to:

- Optimise the extraction, separation and detection method for the wide range of metabolites in *Drosophila*.
- Test the feasibility of *Drosophila melanogaster* as genetic model in combination with metabonomics so that it can provide novel insights into functional genes or into disease states.
- Assess *Drosophila* as a low cost model for drug testing.

- Examine specific fly tissues in combination with RNA interference in order to provide metabonomic information about the functional consequences of mutation of *urate oxidase*.

2. Experimental

2.1 Chemicals

The allopurinol used for this study was purchased from Sigma Chemical Co (St Louis, MO, USA). Acetonitrile was from Fisher Scientific (Leicestershire, UK), and the formic acid was from VWR (UK). All chemicals used were analytical grade. A Direct Q-3 water purification system (Millipore, Walford, UK) was used to produce the HPLC water that was in all of the analyses. All chemicals and reagents are used listed in table 2-1.

Table 2-1 Reagents used in the study

Reagent	Use	Company
methanol	solvent	Fisher Scientific
chloroform	solvent	Fisher Scientific
Tris-HCl	buffer	Fisher Scientific
EDTA	buffer	Sigma Chemical Co
NaCl	buffer	Sigma Chemical Co
SDS	buffer	Sigma Chemical Co
LiCl	buffer	Sigma Chemical Co
KAc	buffer	Sigma Chemical Co
Ethanol	washed	Fisher Scientific
MgCl2	hydrolysis solution	Sigma Chemical Co
Benzonase	hydrolysis solution	Sigma Chemical Co
Phosphodiesterase I	hydrolysis solution	Sigma Chemical Co
Alkaline phosphatase	hydrolysis solution	Sigma Chemical Co
EHNA-hydrochloride	hydrolysis solution	Sigma Chemical Co
esferoxamine	hydrolysis solution	Sigma Chemical Co
NE-PER nuclear extraction reagent kit	Nuclear Protein Isolation	Sigma Chemical Co
PBS	buffer	Fisher Scientific
CER I	buffer	Sigma Chemical Co
protease inhibitor cocktail	inhibitor	Sigma Chemical Co
HCl	hydrolysis solution	Sigma Chemical Co
NaHCO3	salted	Sigma Chemical Co
protein crash plate	Filter	Biotage Ltd.
pRISE	transformation vector	Invitrogen
LR Clonase	recombination	Invitrogen
Oligo nucletotide primers	polymerase	Invitrogen
Qiagen RNeasy Mini extraction kit	extraction	Qiagen
Indigo carmine dye	dye	Sigma Chemical Co

In addition the analytical standards which were used to generate the table of retention times shown in appendix I, were all obtained from Sigma-Aldrich UK.

2.1.1 Buffered methanol-water (MW)

Solvent mixture methanol and water in the ratio (1:1) was previously employed for extraction of *Drosophila* (Kamleh et al., 2008a). Seven-day-old adult flies were collected under CO_2 anaesthesia. Ten flies (male and female) were homogenised in the solvent mixture by using an ultrasonic cell disruptor (Misonix, Inc., USA) for a few seconds; the homogenates were then spun in a centrifuge at 10 000 rpm at 4 ˚C. The supernatant was then collected and kept in the freezer at -80 ˚C prior to the analysis. On the day of analysis, samples were brought to ambient temperature and placed into glass autosampler vials.

2.1.2 Buffered chloroform-methanol-water (MCW)

This method was taken from (Folch et al., 1957) and was modified to suit this experiment. The final ratio of cold solvents methanol/chloroform/water used in the sample quenching extraction method was 3:1:1. Ten adult flies from both genders were collected and anesthetized under CO_2, and collected into the ice cold solvent mixture. Then they were homogenized for few seconds by sonication. The homogenates were then centrifuged for 10 minutes at 4 ˚C. The supernatants were extracted and stored at -80 ˚C until required. Prior to the analysis, samples were kept at room temperature for 30 min. and were then placed into glass autosampler vials.

2.2 Drosophila melanogaster

All the *Drosophila melanogaster* strains which were used in this study were supplied by Professor Julian Dow from the University of Glasgow. The flies studied are listed in table 2-2. The flies were reared either in small ventilated plastic vials for small quantities of *Drosophila* or in large bottles for a large amounts when they were needed (10 adult

flies were selected for each mutant in this study except where otherwise stated. Flies were kept on standard food (Appendix XI) and maintained at room temperature between 20-22 °C in a light-dark cycle 12h: 12h with relative humidity between 35-40%(Ashburner, 1990). Every two days, flies were transferred into new medium.

Table 2-2 Fly stocks used in this study

Name	Resource	phenotype	Reference
OregonR *OR*	(BSC)	Wild type	http://flybase.org/reports/FBst0000005.html
Canton S *CS*	BSC	Wild type	http://flybase.org/reports/FBst0304357.html
White w^{1118}	BSC	White mutant	http://flybase.org/reports/FBal0018186.html
Urate oxidase *uro*	BSC	Uro mutant	http://flybase.org/reports/FBgn0003961.html
Rosy ry^{506}	BSC	rosy mutant	http://flybase.org/reports/FBgn0003308.html
Bestrophin $best^{c04759}$	BSC	Best2 mutant	http://flybase.org/reports/FBgn0035696.html
Yellow *y*	BSC	Yellow mutant	http://flybase.org/reports/FBgn0004034.html

2.3 Fly Larvae

Laboratory grown wild-type Oregon R species of *Drosophila melanogaster* were used as the control for the *y* mutant. Larvae were raised on standard medium on a 12h:12 h L:D cycle, at 23 °C, and at 55 % room humidity until they reached the third-instar stage for the metabolomic analysis. Ice cold methanol/chloroform/water (3:1:1) was used in the

sample quenching and extraction method. Ten larvae from both genders were collected and anesthetized under CO_2, they were then homogenised in the solvent mixture (1 mL) and this was followed by a few seconds of sonication. The homogenate was then centrifuged for 10 minutes in a centrifuge at 4˚C and the supernatants were collected into a fresh tube and stored at -80 ˚C until required.

2.4 DNA/RNA hydrolysis

DNA/RNA was extracted from 100 larvae for each biological replicate using the phenol-chloroform extraction method (Sambrook et al., 1989). A total of 4 biological replicates were prepared for both Oregon R and *y* mutant. Briefly, the DNA extraction procedure was as follows. Whole larvae were ground in a 1.5 ml microcentrifuge tube and subsequently sonicated briefly using a Microson Ultrasonic cell disruptor (Misonix Inc, USA) in 400 µl buffer A (100 mM Tris-HCl (pH 7.5) and 100 mM EDTA, 100 mM NaCl, 0.5% SDS). After incubation at 65 °C for 30 min, 800 µl of LiCl/KAc mixture (1 part 5 M KAc: 2.5 parts 6 M LiCl) was added. The samples were spun for 15 min at room temperature (RT) at maximum speed in a table-top microcentrifuge. Floating curd was removed using a pipette tip and 1 ml of supernatant was taken into a new tube. Then, 600 µl of isopropanol was added and the sample was mixed up and down using pipette. Another round of centrifugation was performed at RT for 15 min. The supernatant was discarded and the pellet was washed with 70 % ethanol and dried for 15 min at RT. The dried pellet was re-suspended in 100 µl of nuclease-free water. DNA/RNA was quantified using a NanoVue plus spectrophotometer (GE Life Sciences, UK). For DNA/RNA hydrolysis, a method was adopted from Kriaucionis *et al.* (Kriaucionis and Heintz, 2009). Briefly, 100 µg amounts of DNA/RNA were incubated in the hydrolysis solution (100 mM NaCl, 20 mM $MgCl_2$, 20 mM Tris pH 7.9, 1 U/µl Benzonase, 600 mU/ml Phosphodiesterase I, 80 U/ml Alkaline phosphatase, 36 µg/ml EHNA-hydrochloride, 2.7 mM desferoxamine). Hydrolysed DNA/RNA was filtered using an Amicon microcon 10 kDa cut-off centrifugal filter unit (Millipore UK Ltd.).

The hydrolysate was used for subsequent chromatography and LC-MS analysis after diluting (1:4) with acetonitrile.

2.5 Nuclear Protein Isolation

For histone analysis, the nuclear protein fraction was extracted using NE-PER nuclear extraction reagent kit (Thermo Scientific, UK). Briefly, 50 larvae were washed in phosphate buffer saline (PBS) 3 times. Using a pipette, all the residual PBS was removed and the larvae were homogenized at 4 °C in ice-cold CER I buffer (including 1:100 protease inhibitor cocktail from Sigma Aldrich, UK). The rest of the extraction was performed according to the manufacturer's protocol. Finally the nuclear fraction was collected and protein quantity was measured using a Bradford colorimetric protein assay kit (BIO-RAD, UK). A total of 80 µg of nuclear protein was used for the hydrolysis as follows. The protein in a total of 80 µl was mixed with 160 µl of constant boiling HCl in a vial. The vial was sealed and heated in an oven at 145 ˚C for 4 hours. The mixture was cooled and 160 µl of 3 M sodium bicarbonate was added. Then 0.4 ml of acetonitrile was added to a protein crash plate (Biotage Ltd, Sweden) followed with 0.2 ml of hydrolysate. Salts were allowed to precipitate for 10 min and then the sample was filtered. The filtrate was used for the subsequent chromatography and LC-MS analysis.

2.6 RNA interference (RNAi)

RNAi is a powerful tool for reverse genetics and can be used to silence gene expression, and is most frequently used in *Drosophila melanogaster in vivo*. It involves construction of an inverted cDNA sequence to target a specific gene and germline transformation into flies for inheritance into successive generations. The uro-RNAi was constructed in the following manner:

- Cloning the double-stranded RNA into the vector
- Germline transformation of the vector into white background embryos

- Balancing and crossing with w^{1118} again to test whether the expression of the construct has an effect on fly development.

The double stranded RNA was cloned into pRISE with the help LR Clonase. Cloning vectors contain selectable markers such as the *mini-white* gene to distinguish the transformed flies from nontransformed and also contain a UAS promoter to induce expression using a GAL4 fly.

After constructing the appropriate plasmid, DNA samples were sent to Bestgene *Drosophila* Service, USA for introducing into *white* background flies to generate a new generation (G_0). Progeny of this cross were then characterized by red eyes because they carry eye marker (*mini-white* gene). Afterward, adult flies that have red eyes were chosen again to cross with *white* flies producing a stably transgenic line as seen in the Figure 2-1.

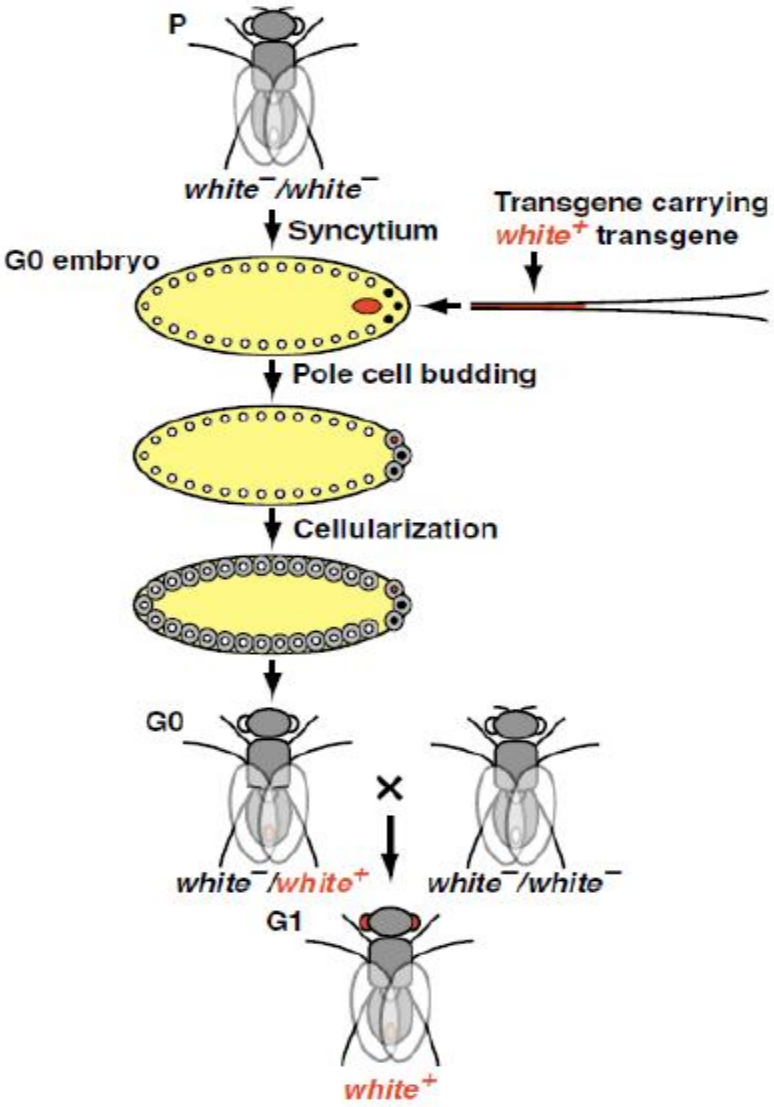

Figure 2-1 Germline transformation of *Drosophila* showing it is conducted by injecting embryos from *white*⁻ strains with a P-element shuttle vector containing the gene of interest and a marker *mini-white* gene, along with a 2-3 helper plasmid. The flies from these embryos are crossed with *white*⁻. Progeny of this cross are then screened for red eyes, implying they carry *mini-white* and thus transgenic. The red-eyed adult flies are then back-crossed to *white*⁻ and selected to produce a stably transformed line.

2.7 Tissue dissections

Adult flies were cut into three major parts: thorax, head and abdomen. In addition, specific tissues were dissected using a simple method illustrated in figure 2.2 adopted from Dow and co-workers(Wang et al., 2004). Flies were anaesthetized on ice, dissected immediately and transferred to a Petri dish containing Schneider's medium (Invitrogen UK)(Boy et al., 2010).

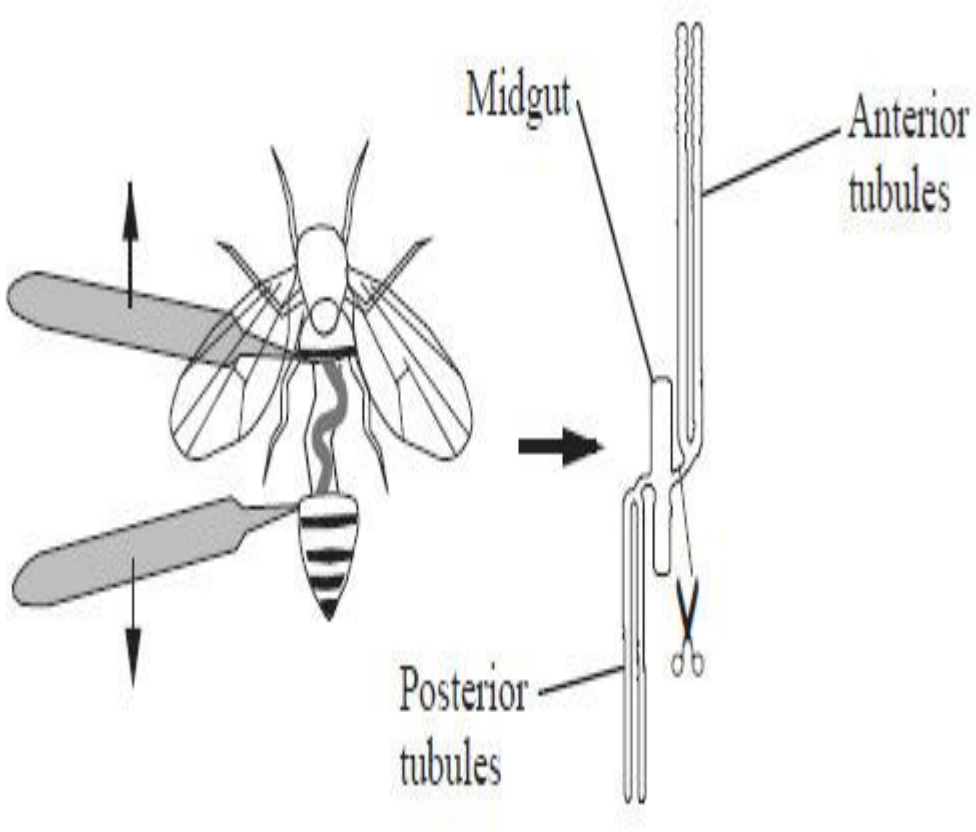

Figure 2-2 Malpighian tubule dissection method where the forceps hold fly from its thorax region and with the other hand, the tubule is slowly and gently is pulled very end part of the fly. At this point the Malpighian tubules will start to appear

2.8 Validation by Quantitative PCR for gene knockdown

This experiment was performed for measuring the expression of lysine-ketoglutarate reductase (*lkr*) and urate oxidase (*uro*). (qRT-PCR) for *lkr* was run on the RNA samples extracted from the third-instar larvae of the *yellow* mutants and Oregon R wild type while (qRT-PCR) for *uro* was run on the RNA samples extracted from dissected tubules of uro-GAL4 flies, uro RNAi flies and their progeny.

Oligo nucletotide primers to detect *lkr* and *uro* were designed by MacVector 10.0 software then the selected pairs were sent to the MWG Biotech custom primer service where they were synthesized

dLKR-F: TGCCTTCGAGCGGGATGAACG
dLKR-R: GCCGGCTTGCCCACAGTCAT
Uro-R: 5'- ACCACGGTGCTAAAGATGCG - 3'
Uro-F: 5'- AAGTGCGAGAACGGAGTCCAAG - 3'

The extraction of mRNAs was carried out using a Qiagen RNeasy Mini extraction kit. The total RNA was extracted and quantified using a Nanodrop™ 1000 spectrophotometer. Using Superscript II reverse transcriptase, first strand complementary DNA or cDNA was generated from 1000 ng of messenger RNA. A quantitative real-time PCR (qPCR) was carried out on the cDNA samples. The PCR conditions include initial denaturation at 95°C for 10 min, then each cycle (repeated 30 times) containing a denaturation step at 95°C for 10s (to denature the each end PCR products), annealing step for 30 s at 56 °C, extension step for 30 s at 72°C. A final extension step was included for 10s at 72°C. At the end of each cycle, CyberGreen fluorescence was read that reflects the amplification of the products. Primers were specific in amplifying one desired product that was evident from the melting curve plot. Then the expression data were normalized to the alpha-Tubulin84B gene as the reference control. Statistical measures (standard error mean and *P*-value) for four

independent replicates were used for each sample under study and presented using GraphPad Prism statistics software (GraphPad Software USA).

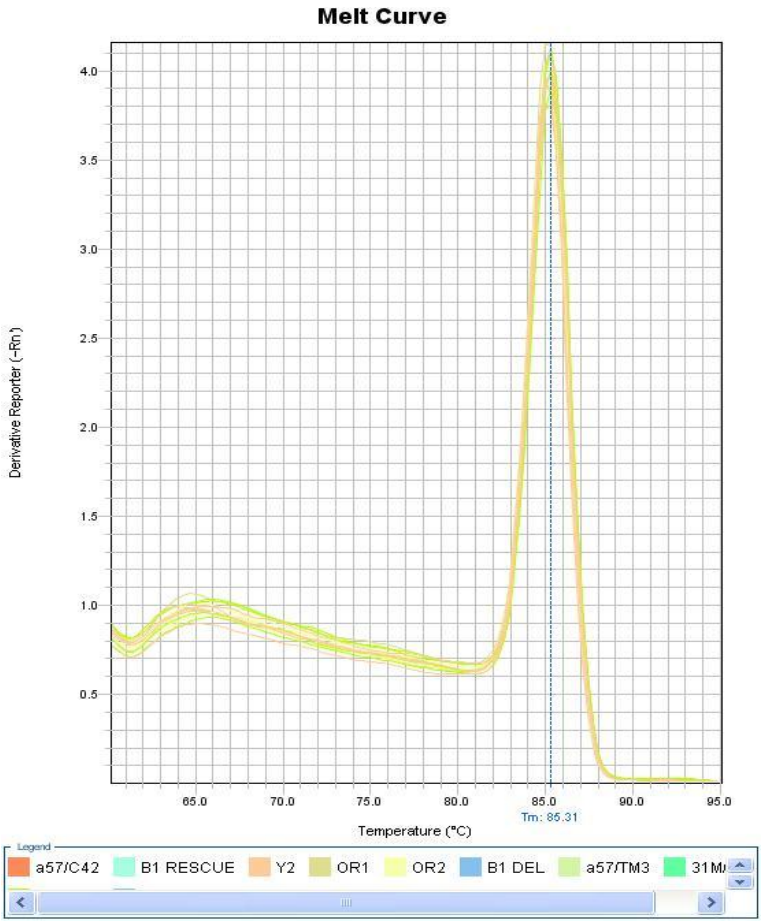

Figure 2-3 showing the right *q*PCR product for *lkr* where it was identified using melting curve.

2.9 Allopurinol treatment of flies

110 µg/ml of allopurinol was prepared and then was added to fly food that was freshly prepared. The drug was added on the surface of the fly food (agar) and kept for one day to dry. The vials were immediately closed with cotton wool. Seven day old Oregon R flies were chosen for feeding with the drug over a time course that included 6, 24 and 48 hours. The experiment was designed to use treated groups against untreated groups at each time point.

2.10 Salt diet and survival assay

Flies (males or females) were fed separately on 4% NaCl via adding salt into their normal growth medium and the experiment was performed based on a previously described method (Stergiopoulos et al., 2009). To test for survival under salt stress conditions, 20 adult flies were transferred into vials that were freshly prepared as described above. Every 2 days, flies were transferred into new vials and the number of dead flies was counted every 12-24 h. The percentage of survivors was calculated using the Kaplan-Meier survival curve as means ± SEM using (GraphPad) software.

2.11 Salt eating behaviour assay

This test was performed using of Indigo carmine dye to show the satiety of the fly with regard to the NaCl diet based on Stergiopoulos's method, (Stergiopoulos et al., 2009) (500 mg/ml). Dye was added into fly's food and then 20 adult flies (males or females) were transferred into vials containing 4% NaCl plus normal food. Their ability to eat salt containing food was tested after 24 h by observing the blue colour present in the fly gut under a light microscope.

2.12 High-performance liquid chromatography (HPLC) analysis

HPLC was carried out using three different column formats, providing a large amount of data, were used to over a wide range of metabolites in *Drosophila*. HILIC and silica columns were utilized to examine polar, mid polar and non-polar compounds in order to provide comprehensive metabolite coverage.

2.12.1 The ZIC-HILIC Column

A ZIC –HILIC column 5µm (150 × 4.6mm, HiChrom, Reading UK) was used in all analyses and a method was developed which produced good separation, solvent A was 0.1 % v/v formic acid in HPLC grade water and solvent B was 0.1 % v/v formic acid in acetonitrile. A flow rate of 300 µl/min was used and the injection volume was 10 µl, the gradient used was as follows: 90%B at (0 min) - 50%B at (16 min) - 20%B at (18min) - 20%B at (28min) - 90%B at (36 min). Samples were kept in a vial tray which was set at constant temperature of 3 ˚C to avoid any possible degradation of samples.

2.12.2 ZIC-pHILIC column

A ZIC pHILIC column (150 x 4.6 mm 5 µm particle size, HiChrom, Reading U.K.) was used in some analyses. Solvent A was only acetonitrile and solvent B was 10 mM ammonium carbonate buffer, pH 9.2. A flow rate of 300µl/min was used and the injection volume was 10 µl, the gradient used was as follows: 80% A 20% B) to 20% A (80% B) in 30 min. Samples were kept in a vial tray which was set at constant temperature of 3 ˚C to avoid any possible degradation of samples.

2.12.3 Silica column

An ACE silica gel column (3mm x 150 mm x 3 µm, HiChrom Reading U.K.) with hydrophilic interaction chromatography (HILIC) mode was used which produced good separation of lipids, Solvent A was 20% 2-propanol (IPA) in 20 mM ammonium formate

(v/v) and solvent B was 20 % IPA in acetonitrile. A flow rate of 300µl/min was used and the injection volume was 10 µl. The gradient used was as follows: 90%B at (0-5 min) - 70%B at (9 min) - 65%B at (13min) - 60%B at (23min) - 55%B at (28-30 min) – 90%B for 31-40 mins. Samples were kept in a vial tray which was set at constant temperature of 3 ˚C to avoid any possible degradation of samples.

2.13 Mass spectrometry of polar metabolites

MS data was obtained from experiments that were carried out by a Finnigan LTQ Orbitrap (Thermo Fisher, Hempsted, UK). The instrument was tuned according of the manufacturer's instructions approximately each week and set at 30000 resolutions. This enabled mass accuracy of < 2ppm to be routinely achieved. Samples were analysed in positive ion mode with a needle voltage of + 4.5 kV and with a capillary temperature of 250 ˚C. Sheath gas flow 40ml/min and auxiliary gas was 10 ml/min, while the mass scanning range was (75-1500) Dalton. The whole instrument was controlled by Xcalibur software version 2.0 (copyright© Thermo Fisher Co). The instrument was also used to carry out MS^2 experiments with various collision energies in order to assist with metabolite identification.

2.14 Mass spectrometry of lipids

In order to get comprehensive coverage of the lipids an Accela HPLC pump interfaced with Orbitrap Exactive mass spectrometer was used in positive/negative switching mode. The instrument was calibrated according to the manufacturer's instructions. The needle voltage was 4.5kV in positive mode and -4.0 kV in negative ion mode, the heated capillary temperature was 320°C and the sheath and auxiliary gases 50 and 17 arbitrary units, respectively. The background ions 195.0876 (+ve), 166.045 and 219.175 (-ve) were used as lock masses. The HPLC conditions were as described in 2.12.3.

2.15 Metabolite identification

Accurate mass measurement to below 2 ppm was sufficient to limit possible elemental compositions for each ion to a few choices. In practice there are certain rules that

eliminate unlikely formulas such as the presence of phosphorus in a biomolecule requires at least four oxygens, for compounds with a MW < 1000 the presence of more than 6 nitrogens and two sulphurs is unlikely, compounds which do not contain a nitrogen have to have odd MWs under ESI conditions. Generally by following such simple rules and with a mass accuracy of < 2ppm only one sensible elemental composition is generated for compounds with a MW < 300 amu. A simple and automated way to search metabolic databases is another important step in reducing the number of candidates to just one formula although in some cases there may be more than one isomer with this formula such as in the case of hexoses and hexose phosphates. The software used in the metabolite identification steps in the current work is detailed below (figure 2-4). These steps begin with the raw data, which is saved in the native format in the Xcalibur software, and end with metabolite profiling confirmation data.

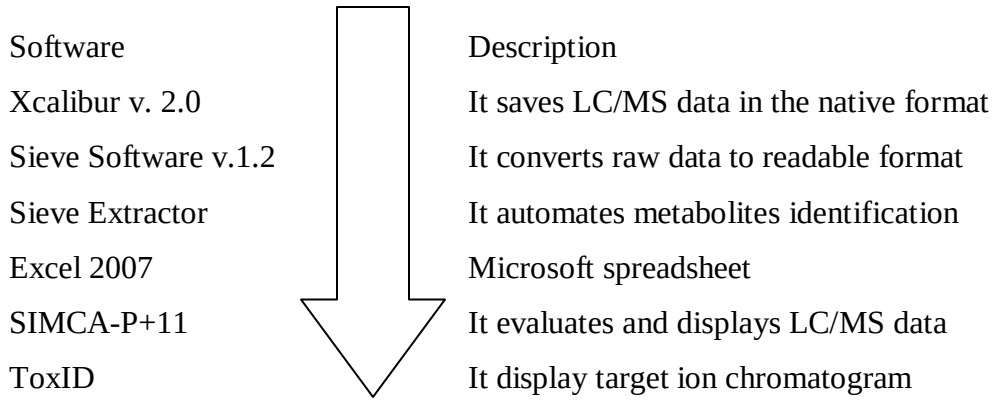

Figure 2-4 Workflow of the metabolomic software used in the current study**.**

Raw data contains the retention time and the mass/charge ratio of the metabolite. Thus, any data analysis process, especially the metabolomic approach, has to exactly identify the metabolite extracted. The three steps of data analysis used in this study are clearly described here.

Firstly, data obtained from Xcalibur software were exported into Sieve Software 1.2 (Thermo Fisher Co.) to be converted into a readable format that allows for further data processing. The Sieve program deals with two sample groups, as mentioned in the previous chapter: in the current study, wild type samples make up the control group while mutations make up the treatment samples. The software then searches for metabolites according to this categorization. Sieve software aligns and frames chromatograms offering retention time, observed mass, ratio for the mean peak areas, mass intensity and p-value or t-test and other features between chromatographic peaks of the control group (normal wild type) and the treatment group, as shown in figure 2-4. It also should be noted that the alignment and mass intensity of ion chromatograms may vary from run to run due to issues with chromatographic stability and detector stability and it is important to minimise these factors as far as possible in order to be able to observe significant differences between sample sets. Figure 2-5 shows the alignment of two peaks by Sieve software.

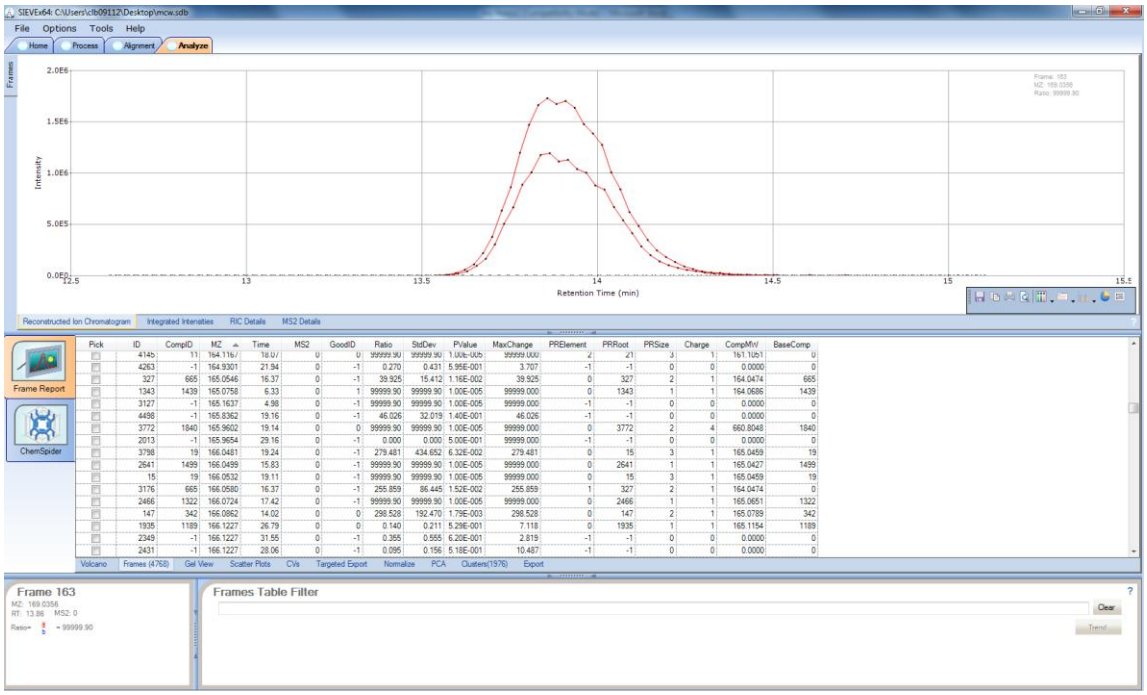

Figure 2-5 Typical screenshot of the alignment step in Sieve

Secondly, as the annotation step in Sieve software is limited, there is an urgent need for software that helps in naming ion masses extracted from the Sieve program. Thus, the Sieve Extractor program was designed in-house to compare accurate masses obtained experimentally with the accurate masses of 41,623 potential metabolites from databases Metlin, Kegg, HMDB and LipidMaps. Data obtained from Sieve are copied and pasted into Sieve Extractor (SE) and compared against the database and the software returns putative identities for the metabolites present in the data set (figure 2-6).

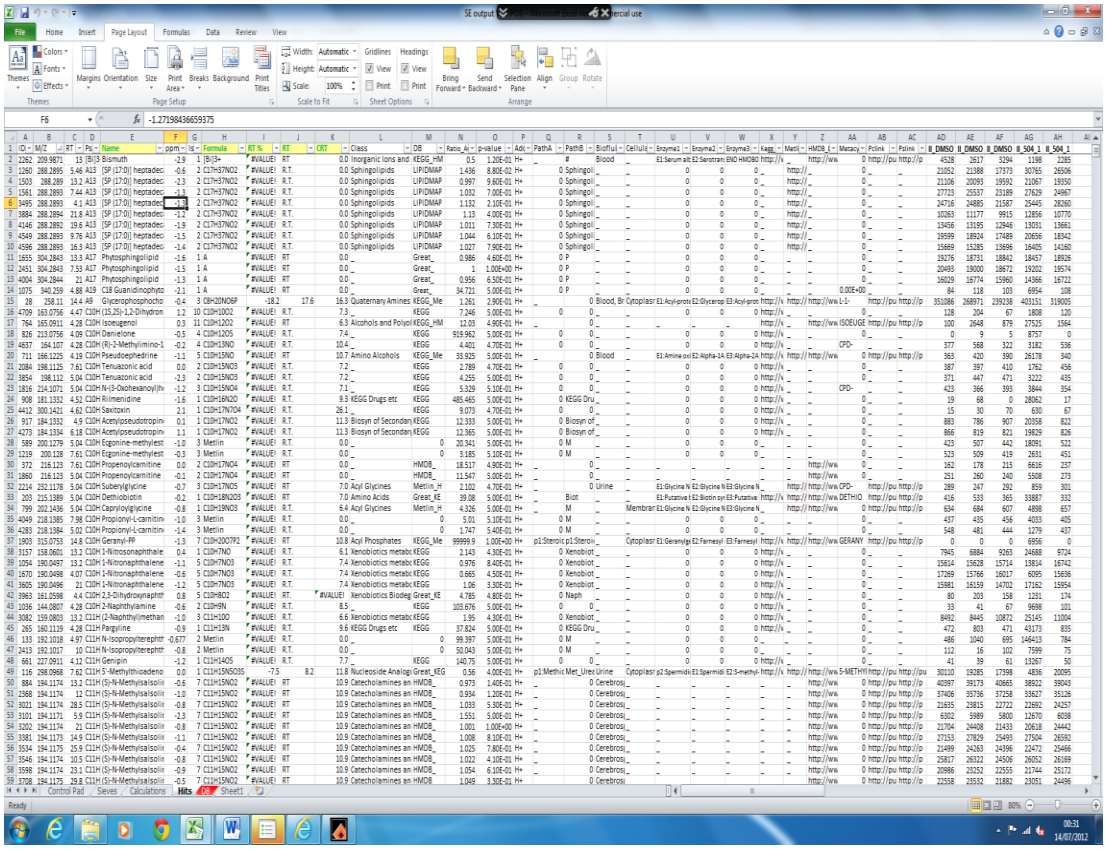

Figure 2-6 Sample output from Sieve Extractor (SE) Programme

Thirdly, in some cases, novel metabolites not present in data bases can be observed as significantly different values from the control samples. Therefore, manual checking for extracted ion chromatograms from the original Xcalibur files is necessary because Xcalibur software shows a single clear peak across the time range of the chromatogram. This approach has two principal steps: mass of the ion determined from the Sieve software is entered into Xcalibur in order to explore its chromatographic peak, which should appear as a perfect sharp peak; then, possible elemental compositions for the ion chromatogram are generated with < 2 ppm mass accuracy. In order to assign unknowns larger databases such as Pubchem can be searched. Finally fragmentation using MS^2 can be used to help elucidate the structure of the unknown.

3. Optimization of the Extraction and Mass Spectrometric Analysis of the *Drosophila* Metabolome.

3.1 Optimization of sample extraction: the choice of buffer

Several strategies are used for the determination of metabolites in different organisms; there is no literature on a global method of extracting the wide range of chemical compounds in *Drosophila*. Such a method needs to be comprehensive. The biosamples are commonly classed as polar, nonpolar and volatile metabolites. All these classes of metabolites can be found in any *Drosophila* sample. There is no available method to extract all three groups of metabolites simultaneously. In this study, two different quenching methods for the extraction of *Drosophila* were examined. Quenching with buffered 50% methanol-water and buffered chloroform-methanol-water (1:3:1) (sections 2.1.1 and 2.1.2) used applied in order to obtain the maximum number of identified metabolites within a broad range of metabolite classes. The differences between the two quenching methods with regard to metabolite recovery from *Drosophila* will be discussed in the following section.

3.1.1 Sample extraction evaluation

In order to evaluate the new extraction method of buffered chloroform/methanol/water, called the MCW method, in comparison to the buffered methanol/water method, called the MW method, the metabolic profiles of MW were compared to the metabolic profiles obtained by the MCW method. The relative standard deviation of metabolite levels and their ratios of their peak areas can be applied in the comparison between the two methods, and p-values are used to highlight any significant changes in the putatively identified metabolites. The results of the comparison of the MW and MCW extraction methods for selected metabolites are summarized in Table 3.1. Additionally, soft independent modelling by class analogy (SIMCA) was used to assess and cluster obtained data from LC-MS for the two quenching methods. The red circles represent the buffered MCW solution and the green circles represent the buffered MW solution (figure 3.4). It is evident that solvent extraction method can produce a separation of samples on the basis of selective extraction.

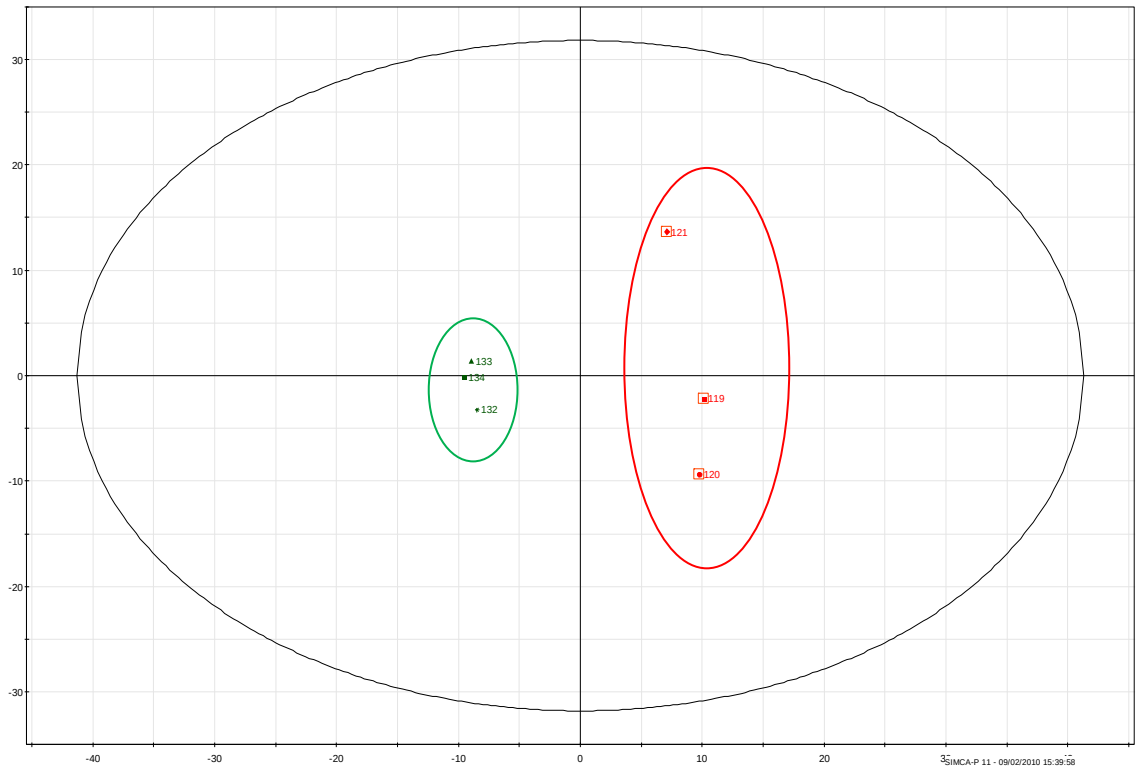

Figure 3-1 Comparison of two different extraction solvents for metabolic profiling in *Drosophila*, Red: MCW and Green: MW.

As shown in the plot, the distance between the samples in the buffered MCW solution is larger than that in the buffered MW solution, which reflects the reproducibility of quenching methods. This means the addition of chloroform to the extraction method resulted in lower reproducibility. Total ion current (TIC) and mass spectra profiles (whole mass range from 50–850) of metabolites for both extractions in positive mode are shown in figure 3.5. The TICs and electrospray mass profiles are slightly different for MCW versus MW. Here, it can be seen that the biggest differences are coloured red, thereby confirming that the MCW method adds metabolites with greater chemical diversity to the list of identified metabolites that were previously obtained by MW (more details in Section 3.15). Figure 3.6 also underlines this point where more ions are present in the MCW extraction.

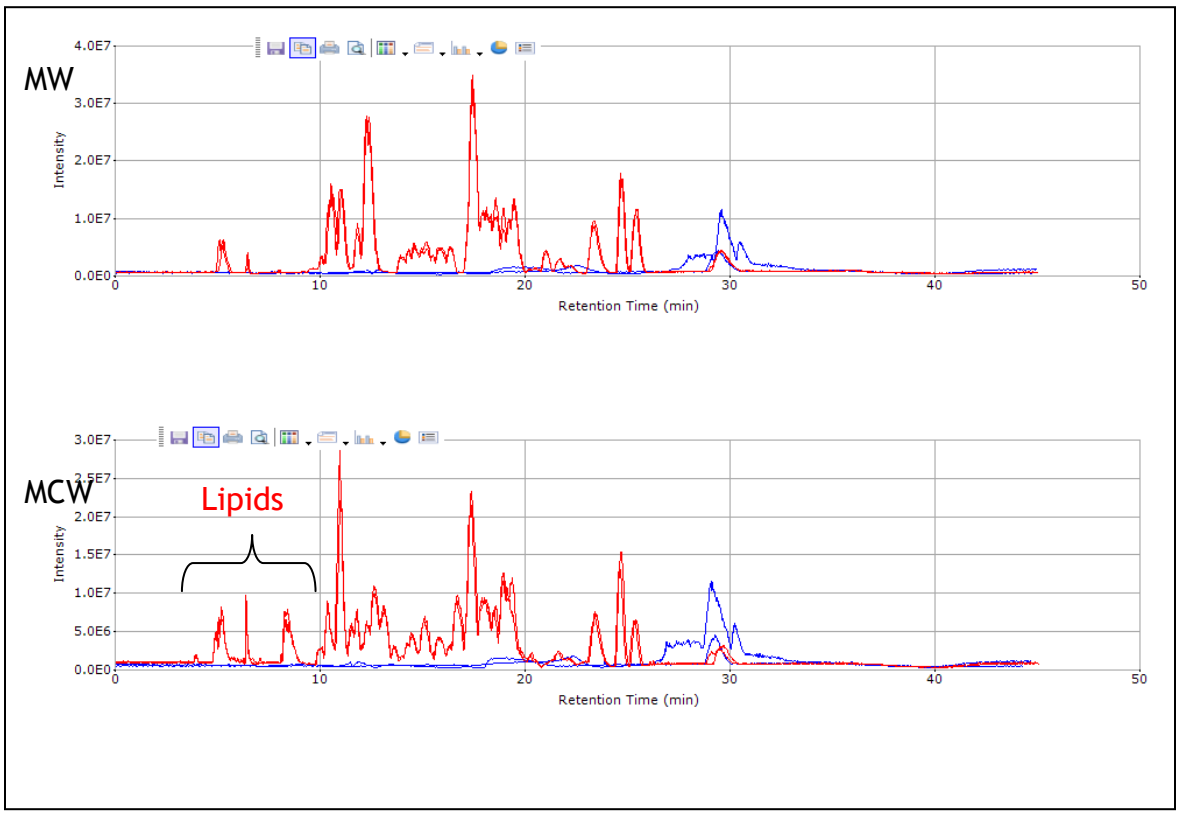

Figure 3-2 Upper panel shows TIC (conditions as in 2.12.1) for *Drosophila* extracted by MW coloured red against blank (no *Drosophila* present) coloured blue while lower panel shows TIC *Drosophila* extracted by MCW coloured red against blank (no *Drosophila* present) coloured blue.

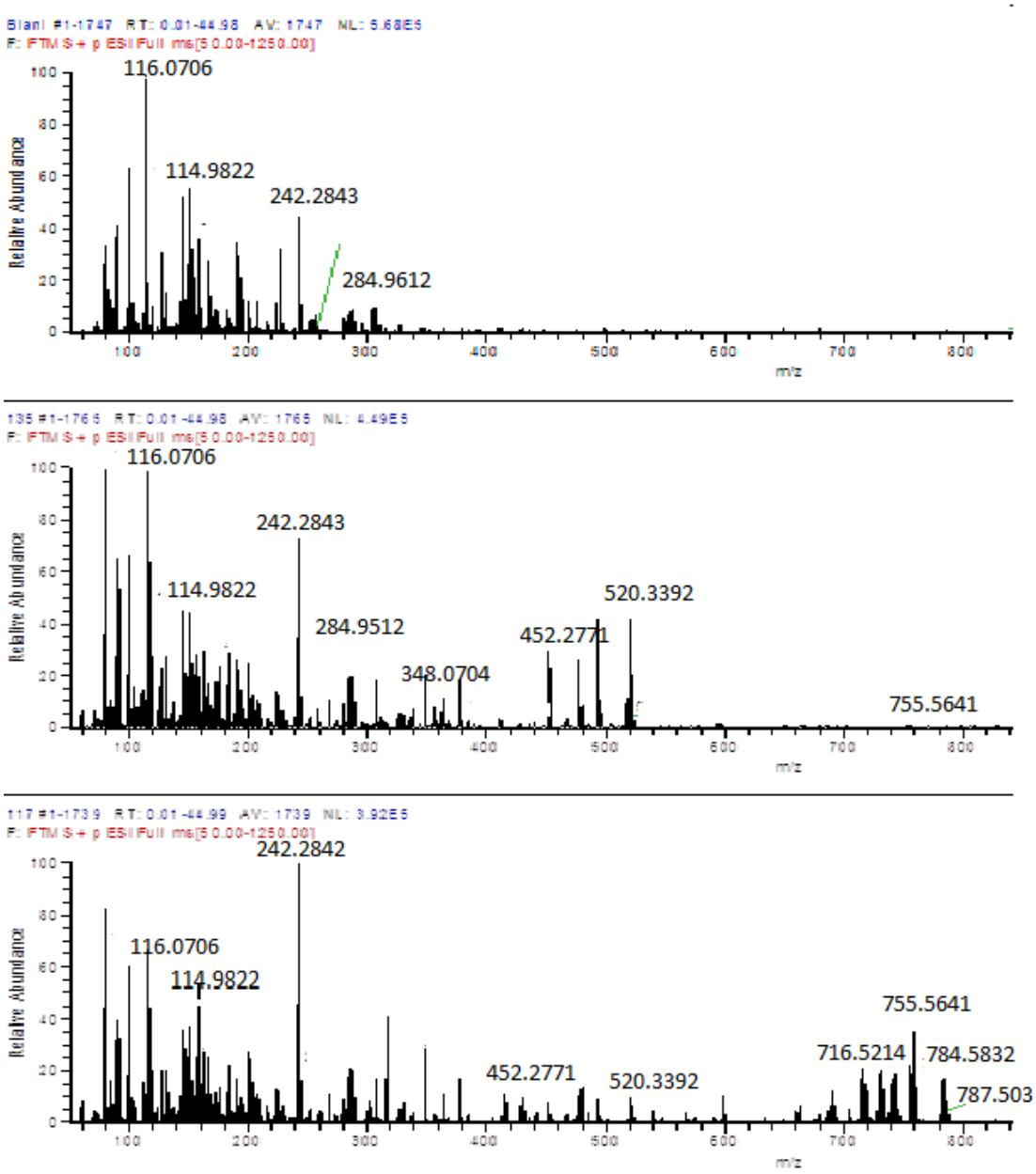

Figure 3-3 Electrospray mass spectra of metabolites (whole m/z range,75-850/whole time range) of : (upper panel) blank (no fly present); (central panel) *Drosophila* extracted by MW; (lower panel) Drosophila extracted by MCW.

Importantly, any quenching method has to extract as many metabolites as possible and must provide the best outcomes according to the total number of metabolites detected and their reproducibility. The MCW method had the highest number of metabolites with

ca 250 different metabolites, excluding lipids, but with a higher variability based on their relative standard error when compared with the MW method. On the other hand, the MW method has a lower number of identified metabolites, which was 198 different metabolites but it had the lowest variability. The observed difference in metabolic profiles between the two methods was due to the presence of chloroform resulting in the extraction of a broader range of compounds including more lipophilic compounds. The distribution of the 230 putatively identified compounds that were detected in the two extraction procedures according to their intensity ratio is shown in Figure 3-7. Around 33% of all identified compounds between 0.8–1.2 did not seem to vary a lot between MCW and MW. About 36% of the metabolites showed higher intensity levels in samples extracted with MCW compared to those extracted with MW. Whereas nearly 30% of all the metabolites demonstrated an increase in intensity with MW extraction compared to MCW extraction. Table 3.1 shows some of the metabolites extracted by using the two different methods.

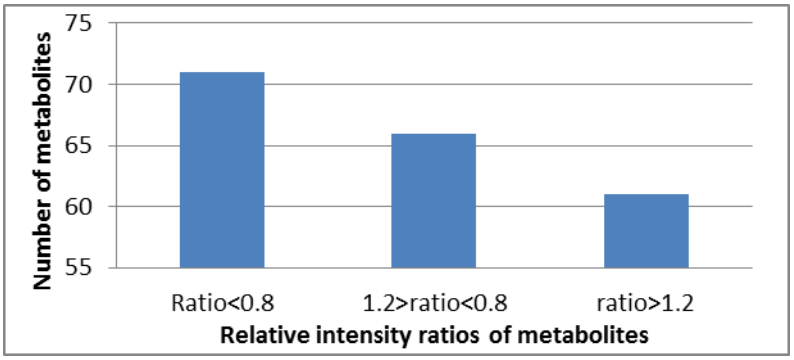

Figure 3-4 Distribution of 230 different detectable metabolites related to their intensity ratios using the two extraction procedures where ratio is MW/MCW.

Table 3.1 Variation in metabolite profiles MW versus MCW (MW/MCW) mean of n=3 for each method.

Metabolites	%RSD MCW	%RSD MW	ratio
Lipids			
Sphinganine	5.24	--	0.00
Dodecanedioic acid	6.50	--	0.00
Dehydrosphinganine(Sphingosine)	11.51	--	0.00
PE(18:0/14:1(9Z))	22.48	--	0.00
PE(16:1(9Z)/16:1(9Z))	3.94	--	0.00
Butoctamide semisuccinate	6.50	--	0.00

Dodecanamide	12.94	34.51	0.01
GPEtn(16:0/18:2(9Z,12Z))	4.92	20.42	0.02
Oleamide	13.19	94.25	0.06
palmitamide	14.23	74.07	0.09
palmitoleamide	14.28	73.64	0.09
Linolylcarnitine	9.05	21.58	0.11
1-Decanol	14.91	26.43	0.12
Myristamide	14.74	72.68	0.14
L-Palmitoylcarnitine	16.16	22.46	0.16
Linolenylcarnitine	12.64	5.81	0.17
C19 sphinganine	5.89	93.83	0.24
O-Acetylcarnitine	9.65	4.69	0.59
Amino acids			
O-Acetyl-L-homoserine	11.06	8.96	3.96
L-Aspartate	24.72	12.44	0.69
L-Lysine	88.67	6.73	0.74
methylxanthine	12.18	35.47	0.74
Alanine	22.23	1.33	1.22
GABA	17.70	3.53	1.22
O-Acetyl-L-serine	20.72	11.93	1.23
L-Arginine	35.23	7.14	1.24
Choline	7.04	3.01	1.26
valine	0.53	4.01	1.29

Purines and Pterins			
Inosine	19.68	9.20	1.33
drosopterin	17.32	6.16	1.64
Biopterin	31.52	9.43	1.67
Butyrylcarnitine	16.07	14.21	1.71
Urate	12.66	2.21	1.72
Dihydroxanthopterin	22.11	6.18	1.73
pterin	21.91	6.36	1.81
Dihydrobiopterin	13.23	5.46	1.87
dehydrosepiapterin	21.63	21.76	1.95
Isoxanthopterin	21.99	20.96	2.18
sepiapterin	25.41	10.37	2.35
Xanthurenic acid	18.37	10.99	2.49
Hypoxanthine	25.73	15.58	3.97
IMP	26.54	14.87	4.00
Adenosine	3.06	23.57	0.66
Adenine	2.45	22.21	0.67
Niacin/Nicotinate	16.71	6.87	0.67
uridine monophosphate	16.21	21.82	0.69
Acetylarginine	19.01	8.10	0.71
AMP	21.69	19.80	0.73

In this study, the amounts of most amino acids extracted were similar, except for aspartate (Asp), serine N-formate and O-Acetyl-L-homoserine (AcSer) (0.6, 1.4 and 3.9

fold, respectively), when MW is compared to the MCW method. The nucleotide pool levels were increased in MCW, except IMP, which has a higher level in the MW method. Additionally, the majority of phosphorylated, organic acid and lipid compounds were abundant in MCW quenched samples. In summary, non-polar and mid-polar compounds had higher intensity levels in the MCW quenched samples. On the other hand, polar compounds showed lower levels after MCW quenching. Although MCW extraction had the highest average standard error of 15% RSD, it provided the best coverage for metabolites, particularly for phospholipid compounds. A lot of these were detected in higher intensities in MCW extracted samples and phosphatidylcholine, phosphatidylethanolamine, glycerolipids and fatty acids were only present in the MCW quenched method. The MCW method was shown to work very efficiently and gave satisfying outcomes for several classes of phospholipid compounds (more data in Section 3.3). Two different extraction strategies were examined in terms of reproducibility, number of metabolites and metabolite yield in order to enhance extraction efficiency. Considering all these evaluation criteria, we can conclude that the extraction method by MCW was preferable for global metabolomics studies in *Drosophila*. On the other hand, our results show that the MW extraction method could be suitable in target analysis for specific compounds such as xanthine, inosine and urate. This study laid the groundwork for further investigations in the metabonomics field with *Drosophila melanogaster* as a model organism.

3.1.2 Stability and storage of extracts

An assessment of the stability of Drosophila metabolites in a wide-range metabolic investigation was essential for accurate and valid studies when comparing mutant strains to WT strains. The goal of this study was to assess the impact of sample storage on the results obtained. In order to assess the effect of sample storage on the metabolite concentration, two batches were put through the same extraction method and run conditions but were stored for 1 and 8 weeks prior to analysis. Figure 3.8 shows the

comparison of the two batches after different times of storage. Strikingly, the intensity levels of amino acids are higher in the group stored for 8 weeks. This may be because deep freezing for an 8-week period decreases peptide levels. In this case, glutathione disulfide (GSSG) contains two molecules of glutathione (GSH) that can be linked by disulfide bonds. GSH is a tripeptide (three amino acids together) γ-glutamylcysteinylglycine. The levels of GSH and GSSG fell after 8 weeks while the levels of glycine, glutamate and cysteine increased possibly due to peptide degradation (many compounds do not change much with storage and a table of these is shown in appendix III). This may provide evidence of the influence of storage in metabolome analysis, and we can conclude that the extractions of mutant samples and the controls must be stored for the same period and analysed under the same conditions. Variability between samples should be avoided whenever possible to minimize the chemical changes that affect the reproducibility of the metabolomics methodology.

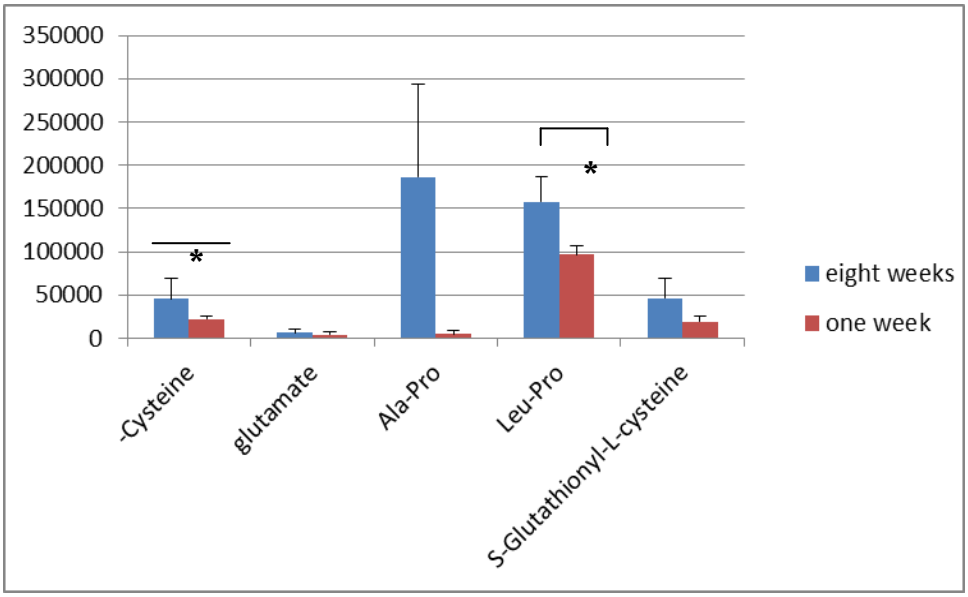

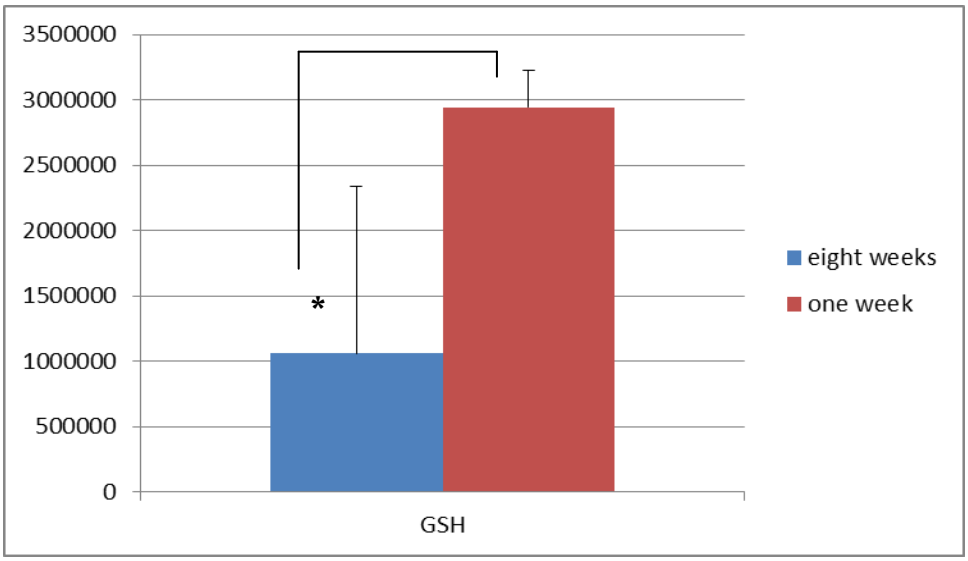

Figure 3-5 Levels of GSH and glutamate following storage at -80°C for 1 and 8 week periods. Data are shown as mean ±SEM for N=3 independent experiments. Data that differ significantly are marked with asterisks are analyzed by Student's *t*-test two tailed.

3.1.3 Chromatographic evaluation of HILIC columns for separation of metabolites

A critical group of metabolites for analysis is that of nucleotide derivatives such as ATP, which serve as building blocks for cells and organisms. This group of metabolites generates energy and is involved in a variety of cellular functions including transport and mechanical and signalling work. The ZIC-HILIC column based on Silica, in combination with 0.1% formic acid/acetonitrile and 0.1% formic acid/water as mobile phase, is not able to catch or separate all nucleotide derivatives, particularly di- and tri-phosphate conjugates and this is probably due their ion suppression by strong ion-pairing with traces of inorganic ions such as sodium and potassium in the mobile phase. Recently, Tomas and co-workers have reported that ZICpHILIC can offer acceptable peak shape for these compounds (Chester, 2012). This column is based on the hydrophilic interaction (HILIC) system and contains a zwitterionic layer similar to the ZIC-HILIC column; however, since it is based on a polymeric coating matrix it is stable at higher pH values. Thus ZICpHILIC can be eluted with at a high pH and this allows the use of ammonium carbonate buffer pH 9.2, the high ammonium ion content in this phase ensures that strong ion pairs do not form with traces of inorganic ions in the system thus allowing the analytes that are extremely polar to be detected at higher pH values due to suppression of inorganic ion pairing. Fundamentally, as mentioned in the previous chapter, the HILIC separation mechanism can be normal-phase/adsorption interaction, partitioning between mobile phase and water layer formed on the stationary phase, hydrogen bonding and electrostatic interaction depending on the column used and separation conditions such as type and amount of buffer and amount of water in the mobile phase. Figure 3.9 (upper pane) shows the extracted ion chromatograms for AMP, ADP and ATP extracted from Drosophila samples that give acceptable peak shapes by using the ZICpHILIC column. Figure 3.9 (lower pane) shows the peaks obtained for AMP, ADP and ATP on a ZICHILIC column. Only AMP gives a satisfactory peak on the ZICHILIC column with 0.1% v/v formic acid as the modifier.This is probably as a result of strong ion pair formation with inorganic ions under low pH conditions where

the hydrogen ion is a relatively weak counter ion. In addition extraction of ATP from Drosophila may be a problem because the harsh grinding conditions required to dirupt the cuticle causing ATP to breakdown into AMP due to the lack of rapid quenching. In our experience is generally easier to obtain high levels of ATP from soft tissues such as cell cultures.

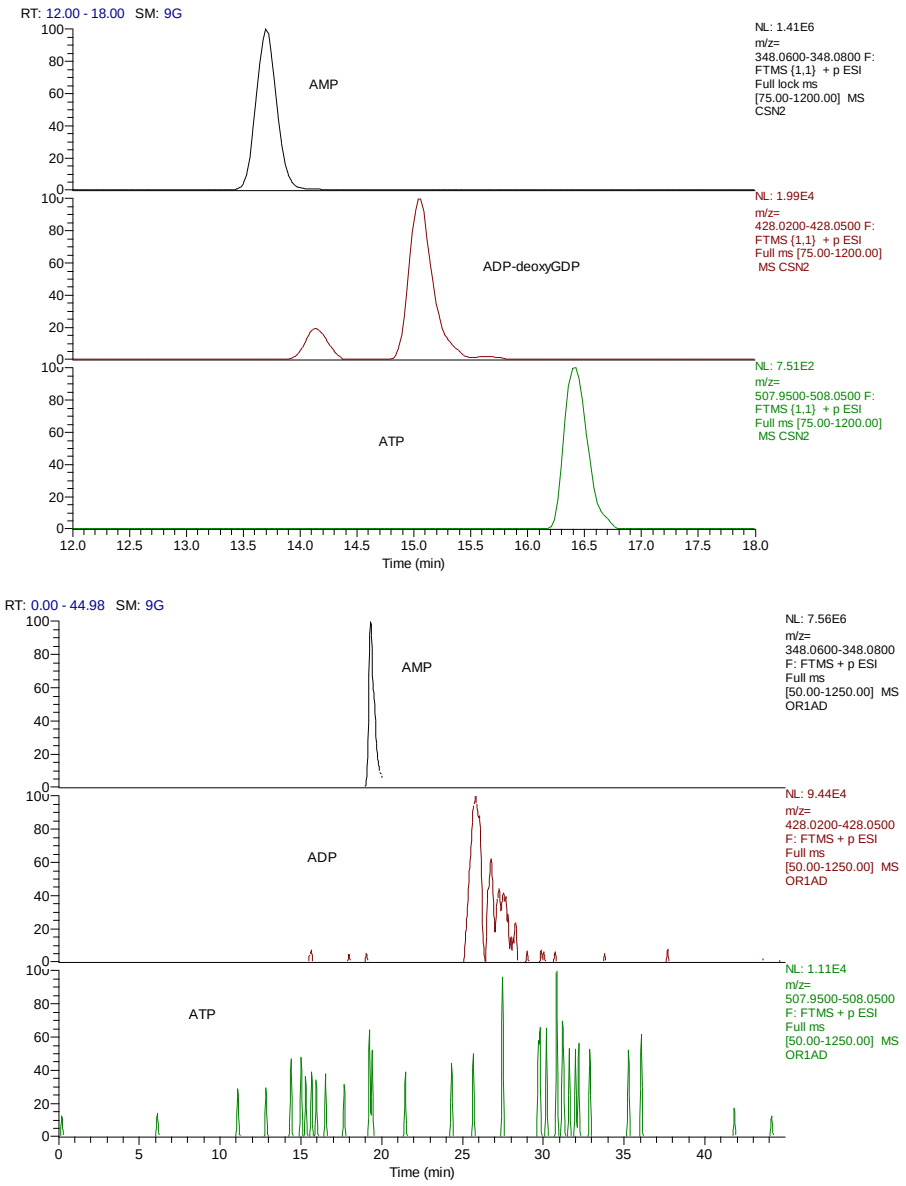

Figure 3-6 Extracted ion chromatographs of AMP, ADP and ATP on ZICpHILIC (upper panel) and on ZICHILIC (lower panel) extracted from *Drosophila*.

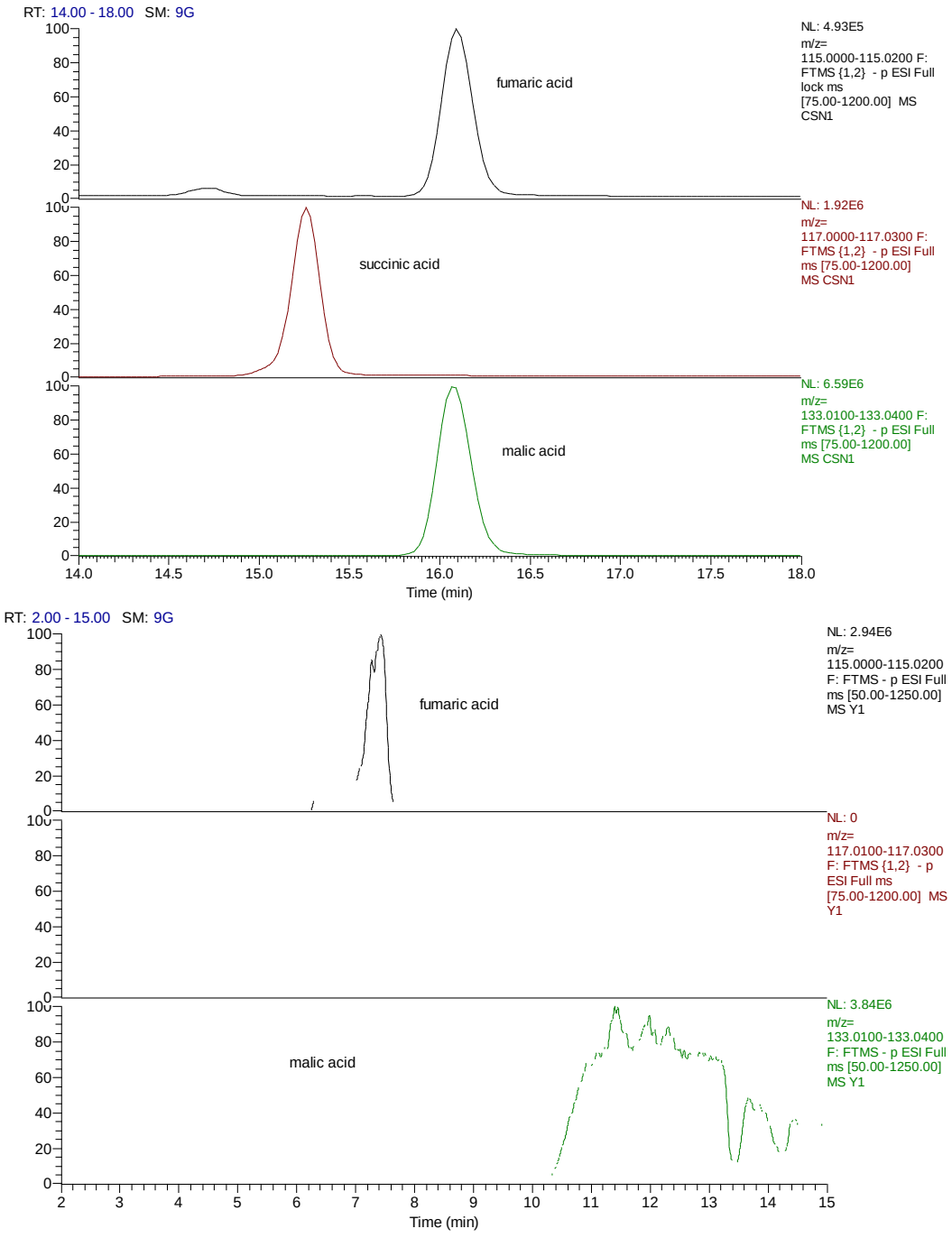

Figure 3-7 Extracted ion chromatograms for fumaric, succinic and malic acids on ZICpHILIC (upper panel) and ZICHILIC (lower panel).

On the other hand, the performance of both columns is similar for amino acids and amino acid derivatives because they are neutral. Although a similar conclusion has been recently published (Johnsen et al., 2011, Zhang et al., 2012),it can be conclude that the basic mobile phase leads to poor performance for basic metabolites under the ZIC-pHILIC column whereas the acidic mobile phase leads to poor separation of acidic metabolites and an inability to separate compounds containing di- and tri-phosphate groups. Figure 3.10 shows the separation of some acids on ZICpHILIC and HILIC. The acids chromatograph much better on ZICpHILIC, fumarate is almost acceptable on ZIC-HILIC but more polar acids such as malic acid give very poor peak shapes.

3.2 Metabolite Coverage

The MCW quenching method was chosen to extract three general classes of metabolites, polar, medium polar and non-polar metabolites, from *Drosophila* samples. This method can be used for profiling analytes of interest, such as amino and non-amino organic acids, sugar phosphates and sugar alcohols, carbohydrate, peptides, nucleotides, vitamins and four classes of phospholipids. Although similar lists have been observed using normal phase columns, the lipid content in Drosophila has not been comprehensively investigated. Thus, this work offers a more comprehensive profile of metabolite content than that in work that has been previously published (Kamleh et al., 2009c, Hammad et al., 2011). Furthermore, a metabolite identification step was accomplished using a validated method based on available standards. A table of standards is shown in appendix I, the retention time of the standards on ZICHILIC decreases by *ca* 1.5 min over three months of usage due to gradual loss of stationary phase. Thus reported retention times in individual experiments may not be exactly the same as those in appendix 1. A newly developed method based on HILIC on silica gel was also used to detect and characterize phosphatidylcholines, lysophosphatidylcholines, phosphatidylethanolamines, lysophosphatidylethanolamines, phosphoinositols, lysophosphoinositols and triglycerides. Apart from metabolite retention time, accurate mass and correlation between MS/MS fragmentation pattern and metabolite structure,

can be used to confirm the identity of putatively identified metabolites. The elution of polar metabolites using the ZIC-HILIC column can be divided into five regions according to their physicochemical properties, as seen in Figure 3-11. Area 1 starts at 5 min, finishes at 12 min and consists of the following chemical groups: lipids, acids and neutral compounds. Area 2 starts at about 9 min, finishes around 15 min and includes sugars and sugar alcohols. Area 3 starts at 12 min and finishes at 19 min for di-peptides and quaternary amines. Area 4 starts at 16 min and finishes at 22 min for phosphate compounds. Compounds with two amine groups occur in area 5, which starts at 21 min and finishes at 28 min. Exploring the best method for separating the wide range of chemical groups requires optimal chromatographic conditions as mentioned in Section 2.14. In terms of HILIC, the critical solvent combination required for the mobile phase system is important in enhancing the molecular ionization in the electrospray ion source of the mass spectrometer and producing enough variation in solvent strength to distribute metabolite elution in different areas according to hydrophilicity and polarity. An increase of the water phase in the eluent leads to decreased retention. Indeed, different mechanisms for metabolite retention in the ZIC-HILIC column may be attributed to partitioning, adsorption and even ion exchange, based on the nature of analytes and the solvent composition. Therefore, the prediction of the behaviour of metabolites regarding their retention is recently possible according to the quantitative structure retention relationship (QSRP) model (Creek et al., 2011, Zhang et al., 2012). Using the QSRP model can be helpful in metabolite identification of compounds that are not commercially available since a prediction of retention time can be made.

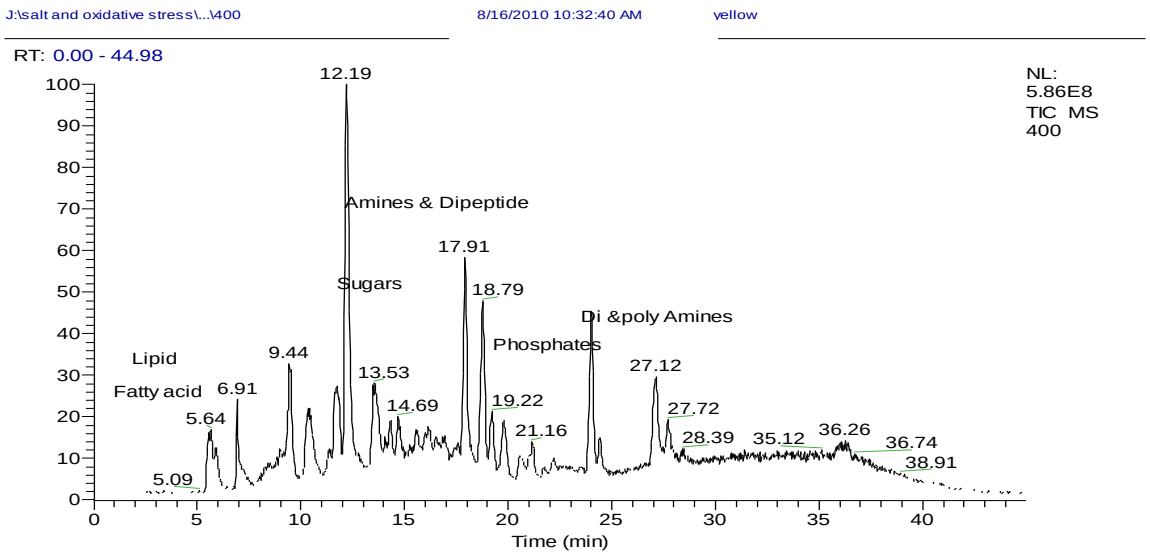

Figure 3-8 TIC for metabolites extracted from adult Drosophila run in positive mode. The sample was analysed by ZIC –HILIC column as in section 2.12.1.

HILIC mode carried out using a silica column allows the elution of phospholipids to be divided into four areas based on diversity of head groups that are linked to phosphate group at the *sn-3* position (figure 3-12). Phosphatidylcholines and their lyso derivatives are retained on the silica gel column, between 19 min and 22 min. They are retained for a relatively long time because they have a choline group with quaternary amine functionality, which interacts strongly with the silanol groups of the stationary phase. Area 2 represents phosphatidylethanolamines and their lyso derivatives, which start at 10 min and finish at 14 min. This area represents a mobile phase combination of 30% aqueous phase and 70% organic phase that produces enough strength to elute these groups due to their head group being less ionised than the choline group in PCs. Thus, the separation of phosphatidylethanolamines in this area seems to be a result of the partitioning mechanism, as the elution of phospholipids is according to the decrease in lipophilicity of the compounds, as seen in the figure. Phosphoinositols and lysophosphoinositols are ionized in the negative mode and start at 3 min and finish at 6 min. They are negatively charged due to the presence of a phosphate group alone without any basic centre. The elution of phosphoinositols in Area 3 has a shorter

retention time compared to the elution of phosphatidylethanolamines and phosphatidylcholines because their only mode of interation with the stationary phase is via hydrophilicity since there is no possibility of the cation exchange interactions which occur with the basic centres in PC and PE lipids. In addition to phospholipids, acylglycerols that are mono, di and tri-subsituted with fatty acids are present in *Drosophila* samples and can be detected by using the silica column as positively charged ammoniated product ions at 3 min. These classes elute around the column void volume and are detected in positive ionisation mode.

The goal of this part of the study was to create a *Drosophila* metabolite list prior to applications of the methods to fly mutations. This data can be used for the identification of unknown metabolites that come from different *Drosophila* mutants by mass spectral matching. This generated list should depend on sample extraction and the measurement procedure used. The methodology should also be able to discriminate between isomeric metabolites as far as possible. Table 3.2 shows a list of putatively identified, mainly non-lipid, metabolites present in Drosophila. Putative identification was according to accurate mass, generally sub 2ppm, matched against the database as described in section 3.1. It is not completely possible to rule out isomers unless chromatographic resolution of the isomers is proved but in general one of two isomers of a particular elemental formula are more common in nature. Also some of the minor components may arise as fragments of more abundant metabolites. Table 3.3 shows a list of lipid metabololites putatively identified in *Drosophila*.

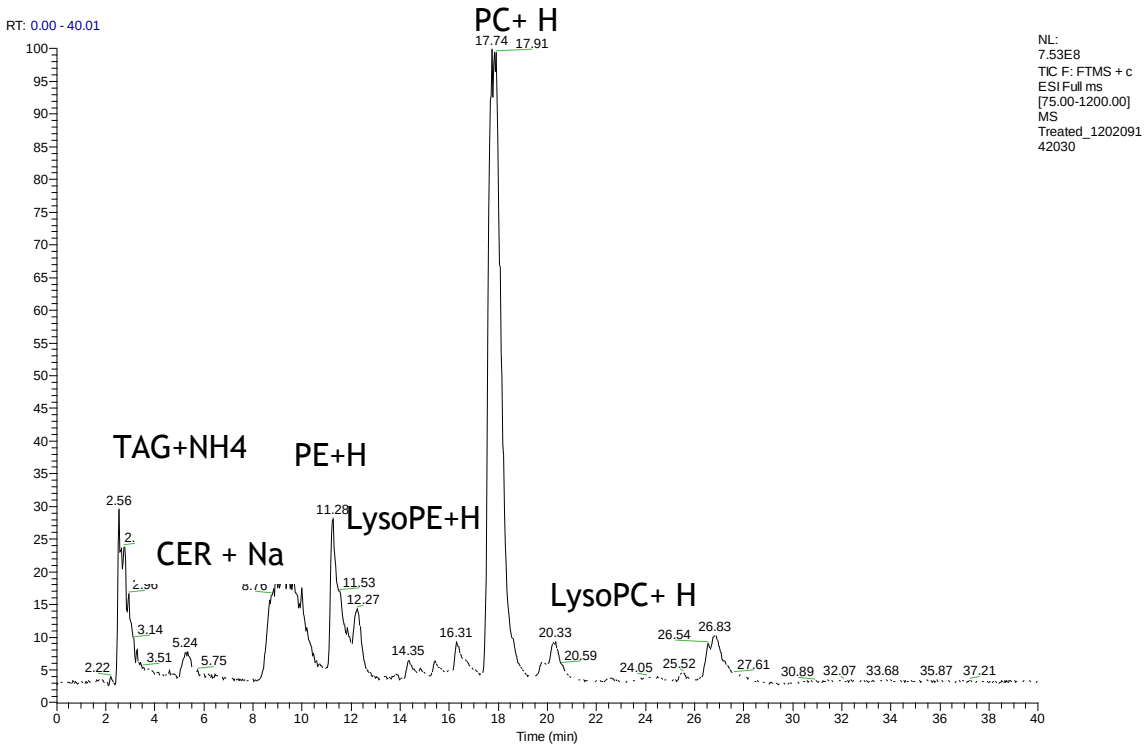

Figure 3-9 TIC for lipids extracted from adult *Drosophila* run in positive mode. The sample was analysed on a silica column as described in section 2.12.3.

Table 3.2 Complete list of metabolites putatively identified in adult *Drosophila* between 70 amu and 700 amu using ZICHILIC chromatography as described in section 2.12.1.

Compounds	MZ	RT	Compounds	MZ	RT
Positive mode					
Iminoglycine	74.02365	19.5	Dihydroxyfluorene-9-one	215.0696	18.7
Glycine	76.03931	19.9	phosphoethanolamine	216.0633	19.4
butanedione	87.04408	16.3	gamma-Glutamyl-gamma-aminobutyraldehyde	217.1185	8.3
butanedione	87.04409	18.8	Acetylarginine	217.1295	18.6
Butanoic acid	89.05979	8.3	Propionyl carnitine	218.1388	14.4
Alanine	90.05495	19.9	Pantothenate	220.1177	8.2
Alanine	90.05498	18.8	5-Hydroxy-L-tryptophan	221.0921	14.6
GABA	104.0706	18.8	Pyrimidodiazopterin	222.0985	12.1
Choline	104.107	19.4	L-Cystathionine	223.0747	23.3
L-Serine	106.0499	19.9	7,8-Dihydro-7,8-dihydroxykynurenate	224.0554	
Diethanolamine	106.0863	20.9	3-Hydroxy-L-kynurenine	225.087	16.2
Ethylbenzene	107.0856	5.2	Methyl jasmonate	225.1487	5.3
p-Benzoquinone	109.0284	19.1	Myristamide	228.2322	5.4
Cytosine	112.0506	20.2	Leu-Pro	229.1547	16.6
Histamine	112.087	29.1	Leu-Pro	229.1547	15.2
Hydroxymethylphosphonate	112.9999	17.4	Leu-Pro	229.1548	14.1
Uracil	113.0346	11.6	Dodecyldimethylamine oxide	230.2479	11.6
cis-1,2-Dihydrobenzene-1,2-diol	113.0598	8.2	Butyrylcarnitine	232.1544	13.7
L-Proline	116.0704	17.8	1,1,3-tris(ethoxymethyl)urea	235.1653	18.0
Indole	118.0652	14.7	dehydrosepiapterin	236.0777	10.8
valine	118.0862	18.0	N-Formylkynurenine	237.087	14.9
glycine betaine	118.0863	16.6	Biopterin1	238.0936	14.3
L-Threonine	120.0655	18.9	Biopterin2	238.0936	11.2
Indoline	120.0808	14.4	Dihydrobiopterin	240.1091	15.2
L-Cysteine	122.0271	17.1	Pirbuterol	241.1547	16.7
Phenethylamine	122.0966	14.9	Inositol cyclic phosphate	243.0265	19.1
Niacin/Nicotinate	124.0394	8.3	Inositol cyclic phosphate	243.0265	20.3
Taurine	126.0218	18.3	Cytidine	244.0929	20.3
1,2,3-Trihydroxybenzene	127.039	20.3	Uridine	245.0769	11.6
2,3,4,5-Tetrahydropyridine-2-	128.0708	6.5	Ethyl-Acetyl-Arginine	245.1609	16.4

carboxylate					
Pyrroline-4-hydroxy-2-carboxylate	130.0499	18.5	N,N-bis(butoxymethyl)-2-methylpropan-2-amine	246.2429	12.6
Pyrroline-4-hydroxy-2-carboxylate	130.05	19.5	palmitollinoleide	252.2323	12.5
methylproline3	130.0863	25.4	palmitoleamide	254.2481	5.3
guanidino butanal	130.0974	17.5	phosphoarginine	255.0854	23.7
beta-Ketoisocaproate	131.0703	8.2	glycyl-dopa	255.0977	19.9
Glutamate 5-semialdehyde	132.0656	18.4	palmitamide	256.2632	5.3
L-Leucine	132.1018	14.9	GPC	258.1098	21.3
isoLeucine	132.1019	16.0	D-Glucosamine 6-phosphate	260.0531	19.2
2-(Hydroxymethyl)-4-oxobutanoate	133.0495		Glucose phosphate	261.0371	19.2
L-Asparagine	133.0608	19.9	Fructose phosphate	261.0371	20.3
L-Aspartate	134.0448	19.1	Glutamyl-leucine	261.1445	14.3
L-Aspartate	134.0449	5.5	Tyrosine phosphate	262.0475	20.7
Adenine	136.0618	14.7	thiamine(+) 2	265.1116	28.2
Hypoxanthine	137.0458	11.8	Adenosine	268.104	14.6
Hypoxanthine	137.0459	17.8	Deoxyguanosine	268.1041	13.6
Phenylacetic acid	137.0597	8.0	Inosine	269.0881	12.8
4-Aminobenzoate	138.055	17.7	narigenin	273.0752	18.5
Urocanate	139.0503	16.0	Glu-gln	276.1189	19.3
Ethanolamine phosphate	142.0264	21.3	Stearidonic acid	277.2161	5.1
Proline Betaine	144.1019	16.6	C10H11O5N4	278.0636	20.3
Octanoic acid	145.1224	6.0	alpha-Ribazole	279.1338	15.7
Amino-3-oxohexanoic acid	146.0812	25.5	(9Z,12Z,15Z)-Octadecatrienoic acid	279.2322	5.0
guanidino butyric acid	146.0923	17.2	Methyl adenosine	282.1198	18.9
acetylcholine 1+	146.1176	17.3	Oleamide	282.2794	5.3
acetylcholine 1+	146.1177	16.3	Guanosine1	284.099	14.9
Glutamine	147.0764	19.5	Guanosine2	284.099	15.9
L-Lysine	147.1129	25.4	C13H12N4O4	288.0843	17.9
glutamate	148.0604	18.6	C17 sphinganine	288.2897	11.8
N-Acetyl-L-serine	148.0606	5.4	N-(L-Arginino)succinate	291.13	
(R)-Pantoate	149.0806	19.5	17-Hydroxylinolenic acid	295.2271	5.0
Indole-5,6-quinone	150.055	14.6	5'-Methylthioadenosine	298.0967	11.9
L-Methionine	150.0583	15.8	Dehydrosphinganine(Sphingosine)	300.2893	11.9
Methyladenine	150.0774	17.7	Sphinganine	302.3046	
Methylhypoxanthine	151.0617	15.8	Phytosphingolipid	304.2846	11.8
Guanine	152.0567	13.3	GSH	308.0908	17.5
(Z)-4-Hydroxyphenylacetaldehyde-oxime	152.0706	16.2	Fructosyllysine	309.1657	25.4
Xanthine	153.0407	11.2	2-aminodimethyladenosine	311.1465	24.9

N-acetylhistamine	154.0974	18.2	Butoctamide semisuccinate	316.2113	13.0
L-Histidine	156.0766	24.7	Butoctamide semisuccinate	316.2119	14.0
2-Aminomuconate	158.0448	9.7	C19 sphinganine	316.3209	11.6
Guanidine proline+	158.0925	16.5	cytidine monophosphate	324.0593	21.0
(S)(+)-Allantoin	159.0513	15.3	uridine monophosphate	325.0434	17.1
2-amino octanoic acid 1	160.1332	16.6	Difructose anhydride isomer	325.113	17.7
2-amino octanoic acid 2	160.1332	12.8	Difructose anhydride isomer	325.1131	19.2
indole carboxylic acid1	162.055	10.0	c AMP	330.0602	16.3
O-Acetyl-L-homoserine	162.0762	15.9	Nicotinamide D-ribonucleotide	335.0638	20.0
Carnitine	162.1123	18.4	2'-Deoxyinosine 5'-phosphate	335.0738	19.1
Dihydroxy-5-(methylthio)pent-1-en-3-one	163.0423	9.2	Dihydroneopterin phosphate	336.0695	19.9
3,3-Dimethylmalate	163.0601	18.3	Histidine lipid	336.2282	12.5
pterin	164.0566	13.1	S-(Hydroxymethyl)glutathione	338.1016	18.1
5-Pyridoxolactone	166.0499		Hisitidine lipid	338.2437	12.4
L-Methionine S-oxide	166.0532	19.4	Dodecamide	338.3414	5.2
L-Phenylalanine	166.0863	14.4	Sucrose	343.1234	18.3
Urate	169.0356	14.3	cGMP	346.0547	16.2
1-Methylhistidine	170.0925	24.9	AMP isomer 2	348.0703	20.1
Glycerolphosphate	173.0209	18.0	AMP isomer 2	348.0703	19.1
Quinaldic acid	174.0551	14.6	IMP	349.0544	17.9
L-Arginine	175.1187	25.5	sugar adduct	360.1501	18.3
N-Formyl-L-glutamate	176.0554	9.8	Histidine adduct	362.2434	12.3
Spermidic acid	176.0918	15.9	GMP	364.0654	19.7
L-Citrulline	176.1029	20.2	Histidine adduct	364.2586	12.1
D-Glucono-1,5-lactone	179.0549		drosopterin	369.1531	20.4
Isoxanthopterin	180.0517	13.2	Riboflavin	377.1455	10.4
D-Galactosamine	180.0867	20.4	Succinyladenosine	384.1151	11.9
Dihydroxanthopterin	182.0673	13.3	Ergosta-5,7,22,24(28)-tetraen-3beta-ol	395.3311	5.7
L-Tyrosine	182.0811	16.6	L-Palmitoylcarnitine	400.3422	11.6
Choline phosphate+	184.0734	24.3	Xanthomatin	424.0776	14.6
Ala-Pro	187.1078	19.1	Linolenylcarnitine	424.342	11.6
N-acetylspermidine	188.1758	28.2	Linolylcarnitine	426.3575	11.6
N6-Acetyl-L-lysine	189.1233	15.6	S-Glutathionyl-L-cysteine	427.0951	22.7
7,8-Diaminononanoate	189.1597	25.9	ADP	428.0368	24.4
Kynurenic acid	190.0499	8.7	Oleoylcarnitine	428.3733	11.5
N-Acetyl-L-glutamate	190.0711	8.8	CDP-ethanolamine	447.0678	22.0
meso-2,6-Diaminoheptanedioate	191.1027	19.2	N6-(1,2-Dicarboxyethyl)-AMP	464.0813	17.1
5-Hydroxyindoleacetate	192.0656	14.7	DHAP(18:0)	478.2923	10.9
Dopamine acetate	196.0968	6.8,7.	Raffinose	505.1765	18.3

		8			
DOPA	198.0761	18.9	UDP-N-acetyl-D-glucosamine	608.0888	21.0
Dodecanamide	200.201	5.4	NAD+	664.1163	20.6
Dodecanamide	200.201	12.9	Stachyose	667.229	18.3
O-Acetylcarnitine	204.1227	15.4	Cellopentaose	829.2809	20.4
L-Tryptophan	205.0973	15.1	Val Ser	205.1183	19.0
Xanthurenic acid	206.0447	10.2	L-Kynurenine	209.0921	14.7
Val Ser	205.1184	24.0	4-Hydroxyphenylacetylglycine	210.0761	17.1
Negative mode					
Butyric acid	87.0452	6.3	Glycerylphosphorylethanolamine	215.0559	8.0
Lactic acid	89.02444	7.8	3-Hydroxyhippuric acid	216.028	19.0
beta lactic acid	89.02446	6.8	Glycerol 3-phosphate	217.012	17.8
Glycolic acid	105.0194	7.3	Homoveratric acid	217.0483	16.0
Fumaric acid	115.0038	7.5	4-Amino-2-methyl-5-phosphomethylpyrimidine	218.0329	16.1
Succinic acid	117.0193	8.1	Pantothenic acid	218.1034	8.1
Hydroxypentanoic acid	117.0558	6.5	2'-Deoxysepiapterin	220.0841	11.0
Erythrose	119.0351	16.7	N-Acetyl-L-phenylalanine	228.0644	23.3
Glutaconic acid	129.0194	12.0	Glycero Phosphoserine	230.0072	19.0
pentanedioic acid	131.0351	6.2	Glycero Phosphothreonine	244.0229	18.6
2-aminobutanedioic acid	132.0303	19.0	Glycerophosphoglycerol	245.0433	16.4
malic acid	133.0143	10.6	2-Ethylhexyl 4-hydroxybenzoate	249.1497	5.1
Deoxyribose	133.0507	8.2	3-Methyluridine	257.0781	7.9
Erythronic acid	135.03	6.8	Epicatechin	271.0607	18.4
Oxoglutaric acid	145.0143	8.5	Acetylvanilalanine	274.07	23.3
Adipic acid	145.0507	6.4	Alpha-CEHC	277.1445	4.7
Citramalic acid	147.0299	9.1	Sedoheptulose 7-phosphate	289.0331	19.2
Mevalonic acid	147.0663	8.2	Gingerol	293.1759	5.3
pentose	149.0457	12.5	Aminoparathion	306.058	11.5
3,4-Dihydroxyphenylacetaldehyde	151.0401	5.4	1-(sn-Glycero-3-phospho)-1D-myo-inositol	333.0593	19.0
D-Xylitol	151.0613	15.1	N-Acetylaspartylglutamic acid	349.0889	9.4
Glycylproline	153.067	6.4	3-Methoxy-4-hydroxyphenylglycol glucuronide	359.0984	8.1
Orotic acid	155.01	12.4	Lactosamine	376.1015	19.6
Tiglylglycine	156.0667	24.8	Sphingosine 1-phosphate	424.247	11.1
Furoic acid	157.0143	9.6	15-Keto-prostaglandin E2	387.1578	8.1
Oxoadipic acid	159.03	11.9	7-Deoxyadriamycinone	397.0932	16.2

(R)-2-Hydroxycaprylic acid	159.1027	5.6	Columbiananin	406.26	5.3
Hydroxyoxoglutaric acid	161.0092	6.4	Leukotriene B4 dimethylamide	408.2753	5.3
Arabinonic acid	165.0406	15.6	(R)-gamma-Tocotrienol	409.3113	5.0
Homovanillin	165.0558	5.8	Hexadecanedioic acid mono-L-carnitine ester	410.2908	5.2
3,4-Dihydroxymandel-aldehyde	167.035	5.7	Demethylphylloquinone	436.3341	4.0
Glyceraldehyde phosphate	168.991	17.8	Doconazole	479.0937	19.0
Glycerol 3-phosphate	171.0064	17.8	Ubiquinone Q4	489.2774	3.7
Aconitic acid	173.0093	10.2	Isovalerylcarnitine	489.3185	13.8
Ascorbic acid	175.0248	9.6	trihexose	503.1619	19.1
3-Keto-b-D-galactose	177.0405	11.9	Oxidized glutathione	611.1436	21.9
hexose	179.0561	16.7	tetrahexose	665.2147	19.6
D-Alanyl-D-alanine	181.0604	16.7	pentahexose	863.2428	20.6
hexitol	181.0718	15.9	3-Isopropenylpimelyl-CoA	948.2021	19.0
Homocysteic acid	182.0129	9.4	Quinic acid	191.0563	13.9
cis-2-Methylaconitate	187.0249	8.4	N-a-Acetylcitrulline	198.0885	18.4
Isocitric acid	191.0198	12.1	Tryptophanol	196.0544	16.4
N-Acetyl-b-glucosaminylamine	201.0881	9.2	2-Methyl-3-hydroxy-5-formylpyridine-4-carboxylate	202.0124	19.8
Gluconic acid	195.051	16.5	Homocitric acid	205.0354	10.4
4-heptoxyphenol	207.1391	5.2			

Table 3.3 List of lipids detected in Drosophila samples by chromatography on silica gel using the method described in section 2.12.3.

Ion	m/z measured	Time	Fragment
Triacylglycerol			
C38 H76 O6 N	642.5689	2.57	
C39 H70 O6 N	648.5201	2.56	
C39 H72 O6 N	650.5364	2.56	
C39 H74 O6 N	652.5521	2.56	472=C29H60o4 309=C20H37O2
C39 H76 O6 N	654.5675	2.57	
C39 H78 O6 N	656.5834	2.559	
C40 H78 O6 N	668.5835	2.559	
C40 H80 O6 N	670.5988	2.56	
C41 H78 O6 N	680.5833	2.53	472=C29H60O4 309=C20H37O2
C41 H80 O6 N	682.5989	2.559	
C41 H84 O6 N	686.6207	2.56	
C42 H76 O6 N	690.5728	2.563	
C42 H82 O6 N	696.6141	2.56	
C42 H84 O6 N	698.6299	2.56	
C42 H86 O6 N	700.6378	2.574	
C43 H80 O6 N	706.5986	2.511	
C43 H82 O6 N	708.614	2.521	465=C29H53O4
C43 H84 O6 N	710.6296	2.56	
C43 H86 O6 N	712.6456	2.574	
C43 H88 O6 N	714.6523	2.574	
C44 H78 O6 N	716.5886	2.521	
C45 H68 O6 N	718.5184	2.836	
C45 H72 O6 N	722.5271	2.61	
C45 H74 O6 N	724.5152	2.574	
C44 H88 O6 N	726.6614	2.574	
C44 H90 O6 N	728.6688	2.574	
C45 H80 O6 N	730.6105	2.828	
C45 H84 O6 N	734.6298	2.521	491=C31H55O4
C45 H86 O6 N	736.6095	2.828	
C45 H88 O6 N	738.6611	2.574	
C45 H90 O6 N	740.676	2.627	
C46 H80 O6 N	742.5997	2.526	
C46 H82 O6 N	744.6202	2.559	

C46 H84 O6 N	746.6182	2.828
C46 H86 O6 N	748.645	2.56
C46 H88 O6 N	750.6607	2.56
C46 H90 O6 N	752.6769	2.574
C46 H92 O6 N	754.6928	2.65
C48 H70 O6 N	756.5278	2.756
C48 H72 O6 N	758.5776	2.517
C48 H74 O6 N	760.5574	2.836
C48 H76 O6 N	762.5721	2.836
C47 H90 O6 N	764.6769	2.574
C47 H92 O6 N	766.6919	2.574
C47 H94 O6 N	768.6989	2.574
C48 H84 O6 N	770.6335	2.559
C48 H86 O6 N	772.6499	2.805
C48 H90 O6 N	776.6763	2.574
C48 H92 O6 N	778.6924	2.574
C48 H94 O6 N	780.708	2.612
C48 H96 O6 N	782.7189	2.65
C50 H74 O6 N	784.5587	2.756
C49 H92 O6 N	790.6926	2.574
C49 H94 O6 N	792.7076	2.574
C49 H96 O6 N	794.7228	2.65
C50 H94 O6 N	804.7077	2.574
C50 H96 O6 N	806.7233	2.612
C51 H92 O6 N	814.6966	2.517
C51 H94 O6 N	816.7073	2.559
C51 H96 O6 N	818.7234	2.574
C51 H98 O6 N	820.7385	2.65
C52 H96 O6 N	830.7221	2.56
C53 H96 O6 N	842.7231	2.559
C53 H98 O6 N	844.7388	2.594
C53 H100 O6 N	846.7546	2.612
C54 H100 O6 N	858.7553	2.627
C54 H102 O6 N	860.7708	2.65
Diacylglycerol		
C26 H50 O5 N	456.3684	2.597
C35 H68 O5 N	582.5105	2.559
C35 H70 O5 N	584.5263	2.559
C37 H62 O5 N	600.4689	2.397
C37 H68 O5 N	606.5098	2.586
C37 H70 O5 N	608.526	2.56

C37 H72 O5 N	610.5412	2.56	
C37 H74 O5 N	612.5573	2.586	
C39 H68 O5 N	630.5093	2.56	
C39 H70 O5 N	632.5252	2.56	
C39 H72 O5 N	634.5412	2.56	
C39 H74 O5 N	636.558	2.56	
C39 H76 O5 N	638.5741	2.56	
Phosphatidylethanolamine			
C31 H63 O8 N P	608.4293	12.501	
C32 H65 O8 N P	622.445	12.583	
C33 H65 O8 N P	634.445	12.36	
C33 H67 O8 N P	636.4606	12.349	
C34 H69 O8 N P	650.4763	12.382	
C35 H67 O8 N P	660.4617	12.246	
C35 H69 O8 N P	662.4769	12.323	
C35 H71 O8 N P	664.4922	12.32	
C36 H71 O8 N P	676.4935	12.246	
C37 H67 O8 N P	684.4584	12.361	
C37 H69 O8 N P	686.4768	12.241	
C37 H71 O8 N P	688.4933	12.169	
C37 H73 O8 N P	690.5085	12.246	
C37 H75 O8 N P	692.5246	12.316	
C37 H77 O8 N P	694.5309	12.32	
C38 H69 O8 N P	698.5136	12.052	
C38 H71 O8 N P	700.528	12.29	
C38 H73 O8 N P	702.5443	12.299	
C38 H75 O8 N P	704.5595	12.399	
C38 H77 O8 N P	706.54	12.299	
C39 H69 O8 N P	710.472	12.247	
C39 H73 O8 N P	714.508	12.084	573=C35H6604Na
C39 H75 O8 N P	716.5231	12.13	575=C35H68O 4Na
C39 H77 O8 N P	718.5391	12.169	577=C35H70O4Na
C39 H79 O8 N P	720.5562	12.328	
C39 H81 O8 N P	722.5499	12.21	
C40 H71 O8 N P	724.5281	11.972	
C40 H73 O8 N P	726.5076	12.053	
C40 H75 O8 N P	728.5232	12.053	587=C37H7204Na
C40 H77 O8 N P	730.5396	12.053	
C40 H79 O8 N P	732.5548	12.13	
C40 H81 O8 N P	734.5604	12.13	

C41 H71 O8 N P	736.4919	11.939	
C41 H73 O8 N P	738.507	11.939	
C41 H75 O8 N P	740.5218	11.991	
C41 H77 O8 N P	742.5378	12.018	601=C37H7004Na
C41 H79 O8 N P	744.5535	12.017	
C41 H81 O8 N P	746.5682	12.103	
C41 H83 O8 N P	748.5768	12.136	
C42 H73 O8 N P	750.5408	12.253	
C42 H75 O8 N P	752.5593	11.931	
C42 H79 O8 N P	756.5552	11.929	
C42 H81 O8 N P	758.5701	12.052	
C42 H83 O8 N P	760.5855	12.053	
C43 H73 O8 N P	762.5051	11.907	
C43 H75 O8 N P	764.5188	11.982	
C43 H77 O8 N P	766.5346	11.982	
C43 H79 O8 N P	768.5536	11.929	
C43 H81 O8 N P	770.5687	11.982	
C43 H83 O8 N P	772.5855	12.017	
C43 H85 O8 N P	774.6015	12.053	
C43 H87 O8 N P	776.6086	12.13	
C45 H87 O8 N P	800.616	12.012	
Lyso phosphatidylethanolamine			
C19 H39 O7 N P	424.2456	13.78	
C19 H41 O7 N P	426.2619	14.014	
C20 H43 O7 N P	440.2774	13.932	
C21 H39 O7 N P	448.2444	14.014	
C21 H43 O7 N P	452.2771	13.681	434=C21H41O6NP,311=C19H35O3
C21 H45 O7 N P	454.2925	13.889	436=C21H43O6NP,313=C19H37O3
C21 H47 O7 N P	456.2986	13.889	
C22 H47 O7 N P	468.3097	13.834	
C23 H41 O7 N P	474.2592	13.932	
C23 H43 O7 N P	476.2777	13.624	
C23 H45 O7 N P	478.2929	13.596	
C23 H49 O7 N P	482.3244	13.601	
C24 H49 O7 N P	494.3243	13.47	
C25 H41 O7 N P	498.2585	13.897	
C25 H43 O7 N P	500.2747	13.855	
C25 H45 O7 N P	502.2905	13.516	
C25 H47 O7 N P	504.3066	13.601	

C25 H49 O7 N P	506.3242	13.51	
C25 H53 O7 N P	510.3559	13.709	
C27 H41 O7 N P	522.2569	13.84	
C27 H43 O7 N P	524.2731	13.806	
Phosphatidylcholine			
C38 H73 O8 N P	702.5075	19.545	
C38 H75 O8 N P	704.5243	19.573	
C38 H79 O8 N P	708.5455	19.621	
C39 H75 O8 N P	716.5244	19.573	
C39 H77 O8 N P	718.5391	19.58	
C39 H79 O8 N P	720.5552	19.621	
C39 H81 O8 N P	722.5619	19.621	
C40 H73 O8 N P	726.5059	19.573	
C40 H75 O8 N P	728.5236	19.53	
C40 H77 O8 N P	730.539	19.53	494=C24H49O7NP
C40 H79 O8 N P	732.5538	19.58	496=C24H51O7NP
C40 H81 O8 N P	734.5692	19.612	
C40 H83 O8 N P	736.5764	19.621	
C41 H77 O8 N P	742.5393	19.207	
C41 H79 O8 N P	744.5544	19.53	
C41 H81 O8 N P	746.5704	19.573	
C41 H83 O8 N P	748.5853	19.621	
C41 H85 O8 N P	750.5917	19.673	
C42 H79 O8 N P	756.5545	19.176	520=C26H51O7NP
C42 H81 O8 N P	758.5691	19.176	496=C24H51O7NP
C42 H83 O8 N P	760.5842	19.524	
C42 H85 O8 N P	762.6017	19.822	
C42 H87 O8 N P	764.6076	19.621	
C43 H79 O8 N P	768.5542	19.094	
C43 H81 O8 N P	770.5701	19.194	
C43 H83 O8 N P	772.5855	19.176	
C43 H85 O8 N P	774.5996	19.266	
C44 H75 O8 N P	776.517	19.11	
C44 H77 O8 N P	778.5386	19.094	
C44 H79 O8 N P	780.5541	19.061	
C44 H81 O8 N P	782.5698	18.992	520=C26H51O7NP
C44 H83 O8 N P	784.5847	19.114	502= C24H57O7NP
C44 H85 O8 N P	786.5997	19.176	
C44 H87 O8 N P	788.6155	19.524	
C44 H89 O8 N P	790.6222	19.524	

C45 H85 O8 N P	798.6	19.114	
C45 H87 O8 N P	800.6163	19.176	
C45 H89 O8 N P	802.6321	19.266	
C46 H85 O8 N P	810.602	19.114	
C46 H87 O8 N P	812.6163	19.114	
C46 H89 O8 N P	814.6321	19.114	
C46 H91 O8 N P	816.6492	19.573	
Lyso phosphatidylcholine			
C20 H43 O7 N P	440.2775	21.876	
C21 H45 O7 N P	454.2932	21.761	
C22 H45 O7 N P	466.2929	21.652	
C22 H47 O7 N P	468.3085	21.587	
C23 H49 O7 N P	482.3248	21.502	
C24 H47 O7 N P	492.3094	21.398	
C24 H49 O7 N P	494.3247	21.404	476=C24H47O7NP
C24 H51 O7 N P	496.3398	21.331	
C25 H51 O7 N P	508.3406	21.286	
C25 H53 O7 N P	510.3566	21.286	
C26 H47 O7 N P	516.3064	21.404	
C26 H49 O7 N P	518.3243	21.331	
C26 H51 O7 N P	520.3401	21.234	502=C26H49O6NP
C26 H53 O7 N P	522.3552	21.15	504=C26H51O6NP
C26 H55 O7 N P	524.3756	21.471	
C27 H55 O7 N P	536.3693	21.142	
Ceramides			
C30 H57 O3 N Na	502.4471	2.601	
C30 H59 O3 N Na	504.4777	2.718	
C30 H63 O3 N Na	508.4577	2.743	
C31 H59 O3 N Na	516.478	2.704	
C31 H61 O3 N Na	518.4937	2.718	
C31 H63 O3 N Na	520.5093	2.718	
C31 H65 O3 N Na	522.5159	2.718	
C32 H63 O3 N Na	532.471	2.721	
C32 H65 O3 N Na	534.4887	2.718	
C32 H67 O3 N Na	536.505	2.718	
C33 H63 O3 N Na	544.5093	2.721	
C33 H65 O3 N Na	546.525	2.721	
C33 H67 O3 N Na	548.5045	2.721	
C33 H69 O3 N Na	550.5469	2.718	

C34 H61 O3 N Na	554.5147	2.718
C34 H63 O3 N Na	556.5303	2.627
C34 H65 O3 N Na	558.486	2.718
C34 H67 O3 N Na	560.5018	2.718
C34 H69 O3 N Na	562.5199	2.704
C34 H71 O3 N Na	564.5371	2.721
C35 H67 O3 N Na	572.5401	2.698
C35 H69 O3 N Na	574.5563	2.718
C35 H71 O3 N Na	576.5356	2.721
C35 H73 O3 N Na	578.5518	2.721
C36 H63 O3 N Na	580.53	2.721
C36 H65 O3 N Na	582.5463	2.718
C36 H67 O3 N Na	584.4976	2.797
C36 H69 O3 N Na	586.5176	2.721
C36 H71 O3 N Na	588.5333	2.721
C36 H73 O3 N Na	590.5513	2.704
C36 H75 O3 N Na	592.5673	2.698
C37 H73 O3 N Na	602.512	2.721
C39 H65 O3 N Na	618.5174	2.754
Lysophosphatidylinositol		
C23 H46 O12 P	545.2734	6.976
C25 H46 O12 P	569.2736	6.947
C25 H48 O12 P	571.2788	6.947
C27 H46 O12 P	593.2731	7.283
C27 H48 O12 P	595.2886	7.283
C27 H50 O12 P	597.3045	7.283
C27 H52 O12 P	599.3207	7.75
Phosphatidylinositol		
C39 H72 O13 P	779.4722	3.071
C41 H74 O13 P	805.4875	4.785
C41 H74 O13 P	805.488	3.071
C41 H76 O13 P	807.5035	4.785
C41 H76 O13 P	807.5037	3.071
C41 H78 O13 P	809.5104	3.071
C42 H76 O13 P	819.5029	6.37
C42 H76 O13 P	819.5034	3.071
C43 H74 O13 P	829.4877	4.785
C43 H74 O13 P	829.4878	3.071
C43 H76 O13 P	831.503	4.785

C43 H76 O13 P	831.5034	3.071
C43 H78 O13 P	833.5183	4.785
C43 H78 O13 P	833.5185	3.071
C43 H80 O13 P	835.5319	4.785
C43 H80 O13 P	835.533	3.071
C43 H82O13 P	837.54	3.071
C44 H80 O13 P	847.5352	3.071
C45 H74 O13 P	853.4876	3.134
C45 H76 O13 P	855.5031	3.134
C45 H78 O13 P	857.5179	3.134
C45 H80 O13 P	859.5329	3.134
C45 H80 O13 P	859.5333	4.785
C45 H82 O13 P	861.5485	4.785
C45 H84 O13 P	863.5644	3.071
Cardiolipins		
C73 H133 O17 P2	1343.9	10.371
C75 H135 O17 P2	1369.915	10.362
C75 H143 O17 P2	1377.992	11.498
C75 H144 O17 P2	1378.997	11.498

3.3 Structure elucidation for phospholipids

Structural information regarding the acyl chain substitution in lipids can be obtained by MS^2 fragmentation, which is a potential method for confirming the identity of metabolites in complex biological samples. Using the LTQ Orbitrap analyzer, fragmentation experiments are able to provide more accurate mass measurements in multistage MS^n for compounds than those obtained by low-resolution analyzers. Collision-induced dissociation (CID) at 40KV was used to explore fragmentation pathways for phospholipids using the silica column based on the condition and parameter outlined in Section 2.12.3. MS^2 fragmentation was used for each individual phospholipid, particularly phosphatidylcholines and phosphatidylethanolamines in the positive polarity mode using data dependent acquisition fragmentation that was operated simultaneously with full scan. Different fragment patterns could be observed for each

lipid class. Figure 3.13 shows the MS^2 spectrum for a PE lipid with m/z 740, the major ion at m/z 599 results from the loss of the PE head group. In contrast, phosphatidylcholine and lysophosphatidylcholine compounds produces the specific mass $C_5H_{15}O_4NP^+$, *m/z* 184.07, which is a diagnostic fragment for all phosphatidylcholine species. This class of phospholipid also underwent elimination of a ketene type fragment to form a lysolipid, which produces a minor peak e.g. the ion at m/z 494 resulting from the loss of the ketene fragment derived from palmitoleic acid (figure 3.14). Lysophosphatidylcholines show the main fragment at [M-18], which represents the elimination of water from the molecular ion (Figure 3.15). Acylglycerols were extracted from the *Drosophila* sample and were characterised by MS/MS fragmentation, where the structure of fatty acids attached to the glycerol backbone can be characterized from the fragmentation of specific mass to charge ratio via neutral losses of free fatty acid, $[M - R_1COOH]^+$. For example Figure 3-15 shows the fragmentation of a TAG bearing short chain acids. The ion at m/z 500 corresponds to a loss of a decatrienyl fatty acid from the molecular ion.

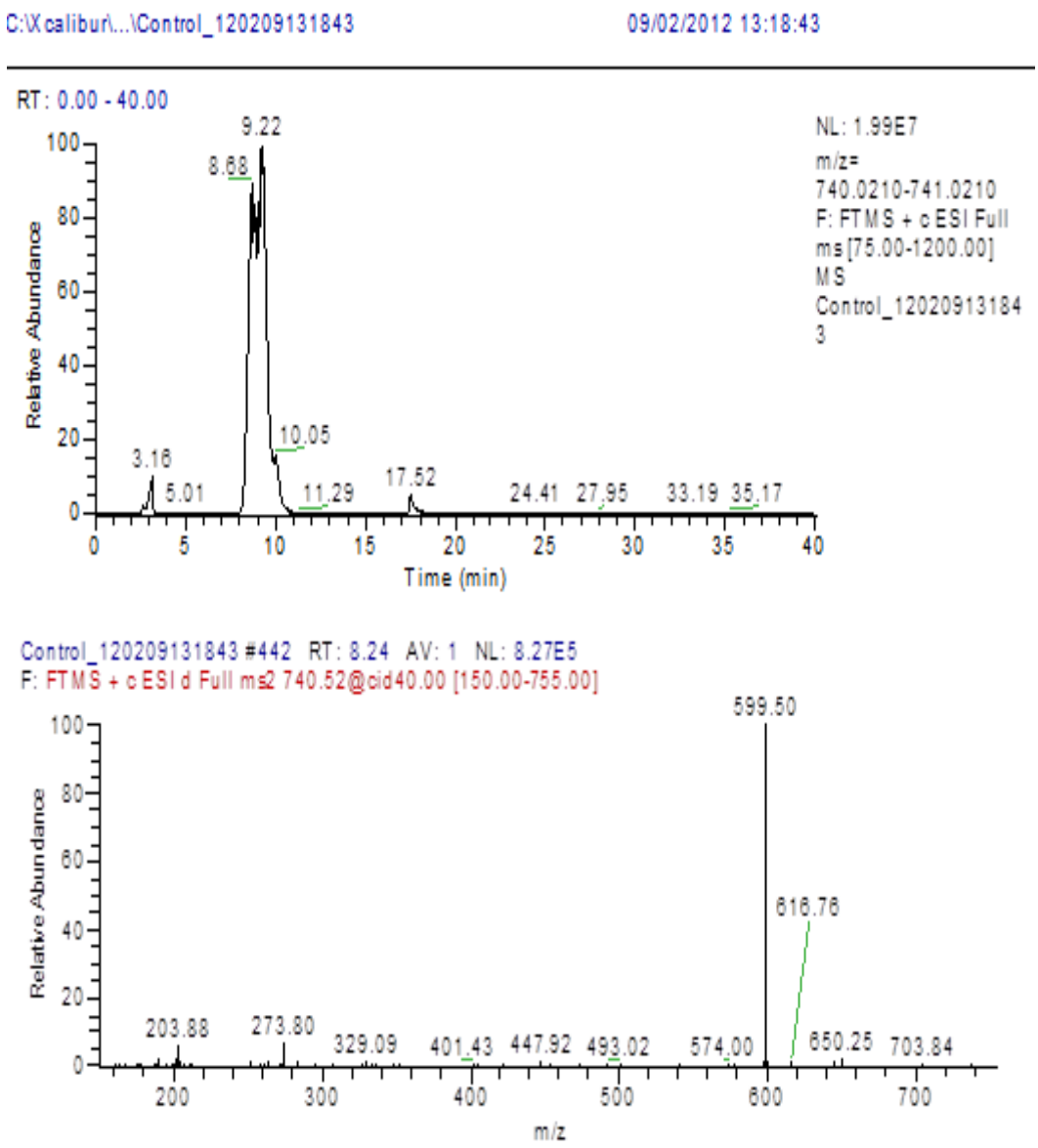

Figure 3-10 This diagram shows the electrogram of the traces of PE.Upper trace, extracted ion chromatograms of PE m/z 740.5. Lower panel, MS/MS spectra of PE m/z 740.5 showing fragment peak for 599.5 formed as a result of loss of phosphoethanolamine. Chromatograms were generated by using Chromatographic conditions as in 2.12.3.

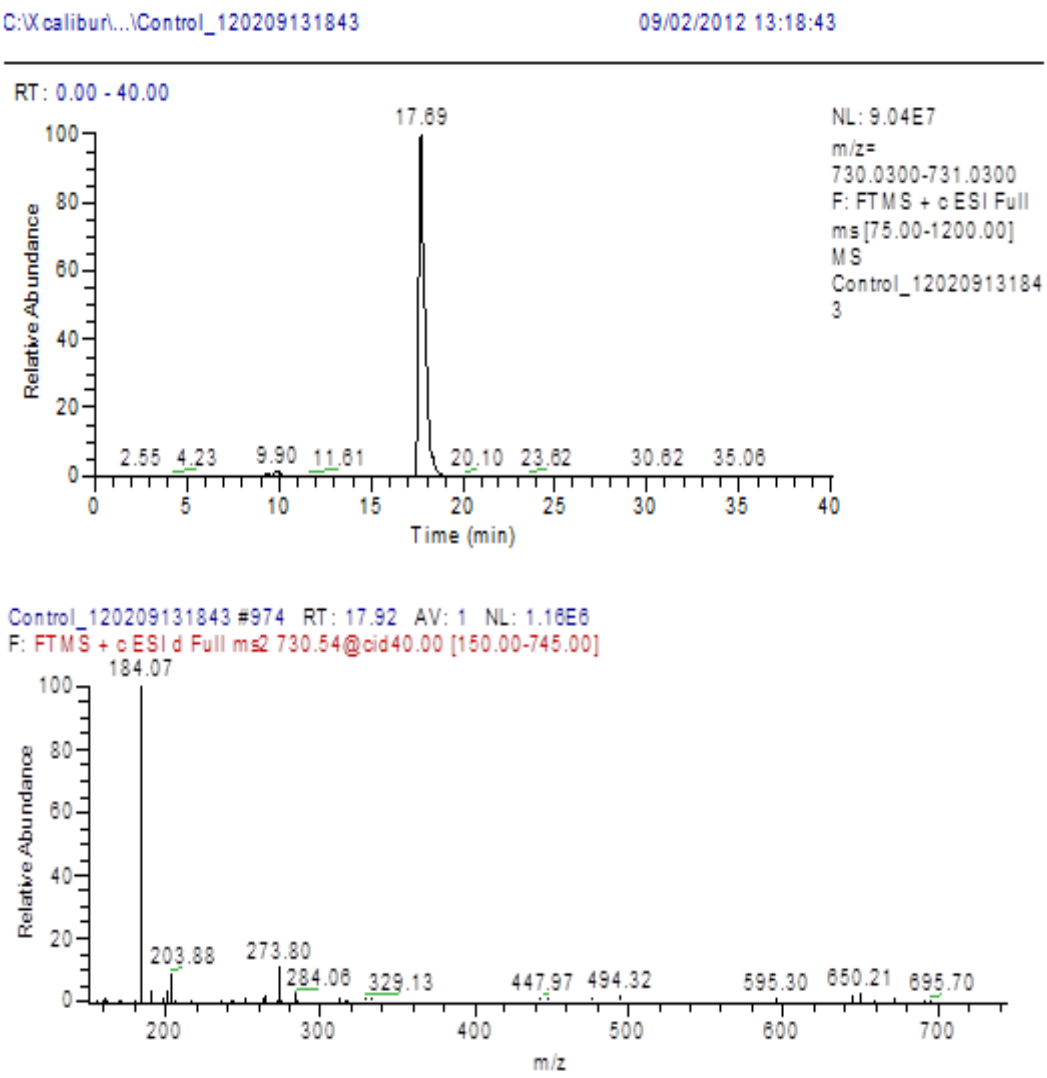

Figure 3-11 This diagram shows the electrogram of the traces of PC. Upper trace, extracted ion chromatograms of PC m/z 730.5; lower panel, MS/MS spectra of PC m/z 730.5 showing fragment peaks for 494.3 formed from $C_{24}H_{49}O_7NP$ and 184 formed from $C_5H_{15}O_4NP^+$. Chromatograms were generated by using Chromatographic conditions as in 2.12.3.

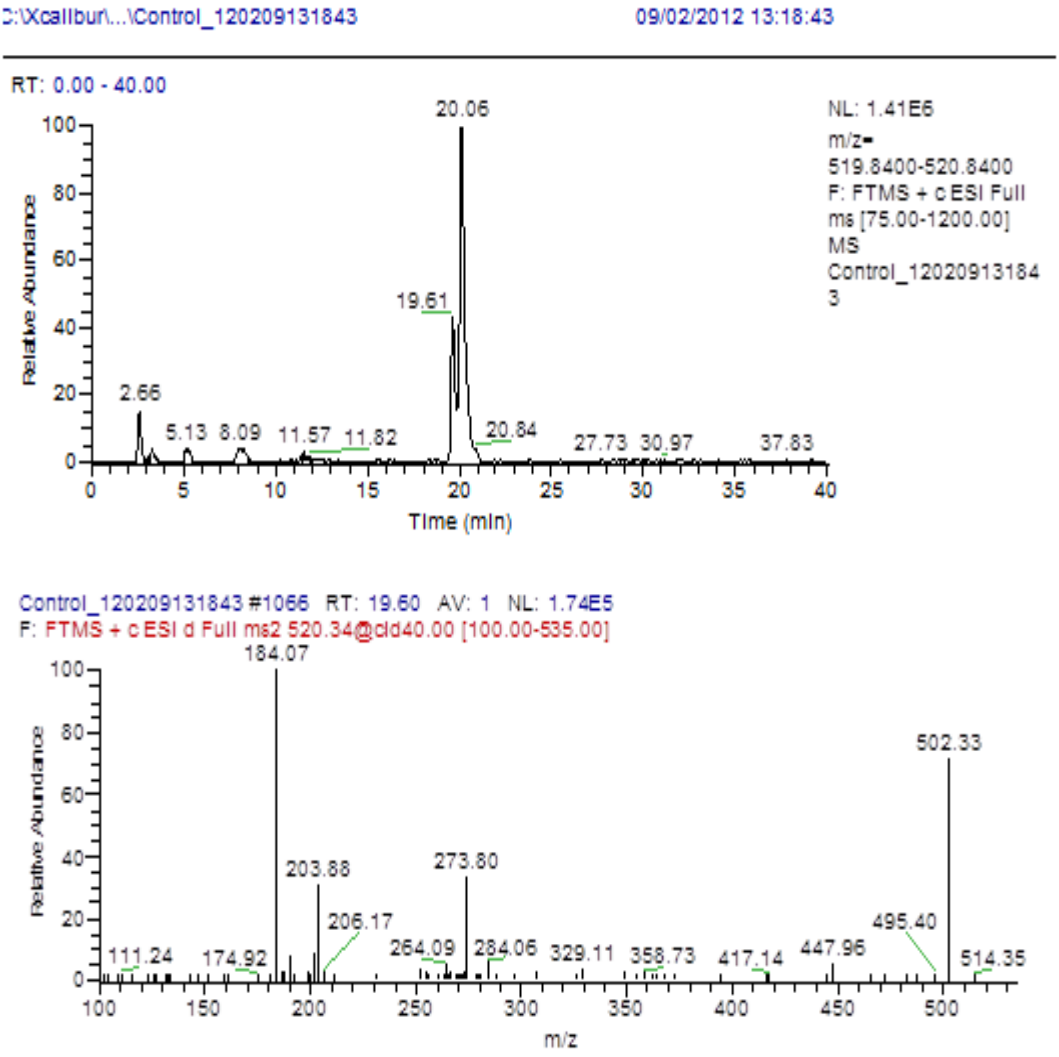

Figure 3-12 This diagram shows the electrogram of the traces of lysoPC. Upper trace, extracted ion chromatograms of lysoPC m/z 520.3; lower panel, MS/MS spectra of lysoPC m/z 520.3 showing fragment peaks for 502.3 formed from $C_{26}H_{49}O_6NP$ after loss of water and 184 formed from $C_5H_{15}O_4NP^+$. Chromatograms were generated by using the chromatographic conditions as in 2.12.3.

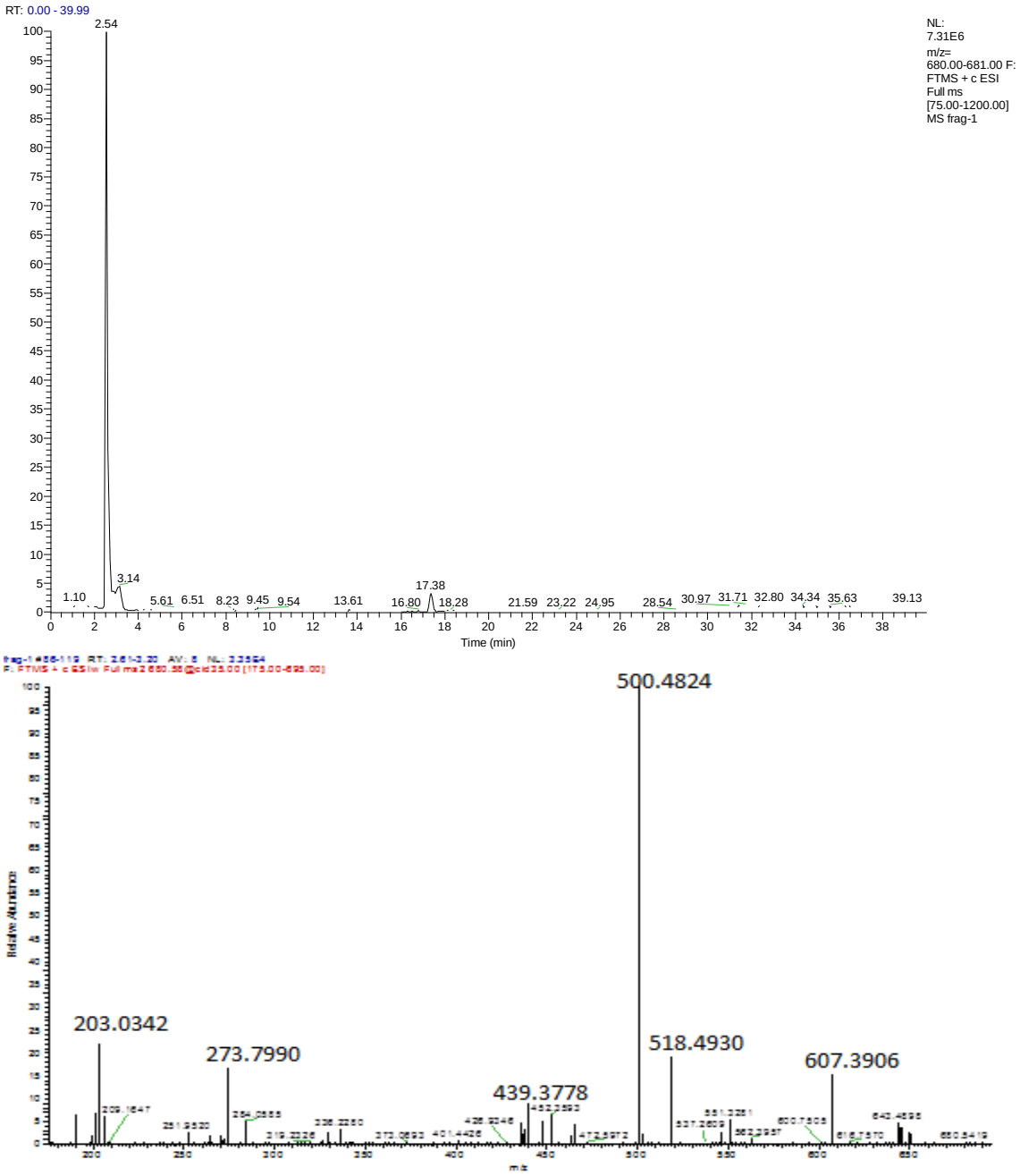

Figure 3-13 This diagram shows the electrogram of the traces of TAG. Upper extracted ion trace, ESI-MS spectra of ammoniated molecular ion at m/z 680.583; lower panel, MS/MS spectra of TAG m/z 680.583. Chromatograms were generated by using the chromatographic conditions as in 2.12.3.

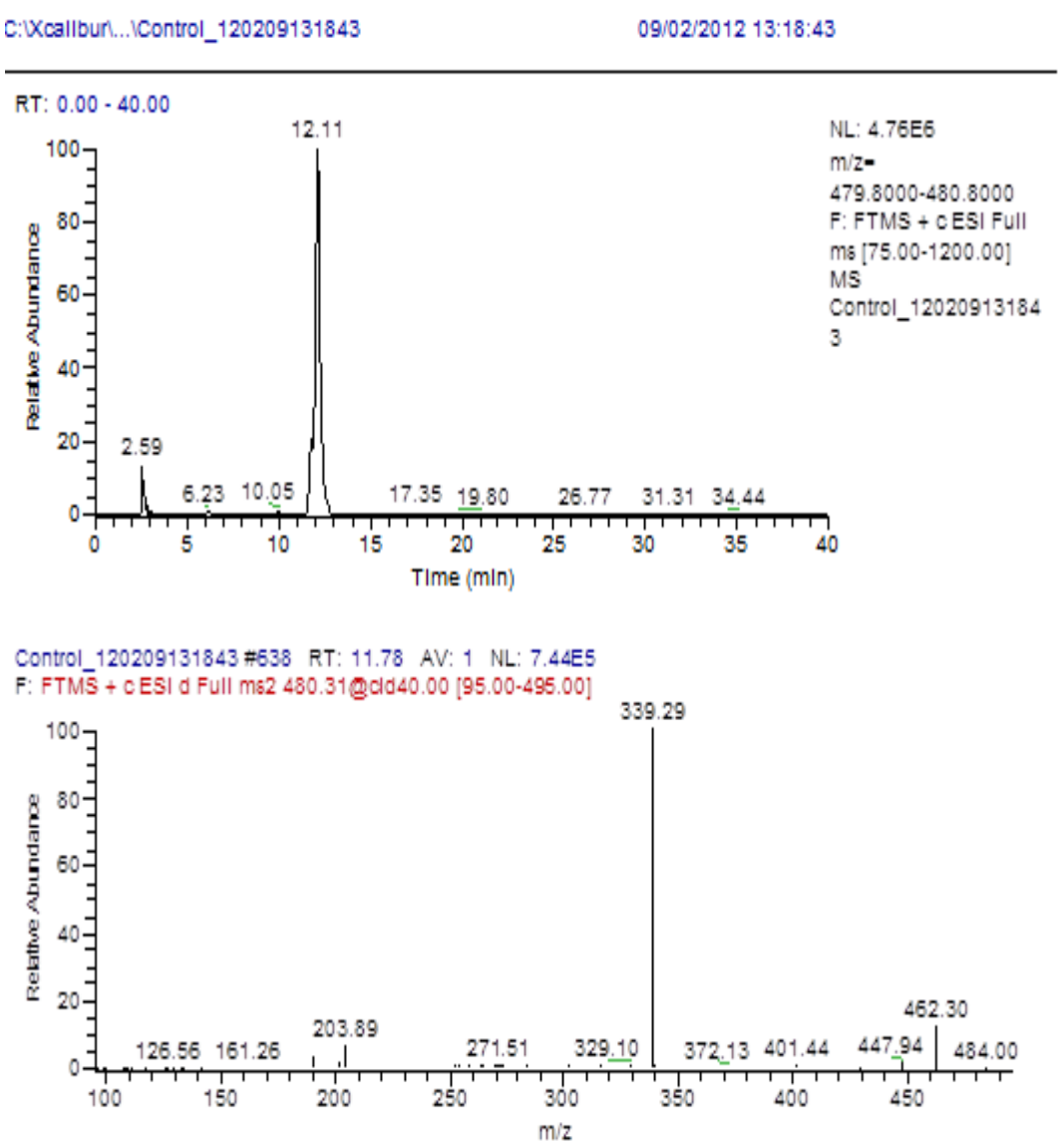

Figure 3-14 This diagram shows the electrogram of the traces of lysoPE. Upper trace, extracted ion chromatograms of lysoPE m/z 480.3; lower panel, MS/MS spectra of lysoPE m/z 480.3 showing fragment peaks for 462.3 formed from $C_{23}H_{77}O_6NP$ after loss of water and = 339 formed from $C_{21}H_{39}O_3$. Chromatograms were generated by using the chromatographic conditions as in 2.12.3.

3.4 Statistical analysis

Comparative data analysis was carried out according to the standard deviation for each metabolite peak and the fold change that identified metabolite ratios between the treatment and control groups. Fold change was calculated based on the treated or mutant condition against the control or wild condition. Where appropriate, fold gives the absolute ratio between the average peaks of sample groups, so the ratio values were considered significant if $0.5 > \text{ratio} > 1.5$ with Student's two-tailed t-test < 0.05. Statistical comparisons are provided by Sieve software for peak areas.

3.5 Method validation

Electrospray ionisation mass spectrometry has been validated in previous studies for qualitative and quantitative analysis of several *Drosophila* species that suffer from single gene mutation(Kamleh et al., 2009d), which have a significant impact on specific metabolic pathways. None of these studies have been validated, either quantitatively or qualitatively, for single genes that are implicated in multiple metabolic pathways. In order to accomplish this goal, a metabolomic approach based on high performance liquid chromatography was applied to spontaneous or classical and directed mutations to test the ability of these techniques to either reproduce classical findings or confirm and measure the efficiency of the knockdown for the gene of interest. The general work flow of metabolomic approach can be seen in fig 3-15

General protocol to study a specific gene in *Drosophila* by metabolomic approach

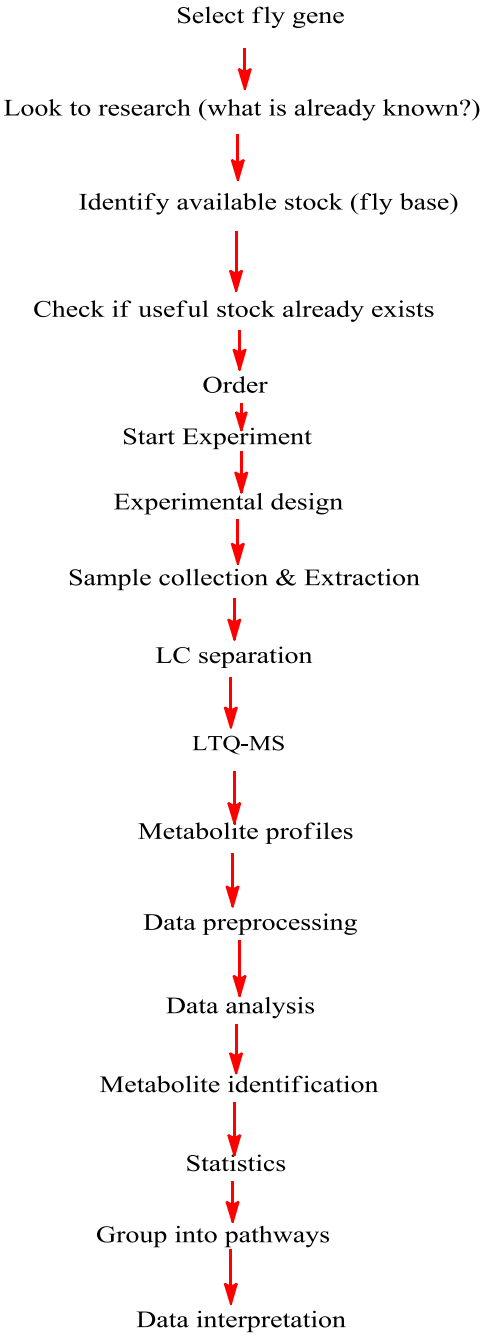

Figure 3-15 Work flow for metabolomic approach on *Drosophila* samples.

Part 2 Case studies

4. Chapter four: Validation of the knockdown of Urate Oxidase Using Metabonomics

4.1 Making of transgenic fly lines and their validation

Polymerase chain reaction (PCR) analysis is the most common method of quantifying and qualifying changes in gene expressions of interest. However, a metabolomic approach using a HILIC column coupled with electrospray mass spectrometry might be an alternative approach in molecular biology and medicine. Unlike PCR analysis, validation by metabolomics does not require complicated procedures either to isolate DNA or to prepare reaction mixtures to run a PCR analysis. To do this, a Gateway™ recombinant vector pRISE was used as described in section 2.5 to insert *urate oxidase (uro)* into w^{1118} background fly embryos reducing the transcription of the normal mRNA as seen in figure 4-1.The percentage of knockdown for *uro* was quantified by metabolomics in order to proceed to functional studies as in figure 4.2.

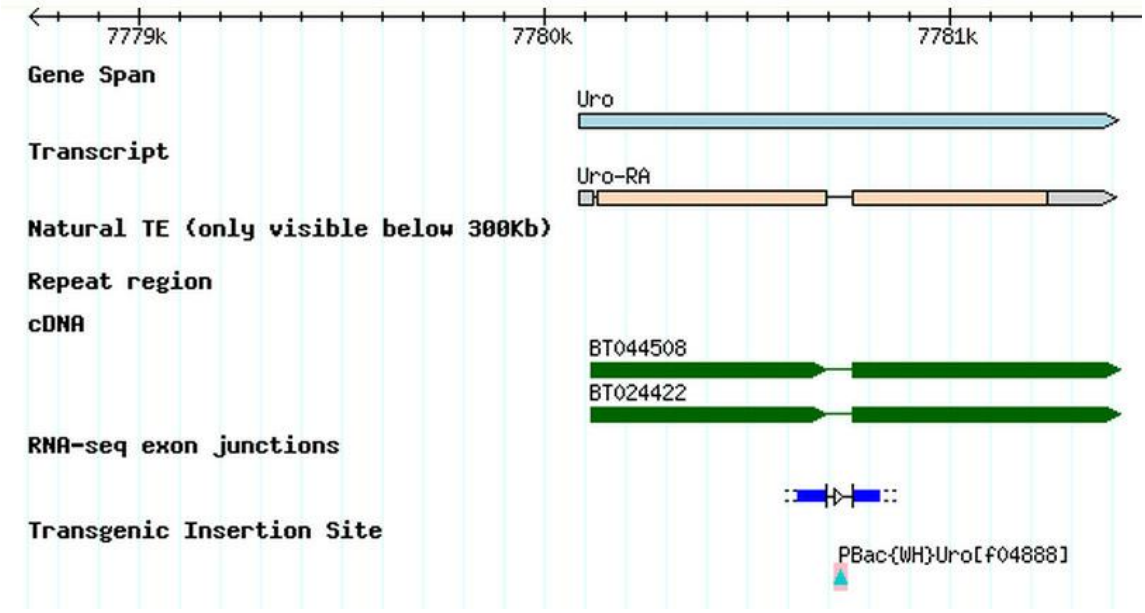

Figure 4-1 The pBac transgenic insertion site on the uro gene obtained from Flybase.org on 15th June, 2012

Broadly, the *uro* gene encodes the urate oxidase enzyme which is one of the purine processing enzymes in *Drosophila melanogaster*, helping with elimination of

nitrogenous waste products (Vogels and Van der Drift, 1976, Kral et al., 1986). Unlike in the human body, fruit flies need to carry out further degradation of uric acid because it is a water insoluble, removing the demand for water to dilute it and reducing its toxicity until it is metabolised to water soluble metabolites (Chapman, 1998). However, the *uro* function is found in a variety of organisms ranging from bacteria to mammals, excluding humans and primates, and its function in *Drosophila* species varies according to their life stages (Friedman and Johnson, 1977). For example, in *Drosophila melanogaster*, *uro* is expressed in the third instar larvae and in adults, while it completely disappears in the pupal stage. In *Drosophila virilise* and *Drosophila pseudoobscura*, the enzyme activity is active in the third instar larvae only and in the adult stage, respectively (Friedman and Johnson, 1977). All *Drosophila* species share the same location of expression for the urate oxidase enzyme, where it is exclusively expressed in Malpighian tubules. In terms of biochemistry, the urate oxidase enzyme has four active sites existing in the form of a homo-tetramer. Unlike oxidase enzymes, such as xanthine oxidase, the hydroxylation process of uric acid conversion to 5-hydroxyisourate (5-HIU) does not require a co-factor or metal cation to function. Thus, two mechanisms were proposed to explain how urate oxidase behaves. An inducing factor, closely located to the gene that stimulates the production of enzymes found in heaemolymph was a first suggested mechanism. Second, an autonomous intracellular clock-like function found in the adult tubule controls the timing of the changes. Like peroxisomal enzymes, urate oxidase generates free radicals during purine catabolism and such enzymes have been associated with diseases such as cancer, heart disease and aging diseases. Thus antioxidant agents are an important means of fighting free radicals to protect against causative agents for diseases. Among these agents is urate, which reacts with free radicals, converting them to a more stable form such as water in order to avoid or at least reduce cell damage.In fruit flies, urate oxidase contributes to the breakdown of purine substrates as seen figure 4-2, in particular the conversion of uric acid to 5-HIU and then to allantoin by 5-hydroxyisourate hydrolase.

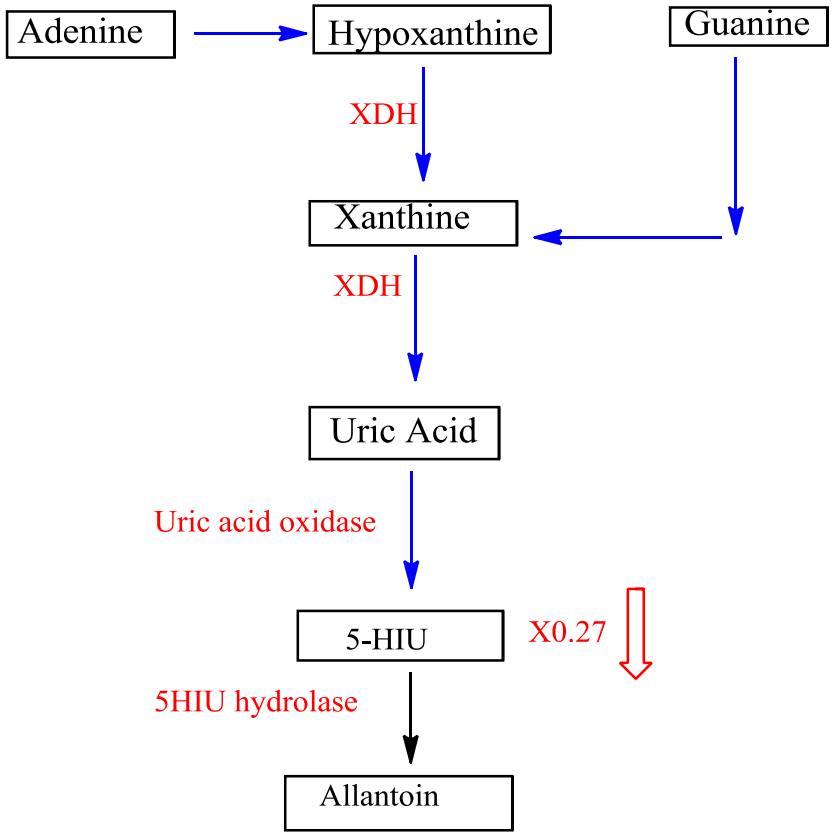

Figure 4-2 Impact of *uro* knockdown on purine catabolism with known *Drosophila* enzymes indicated, and fold changes for metabolites for uro RNAi knockdown versus their parents, with fold changes superimposed .

4.2 Tissue specific knockdown of urate oxidase activity

As mentioned above, the Malpighian tubule is the site of *uro* expression, so flies were crossed with urate GAL4 lines to drive RNAi expression exclusively in the tubules. Then, week-old adult flies were selected in order to dissect tubules from parents and progeny. Fly dissection was performed according to the dissection protocol in section 2.6. Validation by using a metabolomic approach was performed in order to determine

the key metabolic changes that originate from *uro* knockdown. From figure 4.4 we can see that there was a substantial decrease in the amount of gene expression in progeny flies compared with their parents, where the *uro* gene was reduced by 70% in the dissected tubules in *uro*-RNAi progeny according to the levels of HIU and allantoin measured. Validation by qPCR (more details in section 2.8) showed an 80% reduction in gene expression as seen in figure 4.3. Thus the two methods produced results which were in quite close agreement.

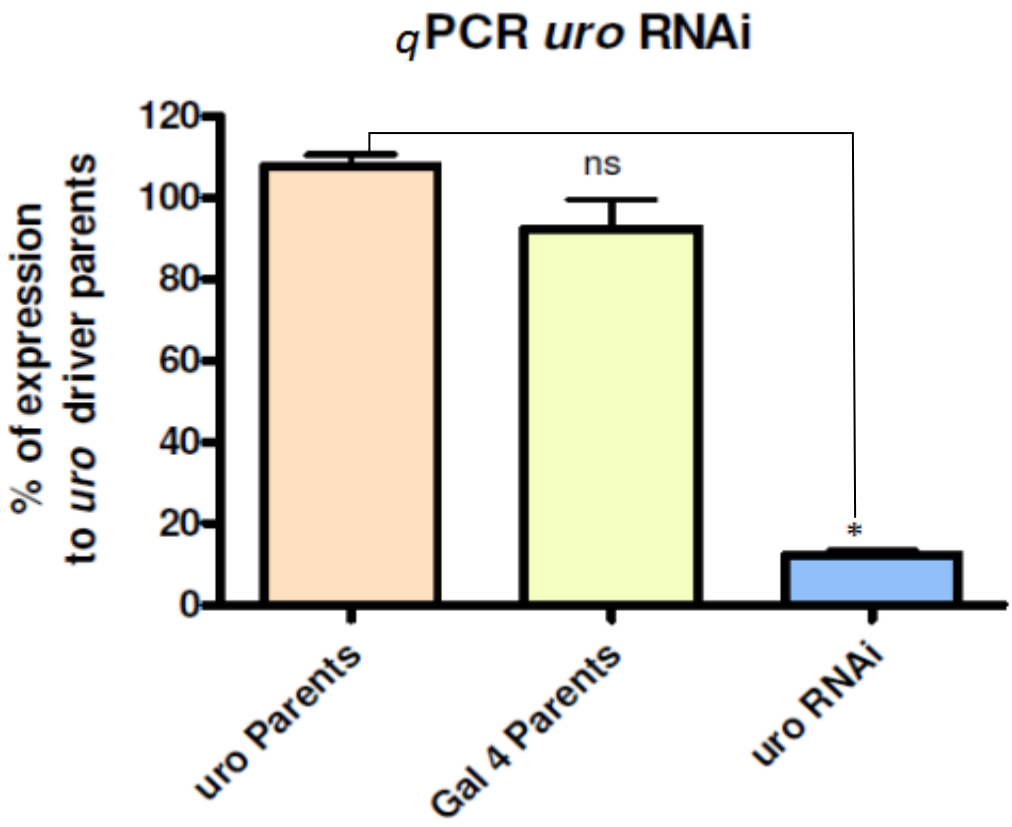

Figure 4-3 *uro* RNAi knockdown validated by *q*PCR approach. It shows *uro* gene knockdown expression dissected from tubules compared to parental lines. Approximately 80% lower expression was observed. Data are shown as mean ±SEM for N=4 independent experiments. Data that differ significantly are marked with asterisks are analyzed by Student's *t*-test two tailed

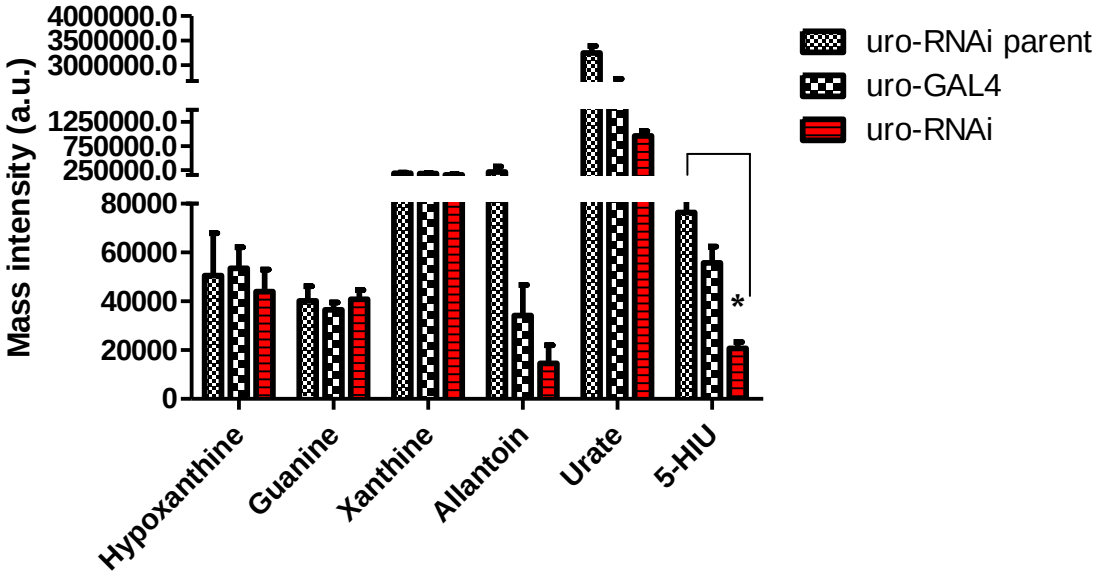

Figure 4-4 *Uro* RNAi knockdown validated by metabolomics approach. It shows the impact of uro gene knockdown expression on purine metabolite levels in dissected tubules compared to parental lines. Approximately 70% lower expression. Data are shown as mean ±SEM for N=4 independent experiments. Data that differ significantly are marked with asterisks are analyzed by Student's *t*-test two tailed

4.3 Conclusion

In this experiment it was shown that a metabolomic approach could be used to validate tissue specific RNAi knockdown of a particular gene.

5. Chapter five: Phenocopying the rosy gene

5.1 History

The identification of the white gene by Morgan was followed by the discovery and the identification of the rosy (*ry*) gene in the fruit fly (Julian A.T, 2007). Depletion in drosopterin (a precursor of red eye pigment) leading to a dull-red eye colour is a phenotype for the *ry* mutant. Although this phenotype is not restricted to the *ry* mutant, several mutants share the same eye colours such as maroon like mutants and other ones (Kamleh et al., 2009c). The ry mutant was recently characterized by the accumulation of hypoxanthine and xanthine and a decrease in uric acid levels because of the absence of xanthine dehydrogenase (XDH) (Kamleh et al., 2008a). Thus purine metabolism is a sensitive pathway to mutation in the *ry* gene. This conclusion was in agreement with an observation that the longevity of *ry* mutant fly was directly reduced in comparison with the wild type when they were fed with a purine enriched diet (Collins et al., 1970). Eye phenotype in the ry mutation gene was considered to be mainly located in the eye tissues and transported into pigment granules but not functionally expressed (Reaume et al., 1989). However, Flyatlas provided a contrasting view whereby the *ry* gene is ubiquitously expressed in most tissues including the eyes but mainly in the tubules (Chintapalli et al., 2007b). Furthermore, xanthine oxidoreductase (XOR) consists of XDH and xanthine oxidase (XO) and both of them utilise hypoxanthine and xanthine as substrates in the oxidation of purines (Meneshian and Bulkley, 2002). However, the cofactors utilized to activate the the two enzyme reactions are different where NAD^+ cofactor is used by XDH as an electron acceptor in order to produce NADH, while XO uses oxygen as an electron acceptor producing free radical species in particular H_2O_2 and O_2^-. Interestingly, both enzymes are encoded by the same gene and they exist in interchangeable forms (Chung et al., 1997). Although the gene product is found in the dehydrogenase form in normal cells, in some pathophysiological circumstances such as injury, the oxidase form is predominant. This interconversion between XDH and XO could be counteracting oxidative stress and may serve as a defence mechanism under adverse conditions (Chung et al., 1997). When a body suffers from an acute loss of oxygen such as in the case of ischemia, it tries to supply oxygen immediately to affected

tissues. This flux of oxygen into the cells sometimes causes undesirable effects ranging from cellular damage to proteins and DNA. So the switch from XO to XDH may prevent cells from death by the use of excess O_2 and rescue the body from oxidative stress by generating less harmful compounds. The interconversion can occur by sulfoxidation of XDH to produce the oxidase form and back to the dehydrogenase form via a reduction process. Proteolysis is also possible for conversion of XDH to XO but this mechanism is irreversible. Chemically, XDH/XO has two subunits with a total size of approximately 300 KDa. Each subunit contains four active cofactors: one molybdenum, one flavin adenine dinucleotide (FAD) and two non-identical centres containing ferrous sulphide Fe_2S_2(Vorbach et al., 2003). This structure plays a vital role in immunity and detoxification systems by modulating ROS and RNS (reactive nitrogen species). In this chapter, we confirm the previous studies showing that *ry* is expressed in all tissues and extend the study of *ry* in an attempt to phenocopy the effects of the *ry* mutation by using allopurinol an inhibitor of XDH and observe the metabolic effects.

5.2 Expression sensitivity to *ry* localization

Like the microarray approach, we sought to measure relevant metabolites in different tissues that should be directly influenced by the expression of the *ry* gene. Thus the activity of XDH/XO could be assessed by measuring the level of uric acid and xanthine viewed in different tissues. So dissected head, thorax and abdomen (n=4) from 7day old adult wild type flies (10 flies of mixed sexes) were well homogenised in ice cold buffer and extracted as described in section 2.1.1. From the data presented in Figure 5-1 , Uric acid is far more extensive in abdomen than head or even thorax, and so *ry* is particularly abundant in abdomen and has half activity in head. From physiological view, the abdomen contains the left- side tubule, mid-gut and hind-gut, while thoracic part contains right-side tubule and fore-gut. The head contains the eyes and brain and various other organs (Chintapalli et al., 2012, Coutelis et al., 2008). The abundance of XDH/XO is relatively low in thorax part since uric acid and xanthine were found in low levels compared to the abdominal part. So it was expected that uric acid levels would be

high in the abdomen because it is particularly the site of fluid excretion and of the breakdown of toxic compounds, this result confirms the flyatals microarray's result (Chintapalli et al., 2007b) and validated the metabolomic approach in reflecting the previous results(Chintapalli et al., 2007b). The highest levels of uric acid in abdominal part are agreement with the its function in detoxification plus its role as antioxidant agent (Dent and Philpot, 1954).

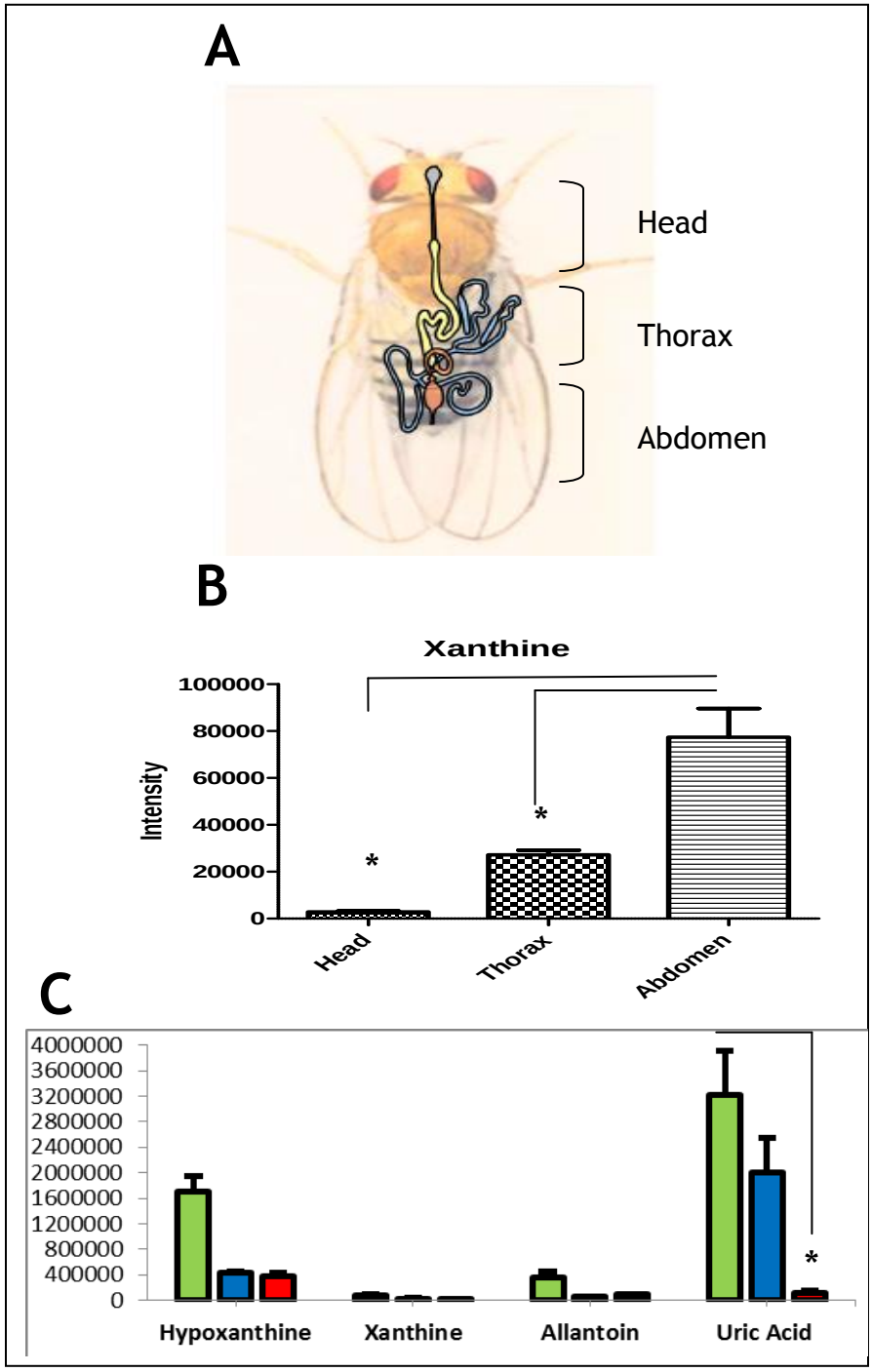

Figure 5-1 *ry* expression across *Drosophila melanogaster* tissues. Effects on hypo xanthine-allantoin axis in the purine metabolism pathway are presented for *ry* against the tissues. The expression is predominant in abdomen for *ry* in panal (B and c according to statistical significance (n=4; *t*-test; $P \leq 0.001$). Panel A shows the internal tissues in *Drosophila.*

5.3 Loss of *ry* results in reduced red eye pigment

Biochemically, XDH/XO is not important only in degradation of nucleic acids to catalyze the oxidation of hypoxanthine to uric acid via xanthine but it also also helps in formation of pteridine pigments in insects (Parisi et al., 1976). Previously, *ry* mutations characterised by a brownish eye colour phenotype, have been shown to suffer from a deficiency in red pigment. Red pigment can be formed via two routes together via two different genes as seen in figure 5-2. *Ry* has a role in the oxidation of pterin to isoxanthopterin while *Sepia* (*se*) has another role in the conversion of sepiapterin to drosopterin. Although the decrease in drosopterin level is linked to the *ry* mutation, the role of *ry* in red pigment formation remains unclear (more details about mechanism of eye pigments are given in chapter six (Ambegaokar and Jackson, 2010). Our results showed that the level of drosopterin was slightly lower in the *ry* mutant than in wild type. However, isoxanthopterin level was one fifth in *ry* mutant flies compared with wild type whereas pterin level was present at 10 fold higher in the *ry* mutant flies. Xanthinuria type I is a descriptive term for excess urinary excretion of the purine base xanthine. Xanthinuria principally results from a deficiency of the enzyme xanthine dehydrogenase and can be diagnosed by an elevation in pterin level accompanied with a decrease in isoxanthopterin level (Boltshauser et al., 1986, Yamamoto et al., 1996, Blau et al., 1996). Therefore, the latter could be another sensitive marker for the activity of XDH/XO. Interestingly, this disorder had been described extensively in *Drosophila* particular *ry* mutants that produce a lot of pterin.

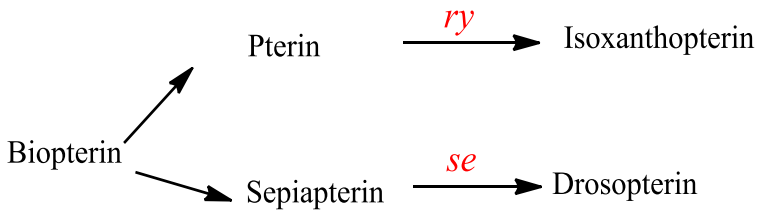

Figure 5-2 Diagram of red pigment formation in Drosophila taken from (Summers et al., 1982)

From the above, *ry* seems to be differently affected in different parts of the body and has three different effects (Hadorn, 1956, Wittkopp and Beldade, 2009). This phenomenon is called pleiotropy where the *ry* flies can be characterised by accumulation of xanthine in the tubule and pterin in the head and depletion in uric acic and isoxanthopterin in addition to the brownish eye phenotype.

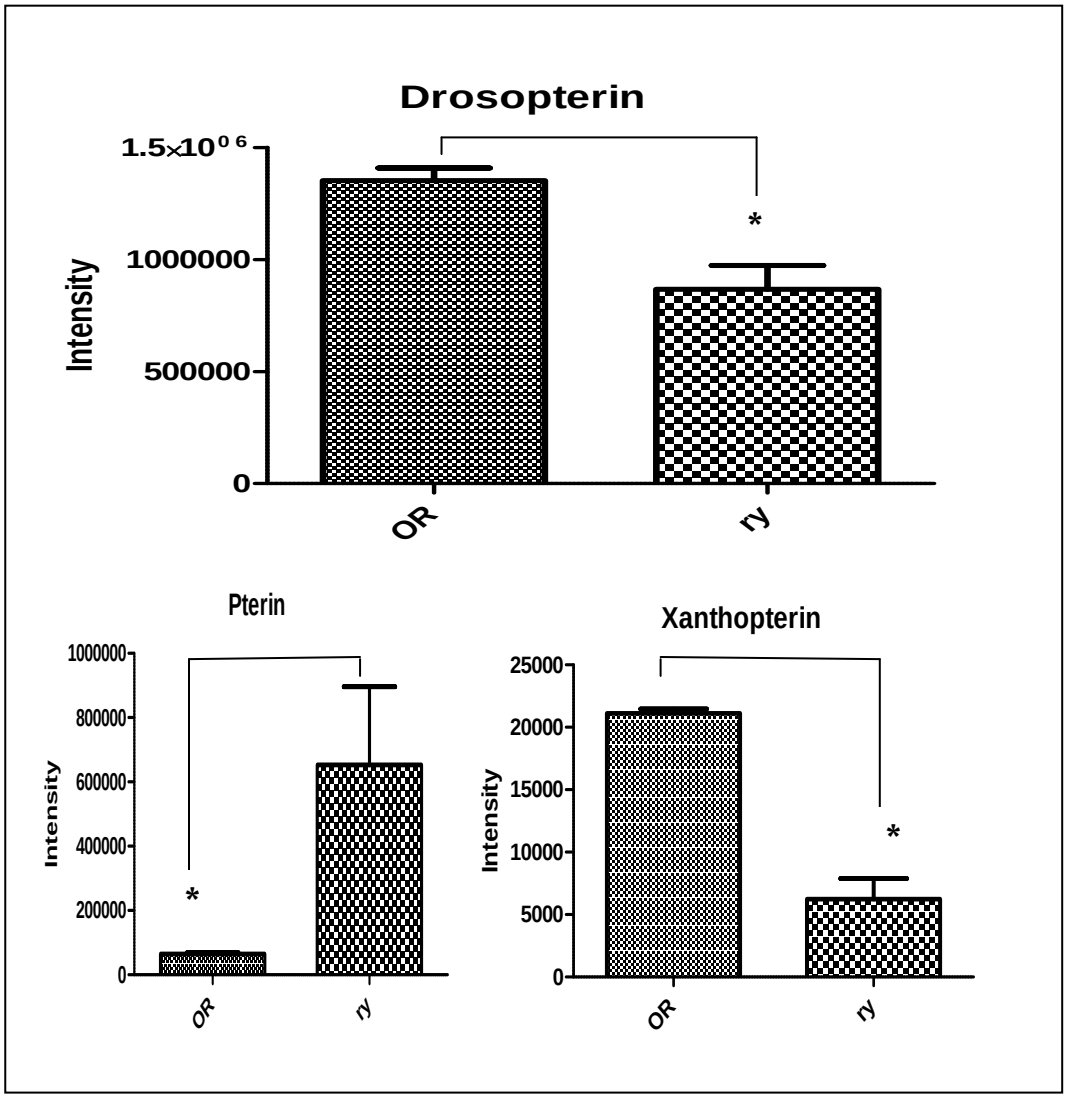

Figure 5-3 Impact of *ry* on red pigment (drospterin , pterin and iosxanthopterin). Data are shown as mean ±SEM for N=4 independent experiments. Data that differ significantly are marked with asterisks are analyzed by Student's *t*-test two tailed

5.4 The effects of allopurinol treatment on Drosophila

Metabolomics as a field of study is expanding rapidly and has the potential to impact in a number of areas including drug discovery, the management of the health of populations and crop improvement (Krastanov, 2010) (Wilcoxen et al., 2010) (Scalbert et al., 2009) (Kamleh et al., 2008c, Dunn, 2008). In order to advance the field further simple model organisms are used since genetic manipulation is more feasible in them than in more complex organisms such as humans. *Drosophila melanogaster* offers a combination of genetic tractability, availability of well-characterised genetic mutant stocks, and organismal complexity (Dow and Davies 2003) and is thus ideal for metabolomic studies. Previous work characterised the metabolomic effects of the *ry* mutation (Kamleh et al., 2008a). The expected changes in the pattern of metabolites directly related to the absence of the xanthine oxidase gene, such as the absence of uric acid and allantoin and the elevation of xanthine and hypoxanthine were observed. In addition, perturbation both in the purine metabolic pathway at a distance from the lesion and in other metabolic pathways was observed. The xanthine oxidase (XO) inhibitor allopurinol is used to treat gout via the inhibition of uric acid formation and is generally well tolerated (Pacher et al., 2006) although it can produce side-effects such as eosinophilia and vasculitis. In principle, administering allopurinol to *Drosophila* should phenocopy the *ry* mutant by inhibiting XO and causing xanthine and hypoxanthine to accumulate and uric acid to deplete. It could potentially also induce the more distant metabolic perturbations seen in the *ry* mutant. Allopurinol is a prodrug and is converted to oxopurinol by the action of XO. Oxopurinol is a suicide inhibitor of XO which replaces the hydroxyl ligand of the molybdenum ion at the active site of XO (Hille and Nishino, 1995), and thus very effectively prevents conversion of hypoxanthine to xanthine and xanthine to uric acid. Inhibition of XO does not prevent xanthine being produced since it can be derived from guanine, and similarly hypoxanthine can be produced from adenine, and the enzymes required for these conversions are not inhibited by allopurinol. There is an on-going interest in allopurinol as a cardio-protectant since the activity of XO is one of the major sources of reactive oxygen species (ROS) in the

human body and it may play a major role in various forms of ischemic and vascular injury (Pacher et al., 2006). However, there is a balance between two effects, since XO also produces uric acid, which is an important antioxidant within the body; and it has been proposed that uric acid is responsible for about 25% the antioxidant capacity of human serum and that dietary antioxidants exert their effects indirectly via increasing plasma uric acid levels (Lotito and Frei, 2004). Metabolomics has the potential to provide a greater understanding of the action of drugs on wider metabolic networks than their intended targets. This might lead to an appreciation of unexpected properties of the drugs allowing serendipitous applications and also give an indication of the physiological basis of side-effects. About 70% of human genes have *Drosophila* homologues, and so the fruit fly is potentially an experimental organism in which drug testing can be conducted with less expense and ethical considerations than in higher animals. The greatest challenge in metabolomics is to be able explain metabolic changes and the greatest confidence in explaining the data obtained occurs when several closely linked metabolic changes are observed e.g. in a single metabolic pathway. In this section the effects of allopurinol on the *Drosophila* metabolome are compared with those produced by the *ry* lesion which were reported previously (Kamleh et al., 2008a). Allopurinol has previously been documented to mimic the *ry* mutation (Glassman, 1965); but given the multiple uses of allopurinol, and unexpected metabolic sequelae of the *ry* mutation, we sought both to confirm the classical results, and to look for novel, undocumented impacts of allopurinol on the metabolome.

5.5 Allopurinol phenocopies rosy, but provides temporal resolution

All masses gave < 2 ppm deviation (usually < 1ppm deviation) from the nominal mass of the metabolite assigned to them which meant generally that there were no competing biologically sensible elemental compositions for compounds although isomers are always a possibility for many compounds. Table 5.1 shows all the putatively identified metabolites which were changed in OR flies as a result of treatment with allopurinol. As expected there was a gradual build up of hypoxanthine and xanthine as a result of their metabolism to uric acid being blocked.

Table 5-1 Metabolic pathways where several metabolites are significantly affected by allopurinol comparing each time point of treatment with untreated flies (batches of 10 male + 10 female flies, n = 4 for each time point). T/C = treatment/control.

			6 h		**24 h**		**48 h**		**72 h**	
	m/z	RT min	T/C	P-value	T/C	P value	T/C	P-value	T/C	P-value
Purines/pterins										
Hypoxanthine	137.0460	11.5	2.3	0.0036	5.2	0.012	3.1	0.0035	6.0	0.0025
Xanthine	153.0407	10.9	3.2	0.0077	7.8	0.0082	12	0.010	12.3	0.0001
Urate	169.0357	14.04	1.1	0.38	1.1	0.085	0.85	0.14	0.72	0.002
Allantoin	159.0514	15.1	0.25	0.00073	0.52	0.007	0.10	0.0011	0.40	0.0028
Pterin	164.0568	12.7	1.3	0.035	1.7	0.000006	1.6	0.0024	1.4	0.000016
Isoxanthopterin	180.0517	13.0	1.1	0.32	1.0	0.9	1.2	0.64	1.0	0.70
Inosine	269.0882	12.7	0.84	0.19	1.0	0.91	0.74	0.0012	0.67	0.00026
Drosopterin	369.1534	19.2	1.1	0.26	1.1	0.13	1.3	0.012	1.0	0.43
Oxidative stress										

Methionine S-oxide	166.0532	19.1	0.99	0.98	2.77	0.00072	1.5	0.0019	1.4	0.83
Ascorbic acid	175.0248	13.7	ND	-	ND	-	ND	-	ND	-
GSH	308.91	17.0	0.51	0.0054	0.40	0.01	0.52	0.0077	0.45	0.0059
Riboflavin	377.1458	10.2	1.0	0.84	0.47	0.0067	0.31	0.000084	0.26	0.000048
GSSG	613.1592	21.5	1.4	0.12	2.9	0.011	1.8	0.022	1.4	0.06
Pentose phosphate pathway										
Deoxyribose	133.0506	8.4	0.42	0.033	0.30	0.11	0.6	0.087	0.36	
Sedoheptulose 7-phosphate	289.0331	20.3	0.73	0.022	1.0	0.33	0.75	0.0031	0.71	0.0075
Aldose reductase										
Gulonolactone	177.0405	12.2	0.30	0.029	0.32	0.034	0.26	0.026	0.52	0.090
glucitol	181.0718	16.3	0.29	0.031	0.50	0.073	0.42	0.048	0.43	0.048
Gulonic acid	195.0511	16.9	0.46	0.020	0.44	0.020	0.36	0.012	0.42	0.021
Kynurenine pathway										
Niacin/Nicotinate	124.0393	8.2	0.72	0.029	0.79	0.034	0.44	0.0016	0.44	0.002
Oxoadipic acid	159.0300	12.2	0.28	0.003	0.31	0.029	0.24	0.0027	0.54	0.1
Dihydroxy-quinoline	162.0548	9.1	1.4	0.039	1.7	0.00066	1.2	0.090	0.94	0.65
Xanthurenic acid	206.0448	11.7	0.86	0.011	0.96	0.47	0.70	0.001	0.80	0.0011
L-Kynurenine	209.0922	13.4	0.71	0.0008	0.69	0.012	0.62	0.000019	0.41	0.000019
3-Hydroxy-L-kynurenine	225.0868	15.1	0.90	0.15	0.83	0.027	0.85	0.00069	0.63	0.00069
N-Formylkynurenine	237.0871	13.9	1.1	0.58	0.45	0.30	0.23	0.0027	0.53	0.0027
Miscellaneous										
L-Tyrosine	182.0812	15.7	0.73	0.024	0.87	0.043	0.61	0.0069	0.75	0.0069
2-Amino-4-	196.0831	11.1	5.6	0.029	23.9	0.21	199	0.025	4.0	0.025

hydroxy-6-hydroxymethyl-7,8-dihydro-pteridine										
5-Hydroxy-L-tryptophan	221.092	13.6	0.41	0.0043	0.18	0.00021	0.19	0.0023	0.32	0.0023
Linolelyl carnitine	424.3421	10.1	0.66	0.003	0.95	0.5	0.63	0.0023	0.57	0.0013
oleylcarnitine	426.3576	10.1	0.81	0.0088	1.1	0.21	0.75	0.0084	0.73	0.0020

Figure 5-5 shows extracted ion chromatograms showing the rise of hypoxanthine over 72 hours and also a gradual increase in a peak for allopurinol which is isomeric with hypoxanthine but elutes earlier from the ZIC-HILIC column. Surprisingly there was only a very slow change in uric acid levels during the course of the experiment indicating that the rate of elimination of uric acid from the flies is slow. This is consistent with the accumulation of uric acid crystals in tissues such as eye, fat body, or the lumen of the tubule of normal flies – termed “storage excretion” (Wigglesworth, 1939). In *ry* mutants, urate is undetectable (Kamleh et al., 2008a); this is because XO activity is never present throughout the life of the insect. Although the ultimate metabolic destination is similar, allopurinol application thus allows a *ry*-like phenotype to be imposed on an otherwise normal animal, revealing temporal information that is unavailable in the mutant. The levels of pterin also rose following allopurinol treatment; pterin is also a substrate for XO and is normally oxidised to produce isoxanthopterin, but this process is also blocked by allopurinol. It was found previously that isoxanthopterin was absent from *ry* mutants (Kamleh et al., 2008a), however, in the current study isoxanthopterin levels were not affected by allopurinol over the time course of the experiment possibly indicating that it is only metabolised slowly by the flies.

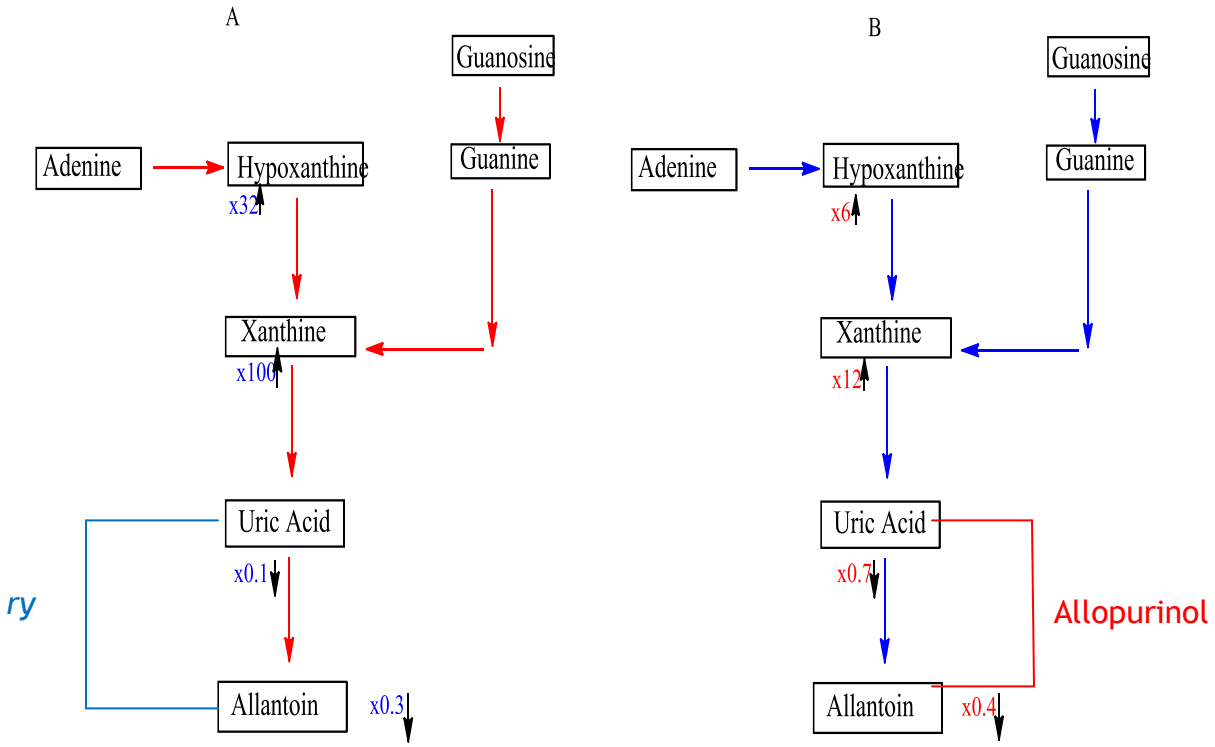

Figure 5-4 Impact of *ry* (A) and allopurinol (B) on the uric acid pathway, with fold changes superimposed.

5.7 Pharmacokinetics

Also we can observe in the figure 5-5 that allopurinol has relatively short time in our model while the half- life of oxypurinol is much longer (Pea, 2005). Thus oxpurinol has much effect on purine metabolism and acts as negative regulator of XDH/XO. Allopurinol cannot be seen before treatment in extracted ion traces while it can be observed that the levels of allopurinol rise gradually after allopurinol treatment.

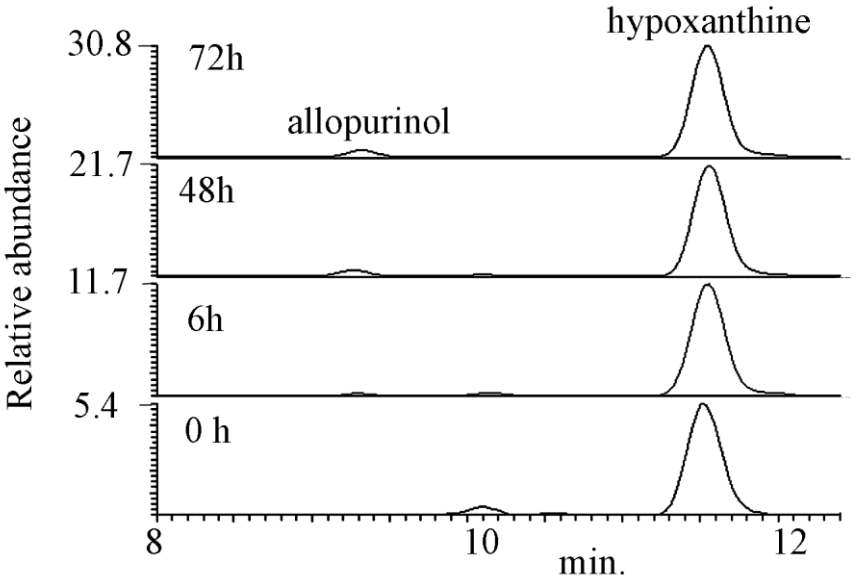

Figure 5-5 Increase of hypoxanthine and allopurinol levels with time in *Drosophila* treated with allopurinol. Chromatograms were generated by using chromatographic conditions as in 2.12.1.

1.7 Allopurinol impacts on ascorbate metabolism

Strikingly, even after only 6 h of treatment with allopurinol, ascorbic acid levels in the flies fell to below the limit of detection and remained so up to 72 h; this can be seen in the extracted ion traces shown in figure 5-6. It can be observed that the levels of glutathione (GSH) fall rapidly after allopurinol treatment (table 1) to around half the pre-treatment levels and correspondingly concentrations of GSSG rise. GSH is the co-factor for thioredoxin which recycles ascorbic acid and the lowered levels of GSH may account for the loss of ascorbic acid. Methionine sulphoxide is another marker of oxidative stress and it was also found to increase following allopurinol treatment. The lowered levels of riboflavin may also indicate oxidative stress, since the vitamin degrades rapidly under such conditions. What part of the metabolic network is being affected by allopurinol and causing the oxidative stress? GSH levels are maintained by glutathione reductase, an enzyme which uses NADPH as its co-factor. The main source of NADPH

is from glucose-6-phosphate dehydrogenase (G6PDH) which oxidises glucose-6-phosphate to glucono 1,5 lactone 6-phosphate. This reaction is the rate limiting step in the pentose phosphate pathway. The levels of the pentose phosphate metabolites sedoheptulose phosphate, ribose phosphate, deoxyribose phosphate and deoxyribose are lowered relative to the controls possibly indicating that allopurinol is somehow causing inhibition of G6PDH. The deficiency of NADPH is also reflected in the markedly lowered levels of glucitol which is derived from glucose by reduction with alditol reductase which requires NADPH as a co-factor. It is a matter of debate whether or not ascorbic acid can be biosynthesised by insects. Many mammals, apart from primates, biosynthesise ascorbic acid and thus do not require it as a vitamin. The sequence of metabolites in the biosynthesis of ascorbic acid is glucuronic acid-gulonic acid-gulonolactone-ascorbic acid. Gulonic acid and gulonolactone can be putatively identified in the extracts from *Drosophila* and are significantly lower in the allopurinol treated samples; again, this could be a consequence of a lack of NADPH which is required as a co-factor for the reduction of glucuronic acid to gulonic acid. It has recently been observed that *Drosophila* over-expressing G6PDH have an increased lifespan, which gives an indication of the importance of G6PDH as a source of NADPH and thus in protection against oxidative stress (Legan et al., 2008).

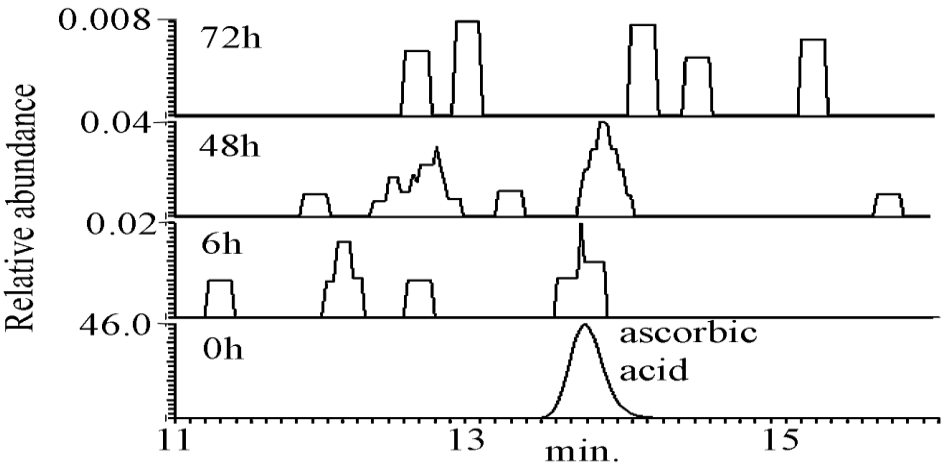

Figure 5-6 Loss of ascorbic acid in *Drosophila* following treatment with allopurinol. Chromatograms were generated by using chromatographic conditions as in 2.12.1.

The induction of oxidative stress by allopurinol is unexpected since there is an extensive literature indicating that it functions indirectly as an anti-oxidant by decreasing production of superoxide as a by-product of XO activity (Pacher et al., 2006), much of the superoxide produced in the human body results from XO activity. However, it is also possible that there is an impact on anti-oxidant levels due to a reduction in uric acid levels, the major concentrations of uric acid are in the Malpighian (renal) tubule and the slow changes uric acid in the whole fly may not reflect the changes in the specific regions of the body. The *ry* mutant, which lacks uric acid, has been shown to be hypersensitive to oxidative stress (Hilliker et al., 1992). Uric acid is believed to be an important anti-oxidant in human serum where it protects ascorbic acid against oxidation possibly via acting as an iron chelating agent (Glantzounis et al., 2005). Depletion of uric acid in serum results in rapid oxidation of ascorbic acid (Sevanian et al., 1991). It was found that mutants of *Drosophila* with impaired XO activity produced higher levels of ROS particularly within their guts (Massie et al., 1991) which might account in the current results for the depleted levels of ascorbic acid in the whole fly. It has been shown that the highest levels of XO in mice occur in the proximal small intestine (Mohamedali et al., 1993). It may be that the allopurinol can affect oxidative stress in two ways; when allopurinol was administered to mice it was found to cause a fall in the levels of both uric acid and ascorbic acid in brain dialysate, but ascorbate levels in brain tissue itself were not reduced (Enrico et al., 1997). It was suggested that the presence of uric acid in extracellular fluids might be more important for stabilising ascorbic acid in extracellular fluid than within tissues.

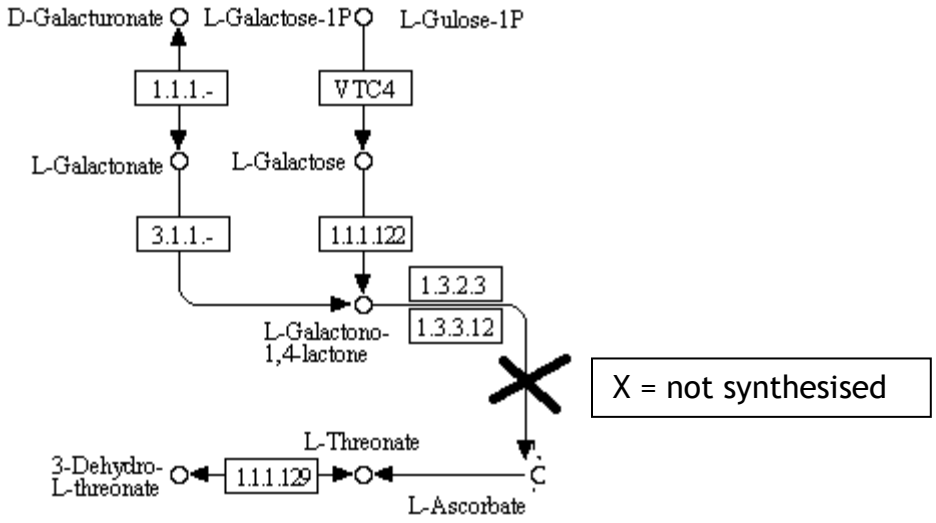

Figure 5-7 Impact of allopurinol on the ascorbic acid pathway: extracted from the KEGG pathway map.

5.5.1 Allopurinol and the kynurenine pathway

Lowered levels of antioxidants may have an effect on the kynurenine pathway. The rate determining step in the pathway is the conversion of tryptophan into formylkynurenine. The enzyme carrying out the conversion is indolamine dioxygenase (IDO) which is a haem based enzyme requiring the iron to be in the iron (II) form for the conversion to occur (Botting, 1995) (Batabyal and Yeh, 2007). *In vitro* ascorbic acid is used as a co-factor for the enzyme since it restores it to its iron (II) form by reducing iron (III), however, *in vivo* the co-factor is not known. In the allopurinol treated flies, levels of formylkynurinine and the downstream metabolites kynurenine, hydroxykynurenine, xanthurenic acid, nicotinic acid and oxoadipic acid are lower than those in the untreated flies. Dihydroxyquinoline, which is also in the kyurenine pathway, goes against the trend and is significantly elevated in allopurinol treated flies. It is possible that the depletion of ascorbic acid impacts on the kynurenine pathway either directly or through failure to maintain a reducing atmosphere and as a consequence

failure to maintain iron in its iron (II) state. However, alternatively the reduction in levels of metabolites in the kynurenine pathway may be due to a reduction in the availability of the superoxide anion which is a co-factor for indolamine 1,3 dioxygenase (IDO) (King and Thomas, 2007). The effects on allopurinol on tryptophan metabolism are of interest since allopurinol is well established as a drug in the management of schizophrenia (Buie et al., 2006), (Dickerson et al., 2009). It has been proposed that its effectiveness in treating schizophrenia is through inhibiting the conversion of adenosine into guanosine since lowered adenosine levels may have a role in the condition. However, it is also well established that schizophrenia and other types of brain disorder can be correlated to increased degradation of tryptophan via the kynurenine pathway (Barry et al., 2009). In addition, in recent years allopurinol has been used as an experimental drug in the treatment of patients who have suffered a stroke (Muir et al., 2008). The severity of a stroke has been correlated with increased degradation of tryptophan via the kynurenine pathway (Darlington et al., 2007). IDO also has a key role in modulating the immune response (King and Thomas, 2007). The picture here is not entirely clear with IDO being induced by interferon-γ in response to infection resulting in increased tryptophan degradation which boosts immune response but at the same time IDO induction has a role in the adaptive immune response and causes immune-suppression which has led to an interest in it as a target for anticancer drugs (Macchiarulo et al., 2009). Some of the difficulty interpreting such contradictory roles for IDO might be attributed to specific co-regulation of enzyme activity and also to localisation of its activity. It has been proposed that IDO and inducible nitric oxide synthase (NOS2) are regulated in a reciprocal fashion (King and Thomas, 2007)) and it was found that in the *ry* mutant that both innately and following infection higher levels of NO were observed (Kim et al., 2001). Thus an increased production of NO can be linked to a removal of xanthine oxidase activity and hence possibly to the reciprocal regulation of NOS2 and IDO with XO also playing a role. In earlier work it was observed that down regulation of kynurenine and hydroxykynurenine occurred in male *ry* flies but not females (Kamleh et al., 2008a). Such arguments become increasingly

tenous but highlight the benefits that would be obtained from bringing in transcriptomics data to support such observations of the metabolome.

5.6 How similar are *ry* mutant and phenocopy of rosy

Although the involvement of *ry* in several biochemical pathways has been demonstrated, the effects of allopurinol are not similar to the effects of *ry*. This might be explained by the fact that the effect of allopurinol is a transient while the effect of lacking *ry* is permanent from birth. Elevated hypoxanthine and xanthine as a result of absence of XDH/XO are accompanied by accumulation of glycerophosphocholine (GPC) and other osmolytes to prevent denaturing of proteins and maintain cell volume. The absence of uric acid in *ry* mutants leads to increase nitrogenous wastes which require more water to excrete them out and eliminate their toxicity. Thus, the hydrolysis of phospholipids may be correlated to the change in cell membrane by alteration of the hydrophilic / lipophilic balance in those compounds conserving water. The *ry* mutant is characterized by significant accumulation of GPC, CDP-choline and CDP-ethanolamine. However, when phenocopied by using allopurinol treatment untreated flies become clearly distinguishable from treated flies. Flies treated with allopurinol show a decrease in those osmolytes to approximately half amounts as normal as seen in figure 5.8. Actually, the attempt to understand how *ry* affects the metabolome has furthered our understanding of the role that lipid degradation may play in osmoregulation, where knowledge is scarce, thus it will be interesting if it is possible to shed light on the impact of salt stress on a specific gene (more details in chapter 7).

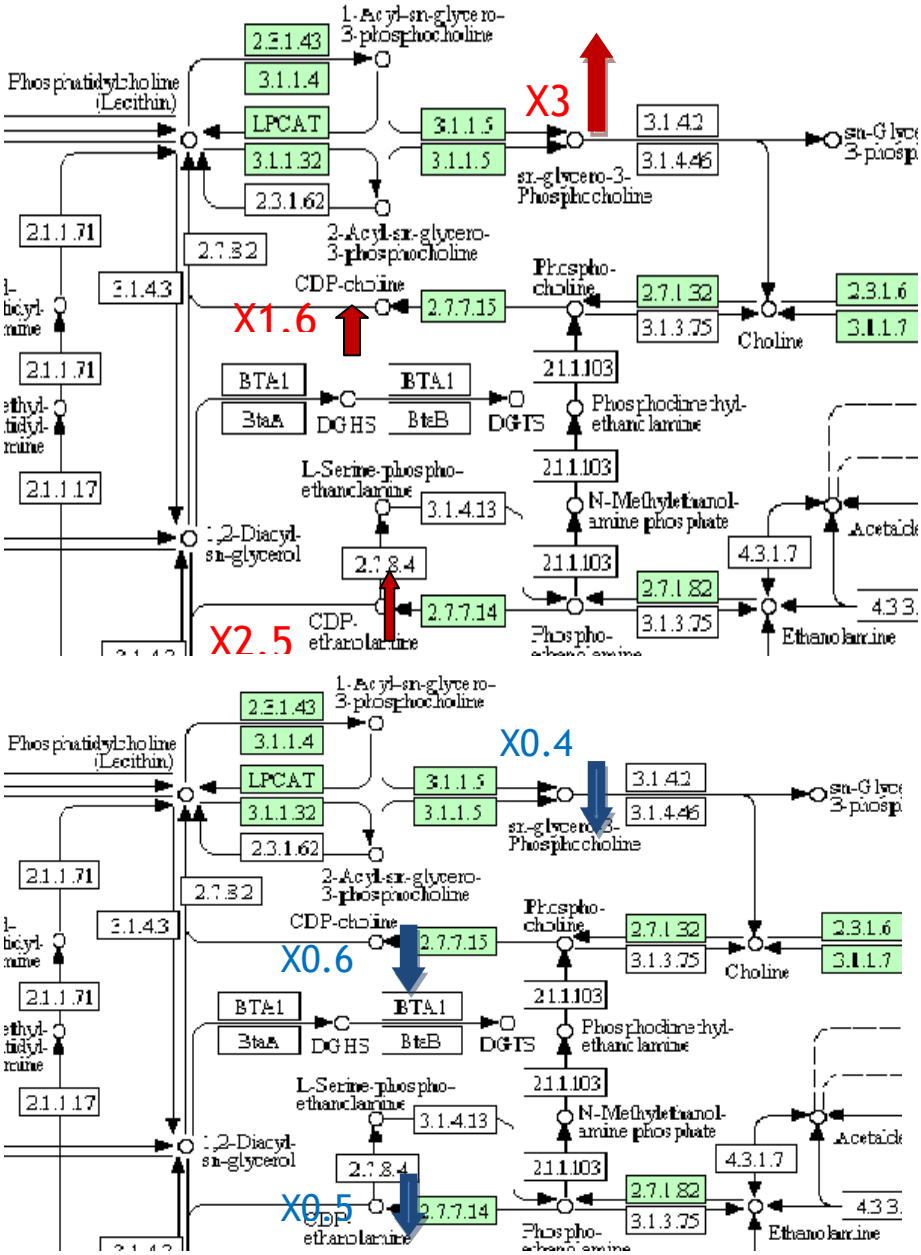

Figure 5-8 Comparison the effect of lack of rosy (upper panel) and allopurinol (lower panel) on osmolyte biosynthesis: extracted from the KEGG pathway map where green colouration indicates to enzymetic pathway involved in lipid matabolism.

5.7 Concluding Remarks

The current chapter has demonstrated the potential value of *Drosophila* as a model organism for uncovering the wider effects of drug molecules. The goal of the study was to phenocopy the effects of the *ry* mutation by using allopurinol and also to observe the metabolic effects. While the expected effects on uric acid metabolism were observed there were a number of unexpected metabolic changes. Most marked was the disappearance of ascorbic acid in the flies. Of most interest in terms of the therapeutic indications for allopurinol was its effect in reducing tryptophan metabolism which ties into the established use of allopurinol in treating schizophrenia and its experimental use in the treatment of patients who have suffered a stroke. It would also be possible to hypothesise on the basis of the effects of allopurinol of tryptophan metabolism that allopurinol might have some value as an immune-modulator. These insights could be accomplished using a simple organism which costs little to procure and maintain and also is very amenable to the production of knock out lines. The introduction of transcriptomic methods to support metabolomic experiments with *Drosophila* will provide a very powerful technique for understanding the ramifications of both genetic mutations and drug action.

6. Chapter six: Study of the Yellow (y) gene using metabonomics

6.1 Introduction

The *Yellow (y)* mutant was one of the first *Drosophila* mutants discovered (Lindsley, 1968). The *Y* mutant encodes a multifunctional protein with close similarity to the major royal jelly protein of honeybees, and similarly contains a 6-bladed beta – propeller motif. According to the *Drosophila* gene expression database, FlyAtlas.org (Chintapalli et al., 2007a), *y* is specifically expressed only in larval salivary glands, suggesting a secretory or digestive function. Royal jelly is secreted from analogous glands in the heads of honey bee workers, suggesting a conserved role for *y*. *Y* proteins share structural similarities with royal jelly proteins and it has been proposed that in the honeybee, such proteins may regulate development epigenetically by promoting DNA methylation (Foret et al., 2009). However, royal jelly also contains the protein royalactin, which is sufficient to induce body enlargement and ovarian development in both *Drosophila* and honeybees (Kamakura, 2011), so *y* does not directly affect fertility in female bees. *Y* is also extensively expressed in the pupal cuticle, where it plays a major role in melanization (Riedel et al., 2011); and expression in the CNS is required for normal male reproductive behaviour (Maleszka and Kucharski, 2000, Ferguson et al., 2011, Drapeau et al., 2006, Drapeau, 2003a). Additionally, *y* flies are sickly and require careful maintenance. So *y* appears to play multiple, quite distinct roles, although its exact biochemical modes of action are still unknown.

It has been proposed that *y* is a structural protein and that it is involved in forming cross-links with the dopamine derivative indole-5,6-quinone during melanisation (Drapeau, 2003a). Another theory is that it acts downstream of DOPA in the formation of melanin; and there is some sequence homology between the *y* protein and dopachrome conversion enzyme (DCE). It has been proposed that to account for the various effects of *y* it must be a hormone-like molecule regulating various processes (Drapeau, 2003b). In previous work we have looked at the effects of a known genetic lesion *ry* on the global metabolite profile in *Drosophila* and found effects on metabolites remote from those directly affected by the lesion (Kamleh et al., 2008b) and also attempted to explain an unknown

genetic lesion (Kamleh et al., 2009b). Given the likely biochemical ramifications of the *y* mutation, this chapter reports the application of hydrophilic interaction chromatography in conjunction with Fourier transform mass spectrometry to elucidate the effects of the *y* gene. The aim of the current study was to use mass spectrometry-based metabolomics to explore the biochemical role of yellow protein in *Drosophila melanogaster*, both larvae and adult flies, in a comparison with wild type flies.

6.2 Larval and adult metabolomes differ markedly

Using our standard screening method for metabolites on a ZicHILIC column it is possible to observe around 300-500 non-lipid metabolites in *Drosophila* whole flies (Kamleh et al., 2009b). Since the expression of *y* is highest in larvae it was firstly decided to study the larvae of *y* and OR flies to apply global metabolomics, in order to seek insight as to its function; and to test the specific hypothesis that *y* impacts on histone function either through histone methylation or DNA methylation. In previous work it has been found that even in a model system such as *Drosophila* metabolic differences within a strain can disappear upon repetition of an extraction experiment (Kamleh et al., 2009b). Thus it is preferred to repeat extractions at least twice several days apart in order to be confident that metabolic differences are stable. In the current case the extractions were repeated three times over a period of two months. It is not feasible to consider such repeat runs in a single group since drifts in chromatographic retention time and instrument sensitivity make it difficult to compare data sets acquired where there is a significant time lapse between acquisition. The most striking observation from the data in Table 6-1 is that there are a number of metabolites present which are simply not observed in the adult flies. Table 6-5 lists the metabolites which vary least between *y* and OR to give some confidence that there is a degree of normalisation between the two sample types.

6.3 Metabolic differences between y and wild-type in larval stage

Table 6-1 summarises the putatively identified unusual metabolites present in the larvae and also metabolites where there is a marked variation between *y* and OR. Novel metabolites were individually curated, requiring a mass accuracy within 1.5 ppm of the proposed structure, and with no sensible elemental composition within 3 ppm of the assigned elemental composition based on the elements C, N, H, O, P and S. All the metabolites listed in table 1 were also checked manually to confirm that they were not isotope peaks, adducts, fragments or dimers of more intense ions. Table 6-2 shows the MS^2 data for some the more unusual metabolites which help confirm their structures. The unusual metabolites present include a compound putatively identified as tyrosine phosphate. It does not vary between *y* and OR but its presence in the larvae is not readily explained unless it serves as a high energy phosphate metabolite or possibly and osmolyte. Arginine phosphate is higher in OR than *y* and is used extensively in invertebrates as a high energy reserve metabolite analogous to creatine phosphate in mammals. The levels of arginine phosphate are lower in *y* than OR and this might indicate increased levels of physiological stress in *y* during larval development.

Table 6-1 List of metabolites and metabolites displaying significant differences between y and OR analysed. Four extracts of 50 *y* and 50 OR larvae were prepared on 3 occasions over a two month time period. "Ratio" is of y: OR signal.

Compounds	MH^+/M^-	Rt	Replicate 1		Replicate 2		Replicate 3	
		min	Ratio	P value	Ratio	P value	Ratio	P value
Melanin biosynthesis								
Dihydroxyindole	150.0545	8.0	3.30	1.80E-02	4.15	1.90E-02	2.27	5.50E-02
phenylalanine	166.0864	12.4	2.21	7.10E-06	2.18	3.90E-03	1.99	3.10E-04
tyrosine	182.081	14.9	1.73	5.90E-03	2.12	9.30E-02	3.32	1.70E-04
dopamine acetate	196.097	7.5	0.52	1.70E-03	2.30	1.80E-01	0.523	4.00E-01
DOPA	198.0761	17.3	2.67	3.00E-02	3.29	1.30E-03	3.23	5.20E-03
Glycyl-dopa	255.0978	17.1	1.34	2.10E-01	1.96	1.40E-01	1.98	5.80E-02
Dihydroxy indole GSH	455.1231	17.2	0.90	8.20E-01	ND		0.64	3.30E-01
Lysine metabolism								
lysine	147.1129	23.4	2.23	1.20E-02	2.07	3.70E-02	1.62	3.90E-02
methyllysine	161.1287	23.0	0.62	7.70E-04	0.72	4.30E-02	0.83	2.70E-01
2-aminoadipate	162.0763	16.1	2.00	2.20E-02	2.28	2.90E-02	1.38	1.30E-01
carnitine	162.1127	15.4	0.60	2.30E-08	0.60	6.90E-04	0.81	1.50E-02
Dimethyl lysine	175.1442	23.1	0.41	3.00E-05	0.39	1.80E-04	0.56	2.40E-02
Lysine acetate	189.1236	16.4	6.19	4.70E-03	4.50	5.00E-03	3.16	4.70E-05
Trimethyl lysine	189.1599	23.8	0.36	3.30E-03	0.45	2.00E-03	0.61	1.30E-01
diaminopimelate	191.1028	16.6	0.66	1.30E-02	0.51	7.90E-03	0.77	2.80E-03
Aspartyl lysine	262.1397	21.5	0.01	5.80E-05	0.05	1.20E-01	0.064	7.50E-03

saccharopine	277.1395	20.8	8.20	1.80E-02	9.50	5.80E-03	5.093	3.70E-02
Fructosyl lysine	309.1658	23.8	0.47	3.70E-03	0.78	3.30E-02	0.87	5.00E-01
Chitin biosynthesis								
N-acetylglucosamine	222.0975	13.5	0.10	3.20E-02	0.50	5.80E-01	0.198	2.00E-01
N-acetylglucosamine isomer	222.0975	15.0	0.06	3.00E-02	0.54	6.7 E-01	0.045	2.10E-01
glucosamine phosphate isomer	260.0532	19.9	1.55	4.20E-03	0.95	6.30E-01	0.374	2.30E-01
Glucosamine phosphate isomer	260.0532	22.2	0.14	6.50E-04	ND	ND	0.024	4.70E-03
Neuraminic acid	268.1027	20.0	1.71	5.70E-04	3.44	4.40E-04	2.003	2.00E-03
Glycosamine acetate phosphate	302.0638	19.8	0.35	1.20E-02	0.66	4.60E-02	0.58	2.30E-03
cytidine monophosphate	324.0594	20.4	2.40	3.20E-02	7.77	9.80E-03	3.51	4.20E-02
UDP Glc NAc	608.0886	25.8	1.16	1.70E-01	2.01	4.50E-02	1.812	6.50E-03
Tryptophan metabolism								
kynurenic acid	190.05	8.9	2.52	4.80E-03	2.29	4.10E-03	3.289	2.00E-04
Xanthurenic acid	206.0449	10.6	2.31	8.90E-03	2.68	5.90E-02	7.904	2.90E-03
hydroxytryptophan	221.0923	12.8	0.35	4.50E-02	0.12	4.60E-03	0.26	6.30E-02
hydroxykynurenine	225.087	14.2	0.40	3.70E-06	0.35	8.70E-04	0.43	1.10E-02
GSH oxidative stress								
Methionine S-oxide	166.0534	18.3	6.29	3.40E-03	3.78	1.80E-02	3.26	2.00E-04
cystathione	223.0749	21.8	2.13	5.00E-02	2.71	2.90E-02	1.81	1.80E-01
GSH	308.0912	16.3	0.05	9.50E-06	0.00	3.60E-01	0.01	3.30E-01
GSH-cysteine	427.0954	21.0	0.43	1.10E-02	0.41	2.60E-01	0.34	2.20E-01
GSSG	613.1594	20.5	0.52	7.10E-02	0.48	2.10E-01	0.26	1.70E-01
Methylation								
methionine	150.0584	13.9	2.52	2.00E-03	1.47	9.60E-02	1.70	2.90E-02

S-adenosylmethionine	399.1448	24.6	2.25	5.20E-03	2.13	1.50E-02	2.263	1.70E-03
Purine metabolism								
guanine	152.0544	13.9	2.41	4.10E-03	1.39	1.60E-01	1.50	6.20E-02
sepiaterin	238.0936	10.3	0.03	2.90E-03	0.06	1.90E-02	0.246	1.90E-01
biopterin	238.0938	13.2	0.63	1.20E-04	0.56	1.70E-02	0.311	2.20E-01
dihydrobiopterin	240.1093	13.9	0.25	6.50E-04	0.18	6.90E-04	0.263	2.00E-02
methyladenosine	282.1185	19.4	2.70	2.80E-03	10.70	3.80E-03	1.02	8.80E-01
methylguanosine	298.1146	11.1	0.43	3.90E-04	0.25	1.60E-03	0.552	5.20E-02
Misc. Metabolites								
threonine	120.0657	17.4	1.96	7.50E-03	2.43	1.10E-02	1.95	8.20E-03
asparagine	133.0609	18.5	0.49	1.90E-02	0.45	8.30E-03	0.34	2.00E-03
glutamine	147.0765	18.2	0.60	1.70E-02	0.55	7.60E-03	0.71	1.50E-04
histidine	156.0769	22.6	0.63	1.00E-04	0.65	1.40E-02	0.61	4.20E-02
Choline phosphate	184.0734	22.4	0.32	2.00E-03	0.30	9.60E-06	0.41	9.50E-06
dimethylarginine	203.1391	22.5	0.22	2.30E-02	ND	-	0.61	3.10 E-02
cytidine	244.093	17.8	1.66	1.80E-02	2.59	6.70E-03	0.485	1.40E-02
uridine	245.077	10.8	1.17	2.90E-01	2.17	6.80E-02	0.674	2.60E-03
Arginine phosphate	255.0853	22.8	0.56	7.00E-04	0.35	1.40E-04	0.326	3.20E-03
Tyrosine phosphate	262.0475	20.7	1.06	3.50E-01	1.48	1.60E02	0.264	3.60E-02
arginosuccinate	291.1301	22.0	0.38	1.20E-03	0.45	1.60E-02	0.115	7.30E-03
riboflavin	377.1454	9.5	3.23	1.10E-03	2.65	2.10E-02	2.842	1.40E-04

Table 6-2 MS^2 data for some of the more usual metabolites extracted from the larvae. Obtained with a CID of 40V.

Metabolite	MH^+	MS^2 fragments
Arginine phosphate	255	238 (-NH_3), 192 (-OH-HCOOH), 175 (-HPO_3)
Glycyl DOPA	255	76 (glycine)
Tyrosine phosphate	262	216 (-HCOOH), 199 (-HCOOH-NH_3)
Aspartyllysine	262	245 (-NH_3), 147 (-glutamyl)
Neuraminic acid	268	250 (-H_2O), 232 (-2xH_2O), 214 (-3xH_2O)
Saccharopine	277	259 (-H_2O),213 (-H_2O, -HCOOH), 195 ((-2H_2O, -HCOOH).

6.4 Melanisation

Y is famously a visible mutant of melanisation, and antagonistic to *ebony*. However, *y* appears to lack homology to known enzymes in the tyrosinase/dopa pathways, but rather supports the activity of dopachrome-converting enzymes Yellow-f and Yellow-f2 (Han et al., 2002). As might be expected there is thus a marked effect of the absence of *y* protein on metabolites in the pathway of eumelanin biosynthesis (Fig. 6-1) with phenylalanine, tyrosine, DOPA and dihydroxyindole (DHI) consistently accumulating in all three batches of *y* larvae analysed. There is a tendency for levels of dopamine acetate to be lower in *y* but this is not consistent. Dopamine acetate is not an intermediate in melanin biosynthesis but is involved as a cross-linking agent in cuticle development since the acylation of the amine group blocks the possibility of it cyclising to form dopachrome, the presence of a compound putatively identified as DOPA-glycine in the extracts may also fulfil this function. A widespread theory of the action of *y* is that it governs dopachrome conversion. However, the presence of DHI in *y*, which is an immediate precursor of eumelanin, indicates that it is not simply lack of a precursor which blocks eumelanin biosynthesis. The only enzymatic step between DHI and eumelanin is catalysed by tyrosinase which is used twice in the pathway leading to DHI. A clue to the fate of DHI not used in melanin biosynthesis is given by the presence of a

relatively abundant peak which corresponds to the glutathione (GSH) adduct of DHI (Fig6-2). The chromatographic trace shows a typical "thiol reaction product" with four peaks being present which could correspond to the available positional isomers from the reactive sites on the aromatic and indole rings of DHI. The levels of DHI-GSH do not differ between *y* and OR. Apart from the eumelanin biosynthesis pathway there are number of other metabolic pathways that are strikingly affected in *y*.

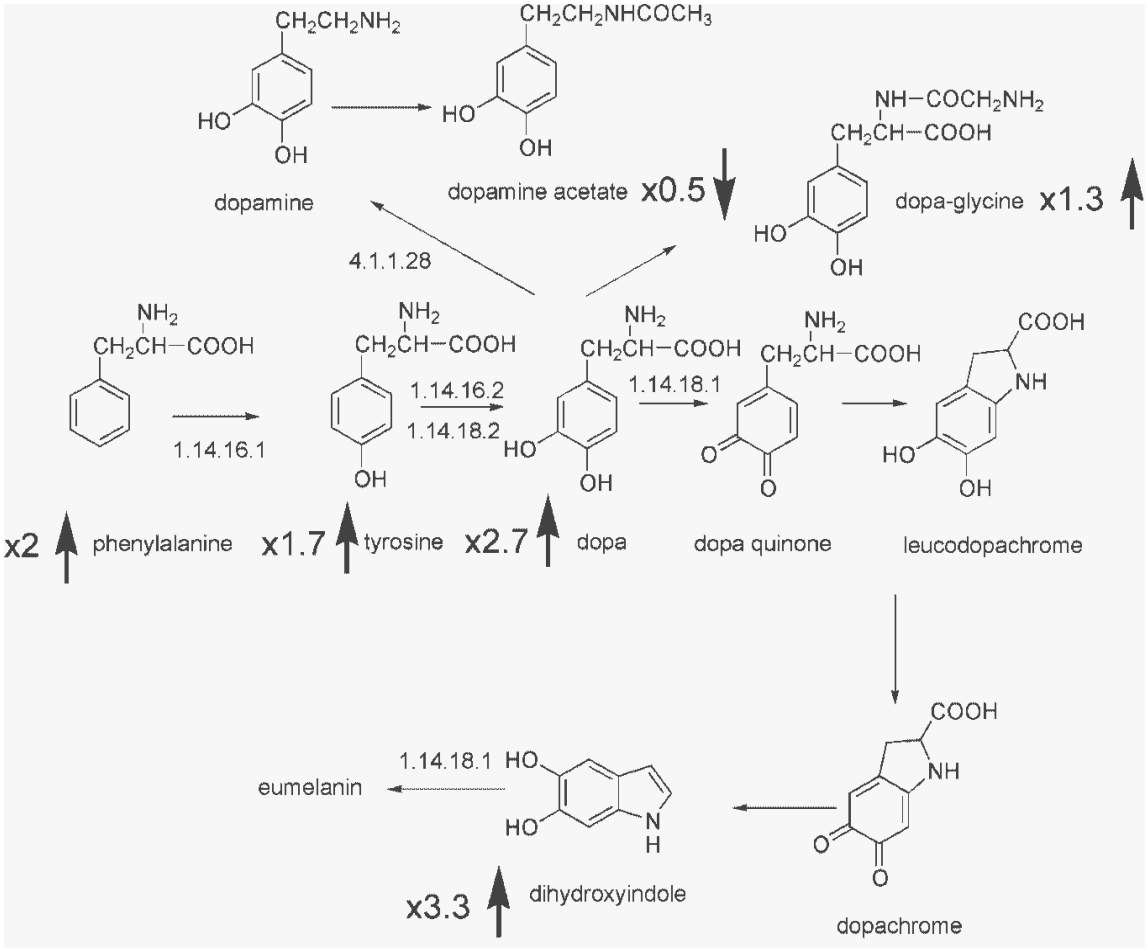

Figure 6-1 Impact of *y* mutation on eumelanin biosynthesis with known *Drosophila* enzymes indicated, and fold changes for metabolites for *y* versus OR (from Table 6-1) shown in arrows.

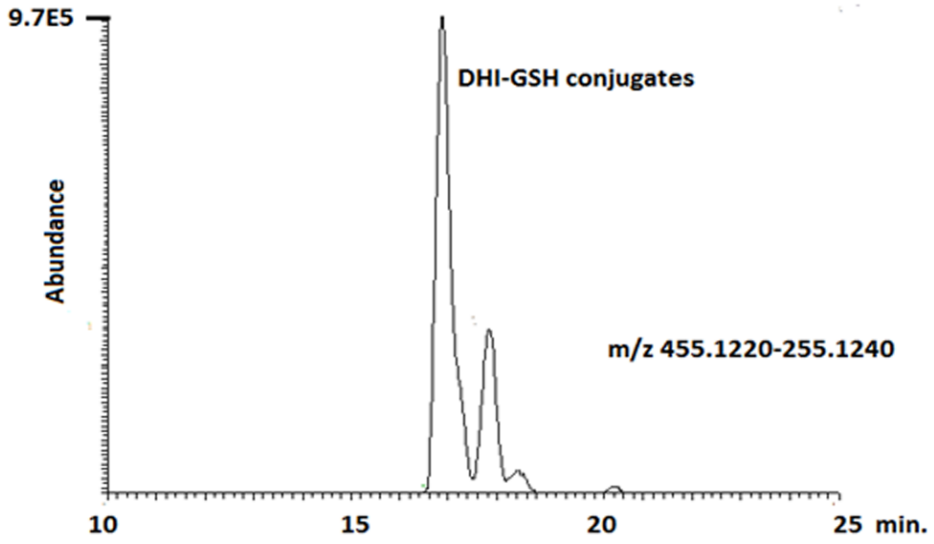

Figure 6-2 Extracted ion trace showing the putatively identified GSH conjugates of DHI

6.5 Lysine Metabolism

The largest number of metabolites within a single pathway that are affected by the *y* mutation are related to lysine metabolism (Fig 6-3). A major metabolite of lysine in the larvae is fructosyl lysine which has only been reported as a non-enzymatic glycation product deriving from the reaction between lysine residues within proteins and glucose. Lysine is consistently elevated in *y* about two times and the lysine metabolite saccharopine is elevated between 5 and 10 times compared to OR. The elevated levels of saccharopine are interesting in view of the recent finding that the ketoglutarate reductase (dLKR)/saccharopine dehydrogenase (SDH), the enzyme responsible for saccharopine formation, has been found to suppress ecdysone-mediated cell death (Cakouros et al., 2008). dLKR/SDH suppresses the activity of ecdysone by binding to histones H3 and H4 thus inhibiting arginine methylation within the histone tails. The function of dLKR/SDH appears to be to modulate ecdysone action and its expression was found to be highest at the larval/pupal stage. Ecdysone has been shown to regulate late response genes in the chitin biosynthesis pathway. Reduced levels of *dKLR*/*SDH* expression

caused reduced size of fly wings compared to wild type. In the current case, the presence of high levels of saccharopine suggests an expression of high levels of dLKR/SDH in *y*. The most striking difference in lysine metabolism between *y* and OR was the presence of a dipeptide aspartyl-lysine which is almost completely absent from *y*. There is no literature on this peptide except that it is present in proteins such as collagen where the aspartyl-lysine linkage can be used to cross-link protein chains. The structure of aspartyl-lysine is very similar to that of saccharopine and it is possible that it might compete for the binding site in dLKR/SDH. Modification of lysine residues is an aspect in comparing *y* and OR genes. In *y*, lysine acetate levels are elevated > x3 when compared with OR and methyl-, dimethyl and trimethyllysine are 2-3 times lower than in OR. Both acetyl-lysine and methylated lysines are derived from the turnover of histones and provide two strategies for allowing chromatin remodelling and thus control of gene transcription. Acetylation of lysine removes the electrostatic interaction between the lysine residues in histone and the phosphate backbone of DNA allowing access of transcriptional enzymes (Rahman et al., 2004). Lysine itself can act as a source of acetyl-CoA for the acetylation since the catabolic pathway *via* saccharopine produces acetyl CoA. *Y* larvae also contain elevated levels of aminoadipate which is the next step in the lysine degradation pathway. This indicates that the elevated levels of saccharopine may be due to increased enzyme expression rather than pathway blockage.

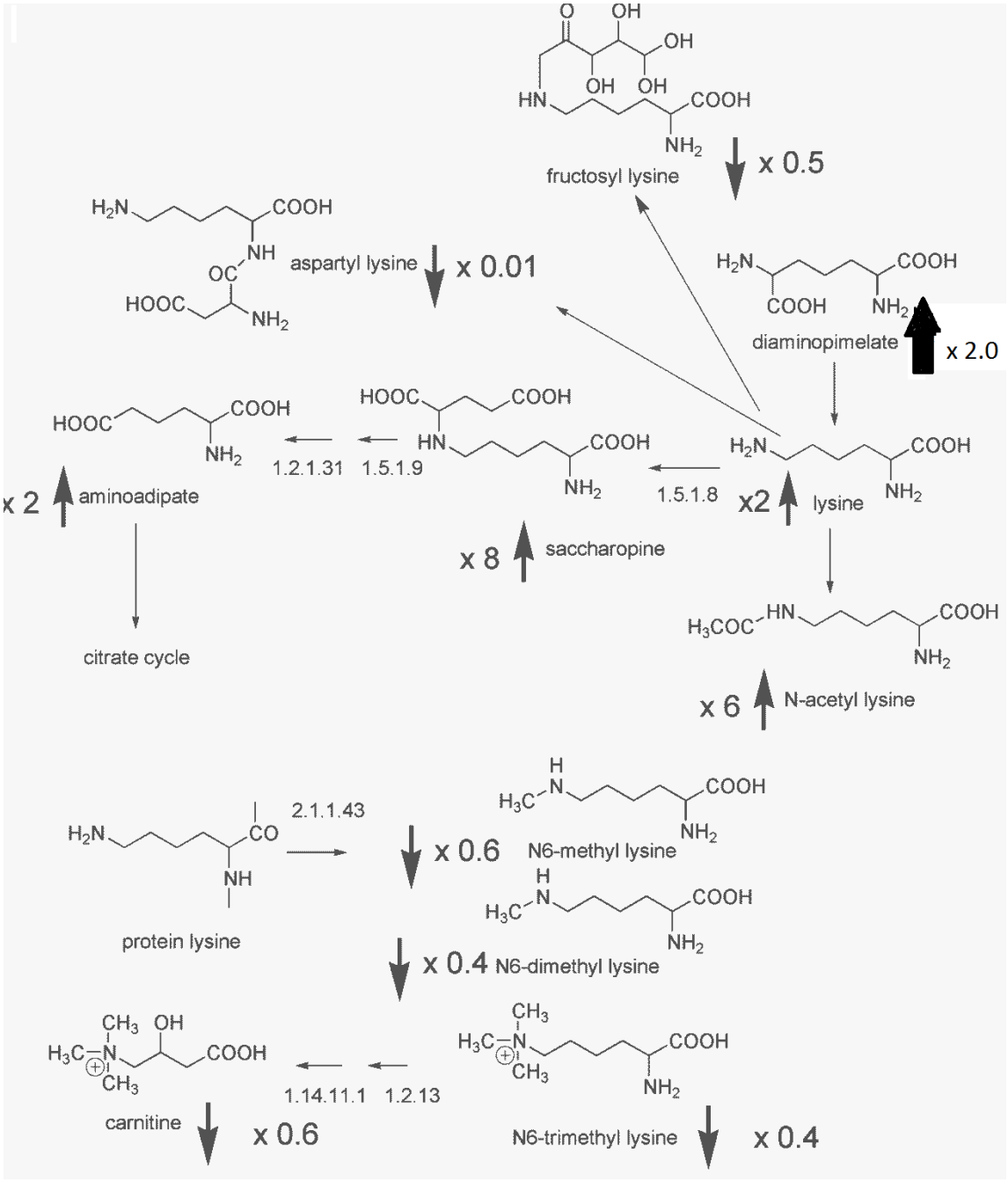

Figure 6-3 Impact of *y* mutation on lysine catabolism with known *Drosophila* enzymes indicated, and fold changes for metabolites for *y* versus OR (from Table 6-1) shown in arrows. Note that there are no enzymes present in drosophila capable of synthesizing lysine; as in other higher animals, lysine is an essential amino acid.

6.6 Impact of *Y* on Histone Methylation

Y is a major constitutent of Royal jelly protein, which when fed to honeybee larvae, is capable of epigenetic reprogramming of drones into queens (Kucharski et al., 2008). It is thus of interest that several metabolic changes observed in *y* larvae were consistent with changed histone modification. Enzymatic deacetylation of lysine acetate within histones results in increased histone-DNA binding and thus gene silencing. Similarly, methylation, particularly trimethylation which introduces a permanent positive charge onto lysine residues within histones, increases the interaction between histones and DNA blocking access of transcriptional enzymes and promoting gene silencing. Methylation of histones and DNA are believed to work in concert to promote gene silencing (Patel et al., 2011). Demethylation of lysine or DNA allows access to transcriptional enzymes and thus reverses gene silencing. Thus, there is some indication from the decreased levels of methylated lysines and elevated levels of acetyl lysine in *y* that the gene might be involved in epigenetic processes involving histone methylation and acetylation. Dimethylarginine which is also found in histone proteins is also found at lower levels in *y* compared with OR. However, there is a limitation in purely metabolomic data since it is simply not known if the modified lysines seen in these samples reflect the rate of degradation of histone proteins. Histone proteins are steadily turned over (Zee et al., 2010) and might be expected to contribute modified methyllysines, acetyllysine and dimethylarginine to the metabolome. If they do, then one might propose that elevated levels of acetyllysine reflect increased expression of certain genes in the absence of *y*. It has been suggested that histone acetylation may occur under stress (Rahman et al., 2004) conditions, for instance where enzyme up-regulation occurs in order to neutralise the effects of reactive oxygen species. It is likely that *y* may suffer from increased oxidative stress because of the absence of melanin and this is reflected in the very low levels of GSH in *y* and the high levels of methionine S-oxide. Alternatively GSH depletion might be through its reaction with a reactive species such as 5, 6-indole quinone since the IDH-GSH conjugate can be observed. This would explain why GSSG is also lower in *y* since the GSH used to neutralise reactive

molecules will not form GSSG which is only formed when it is used as a reducing reagent such as in the conversion of NAD+ to NADH or in the neutralisation of reactive oxygen species. In the case of OR it is possible to propose that the high levels of methylated lysines may be due to a higher rate of histone turnover possibly reflecting some differences in the level of gene expression between OR and *y*. Thus all the metabolite evidence suggests, as proposed by Drapeau (Drapeau, 2003b), that *y* has a broader regulatory role than the simple control of melanin biosynthesis and that a number of biosynthetic pathways are influenced by it. Trimethyllysine derived from protein catabolism is the source of carnitine (Vaz and Wanders, 2002) and elevated levels of trimethyllysine are reflected by elevated levels of carnitine in OR compared to *y*. Methylated metabolites present a theme running through the data. In *y* the precursors required for methylation, methionine and S-adenosyl methionine- accumulate as if they were being underutilised. This suggests some differences in the regulation of methylation between OR and *y*. In order to determine whether or not *y* is directly involved in controlling the level of methylation of histone proteins, histones were isolated from OR and *y* larvae and subjected to a simple acid hydrolysis. Although the isolated proteins were rich in methylated lysine residues, particularly trimethyl lysine, there were no significant differences in the degree of methylation of histones from *y* and OR, at least in this small sample (n=4). In addition to methylated lysines there was an abundance of dimethylarginine present in the hydrolysate from the histones. However, there was no significant difference between dimethyl arginine in hydrolysates from *y* and OR. Table 6-3 summarises the data obtained for methyllysines and arginine in OR and *y* normalised to the mean areas for the peaks for lysine or arginine in the hydrolysate.

Table 6-3. Methylated lysines and arginine obtained by hydrolysis of histone proteins isolated from *y* and OR. Hydrolysis was carried out on 4 aliquots of the extract. The levels are expressed as a % of the mean peak areas compared against the mean peak area for lysine.

Amino acid	MW	Rt	Level in OR % of lysine	Level in *y* % of lysine
Methyl lysine	163.1309	25.4	1.01	0.79
dimethyllysine	175.1437	25.5	2.33	1.91
trimethyllysine	189.1596	26.1	3.58	3.64
dimethylarginine	203.1503	24.9	1.64	1.87

6.7 Impact of *Y* on Cuticle Biosynthesis

The *y* mutation has been found to cause malformation of the cuticle and this leads to *y* larvae moving in an unusual way compared to wild type. Microscopical examination has revealed that the spicules on the surface of the larvae are arranged in a disorganised fashion (Inestrosa et al., 1996). In *y* levels of N-acetylglycosamines (NAG) (glucosamine and galactosamine co-elute from the ZICHILIC column as seen in fig 6-4) and a glycosamine phosphate (this compound elutes earlier than glucosamine and galactosamine phosphate standards) tend to be lower in *y* than in OR. A more immediate chitin precursor, corresponding in retention time to the standard for N-acetylglucosamine 6-phosphate (the standard co-elutes with N-acetylgalactosamine 6-phosphate), is consistently lower in *y*. The rate limiting enzyme in this pathway is glucosamine 6-phosphate synthetase (GPS) which converts fructose 6-phosphate into glucosamine 6-phosphate (Merzendorfer and Zimoch, 2003), glutamine is involved as a co-factor in this conversion and its levels in *y* are about 60% of those in WT as seen in fig 6-5. Uridine diphosphate (UDP)-NAG is formed by the reaction of NAG 1-phosphate with UDP and UDP-NAG can then be employed to form chitin and in other reactions such as glycoprotein formation. UDP-NAG is an allosteric inhibitor of GPS and the

elevated levels of UDP-NAG in *y*, significantly elevated in two batches, would suggest that this pathway may be less active in *y*. The chitin pathway branches at NAG and NAG can go on to make chitin or can go towards N-acetylneuraminic acid (NAN) which becomes incorporated into glycoproteins. Neuraminic acid is more often found in biological systems as NAA but it is the deacetylated form of NAA, neuraminic acid, which is found to be elevated in the *y* mutant suggesting that NAG is being channelled in this direction rather than into chitin. It has been proposed that correct formation of chitin structures within the cuticle is required for correct pigmentation and the lack of pigmentation in *y* might be due to a lack of localisation of the enzymes required to make melanin within the malformed cuticle. The complex effects within this pathway again suggest that *y* is responsible for modulation of several pathways. The levels of chitin precursors are low and this may account for some of the difficulties in finding completely consistent batch to batch differences between *y* and OR in this pathway.

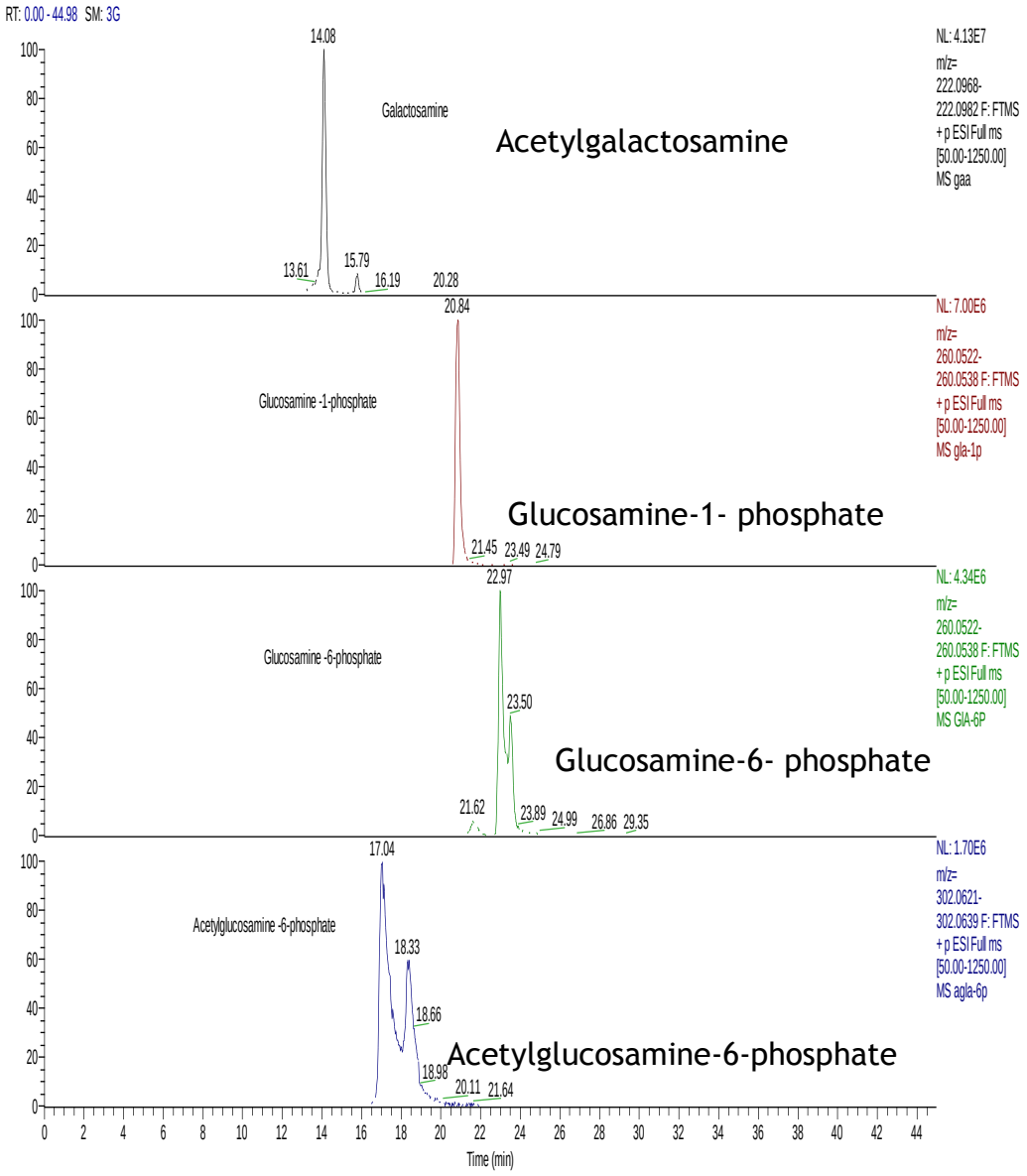

Figure 6-4 Extracted ion traces for Galactosamine, Glucosamine-1-phosphate, Glucosamine-6-phosphate and Acetylglucosamine-6-phosphate showing their elution order by ZIC-HILIC column. Chromatograms were generated by using Chromatographic conditions as in 2.12.1.

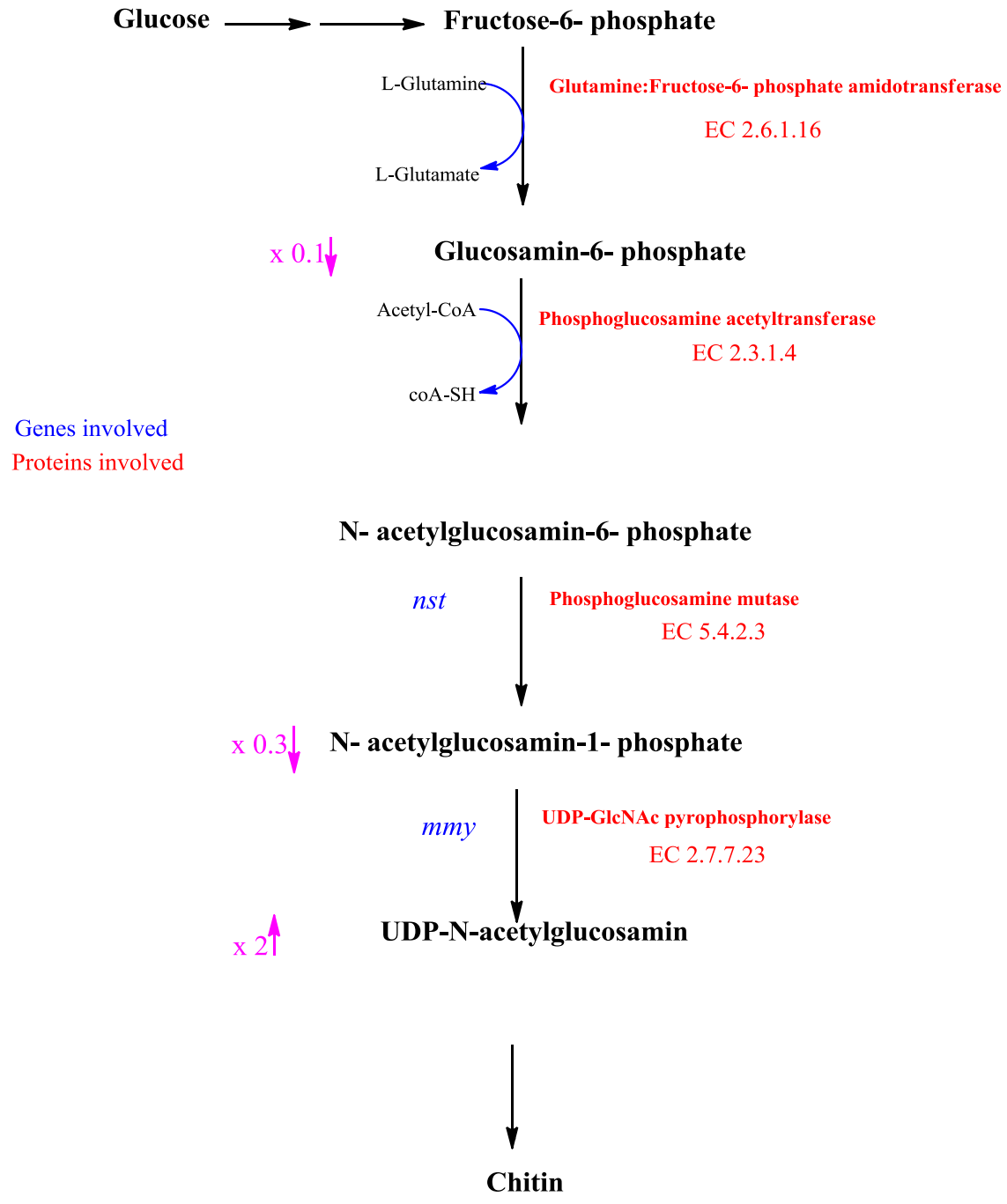

Figure 6-5 taken from (Merzendorfer and Zimoch, 2003) showing Impact of *y* mutation on chitin biosynthesis with known *Drosophila* enzymes indicated, and fold changes for metabolites for *y* versus OR (from Table 6-1) shown in arrows.

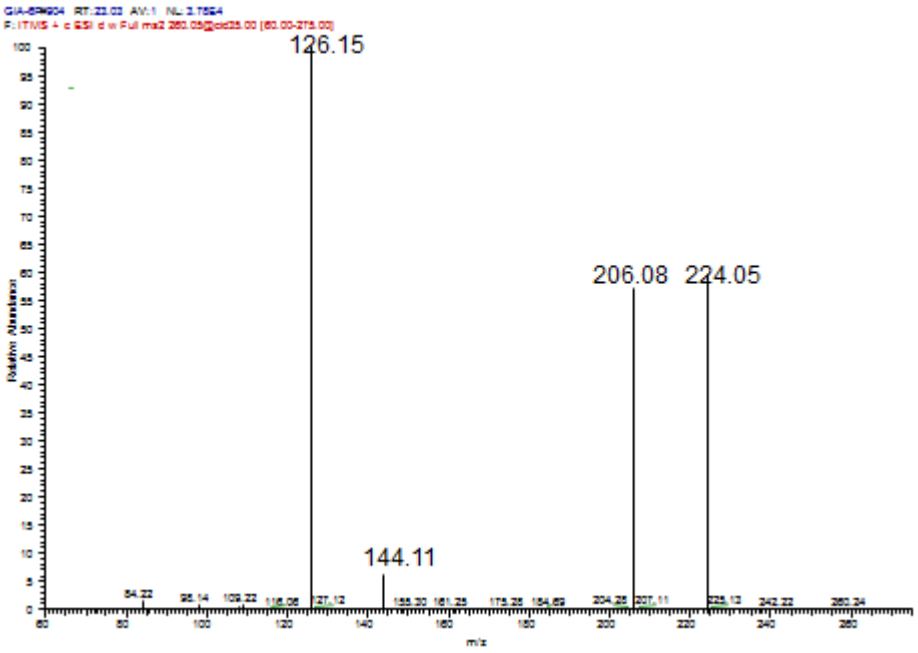

Figure 6-6 Positive ion MS^2 spectrum of Glucosamine-6- phosphate at 35Vgenerated from [M+H] at m/z 260.053 showed product ions at m/z 224 , 206, 144 and 126 which were considered to be $[M+H–2H_2O]^+$, $[M+H–3H_2O]^+$ $[M+H–H_3PO_4-H_2O]^+$ and $[M+H– H_3PO_4- 2H_2O]^+$ respectively.

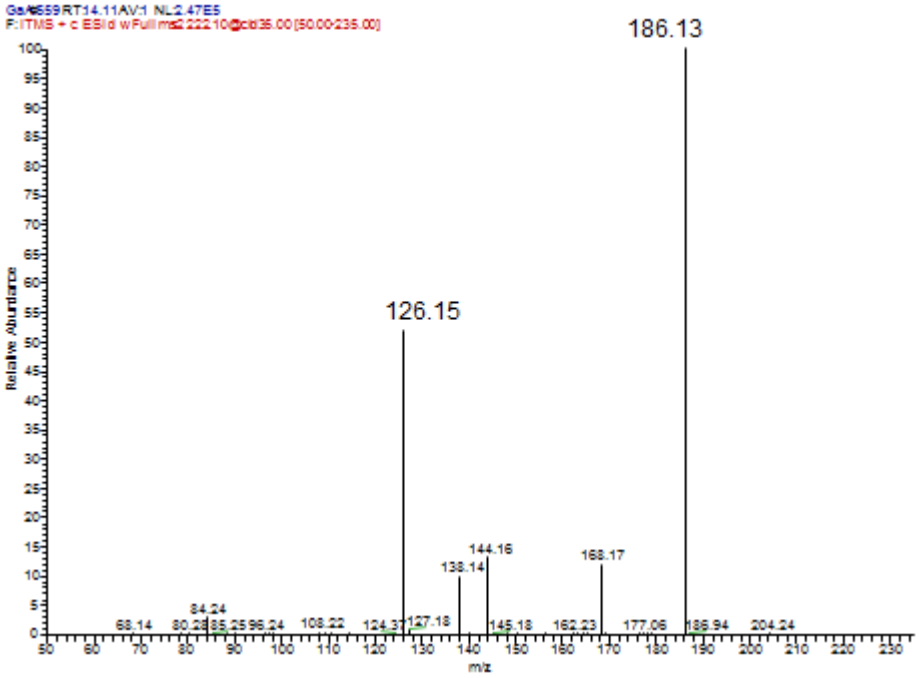

Figure 6-7 Positive ion MS/MS spectrum of acetylgalactosamine generated from [M+H] at m/z 222.975 showed product ions at m/z 186 and 126 which were considered to be $[M–2H_2O+H]^+$ and $[M–C_2H_8O_4+H]^+$ respectively.

6.8 Other Changes

Aside from decreased levels of free methylated lysines in *y* compared to OR, choline phosphate and methylguanine and which require methylation reactions in their biosynthesis, are higher in OR. While methionine and S-adenosyl methionine which supply the methyl groups used in methylation reactions are elevated in *y*. Since it has been proposed that royal jelly proteins may be involved in epigenetic modification of DNA via methylation (Kucharski et al., 2008) and it was decided to examine DNA isolated from OR and *y*. DNA/RNA was isolated from OR and *y* larvae and enzymatically digested to yield free DNA/RNA bases and then analysed by LCMS. All of the methylated bases detected were derived from RNA and contained ribose rather than deoxyribose and no modified DNA bases were detected. It was possible to see methylated bases to a level of *ca* 0.1 % of the non-methylated bases (Fig. 6-8), there was no significant difference in the levels of methylated RNA bases between OR and *y*. Table 6-4 summarises the data obtained for DNA and RNA bases isolated by hydrolysis. The levels of biopterins are much lower in *y* than OR. Dihydrobiopterin is required as a co-factor in the biosynthesis of tyrosine and 5-hydroxytrytophan. 5-hydroxytryptophan levels are lower in *y* but tyrosine levels are high, however, tyrosine may simply accumulate due to lack of its utilisation in melanin biosynthesis. Tryptophan metabolism is also affected in the kynurenine pathway with hydroxykynurenine levels being lower in *y* and levels of the downstream metabolites in this pathway kynurenic acid and xanthurenic acid being elevated. Both kynurenic and xanthurenic acids are produced by the enzyme L-kynurenine:2-oxoglutarate aminotransferase (KOA). The gene coding for this enzyme is orthologous with 2-aminoadipate transaminase (AT) which is responsible for the formation of oxoadipate from aminoadipate in the lysine degradation pathway. KEGG does not list AT as being present in *Drosophila*, however, KEGG does indicate that KOA is present in *Drosophila* thus it is possible that KOA fulfils the same function as AT in *Drosophila*. Thus increased levels of kynurenic acids and xanthurenic acids may be linked to the increase in lysine degradation products.

Table 6-4. DNA and RNA bases present in DNA/RNA extracted from *y* and OR larvae.

DNA/RNA Bases	MW	Rt	Fragments obtained in HCD cell
deoxycytosine	228.0981	19.7	112.05 ($C_4H_6N_3O$ 0.28 ppm)
deoxythymidine	243.0977	7.1	127.05 ($C_5H_7NO_2$ 0.35 ppm)
cytosine	244.0927	22.4	112.05 ($C_4H_6N_3O$ 0.01 ppm)
uridine	245.0767	12.7	113.03 ($C_4H_5NO_2$ 0.3 ppm)
deoxyadenosine	252.1090	15.0	136.06 ($C_5H_6N_5$ 0.80 ppm)
Cytosine deoxyhexose	258.1086	18.0	112.05 ($C_4H_6N_3O$ 0.37 ppm)
methylcytosine	258.1081	21.8	126.0662 ($C_5H_8N_3O$ -0.15 ppm)
thymidine	259.0934	7.4	127.05 ($C_5H_7NO_2$ 0.35 ppm)
deoxyguanosine	268.1040	15.0	152.06 ($C_5H_6N_5O$ -0.17 ppm)
adenosine	268.1040	17.0	136.06 ($C_5H_6N_5$ 0.72 ppm)
methyladenosine	282.1201	15.0	150.07 ($C_6H_8N_5$ 0.05 ppm)
Adenine deoxyhexose	282.1200	14.4	136.06 ($C_5H_6N_5$ -0.75 ppm)
Methyl adenosine	282.1198	18.1	150.07 ($C_6H_8N_5$ -1.5 ppm)
Guanosine	284.1000	16.1	152.06 ($C_5H_6N_5O$ 0.22 ppm)
Dimethyladenosine	296.1356	13.2	164.09 ($C_7H_{10}N_5$ –1.1 ppm)
Guanine deoxyhexose	298.1148	13.4	152.06 ($C_5H_6N_5O$ -0.42 ppm)
Methylguanosine	298.1146	14.1	166.06 ($C_6H_8N_5O$ 0.08 ppm)
Methylguanosine	298.1148	14.5	166.06 ($C_6H_8N_5O$ 0.08 ppm)
Dimethylguanosine	312.1306	13.2	180.09 ($C_7H_{10}N_5O$ -0.37 ppm)

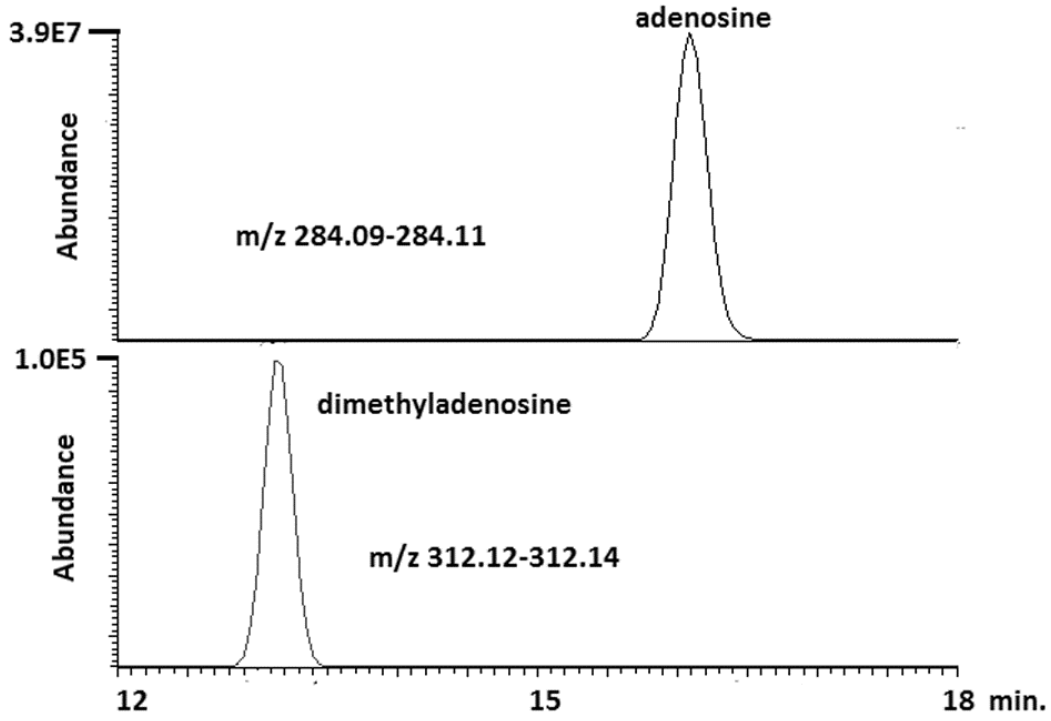

Figure 6-8 Extracted ion traces for guanosine (upper panel) and dimethylguanosine (lower panel) in a RNA/DNA hydrolysate giving an indication of the dynamic range available for detection of modified DNA/RNA bases. Chromatograms were generated by using Chromatographic conditions as in 2.12.1.

Table 6-5 Some stable metabolites which do not vary between OR and *y* larvae for two of the batches.

Mass (amu)	Rt min.	Identity	Ratio *y*/OR	P-value	Ratio *y*/OR	P-value
204.1232	12.5	Acetylcarnitine	0.79	1.70E-01	0.97	5.00E-01
134.0449	17.9	L-Aspartic acid	0.82	1.30E-01	0.84	3.70E-01
104.1071	16.0	Choline	0.83	4.00E-02	0.89	3.00E-01
400.3422	8.8	O-Palmitoyl-R-carnitine	0.86	2.30E-01	0.94	8.80E-01
424.3423	8.8	Linolenylcarnitine	0.87	3.80E-01	1.01	9.80E-01
216.0633	18.7	Glycerylphosphoryl ethanolamine	0.88	1.40E-01	0.80	9.40E-02
398.3265	8.9	9-Hexadecenoylcarnitine	0.90	2.80E-01	0.95	8.80E-01
688.4912	6.5	PE(32:2)	0.91	2.50E-01	0.83	1.90E-01
218.1389	11.5	Propionyl-L-carnitine	0.92	8.00E-01	0.84	4.70E-01
522.356	11.7	Oleoylglycerophosphocholine	0.92	4.80E-01	1.36	2.40E-01
268.1042	12.5	adenosine	0.95	8.80E-01	1.28	2.50E-01
175.119	23.3	L-Arginine	0.96	5.10E-01	1.21	2.30E-01
106.0501	18.5	Serine	0.97	8.30E-01	1.10	2.70E-01
269.0881	12.1	Inosine	0.97	8.30E-01	0.75	1.60E-01
169.0358	13.6	Uric acid	0.98	9.00E-01	1.07	7.70E-01
456.4049	8.6	Arachidyl carnitine	0.98	9.30E-01	1.04	9.20E-01
538.5198	5.3	Ceramide (34:1)	1.02	7.90E-01	1.09	6.10E-01
664.4915	21.1	NAD+	1.05	5.50E-01	1.04	8.00E-01
496.3402	12.0	LysoPC(16:0)	1.05	4.60E-01	1.54	4.20E-02
205.0973	12.9	Tryptophan	1.10	1.30E-01	1.32	1.20E-01
258.1103	20.3	Glycerophosphocholine	1.17	6.10E-02	1.20	3.20E-01
217.1297	15.8	Acetyl-arginine	1.22	3.80E-01	0.85	4.50E-01
146.1177	12.8	acetylcholine	1.29	3.00E-01	1.84	1.30E-01
118.0864	14.6	valine	1.52	6.90E-02	1.27	2.30E-01

6.9 Concluding Remarks

The current study supports the idea that *y* behaves like a regulatory hormone or cofactor affecting a variety of metabolic pathways. The evidence presented here points to it possibly mediating its effects through regulation of ecdysone activity which has been found to regulate genes involved in chitin biosynthesis (Yao et al., 2010). The pathways regulated include chitin biosynthesis and the pathway via DOPA which leads to melanin pigments and also produces tanning compounds. It may be that the regulation of chitin biosynthesis is most significant since formation of the correct chitin structure may be necessary for proper functioning of melanin production and for the tanning process to occur properly. The effects on lysine metabolism are very interesting particularly the effects on methylated and acetyl lysine. In an attempt to get a better understanding of the rate of histidine turnover in *y* and wild type larvae were fed with 13C-labelled lysine. However, although the labelled lysine was incorporated into the growth medium for the larvae the levels of labelled lysine derivatives formed within the metabolome were negligible, possibly since the degree of enrichment of the growth medium with lysine was too low.

7. Chapter seven: Study of the White gene using metabonomics

7.1 Introduction

The *white* (*w*) gene in *Drosophila* is a member of a large ATP-binding cassette (*ABC*) gene superfamily. These genes encode membrane proteins, which typically contain two motifs (Walker A and B) separated by amino acids and an additional element called the C motif. In addition to the *ABC* transporter architecture, *ABC* proteins also contain ion channels and receptors, and these proteins have roles in the assembly and translation in ribosomes. Moreover, *ABC* transporter families are present in all life forms. They are only involved in many substrate transport processes for regulating multiple essential cellular functions. In eukaryotic species, ABC proteins are involved in the transport of hydrophobic compounds, either as a plasma membrane transporter or as a vesicular membrane-bound transporter (Mackenzie et al., 1999). Additionally, *white* protein is classified as a half-transporter because it constitutes only one transmembrane domain (TMD) and one nucleotide-binding domain (NBD). Thus *white* gene products act as dimers with other proteins. A full transporter has two transmembrane domains and two ATP–binding domains acting as a dimer; so in order for *white* protein to be active it should react with another protein to form dimers. This feature of *white* protein is known in the *Drosophila* eye pigmentation phenotype, which dimerises with other proteins, such as brown and scarlet protein, to transport eye precursors which are used to form pigment granules within the cells of the eye.

Interestingly, there are several *ABC* genes found in *Drosophil*a *melanogaster*, which are divided into eight subfamilies ranging from A to H. All of them exist in humans except the H subfamily, which appears to be absent in mammals. Among these genes, the white gene is part of the *ABCG* subfamily (Evans et al., 2008, Dean et al., 2001). The architecture of *ABC* transporters has been known as a conserved domain from vertebrates to invertebrates. In humans there are 48 genes encoding ABC proteins, and among these genes 17 have been implicated in human diseases. The ABC transporter, expressed in the trachea (*Atet*) gene, that shows extensive homology with the *white* gene in *Drosophila* is closely related to the *ABCG1* gene in humans and regulates cholesterol and phospholipid transport (Mackenzie et al., 1999, Klucken et al., 2000, Anaka et al., 2008, Kômoto et al., 2009). Likewise, the white gene appears to be an important transporter for cGMP, and not cAMP, across the tubules in vesicles (Evans et al., 2008).

Moreover, the *white* gene appears to be similar to the human *ABCG2* gene which is associated with gout disease by encoding uric acid transport. Additionally, *ABCG2* is

called a multi-drug resistance gene (MDG), which plays an important role in hydrophobic compound transport in humans. Biological systems have evolved ways to transport hydrophobic substrates across cell membranes according to their specificity and high affinity to bind with transmembranes; thus defects in the function of ABC transporters leads to various diseases and may result in remarkable phenotypes (Woodward et al., 2009).

Morphologically, *white* is predominantly expressed in larval (58x) and adult tubules (40x) (see Table 3). It is also expressed in the eyes (5x) (Note: in the brackets, tissue fold change over adult fly is presented) (Evans et al., 2008). According to the Protein Interaction Database (Biogrid), *white* interacts with numerous proteins, indicating that it might be a multifunctional protein that plays roles besides pigment precursor synthesis; for example, resistance to oxidative stress, at least in tubules.

The previous findings should be addressed in order to establish the impact of the *w* mutation on the fly metabolome. At a molecular level, the *w* transgene wild type is unable to accumulate cGMP inside cells (Evans et al., 2008). Many important cellular activities are engaged by cGMP, including cell adhesion, proliferation and signalling (Sager, 2004). cGMP flux requires *ABC* transporters, particularly *white*, to transport it either intracellularly or intercellularly (Sager, 2004, Evans et al., 2008). Mutation of the *w* gene in the principal cells of the tubule results in a failure of principal cells to excrete cGMP, preventing its recycling. This could help to explain the low level of some purine metabolites and pigment precursors because both GMP and GTP are essential to their metabolism, although this prevention is not completed due to other *ABC* transporters participating in the transport of cGMP (Evans et al., 2008). An increase in cGMP concentrations in cells causes increased fluid and ion secretion along with decreased fluid absorption; thus, it is highly important for fly survival that an excess of intercellular cGMP is kept under control. To do so, flies that suffer from the *w* mutation have a wide range of complicated strategies. One of the options is that an inactivation of guanine cyclase (GC) via an inhibitor or activation of phosphodiesterase (PDE) via a stimulator. Both the GC and PDE proteins contain two types of subunits, including catalytic and regulatory subunits, which require modulation to ensure their function. The

protein modulations are regulated by several events, such as the phosphorylation process.

In this chapter, we confirm the previous studies that have shown that *w* is required for eye pigmentation and extend the knowledge of the functions of *w* to several other cellular processes. Specifically, we show that *w* mutant flies have reduced purine metabolism and increased sensitivity to acute salt stress.

7.2 Where does the regulation of *w* expression occur?

The wild type *w* transgene is able to concentrate tryptophan, kynurenine, 3-hydroxykynurenine, guanine and riboflavin intracellularly (Evans et al., 2008). This knowledge may be used to interpret metabolomics data by measuring the relevant metabolites in different tissues that could be directly influenced by the expression of the *w* gene. Thus, the activity of *w* could be assessed by measuring *w* substrates viewed in abdomen and head tissue. The head and abdomen from 7-day-old adult wild type flies (mixed sexes) were dissected according to the method described in section 2.6 and were well homogenised in ice cold extraction solvent. From the data presented in Figure 7-1, it can be seen that all potential substrates for *white* are far more extensive in the abdomen than the head, so *w* is particularly abundant in the abdomen and shows low activity in head. These findings are consistent with previous observations that the amount of mRNA for the *w* gene in the tubules is higher than in eye tissue. It has been established that *w* is localised in the intracellular vesicles in the principal cells located on the tubule and pigment vesicles located on the eye and maintains eye fluid secretion and eye pigmentation, respectively. Guanine and tryptophan share a common transport system and are precurors of pteridine and ommochrome pigments, respectively.

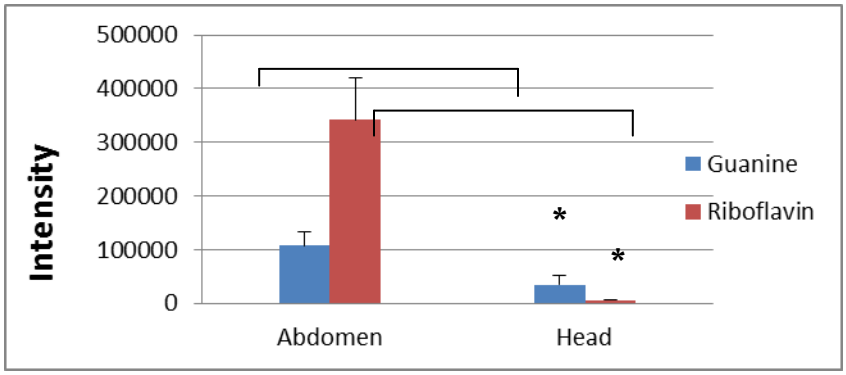

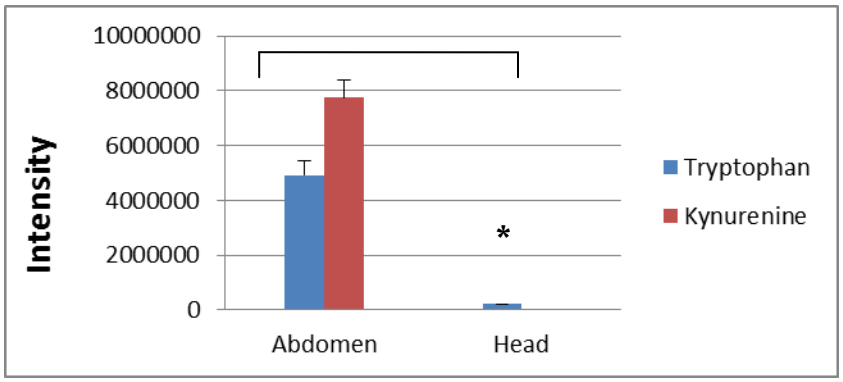

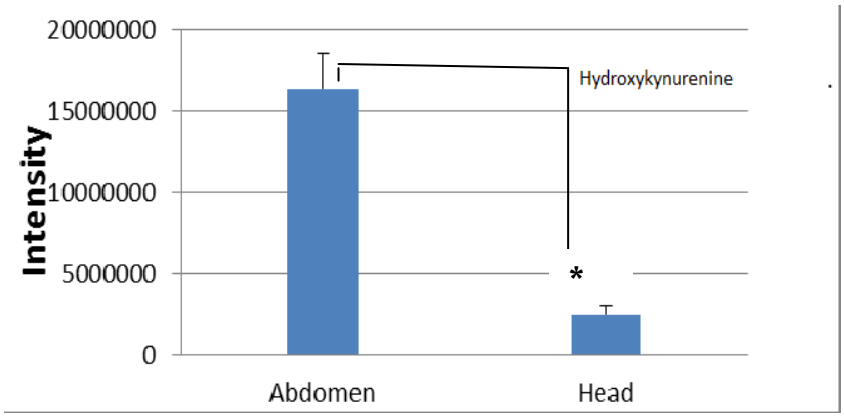

Figure 7-1 Evidence for differential precursors of *w* gene in wild-type according to their avaliblity in the abdomen and heads. All panels showed *white's* substrates are higher in abdomen than head implying that *w* expression was found significantly higher in the abdomen. Data are shown as mean ±SEM for N=4 independent experiments. Data that differ significantly are marked with asterisks are analyzed by Student's *t*-test two tailed. Since the mass of the tissues were different the intensities of the metabolites were normalised relative to protein content determined by the Bradford assay.

7.3 Global metabolomics of *w* and wild-type flies

In the work that follows, an attempt is made to understand the cellular changes resulting from defective transport due to the *w* mutation upon the whole organism. These changes are numerous and are summarised in table 7-1, showing the major alterations that occur inside the fly body. They also include the complex network of metabolites with predicted functional effects on a wide range of cellular activities, including pigmentation, signalling and ion homeostasis. In recent work, several significant differences have been detected in the metabolic profiles of the *w* mutation when compared with the Oregon wild-type. Furthermore, metabolomics gives us a great chance to rapidly confirm results obtained from classical work and extend our knowledge of the fly's biological system when it lacks the *w* protein. This study was able to detect further pigmentation perturbations resulting from the *w* lesion than was previously possible and explore new effects on the xanthine-uric acid-5HIU axis in the purine metabolism pathway, which has not been previously reported. It was found that uric acid and HIU levels were lower in *w* and allantoin was elevated. One of the functions of *white* is urate transport and mutations of the gene in humans causes gout. However, in the current case uric acid levels are lower which does not match expectation. The fact that allantoin, which is downstream of uric acid, is elevated suggests that there may be some type of compensation going on for deficient uric acid transport where the metabolism of urate into allantoin is increased. However, to support this hypothesis further work would be required. The level of hypoxanthine, adenine and inosine was similar in wild type and *w* mutant flies, while the levels of guanine and guanosine in *w* mutants, which are necessary for biosynthesis of petridine pigments, were found to be somewhat lower. Another observation is that the oxidative process for for formation of kynurenine in *w* is deficient, along with decreased 3-hydroxykynurenine, suggesting that the enzyme required for the hydroxylation reaction shows reduced activity along with the FAD co-factor associated with riboflavin. The latter was found in much lower quantities in *w* mutant flies. These observations are reflected in the lower levels of ommochrome pigment xanthomatin which is formed via

the kynurenine pathway. There are some significant biochemical changes during the adaptation of the *w* mutant fly due to the lack of white protein. One of these changes was in glutathione (GSH) which is significantly elevated (about two fold) in *w* mutants. This observation was accompanied with decreased levels of the oxidised form of GSH (GSSG, about half) compared to wild type in males but not in females. This is because GSH acts as an electrophile scavenger that accepts electron pairs from endothelial cells to form a glutathionyl radical ($GS^{\bullet}$) that is oxidised via the glutathione s-transferase enzyme to GSSG, which can be recycled into GSH by the glutathione reductase enzyme (Hansen et al., 2006). GSH has a role in preventing leakage of the reactive compound ROS, formed in redox-reactions, which in turn leads to maintaining the *w* mutant fly's survival. It is likely that *w* would be more prone to oxidative stress since the lack of pigmentation will mean increased exposure of tissues within the fly to radiation. Table 7-1 lists some additional metabolites that showed differences between males and females including osmolyte metabolites, such as glycerophosphocholine (GPC) and glycerophosphoethanolamine (GPEA). Accumulation of osmolytes may be required to combat deficiencies in uric acid transport which is the normal way of eliminating nitrogenous waste while conserving water. Both GPC and GPEA were found to be much higher in the female *w* mutation (about eight times) than the value obtained for the male *w* mutation when they were compared with wild type. These observations imply that females are able to concentrate these compounds to overcome osmotic stress and enhance their survival, but why is the impact on GPC and GPEA required only in females? Is there any relevant link between *w* genomic location and *w* dosage compensation? (More details in 7.4). Gender differences are reflected in a distinct metabolic profile especially for lipid metabolism. Several studies support the proposal that the lipid metabolism is different in females compared to male flies (Chintapalli et al., 2012, Michael et al., 2011). Our results also show that the lipid precursors CDP-choline and CDP-ethanolamine (figure 7.2) are less than half in males compared with females.

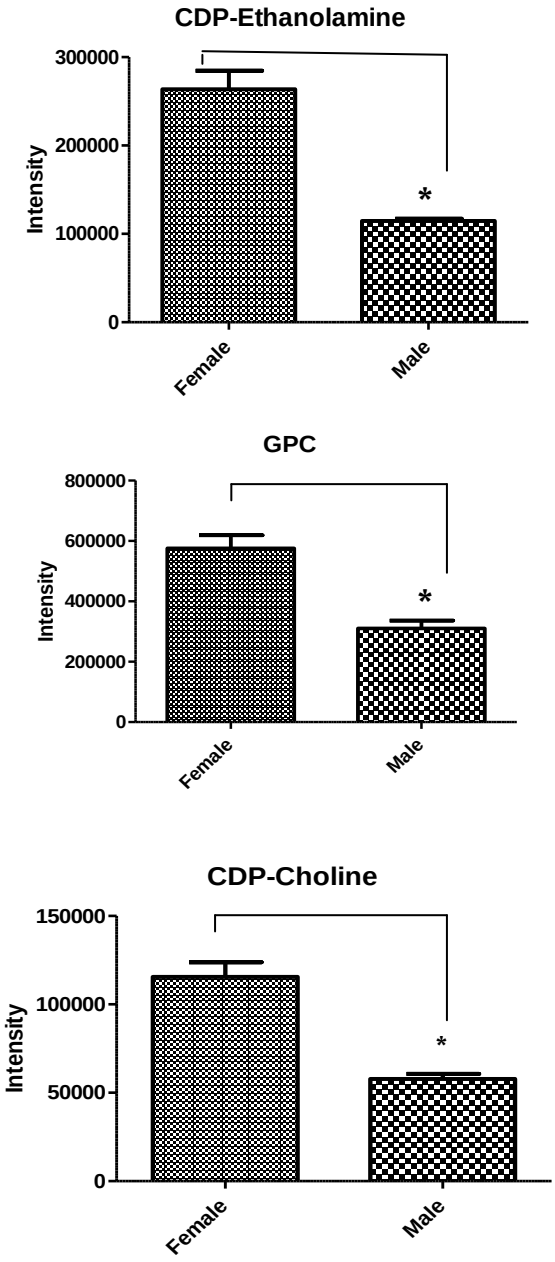

Figure 7-2 Variation in CDP-Ethanolamine, GPC and CDP-choline in male and female *w* flies. Data are shown as mean ±SEM for N=4 independent experiments. Data that differ significantly are marked with asterisks are analyzed by Student's *t*-test two tailed.

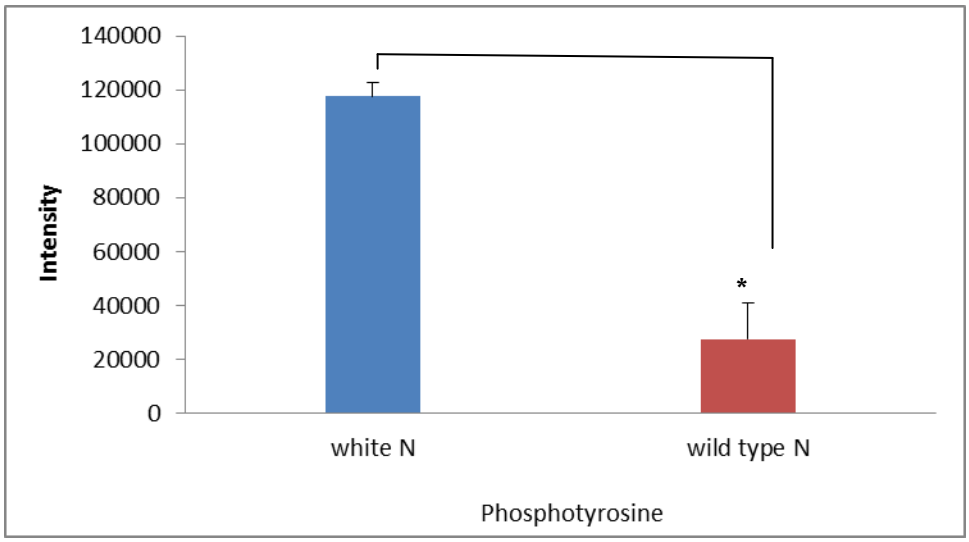

Figure 7-3 Phosphotyrosine levels are higher in *w* mutants than wild type in normal conditions. Data are shown as mean ±SEM for N=4 independent experiments. Data that differ significantly are marked with asterisks are analyzed by Student's *t*-test two tailed.

There was a marked accumulation of phosphotyrosine in *w* (figure 7-3) and it is difficult to explain presence of this compound except possibly as a regulator of osmotic stress.

Table 7-1 List of metabolites displaying significant differences between *w* and wt analysed. "Ratio" is of *w*: wt signal (n=4).

			Female		Male	
Purine pathway	**m/z**	**Rt min.**	***w*/OR**	**P value**	***w*/OR**	**P value**
Hypoxanthine	137.04588	12.18	1.16	0.13622	0.94	0.70895
Guanine	152.05632	13.99	0.71	4.80E-02	0.58	3.70E-05
allantoin	159.0513	15.12	3.99	0.00001	3.55	0.00001
urate	169.03568	13.59	0.18	0.00546	0.18	0.00056
HIU	185.0306	13.80	--	--	0.006	0.009
Inosine	269.08813	12.18	1.15	0.10510	0.96	0.77328
Guanosine	284.09915	13.96	0.26	0.00342	0.14	0.00000
Eye pigments						
pterin	164.05687	12.12	Nd	0.00343	0.00	0.00011
tryptophan	205.09708	13.07	0.3	0.00014	0.18	0.00020
kynurenine	209.09221	12.69	1.2	0.08414	0.05	0.00008
hydroxytryptophan	221.09215	17.02	Nd	0.00423	0.00	0.00051
hydroxykynurenine	225.09515	14.38	Nd	0.00051	0.00	0.00053
sepiapterin	238.09352	10.39	Nd	0.00261	0.00	0.00028
biopterin	238.09354	13.21	0.02	0.00368	0.01	0.00002
dihydrobiopterin	240.10916	13.99	0.01	0.00142	0.01	0.00006
drosopterin	369.15308	18.20	Nd	0.00425	0.00	0.00103
xanthomatin	424.07742	13.78	Nd	0.00473	0.00	0.00568
Isoxanthopterin	180.05156	12.5	Nd	0.00014	0.00	0.00003
Dihydroxanthopterin	182.06744	12.5	Nd	0.00470	0.00	0.00003

GSH oxidative stress						
Methionine S-oxide	166.05344	18.41	1.91	0.02248	0.96	0.62921
cystathione	223.07478	21.98	1.36	0.00998	3.31	0.00086
Methylthioadenosine	298.09692	26.7	4.01	0.01181	0.48	0.02287
GSH	308.09055	16.28	1.93	0.00001	1.49	0.03701
Hydroxymethylglutathione	338.10181	16.96	0.94	0.64930	0.60	0.06198
Cysteineglutathione disulfide	427.09503	21.18	0.69	0.04082	0.42	0.01329
GSSG	613.15912	20.64	0.98	0.78921	0.39	0.03518
Osmolytes						
ethanolamine phosphate	142.0264	20.09	1.43	0.00749	1.20	0.12491
glycerophosphoethanolamine	216.06339	18.72	3.07	0.00086	0.69	0.02341
GPC	258.11005	20.42	3.30	0.00000	0.52	0.00926
CDP-ehanolamine	447.06754	21.58	2.82	0.00002	0.72	0.00066
CDP-choline	489.11444	23.71	1.90	0.00011	0.89	0.13933
Misc. Metabolites						
lysine	147.11284	23.55	2.80	0.00011	1.95	0.00001
glutamine	148.06052	17.12	1.26	0.01401	0.90	0.12949
methyllysine	161.12848	23.09	3.24	0.00124	1.19	0.53045
spermidate	176.09172	14.61	6.48	0.00005	10.78	0.00004
Homocitrulline	190.1187	23.98	0.21	0.00185	0.10	0.00098
Dimethylarginine	203.15031	21.65	1.39	0.00954	0.86	0.06141
Argininosuccinic acid	291.13	22.14	1.32	0.01914	1.85	0.00002
riboflavin	377.14557	9.58	0.72	0.00629	0.08	0.00131

Nd = Not detected

7.4 Eye Development in *Drosophila* a fascinating story

Generally, the mechanism of eye pigmentation in *Drosophila* has been reported extensively during the last century. The pigmentation occurs due to the synthesis of two pigments: ommochrome (from the tryptophan pathway) and drosopterin (from the guanine pathway) (Summers et al., 1982). However, there are several compounds responsible for red pigmentation, including: drosopterin, xanthopterin and pterin. In fact, to form these compounds, the fly needs to break down guanosine triphosphate (GTP), first into dihydroneopterin triphosphate (H_2NTP) by the *punch* gene, which encodes GTP cyclohydrolase (Figure 7-4). H_2NTP requires the *purple* gene, which encodes 6-pyruvoyl-tetrahydropterin synthase (PTPS) to form pyruvyl tetrahydroopterin (PTP). The latter has three routes for its formation. In the first path, it converts into sepiapterin and ultimately into sepiabiopterin via dihydrobiopterin oxidase. In the second route, it converts into pyrimidodiazepine, which requires glutathione as a co-factor. The third pathway is that pyruvyl tetrahydropterin (PTP) converts into pterin via dihydropterin by dihydropterin oxidase (DHO), and then pterin converts into xanthopterin (Sullivan et al., 1979). The end product formation of tetrahydropterin degradation requires a condensation process with two intermediates of PTP, dihydropterin and pyrimidodiazepine, resulting in drosopterin producing the red eye phenotype.

Interestingly, although there is a wealth of information about *Drosophila* eye pattern genetics, little is known regarding how these pigments develop. To explore this, we examined the ability of larvae to synthesise these patterns in wild type, and then compared them to *w* flies in order to observe small changes in their expression. In case of wild-type larvae, metabolomic data suggest that drosopterin levels were completely abolished due to the absence of pyrimidodiazepine, which is considered the rate-limiting substrate for the condensation reaction with dihydropterin. Thus, drosopterin formation was blocked. In fact, the synthesis of pyrimidodiazepine requires two genes to encode pyrimidodiazepine synthase (PDA synthase); one of them is *sepia* which is directly involved in it, while the participation of the *clot* gene is indirect via its maintainance of the glutathione levels. Glutathione is involved as co-factor due to the pyrimidodiazepine structure requiring two more electrons than PTP. Therefore, the level of glutathione plays a vital role in drosopterin synthesis because of its involvement as an electron supplier in the formation of PDA. Glutathione levels were maintained in wild-type larvae, thus the disappearance of

drosopterin may be ascribed to a defect in the expression of the *sepia* gene, suggesting that *sepia* is not functioning normally in the larval stage of wild type. This data confirms that the red pigment is not synthesised in the larval stage, but may begin in the late pupal stage and continue during adulthood, due to the *sepia* gene, which is mainly expressed in the adult head according to the FlyAtlas.

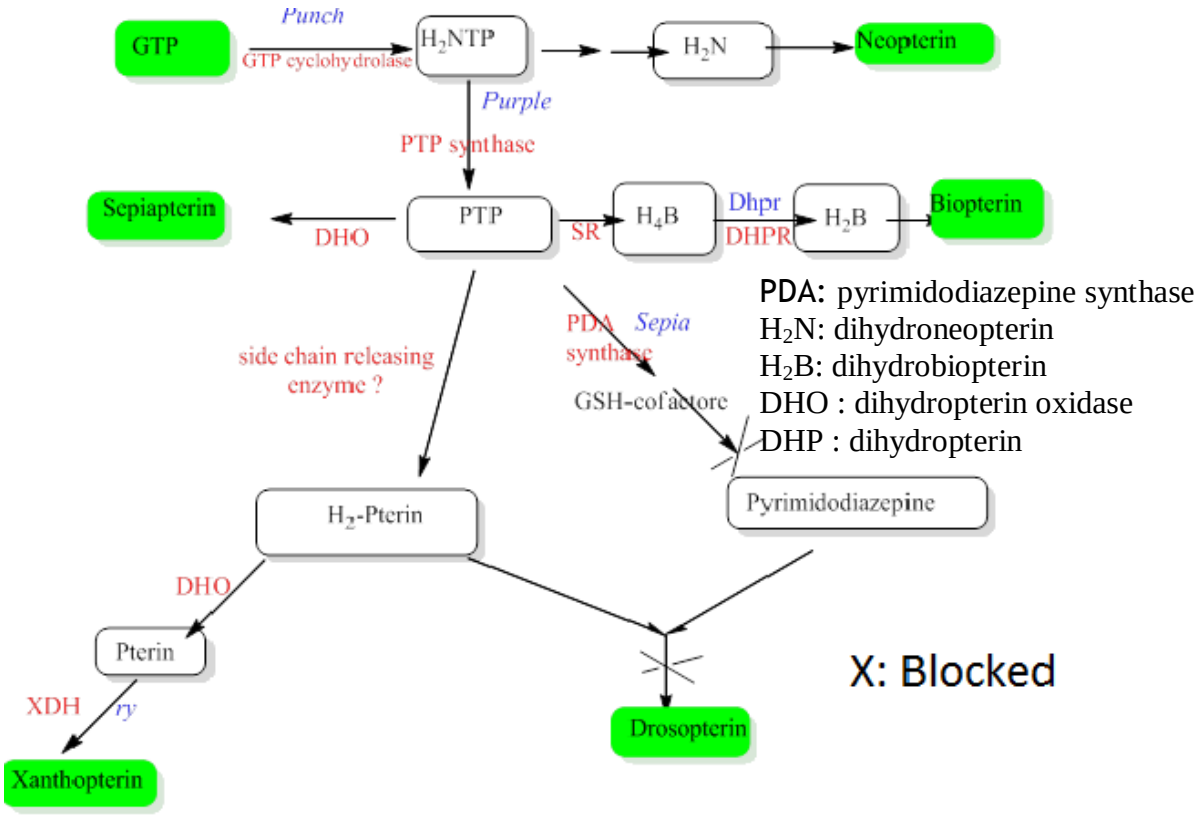

Figure 7-4 Proposed red pigment biosynthetic pathways in *Drosophila* wild-type larvae.

7.5 How could lack of *w* impact on the drosopterin pathway?

In the case of white-eyed flies, the perturbation of red pigments due to the lack of the *w* gene was easily mirrored by the metabolomics results as seen in fig 7-5. The characteristic differences between *w* mutant and wild type flies are with regard to red pigments and are the absence of dihydroneopterin, neopterin, sepiapterin, xanthopterin, pyrimidodiazepine and drosopterin in *w* mutants. However, the

degradation products of 5,6,7,8-tetrahydrobiopterin BH4, such as dihydrobiopterin and biopterin, were significantly present in low levels in *w* mutants, which suggests that the mutation causes a sharp down-regulation in enzyme 6-pyruvoyl-tetrahydropterin synthase levels (PTPS); but the enzyme was not completely absent. On the other hand, *w* flies have an impaired regulatory system, which directly affects dihydropterin oxidase (DHO), sepiapterin synthase, neopterin synthase and drosopterin synthase by preventing the formation of several of the pigments that are involved in red eye pigmentation. Thus, the absence of pterin compounds, which are used as precursors for dihydropterin oxidase, may contribute to blocking the production of red pigments. Moreover, and more specifically, previous research has found that the generation of 7,8-dihydropterin (DHP) from PTP through the release of the three carbon side chain is a cornerstone for the oxidation of DHP to the corresponding pterins. However, the role of white protein in preventing DHP synthesis remains largely unknown (Sullivan et al., 1979, Kômoto et al., 2009, Longo, 2009, Kim et al., 2006, Montell et al., 1992, Thöny et al., 2000).

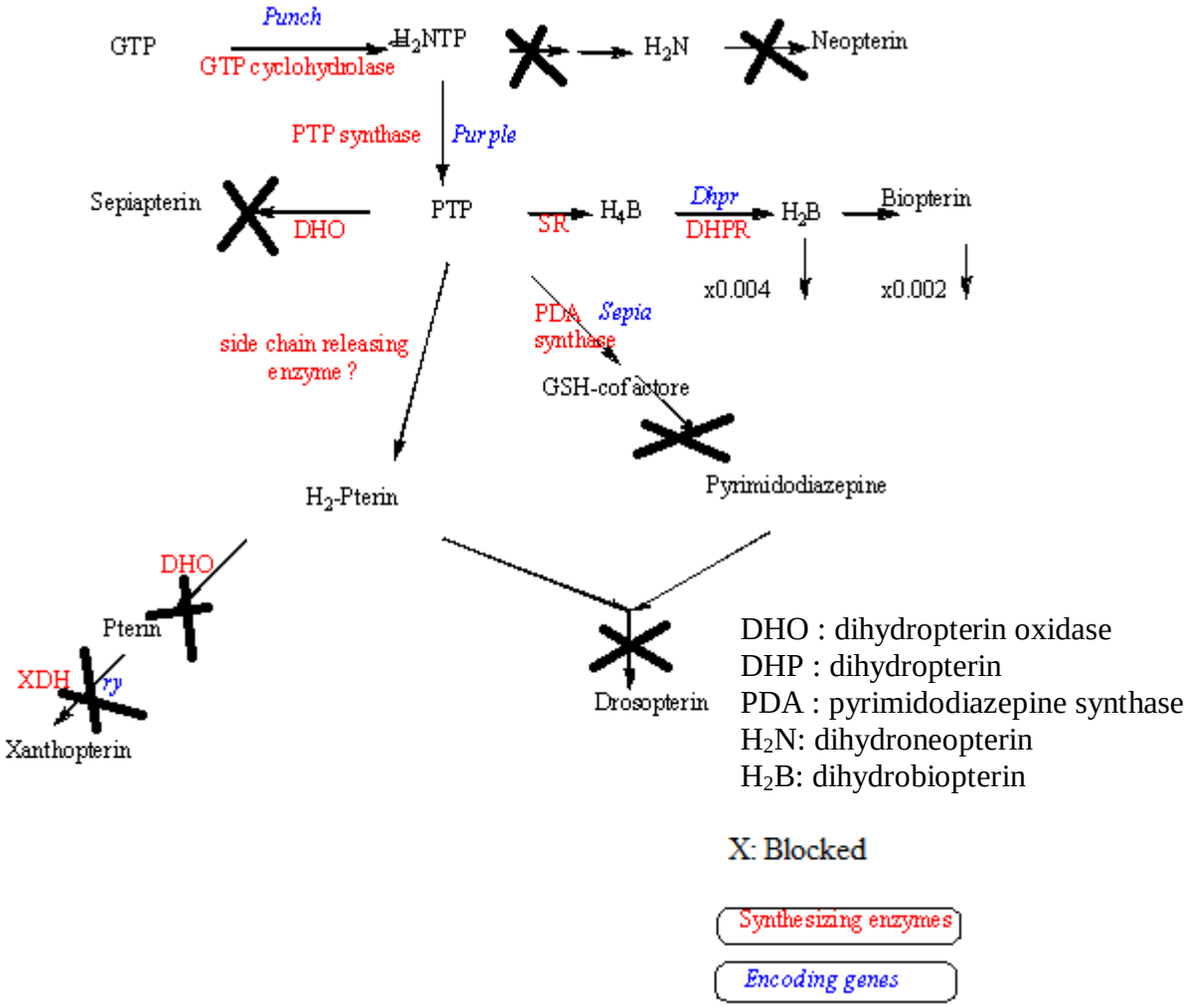

Figure 7-5 Impact of *w* mutation on drosopterin biosynthesis with known *Drosophila* enzymes indicated, and fold changes for metabolites for *w* versus OR (from Table 7-1) shown in arrows.

7.6 How could lack of w impact on the xanthomatin pathway?

Another eye pigment, which is responsible for brown eye colour, results from xanthommatin when it accumulates in the periphery of each ommatidium cell. Xanthomatin is formed from tryptophan metabolism (Figure 7-6). Unlike the red pigments, brown pigments are synthesised and stored in both stages, larval and adulthood. In fact, there are several genes that are implicated in the synthesis of the xanthomatin pigment, and three of them are well characterized: *cinnabar*, *vermilion* and *cardinal*. *Vermilion* encodes tryptophan 2,3 dioxygenase (TDO) and controls the conversion of tryptophan to N-formyl kynurenine, while kynurenine 3-

monooxygenase (KMO) is encoded by the *cinnabar* gene to produce hydroxykynurenine from kynurenine. The condensation reaction that yields xanthomatin occurs through phenoxazinone synthase from hydroxykynurenine via the *cardinal* gene. Unfortunately, the gene that is responsible for the second step in brown pigment biosynthesis has not been identified (Tearle, 1991). However, there are two genes that are thought to be implicated in the transport of tryptophan pathway precursors *w* and *scarlet* and it was proposed (Potter et al., 2000) that tryptophan is transported across the cellular membrane by *w*, whereas kynurenine is transported into cells by *scarlet*. *Scarlet* cannot function unless it forms a dimer with *w*. Here there are interesting differences between male and female *w* flies in that kyurenine is almost absent from male flies but it is slightly elevated in female flies compared with wild type. The presence of tryptophan, kynurenine and hydroxykynurenine only in minute concentrations may prevent xanthomatin formation in *w* flies in comparison to wild type. These findings are consistent with previous findings (Sullivan et al., 1980). The absence of the *w* should not prevent the entry of tryptophan into cells across the plasma membrane, but the pathway of tryptophan transport is reduced substantially, tryptophan is an essential amino acid in *Drosophila* and has to be acquired from the diet. This is observed in table 7.1 where tryptophan levels are much lower in *w*. Furthermore, these outcomes confirm the previous data, which reported that a combination of the two proteins, white and scarlet, is essential for xanthomatin synthesis, where this combination is required for channelling hydroxykynurenine into cells across the pigment granule membrane after being synthesized in the cytoplasm. Therefore, phenoxazinone synthase is available but does not act due to accumulation of hydroxykynurenine outside of the pigment granule cells, while the other enzymes involved in brown eye pigmentation, TDO, KMO and KF, act on the inner cytoplasmic side and do not need white/scarlet hetrodimers to produce their products (Coleman and Neckameyer, 2005, Sullivan et al., 1980, Sun et al., 1995, Li et al., 1999, Le Roes-Hill et al., 2009).

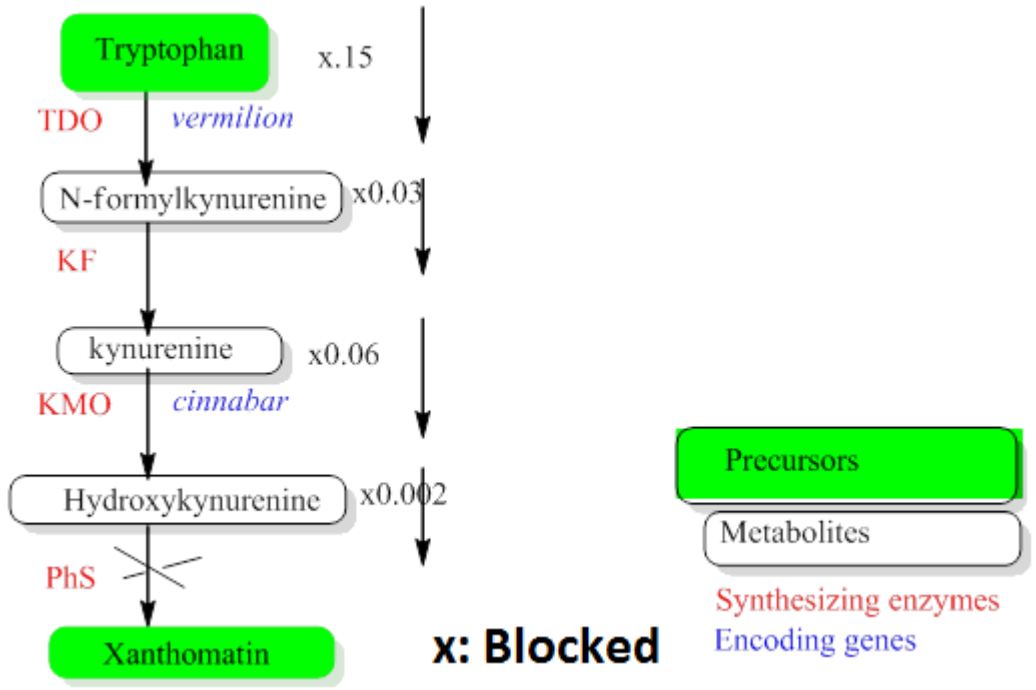

Figure 7-6 Impact of *w* mutation on xanthomatin biosynthesis with known *Drosophila* enzymes indicated, and fold changes for metabolites for *w* versus OR (from Table 7-1) shown in arrows.

7.7 Mini-white rescues the *w* phenotype

Drosophila transgenesis heavily relies on the germline transformation of *white* embryos with the transformation vectors that harbour the *mini-white* marker (*mini-*w^+). This allows the selection of successful transformants on the basis of eye colour (orange to red) depending on their insertion in the genome. The *mini-*w^+ is the truncated form of the *white* gene and partially rescues the eye colour leading to artificial eye-colour in new generations that carry the *p*-element reporter. Integration events of the *p*-element most often occur close to the 5' regulatory regions of genes, and unwanted phenomena can occur during the transgenesis process, such as disruption of a neighbouring gene, or an undesired position effect, or position effect variegation. In order to avoid these drawbacks, several transposons for *Drosophila* transgenesis with a different insertion compatible with *p*-element technology have been used either to improve transposition or to neutralize the position effect, including *piggyBac*, *Minos*, *hobo* and *gyps* (Sun et al., 1995, Bhojwani et al., 1995, Kleinjan and van Heyningen, 1998). To investigate eye phenotypes in terms of their

metabolic differences, which may originate from the *p*-element mediated insertion of the *mini-white* and its expression, we used a metabolomic approach. Transgenic flies that carry one copy of the *w* gene were used along with *white* mutant flies to compare the metabolomic differences and compensation of *white* by *mini-w*$^{+}$. Moreover, many genes that are implicated in eye development and their interference with the *mini-white* gene are revealed for further investigation of the role of the *mini-white* gene in eye pigments synthesis. How much does metabolome of *mini-w*$^{+}$ tell us about the rescue of *white* mutant phenotype? The data obtained from the metabolomic approach revealed that proteins involved in the drosopterin and xanthommatin pathways were positively affected by the *mini-white* gene, as seen in figure 7-7.

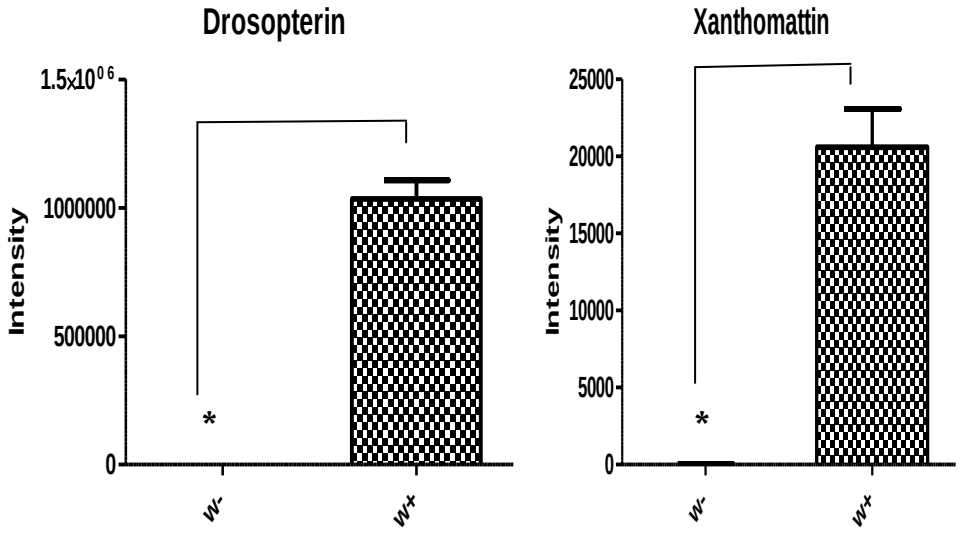

Figure 7-7 Impact of *mini-w*$^{+}$ insertion on drosopterin and xanthomatin showing their sensitivity to mini-*w*$^{+}$. Data are shown as mean ±SEM for N=4 independent experiments. Data that differ significantly are marked with asterisks are analyzed by Student's *t*-test two tailed.

Although the *white* gene is normally expressed on the X chromosome, as seen in fig 7-8, the transposon process does have ectopic consequences, as mentioned above. Thus, metabolomics was used to clarify how the existence of the *mini-white* gene in different chromosomal locations affects metabolic perturbation. Striking changes in enzyme activities that are responsible for degradation of the tetrahydrobiopterin

pathway were observed, with particular effects on dihydrobiopterin and biopterin syntheses being highly induced in transgenic flies compared to *w* mutants (data not shown).

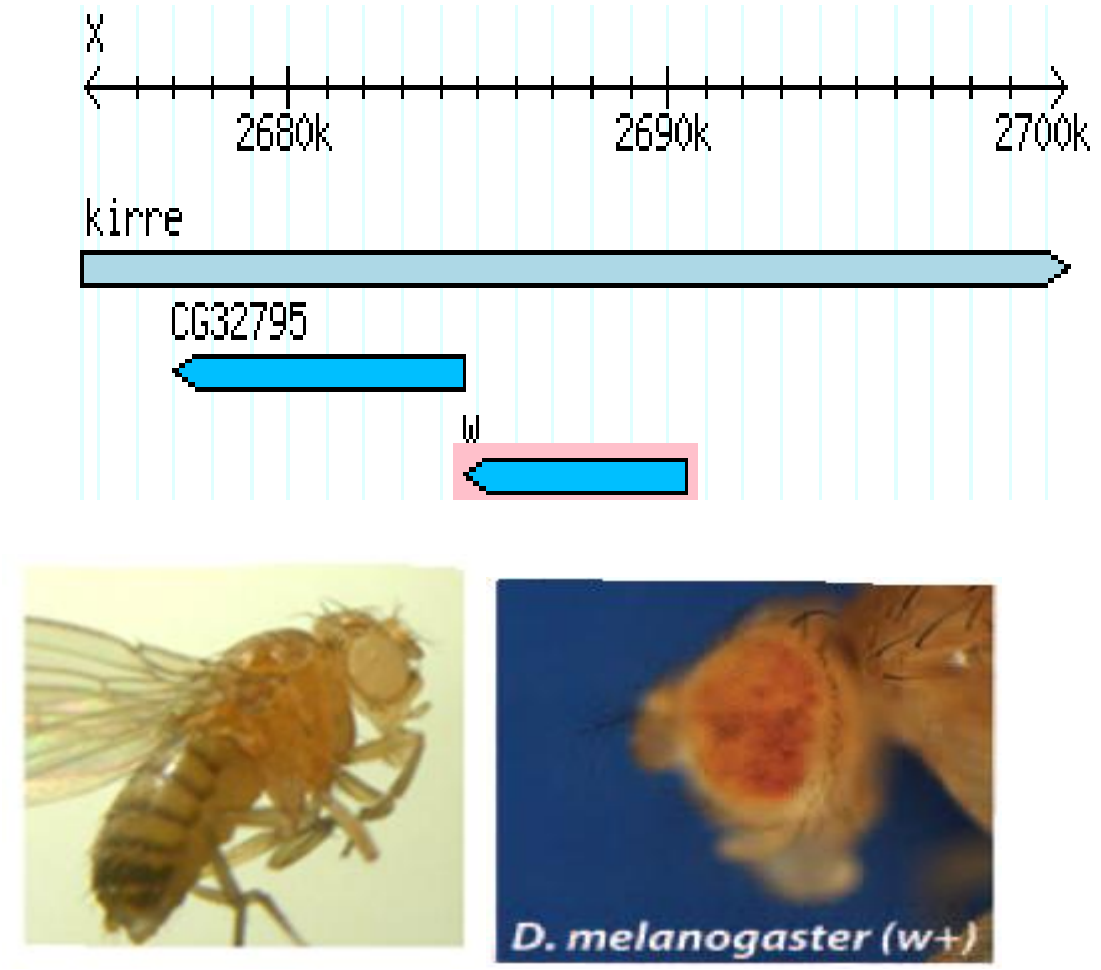

Figure 7-8 Genomic organisation of w (upper panel); lower panel (right) Showing the characteristic red eye colour of *mini-w*$^{+}$ against white eyed flies (*w1118*) (left) (Data obtained from Flybase.org on 10th June, 2012, (Evans et al., 2008) and (Holtzman et al., 2010)

Furthermore, the data showed that tetrahydrobiopterin degradation in *w* mutants was greatly reduced. These results differ from those for *mini-w*$^{+}$ where the levels of dihydrobiopterin and biopterin were elevated. Despite the role of the *mini-white* gene in promoting the syntheses of tetrahydrobiopterin being evident in this study, the biochemical details of *white's* action remain unclear. The *mini-white* gene increases

the activity of dihydropteridine reductase (DHPR) by about 100 fold (data not shown), allowing dihydrobiopterin and biopterin to accumulate at 60 times greater than the level in *w*. However, tetrahydrobiopterin is considered essential for various biochemical pathways as a cofactor, including the metabolism of monoamine neurotransmitters, and it is also required for three nitric oxide synthases (NOS) and for the hydroxylation of glyceryl ether. Therefore, its defects cause disorders such as neurological diseases (Montell et al., 1992, Thöny et al., 2000).

The feedback of *mini–w*$^{+}$ is not confined to its role in producing eye precursors; possible feedback effects of *mini–w*$^{+}$ on purine metabolism were investigated. The xanthine/uric acid arm of this pathway was assessed in *w*$^{-}$ and *mini–w*$^{+}$. *Ry* was upregulated, allowing uric acid and isoxanthopterin to accumulate about 10 and 60 times, respectively, in *mini–w*$^{+}$ compared to white, as seen in figure 7-9. Interestingly, *white's* substrates were concentrated by *mini–w*$^{+}$ (figure 7-10), suggesting that *w* is an important regulator for cell and tissue function. These data are consistent with previous conclusions and extend our knowledge of the effects of the expression of the *mini-w*$^{+}$ gene beyond eye pigmentation.

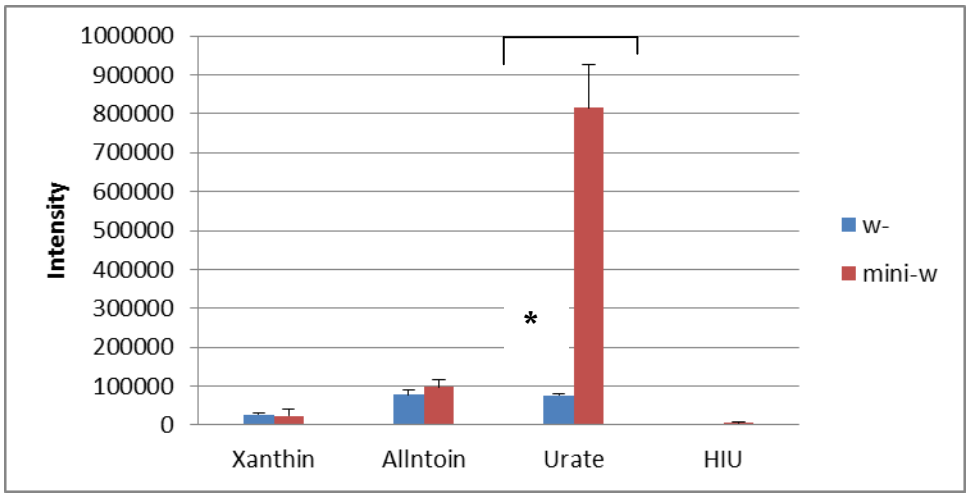

Figure 7-9. Impact of *mini-w*$^{+}$ insertion on uric acid pathway showing *ry* is up regulated 10 times as can be observed from the urate level. Data are shown as mean ±SEM for N=4 independent experiments. Data that differ significantly are marked with asterisks are analyzed by Student's *t*-test two tailed.

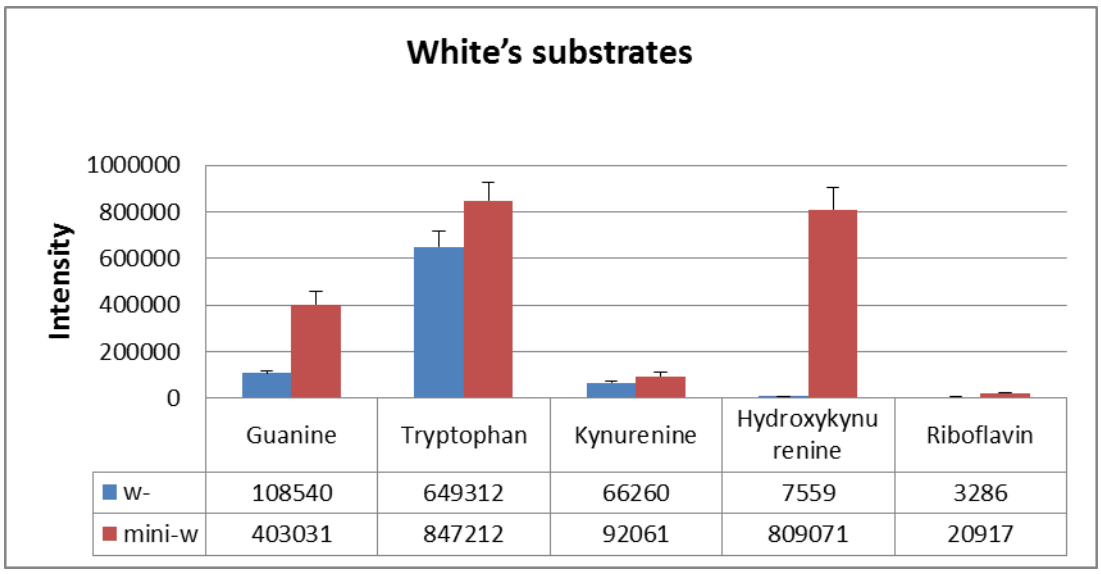

Figure 7-10. Impact of *mini-w*$^{+}$ insertion on white's substrates showing Guanine ,Tryptophan, Kynurenine , Hydroxykynurenine and Riboflvine were accumulated in *mini-w*$^{+}$ flies confirming that these compounds are sensitive to *w* expression at different levels. Data was statistically assessed by Student's *t*-test (two tailed);n=4.

7.8 The sensitivity of eye pigmentation to dosage compensation

Like most metabolomic studies, where the objective is to determine which metabolites are altered in the sexes, we focused here on metabolites that are involved in the biosynthesis of insect pigments - either pigmentation originating from pteridine or from tryptophan. In doing so, we extracted an equal number of flies of each sex carrying the same genetic background (wild-type) in order to determine the differences in the amount of eye pigments between them, and to know the differences between sexes which contribbute to different levels of particular gene expression. These genes have been known as being responsible for pigment synthesis, and loading and delivery into pigment granules. The effect of *w* on the dosage compensation phenomenon was thus investigated. White's role has gained prominence in loading activities and even in pigment synthesis. Accordingly, we hypothesise that the differences in eye phenotype between sexes might be linked to the dosage compensation phenomenon. Broadly, dosage compensation is a widespread process that happens in living organisms to compensate for the transcription of the abundance of genes which are located on the X chromosome.

Males bear a single X chromosome containing one *w* copy and a Y chromosome while females have two X chromosomes containing two copies of *w*. Therefore an adjustment between autosome and chromosome must be made to maintain genetic homeostasis due to the differences in the expression levels of genes on the X chromosome in the sexes. Indeed, the mechanism of this process varies from one organism to another. For example, in humans the dosage compensation occurs by inactivation of one X chromosome in females. In contrast, most of the studies in *Drosophila* support the hypothesis that dosage compensation happens by hypertranscription or activation of X chromosome genes by twofold expression level in males. However, it is still the feasible that hypotranscription or inactivation of an X chromosome occurs in females. The X chromosome bears 20% of the Drosophila genome representing about 3000 genes. Furthermore, regardless of whether or not the mechanism of dosage compensation is hypo or hyper, the transcription process in X chromosome of female or male flies, the process involves changes in transcription levels of relevant genes through chromatin alteration. Thus the transcriptional levels of genes whether these levels are activated or repressed are associated with modified histones. In fact, the acetylation of basic amino acids in histones leads to positive regulation for relevant gene transcription, due to removal of the positive charge on the basic amino acids, thus removing the interaction of histone with the phosphate backbone of DNA. Thus the ability of genes to wrap around histone proteins in forming the chromatin structure is decreased. Methylation of histones in most cases results in an increase in the ability of histone tails to interact with phosphate groups in DNA, and allows chromatin compacting and prevention of gene transcription. Additionally, previous studies have mentioned that in some cases the methylation of lysine on histone H3 is associated with hypertranscription of the genes in the X chromosome due to up-regulation of histone acetylases (Zhang and Reinberg, 2001, Strahl et al., 1999, Shilatifard, 2008). However, little information is known about the mechanism of rapid dosage compensation for the X chromosome, whether it is via activating X-linked genes in males or inactivating the X chromosome in females.

Metabolomics could offer a new insight into *Drosophila* genome by exploring the role of dosage compensation via the expression level of genes spatially in the X chromosome. This compensation which occurs in males only due to the existence of

only one copy of the X chromosome while female flies have two copies, so male flies must be compensated for male survival. Indeed, this X chromosome compensation process is adjusted by male specific lethal factors (MSL) to increase the expression of X chromosome in males. Thus it seems to be sensitive to perturbations related to proteins that interact with the X chromosome. Eye pigmentation compounds have been used as preferential markers to monitor this genetic phenomenon due to the fact that the *white* gene is considered a major factor in the pigmentation process and is located on the X chromosome(Girton and Johansen, 2008, Gilfillan et al., 2004, Hallacli and Akhtar, 2009, Zhang and Oliver, 2010).

In the current study it was found that in male flies, all pteridine derivatives that are involved in red eye pigments were found at significantly higher levels than those in the female flies except drosopterin and pterin, while the level of pyrimidodiazepine (PDA) did not differ between sexes. This implies that the s*epia* gene which encodes PDA synthase to convert pyruvyl tetrahydrobiopterin (PTHB) into pyrimidodiazepine (PDA) appears to be not affected by the dosage compensation process due to its location in *Drosophila*'s genome map on chromosome 3 (table 7.2). In this case, the decreased level of drosopterin in males may be attributed to the condensation of PDA with 7,8-dihydropterin (DHP) not occurring properly due to the trace amounts of DHP reacting rapidly to form pterin via dihydropterin oxidase (DHO) and finally accumulating as xanthopterin by via the action of xanthine dehydrogenase (*XDH)(*Table7.2*).*

Table 7-2. The genetic location for usual genes involved in eyes pigmentation on *Drosophila melanogaster* Chromosomes.

Gene	symbol	Genomic location
ABC transport group		
White	w	x
Brown	bw	2
Scarlet	st	3
Granule group		
carmine	cm	x
carnation	cr	x
claret	ca	3
deep orange	dor	x
orange	or	2
ruby	rb	x
pink	p	3
Brown pigment synthesis group		
cinnabar	cn	2
vermilion	v	x
karmoisin	kar	3
Red pigment synthesis group		
sepia	se	3
clot	cl	2
purple	pr	2
Punch	pu	2

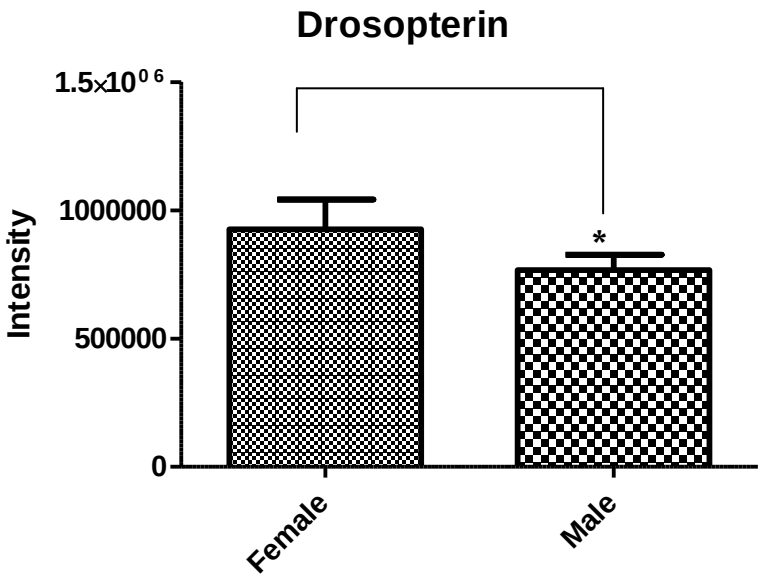

Figure 7-11. Impact of *gender* on red pigment levels showing drosopterin is slightly higher in female flies. Data are shown as mean ±SEM for N=4 independent experiments. Data that differ significantly are marked with asterisks are analyzed by Student's *t*-test two tailed.

In contrast to the pteridine pathway, all the xanthomatin intermediate compounds in male flies were present at significantly lower levels than those in female flies. This conflicting data indicates that the metabolomic approach indirectly allows us to shed light on gene expression compensation. The best evidence that double expression of the male X chromosome does not occur perfectly is that the conversion of tryptophan to formylkynurenine, the first step in the synthesis of xanthomatin pigments, is lower by 90% in males compared with females, suggesting that the *vermilion* gene (located on the X chromosome), which encodes tryptophan 2,3-dioxygenase, is a more actively transcribed gene in females. Actually, this finding is opposed to most of the literature about X linked gene theory in *Drosophila*, where this theory supports the compensation for genes located on the X chromosome in males via hypertranscriptional activity for these genes.

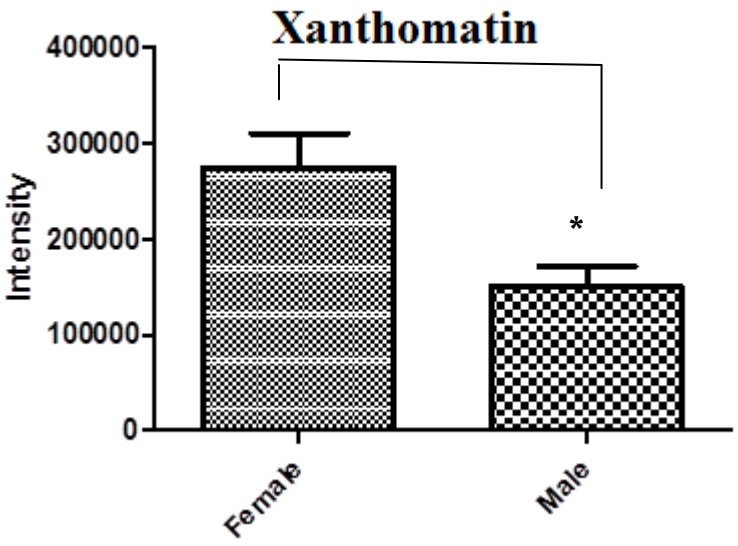

Figure 7-12. Impact of *gender* on brown pigment showing xanthomatin level is doubled in females, reflecting deficit compensation on the X chromosome. Data are shown as mean ±SEM for N=4 independent experiments. Data that differ significantly are marked with asterisks are analyzed by Student's *t*-test two tailed.

Moreover, our data shed much light on the dosage compensation phenomenon that appears to be non-exclusive for genes located on the X chromosome, but for genes that are located away from X chromosome. To support this idea, a higher level of isoxanthopterin was observed in males, indicating that xanthine dehydrogenase activity (*XDH*) was upregulated to form isoxanthopterin from pterin. However, XDH (*ry*) is located on chromosome 3, which did not appear to perturb purine metabolism and the levels of xanthine and uric acid in males were the same as in females. In sharp contrast, kynurenine 3-monooxygenase encoded by the *cinnabar* gene, which is located on chromosome 2, appeared to be downregulated by 70% in males but this may be due to a lack of availability of its substrate formylkynurenine which is produced by tryptophan 2, 3-dioxygenase which is located on the X chromosome apart from eye pigments, metabolomic data can offer new insights into the mechanisms of dosage compensation on the X chromosome. Levels of mono-, and trimethyl lysines and and dimethyl arginine residues are much higher in female flies. Figure 7.13 shows the chromatograms for these metabolites in an extract from 10 male and 10 female flies. Although metabolomics can only look at a static picture

without carrying out labelling studies the presence of high levels of these compounds in female flies might suggest a higher level of methylation of histones and thus gene silencing. In fact, histone modification by methylation can lead to either inhibition or activation of transcription depending on the type and site of the amino acid which is modified within the histone while histone acetylation and phosphorylation are always accompanied by up-regulation of the transcription process. N-acetyllysine was not detected in the samples. The most elevated metabolite in male flies was assigned by the data base search to methylthioadenosine, however, methylthioadenosine is essentially a neutral compound and elutes quite early from the ZICHILIC column. The metabolite assigned to methylthioadenosine elutes at 26.7 minutes which is similar to the retention time of S-adenosylmethionine. However, this compound is detected in male and female *Drosophila* and is not significantly different between them. S-adenosylmethionine is chemically quite unstable and this is relected by the fact that it fragments quite readily in the mass spectrometer source/trap without fragmentation energy being applied to give a fragment corresponding to methylthiodenosine. Figure 7.14 shows chromatograms form S-adenosylmethionine and the unknown metabolite both of which yield an ion corresponding to methylthioadenosine. The mass spectrum of the unknown metabolite had its most intense ion at m/z 355.1550 (figure 7.14) and its accurate mass corresponds to a decarboxylated form of S-adenosylmethionine. There is no record of this compound in any data base, however, chemically it could serve as a source of methyl and aminopropyl in the same way as S-adenosylmethionine. Its accumulation in male flies might be linked to the decreased levels of methyllysines and dimethylarginine in male flies if it is assumed the co-factor is accumulating rather than being used in methylation processes. Thus, it is clear that the mechanism of X chromosome dosage compensation in *Drosophila* needs further investigation and metabolomics in itself cannot give a definitive answer. One strategy for gaining some insight into the significance of lysine and arginine methylation would be to label *Drosophila* by growing them on labelled substrates, then transfer to unlabelled growth medium and observe the rate at which histone proteins degrade.

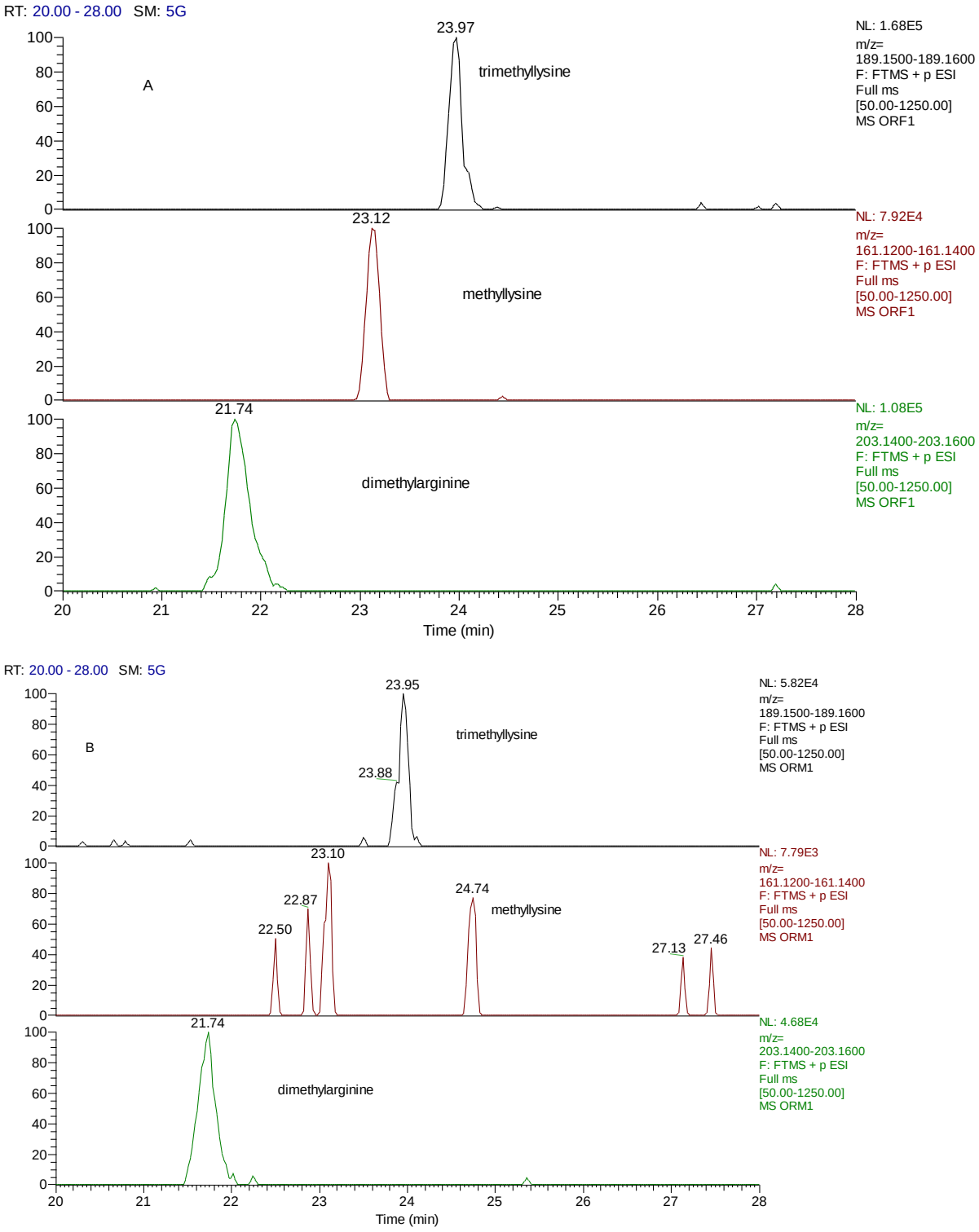

Figure 7-13 Chromatograms comparing methylated amino acids in extracts from 10 female (A) and 10 male (B) flies.

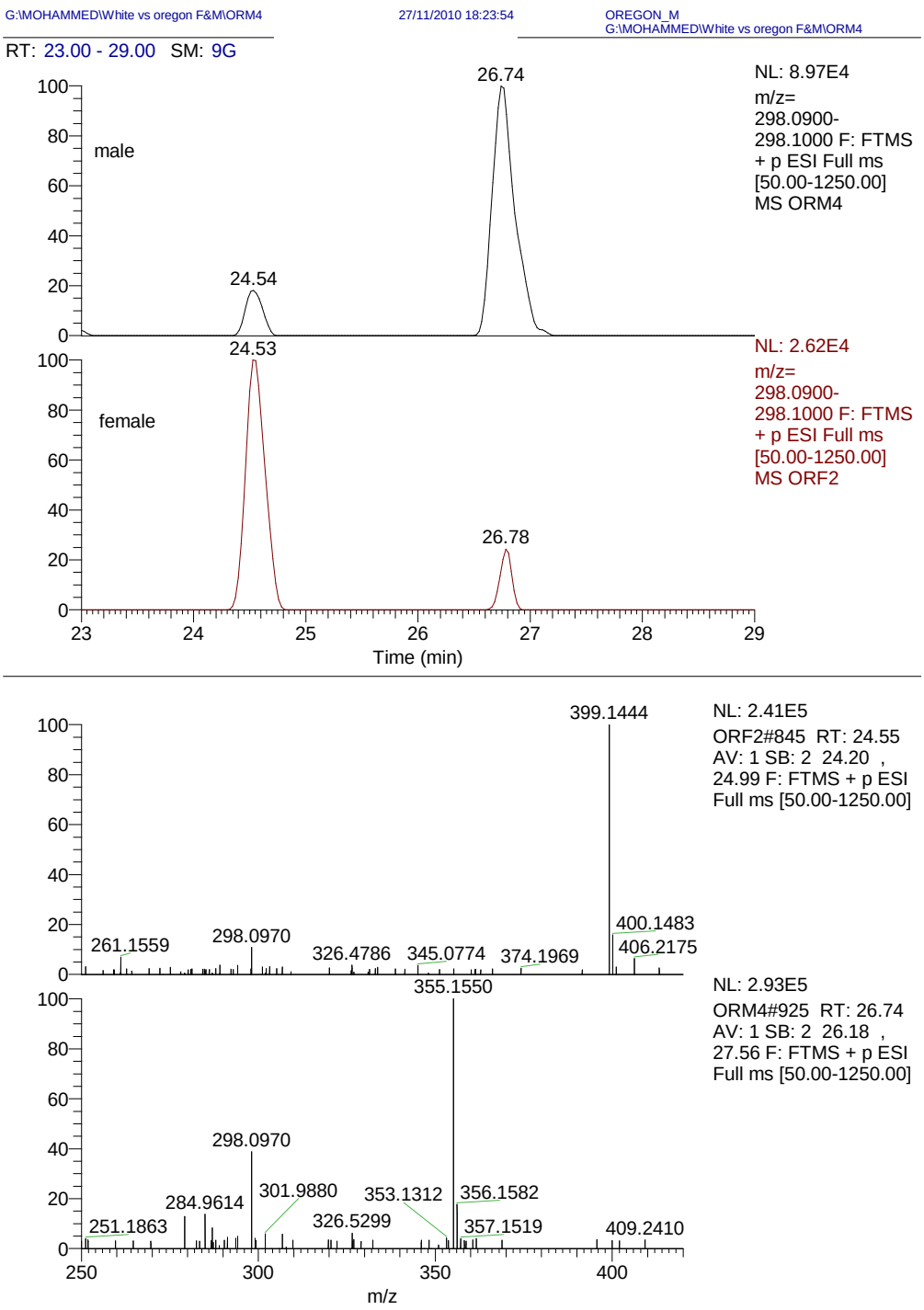

Figure 7-14 High levels of S-adenosylmethylpropylamine occur in male compared to female *Drosophila*

Because most of the series of pteridines and xanthomatins are not present in *white* flies, several genes belonging to the pteridine and ommochrome biosynthetic pathways are not capable of perturbation, so the measurement of dosage compensation theory in eye pigmentation in *white* was not informative, while the methyltransferases for both lysine and arginine residues showed low activity in *white* rather than in wild type. The levels of histone methylation in both sexes remained the same as described above. Taken together, all obtained data highlight the limitations of metabolomics in the investigation of dosage compensation for the *white* gene on the X chromosome. Thus, these data suggest that there is more to learn about this phenomenon. Based on the above information, we sought to identify whether the absence of the *white* gene plays a role in the perturbation of metabolic activities through salt treatment, but it was useful to know the nature of this gene prior to studying acute circumstances for *white*-mutant flies.

Table 7-3. Shows the main difference between sexes. Four extracts of 10 *females* and 10 males adult wild type were prepared. "Ratio" is of males/females peak areas.

Metabolites	MZ	Retention time	Ratio Males/females	P-VALUE
L-Serine	106.0499	18.5	0.42	1.05E-05
Proline	116.07046	17.8	0.71	0.007067
Valine	118.08636	18.0	0.57	0.010278
Taurine	126.02211	18.3	1.43	2.18E-06
Leucine	132.10199	14.9	0.48	0.000787
Hypoxanthine	137.04588	12.5	0.56	0.007187
Acetylcholine	146.11751	17.3	0.41	0.026628
Lysine	147.11284	25.4	0.50	0.00723
Methionine	150.05832	15.8	0.46	3.10E-03
Methyladenine	150.07756	17.7	1.3	0.015517
Guanine	152.05632	13.3	0.60	0.022563
Acetylhistamine	154.09752	18.3	37.76	2.04E-05
Methyllysine	161.12848	23.0	0.05	0.000271
Pterin	164.05687	13.6	0.52	0.026858
Phenylalanine	166.0863	14.4	0.51	0.002903
Isoxanthopterin	180.05156	13.2	18.21	3.32E-05
Dihydroxanthopterin	182.06744	13.3	2.04	0.002082
Tyrosine	182.08113	16.6	0.46	0.000912
Acetylspermidine	188.17595	18.2	1.44	0.038937
Trimethyl lysine	189.16	23.8	0.30	0.001728
Dimethyl arginine	203.15031	24.9	0.29	0.002342
Acetylcarnitine	204.12317	12.5	1.64	0.005832
Kynurenine	209.09221	14.5	0.37	0.000185
Acetyl arginine	217.1297	22.3	1.07	0.598832
Pyrimidodiazopterin	222.09866	12.1	0.47	0.008944
Hydroxy-L-kynurenine	225.08699	15.1	0.65	0.00095
Formylkynurenine	237.08716	13.9	0.10	0.002638
Sepiapterin	238.09352	10.4	2.37	0.000165
Biopterin	238.09354	13.9	2.25	0.000517
Dihydrobiopterin	240.10916	14.1	1.02	0.767009
Phosophoarginine	255.08542	22.5	0.25	0.01373
S-adenosylmethylpropylamine	298.09698	24.6	58.90	0.001372
Drosopterin	369.15308	18.1	0.82	0.282902
Xanthomatin	424.07742	14.2	0.54	0.032491

7.9 Mechanisms for Compensating for Salt Stress

Drosophila melanogaster, is well known for its tolerance for high levels of NaCl (Naikkhwah and O'Donnell, 2011). In general, salt is absorbed into the gut wall, then excreted by the Malpighian tubules and hindgut, as seen in figure 7-15. The balance between the rate of salt absorption and its eventual excretion is considered an important step for maintaining the flux of ions, including Na^+ and Cl^-, into and out of the cell. Indeed, an excess of salt in living organisms is not desirable due to ionic toxicity and it poses challenges to enzymatic reactions (Atack et al., 1995).

The toxicity of Na^+ was reported to affect HAL2 nucleotidase and RNAase MRP by displacing the essential magnesium sites; therefore a reduction in Na^+ absorption and an increase in Na^+ excretion represents the best defence mechanism for surviving well on a salt diet (Dichtl et al., 1997). Actually, when a cell faces a hypersaline environment cell volume will be decreased due to osmotic water loss. In order to neutralise this threat, fruit flies often use two kinds of defence systems. The first defence mechanism is often referred to as a short-term solution and the second is known as a long-term solution. These mechanisms involve a series of enzymes that are the body's main protection systems against osmotically stressful hypersaline conditions (Cohen, 1999). The first defence begins with suspending osmosis by replacing inorganic ions with macromolecular substances. The role of an influx of inorganic ions (Na^+ and Cl^-) inside the cell is to help the cell return its original volume by preventing the loss of water. This process takes place within minutes to hours (Roberts, 2000). Indeed, macromolecular substances vary so widely within living organisms that generalisations are difficult if the species is not considered (Roberts, 2000). Clearly, the action of macromolecular substances or organic osmolytes in osmotic adjustment and osmoprotection plays a vital role in salt tolerance. This role requires accumulation of organic osmolytes in the cytosol and organelles where this accumulation appears to be compatible with cellular processes, so it is better tolerated because intracellular activities are not disturbed. Furthermore, many of the organic osmolytes enhance cell adaptation by decreasing the generation of reactive oxygen species that are considered as the by-products of the hyperosmotic and ionic stresses and lead to the cell dysfunction that leads to cell death. However, a

common feature of organic osmolytes is that these entities can maintain the pH of intracellular fluid and minimise the effects on the charge balance of the cytosol. Imbalance in the charge of the cytosol and extracellular fluid would result in metabolic perturbation.

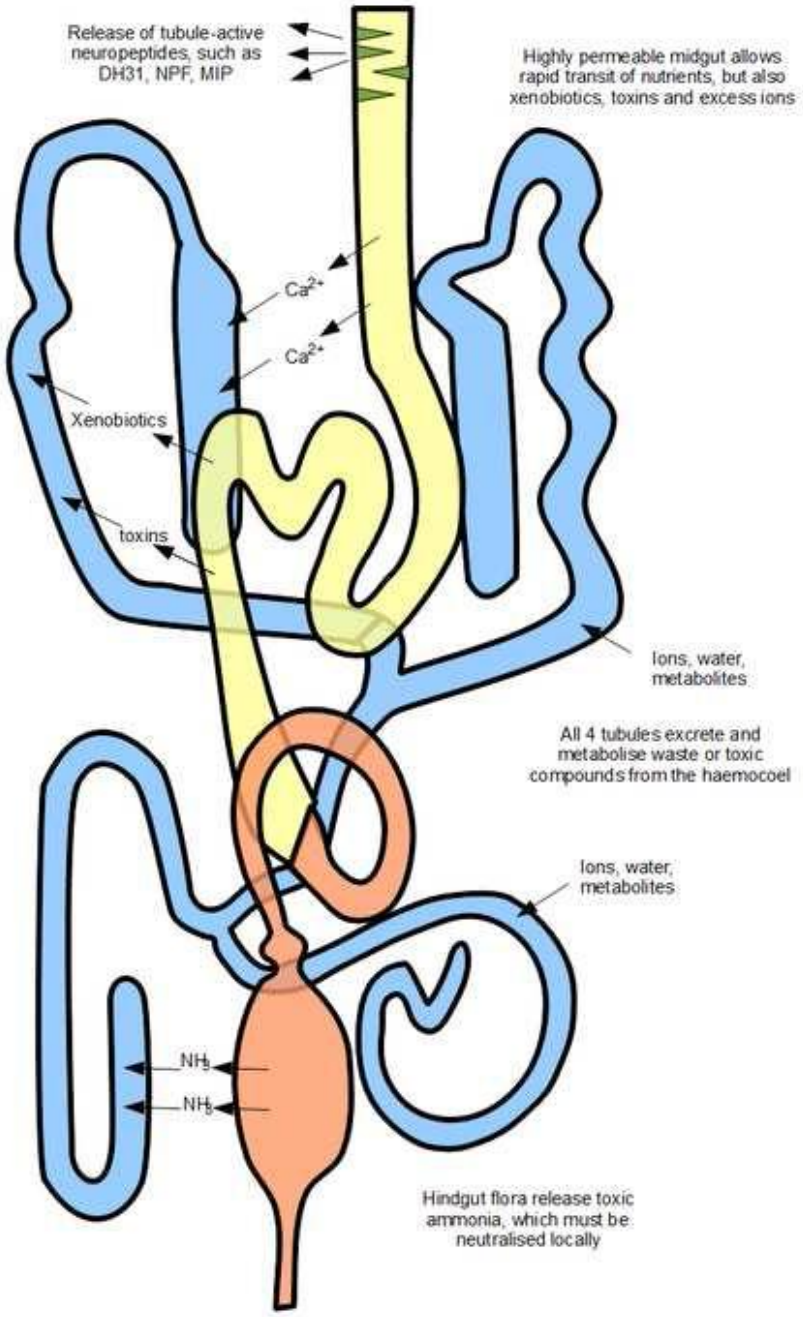

Figure 7-15. Model for universal functions of renal system: tubule (blue), guts (yellow and orange); adapted from (Chintapalli et al., 2012)

Osmoprotective substances can be categorised into two main groups, which represent the compatible osmotic solutes that are produced in response to saline conditions. These include the minority anionic solutes such as phosphate, sulphate and carboxylates, and the majority organic solutes that consist of simple sugars, or monosaccharides (mainly glucose and fructose), disaccharides (sucrose and trehalose), and complex sugars (raffinose and fructans). Others include polyols, amino acids and their derivatives (such as glycerol, proline and betaine). These compounds are accumulated by *de novo* synthesis or by increased absorption or by decreased degradation (Roberts, 2000). Additionally, the elevation of organic solute levels stabilises the protein structure by pushing the equilibrium of protein folding towards its original form, so the shape is stabilised or unaltered. Indeed denaturation can produce a range of effects, from the loss of protein solubility to communal aggregation via reduction in the total area of protein exposed to water (Roberts, 2000).

It has been proposed that cells use stress proteins called chaperones to help protect cellular proteins against a saline environment by promoting protein folding and by stabilising the structure of both protein and membranes during the dehydration process (Beck et al., 2000). To some extent, heat shock proteins (HSPs) have been found as osmotic stress proteins and are involved in maintenance of cellular components. One such protein that has been reported, which belongs to HSP110, is OSP94, which can replace osmolytes in salt stress conditions. Given that the synthesis of a protein takes more time and energy than its destruction, the imbalance in the folding and unfolding process may intervene in other slower enzymatic reactions required for successful protein modification folding, like isomerizames (Cohen, 1999, Roberts, 2000, Beck et al., 2000). This disequilibrium would lead to increased protein oxidation and, in turn, would reduce the ability of the organism to tolerate salt; therefore, the survival of a cell depends on the ratio of folded to unfolded protein. The role of HSPs is thought to be in stabilising cells until the accumulation of macromolecule osmolytes reaches sufficient levels to prevent the influence of saline conditions. In fact, there have been many efforts to understand the molecular mechanism of tolerance to salt stress that allows the cells to sense the

changes in extracellular fluid concentration and activate their defence against this in order to survive and recover from the presence of high external concentrations of salt.

Obviously, from all the above data and as indicated previously, it becomes clear that the cells, in order to survive the salinity, must have molecules that can interact with solutes and sense reduced hydration. The latter process results in macromolecular crowding in the cytosol. There are also other molecules that can recognise changes in plasma membrane structure, and they must include proteins that are quickly activated by alteration in the proton gradient (Serrano et al., 1999, Serrano and Rodriguez-Navarro, 2001).

7.10 Loss of w results in reduced resistance to salt stress

To explore its potential function in salt homeostasis, *w* mutation flies, both males and females, were fed separately on normal food containing 4% NaCl, as reported in section 2.9. The survival curves of these flies were compared in relation to salt conditions. Both male and female white mutation flies showed decreased survival rates from those of the control flies upon the salt feeding, whereas the longevity for both the control and the mutants did not appear different with normal feeding (data not shown). In contrast, it should be noted that the wild type male flies showed higher survival rates than the females upon salt feeding (figure 7.16). This is more evidence of the role of *w* in cellular function.

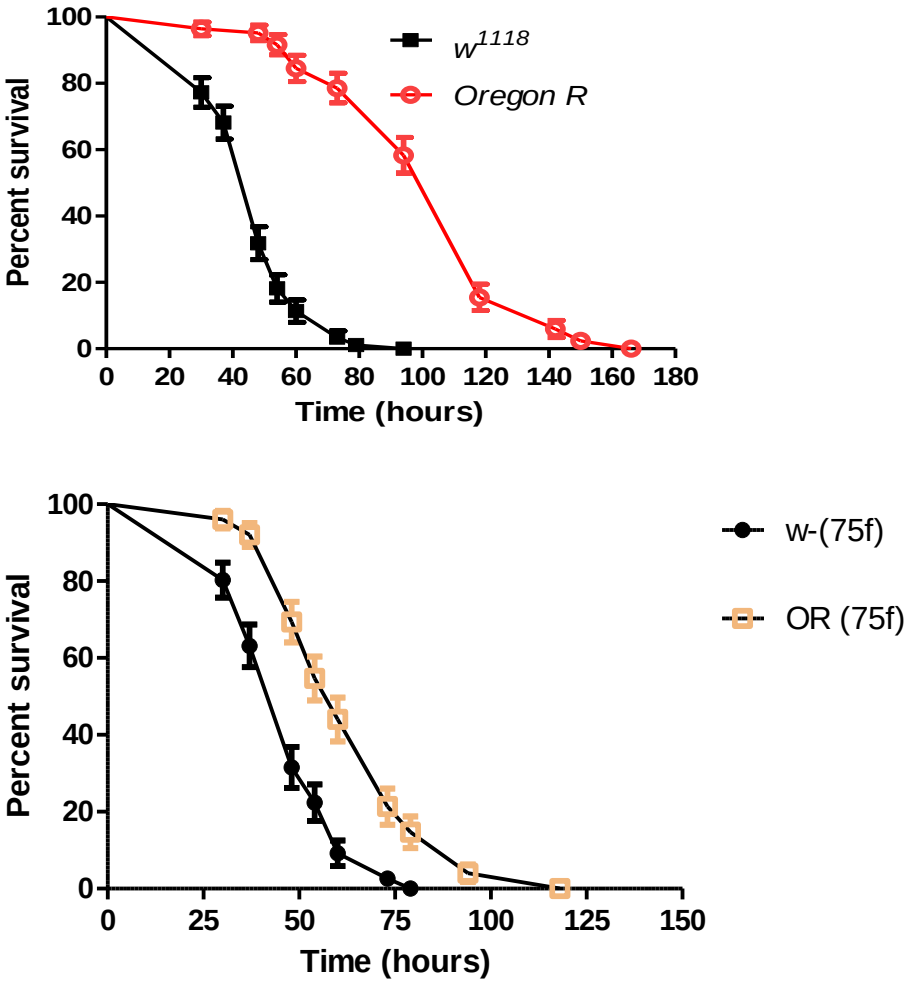

Figure 7-16. Survival curves showing that the *w* mutants are sensitive to salt stress. Salt assays were performed as described in section 2.9. All the assays were carried out separately for males (upper panel) and females (lower panel). Four independent replicates were used to obtain data; a total of 75 flies were used in each of the replicates. Interestingly, females carrying two *w* copies of the wild-type transgene showed decreased resistance over males carrying one copy of the *w* wild type.

7.11 Metabolomic flux response of whole organism to high salt diet

A metabolomic approach was used in an attempt to understand the influence of acute salt stress on the genetic pathways that impact on metabolic activities. It was important to address this question: Is salty food palatable to flies? In order to to avoid misinterpreting the effect of a salt diet on flies, salty food was labelled with a dye marker (indigo carmine dye**)** before adding the fruit flies, in order to investigate the ability of flies to eat salty food since their starvation would not be evident. The blue dye was added to their food, then flies were kept for 48 hours. The results showed that all flies had blue marker dye in their tissues, implying that the flies can eat salty food. These results can be seen in figure 7-17, confirming that the effect of salt loading was real.

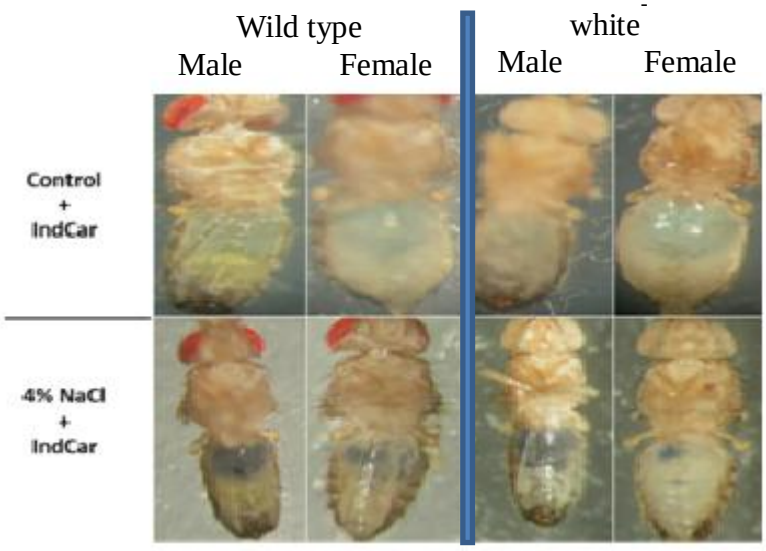

Figure 7-17 Flies eat salty food**.** Fly eating behaviour was assayed according to section 2.10. After one day of feeding, almost all the flies, including *w* mutants had abdomens that were coloured blue (lower panel) implying that they eat food even with high concentrations of salt. However, the changes in intercellular pH were monitored by blue colour, which was more pronounced in salt assays.

Although *Drosophila* do not encounter a salty environment in their normal life, they have evolved complex mechanisms that allow for resistance and adaptation to NaCl stress. These mechanisms can be seen in two different ways: anatomical or physiological and biochemical mechanisms. In fact, physiological mechanisms were

discovered by transcriptomic approaches by using an Affymetrix microarray method as published by Stergiopoulos (Stergiopoulos et al., 2009). However, the exact biochemical mechanisms of the effect of salt on *Drosophila* were still not clear. So, the goal of this study was to be a complementary study to the previously obtained transcriptomic data. Indeed metabolic principles can clearly govern fly stress, sense, response and adaptation. These principles become much clearer if we deal with specific tissues (guts and tubule) rather than the whole body because both the tubule and guts are considered osmoregulatory organs that counter high salt concentrations; therefore the metabolomic flux response of the whole fly and its tolerance to NaCl stress have few metabolic changes.

Table 7-4 List of metabolites that were significantly altered in salt-treated flies compared to controls (normal food) for *w* mutant and wild type. . Four extracts of 10 *w* and 10 wild type adult were prepared. "Ratio" is of treated/untreated signal**.**

Metabolites	MZ	Time	w		wild type	
			R	p-value	R	p-value
Glycine	76.039383	22.5	1.16	0.0665	1.31	0.0188
Alanine	90.054939	23.1	0.96	0.5748	1.00	0.9800
Alanine	90.05497	22.6	0.79	0.0316	0.84	0.0310
Serine	106.04983	22.5	1.65	0.0043	1.37	0.0037
Histamine	112.08691	31.6	0.82	0.0597	0.84	0.0365
Proline	116.07055	20.0	0.92	0.2699	1.06	0.4806
Valine	118.08616	19.8	1.15	0.1607	0.63	0.0321
Glycine betaine	118.08624	21.1	1.05	0.6037	0.52	0.0002
Asparagine	133.06068	22.4	0.89	0.1686	1.00	0.9505
Ornithine	133.09712	27.0	1.16	0.2388	0.88	0.8070
Aspartate	134.04472	21.5	2.01	0.0223	1.56	0.0113
Hypoxanthine	137.04579	14.8	0.29	0.0015	0.53	0.0014
Ethanolamine phosphate	142.02644	22.3	1.05	0.5887	1.29	0.0299
Proline betaine	144.10194	19.9	0.46	0.0003	1.59	0.5049
Glutamine	147.07635	22.0	1.36	0.0042	1.30	0.0053
Glutamate	148.06044	22.6	0.90	0.0555	1.02	0.8747
Guanine	152.05414	18.6	1.01	0.8828	1.30	0.3970
Allantoin	159.05128	17.0	1.21	0.1369	0.44	0.4147
Carnitine	162.11247	23.1	0.67	0.0041	0.86	0.1046
Urate	169.03558	16.0	1.09	0.3490	0.82	0.0928
Arginine	175.1188	27.2	1.03	0.7366	1.24	0.0213
Citrulline	176.10298	22.9	3.97	0.3406	1.66	0.0002
HIU	185.03061	16.0	5.96	0.0274	1.01	0.9460
Homocitrulline	190.11862	27.5	0.00	0.3910	0.41	0.0001
Acetylcarnitine	204.12277	18.8	0.91	0.3945	1.37	0.0261
Propionyl carnitine	218.1385	17.8	0.58	0.0015	0.81	0.1178
Butyrylcarnitine	232.15428	16.8	1.56	0.0344	4.39	0.0000
Cystine	241.03101	24.6	0.35	0.0108	0.23	0.0244
Phosphoarginine	255.08508	25.0	4.42	0.0928	3.40	0.0985
GPC	258.10992	22.6	0.65	0.0019	0.81	0.0051
Tyrosine phosphate	262.04727	21.3	0.99	0.9361	5.10	0.0000
GSH	308.09085	20.1	2.19	0.0087	1.34	0.6780
Linolenylcarnitine	424.34183	14.8	1.15	0.4675	1.05	0.7054
Linolylcarnitine	426.35751	14.7	0.95	0.5774	0.76	0.0897
Oleoylcarnitine	428.37338	14.7	1.45	0.1836	1.39	0.0512
CDP-ethanolamine	447.06744	23.7	0.66	0.0043	2.38	0.0006
CDP-choline	489.11432	25.2	0.80	0.1257	0.99	0.9035
GSSG	613.159	24.2	1.68	0.0510	2.23	0.0003

GSH and GSSG levels increase in both *w* and wild type flies indicating that salt stress is associated with oxidative stress. *W* appears to accumulate GSH to a somewhat greater extent than wild type suggesting that its poorer adaption to the conditions does not relate to impaired antioxidant capacity. The tolerance of fruit flies to salt stress begins from the accumulation of organic solutes, whether these accumulations are a result of fly responses or fly adaptations to acute changes in the salt environment. It is not surprising to find that there is an increase in nitrogen compound levels during salt treatment, especially serine, amino acids may maintain cell functions in both wild type and mutated flies (Shahjee et al., 2002). Serine, glycine and cysteine are non-essential amino acids and so they can be synthesised by the fly via a *de novo* synthesis process. Both the glutamate family, which is composed of four non-essential amino acids (glutamate, glutamine, proline and arginine) (Galinski and Trüper, 1994) that are formed from 2-oxoglutarate metabolism, and the aspartate family, which also consists of two non–essential amino acids (asparagine and asparate) and comes from oxaloacetate metabolism, seem to be unaffected by salt exposure, as seen in table 7-3. Acetyl, propionyl and butylcarnitines are elevated to a marked extent in wild type and these quaternary ammonium compounds could well be functioning as osmolytes. The most marked difference between *w* and wild type is the increase in tyrosine phosphate which occurs in wild type. Free tyrosine phosphate has been reported in Drosophila once before (Moore 1985) but no role has been ascribed to it. It has all the qualities required of an osmolyte being highly charged and having a hydrophobic region which would allow interaction with proteins and membranes. The build up of sodium ions in the cytosol leads to an ion toxicity phenomenon particularly with magnesium being present at sites in many essential enzymes (Zhou and Clapham, 2009, Serrano et al., 1999), phosphate, in the form of tyrosine phosphate, would pair strongly with inorganic cations and thus may reduce the effect of increased sodium ions in the cell

.

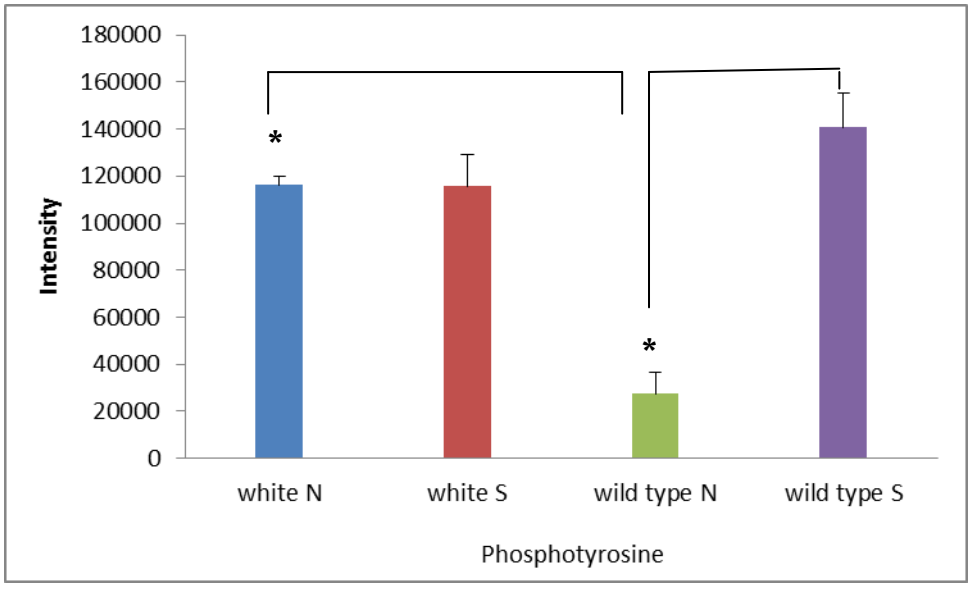

Figure 7-18 Level of phosphotyrosine is more abundant in white mutation flies in both cases (salted and unsalted condition) while in wild type flies under salt condation, phosphotyrosine was accumulated 5 fold than wild type flies fed by normal food Data are shown as mean ±SEM for N=4 independent experiments. Data that differ significantly are marked with asterisks are analyzed by Student's *t*-test two tailed.

Phosphorylation requires ATP and there is likely to be a high demand for ATP in salt stressed cells both as a co-factor in ATP based pumps required to remove ions from the cell and potentially in the production of osmolytes. Arginine phosphate (AP) is markedly elevated both in *w* and wild type. AP plays the same role in invertebrate systems as creatine phosphate does in vertebrate systems by providing a highly diffusible high energy phosphate donor which is used to restore ADP to ATP in situations where energy demand is high (Ellington 2001) ATP diffuses much more slowly than AP and is thus less able to meet demand for high energy phosphate at specific sites within the organism. Normally, cysteine is sulphide compound that plays an important role in protein stability and function due to its ability to form cystine by linking two cysteine molecules via a disulphide bridge (Brosnan and Brosnan, 2006). So, together with methionine, cysteine is a protein degradation biomarker. Thus, the steady accumulation in the fly's body during time treatments by a denaturating agent are a result of the protein refolding process which maintains the stability and function of protein in order to keep the fly alive (Jessop et al., 2004,

Brosnan and Brosnan, 2006). Releasing cysteine from proteins increases local conformational changes that strengthen the association between protein's subunits returning to native state (Burns et al., 2005). In this way the fly tries to minimise the effect of high salt concentrations on cell components (Beck et al., 2000). Primarily, cysteine can be synthesised from serine by eliminating the acetate group from o-acetylserine and adding H_2S via the sulfhydrylation reaction. These steps are widely known in plants and most microorganisms, while in mammals it can be achieved from methionine that is directly converted into L-homocysteine, which later can condense with serine to form L-cystathionine; then cysteine is made via cystathionine γ-lyase. (Voet and Voet, 2006).

The third metabolite in the serine family list is glycine, the production of glycine from serine will give the fly's body chance to delay the dehydration process coming from salinity. Glycine can be formed via serine hydroxymethyltransferase when serine condenses with tetrahydrofolate (THF) forming N^5,N^{10}-Methylene tetrahydrofolate and water, while the reverse conversion is possible by glycine oxidase reaction when N^5,N^{10}-Methylene tetrahydrofolate reacts with free ammonium (Cossins and Sinha, 1966). Furthermore, elimination of excess ammonia by yielding urea is part of the clearance process to avoid toxicity from ammonia accumulation. Therefore one possible way to decrease the amount of ammonia then excrete it as urea is through the arginase pathway, where arginine converts into urea and ornithine via the urea cycle (Morris Jr, 2002). Thus, induction of a urea-metabolising enzyme via the arginase mechanism by high levels of two metabolites, such as ornithine and citrulline, may be demonstrated to occur in fruit flies as a way to counteract salt stress. Additionally, citrulline can be formed in mitochondria by adding carbamoyl residue into orinthine via an oxidation process with ornithine carbamoyltransferase to produce phosphate. Although the role of both rare amino acids orinthine and citrulline in enhancing the immune system is not rigorously demonstrated, their ability to counteract adverse conditions is believed to promote tissue repair, which, in turn, increases fly longevity. From the above results, it is clear that a broad spectrum of enzymes implicated in the metabolism of nitrogen-containing compounds showed upregulation in their levels over the course of treatment in comparison with normal conditions (Beck et al., 2000).

7.12 What is the link between mutation in white gene in drosophila and salt sensitivity?

Unlike wild-type flies, *white* mutant flies were highly sensitive to salt food and died more quickly than the wild type, suggesting that *w* is an essential gene for salt regulation in organisms that face acute salt diets. This interesting phenomenon pushes us to suggest that a secondary molecular signalling (cGMP and its transporter) is involved. Although previous research has shown that the fluid transport is not associated with functional *white*, the mechanism of transport of cGMP throughout the tubules is still unclear; it may be either by free diffusion or active transport (secondary or primary) that facilitates its transport from one compartment to another (Evans et al., 2008).

We know that lipids are mainly synthesised in endoplasmic reticulum (ER) and then transported to other organelles according to need (Blom et al., 2011). After exposure to extreme salt conditions, *w* mutant flies do not only demonstrate greater sensitivity to salt stress than wild type, they also display a lower level of phospholipase A1 than the wild type (Kopf et al., 2012). In figure 7.16 it can be seen that levels of the SN2 lyso PC lipid at m/z 520.3 are markedly reduced in response to salt treatment in *w*. The earlier elution of the SN2 lysolipids was confirmed by treating soybean lecithin with phospholipase A2. The same was observed for the SN1 lysolipids in salt treated *w* (figure 7.19) but to a lesser extent. In comparison salt stress had less effect on PC lysolipids in wild type. Therefore, the reduction in SN2-lysoPC species may lead to membrane disorganisation and some of the changes in membrane properties may occur in *w* mutants. This corresponds to the observation from transcriptomics data that phospholipase falls under salt stress conditions (Stergiopoulos et al., 2009).

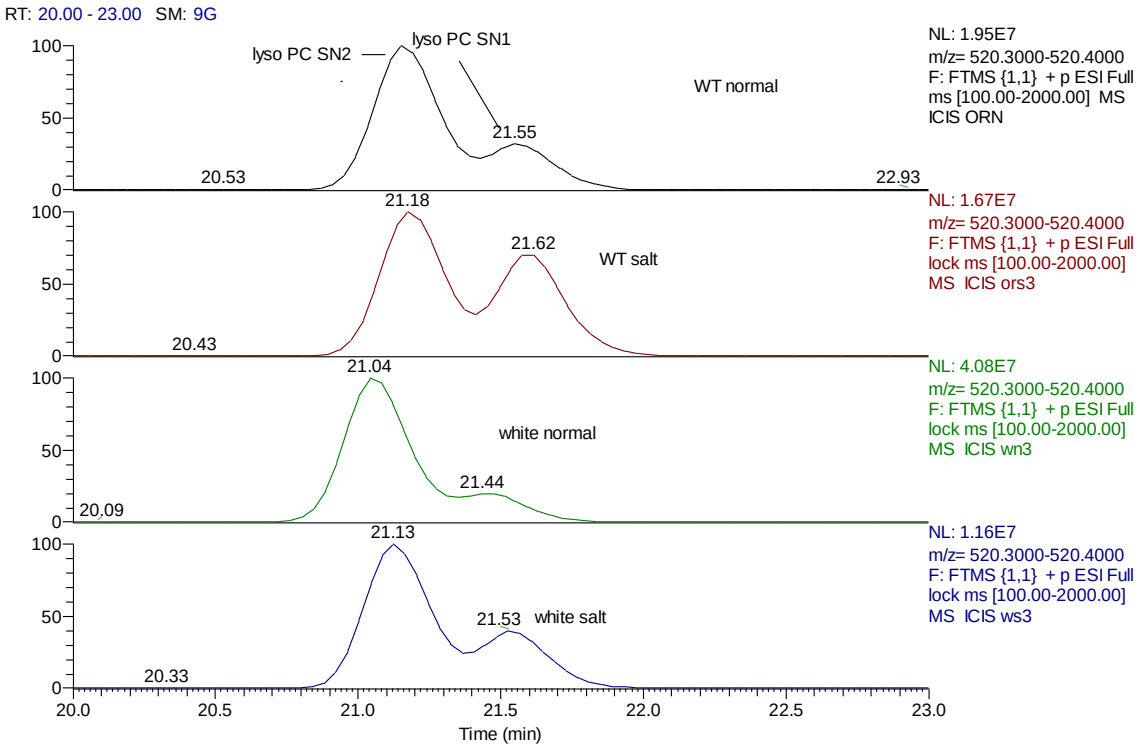

Figure 7-19 Peaks obtained for a typical PC lysolipid for WT and *w* cultured on normal growth medium and under salt stress (chromatographic conditions as in section 2.12.3.

Although the attempt to understand how *w* responds to salt stress has furthered, our understanding of the role lysophospholipid plays in salt conditions is challenging. It would seem that inhibition of phospholipase A1 by salt stress conditions in *w* will prevent the flies from adapting since they are less able to remodel their cell membranes.

During their metabolism, do SN2lysoPC species need to be transported further by the *white* transporter to their new destination? Since this process does not function properly in the *w* mutant this might have an effect on the adaption to salt stress.

The poor adaption to salt stress by *w* might be explained by considering G-protein-coupled lysophosphatidylcholine receptors, which can activate diverse groups of receptors leading to the promotion of many cellular functions, including cell proliferation, cell survival, cell signalling, adhesion, calcium homoeostasis and

Ca^{2+} dependent functions (Xu, 2002, Lim et al., 2011, Radeff-Huang et al., 2004, Meyer zu Heringdorf and Jakobs, 2007). The correlation between GPCRs and certain lysophospholipids was only recently discovered. There are several types of lysophospholipid: sphingosine-1-phosphate (S1P), lysophosphatidic acid (LPA), sphingosylphosphorylcholine (SPC) and lysophosphatidylcholine (LPC) which have been recognised to act as ligands to G- receptors, so GPCRs can be activated or inhibited according to lysophospholipid mediators that have a glycerol or sphingoid backbone and one single acyl fatty acid. Furthermore, GPCRs have been found in *Drosophila* and are characterised by a heterotrimeric structure with three subunits (alpha, beta and gamma) (Yarfitz et al., 1988). Among them, the alpha subunit has been studied extensively and grouped into four major families, including G_i, G_s, $G_{12/13}$ and G_q. In some cases, GPCR coupling to specific G-proteins inhibits cell growth and proliferation, such as with cAMP/PKA and the closely-related cGMP/PKG (protein kinase A, G refers to PKA and PKG, respectively) (Radeff-Huang et al., 2004). From the information above, it can be postulated that lysophosphatidylcholinease A1 and its product sn2 lysoPC – not lysophosphatidylcholinease A2 and its product sn1 lysoPC – play an important role in the salt tolerance mechanism that results in the regulation of many kinds of cellular activities.

Figure 7.19 shows the proposed actions of cGMP within cells. During processing the data from the lipid method used to analyse lipids in Drosophila, which is based on chromatography on silica gel, it was observed that this method seemed to be very good for the analysis of cyclic AMP and cyclic GMP. The ZICHILIC and ZICpHILIC methods only gave weak or no peaks for these analytes. These are very preliminary results and require checking but the peaks for cAMP and cGMP are clear as shown in figures 7.18 and 7.19 give elemental matches at sub 1 ppm and are observed in negative ion as well as positive ion mode. Table 7.5 summarises the findings for the comparison of wild type and *w* untreated and subjected to salt stress. While the levels of cAMP and cGMP do not change very much in WT they are elevated by about x4 in *w* in response to salt stress. In addition GMP can be detected in WT but not in *w*, GMP is formed via the action of phosphodiesterase on cGMP and terminates its action in promoting ion channel conductance. Thus despite the fact

that *w* cannot transport cGMP it can still produce it. It may be that cGMP accumulates since it cannot be transported out of cells and this might be a factor in the failure of *w* to adapt to salt stress. In addition to 3'5' cAMP there is an isomer of cAMP present in the samples (figures 7.21 and 7.22) which may be due to 2'3'cAMP. 2'3' cAMP has been very recently reported as a metabolite of adenosine and is believed to increase under stress conditions, its physiological role remains to be fully characterised (Jackson 2011).

Table 7.5 Effects of salt stress on cAMP and cGMP in *w* and wild type (n=4). The analytes were detected using the lipid analysis method described in 2.12.3.

	m/z	RT	ratio WT S/N	P-value	Ratio *w* S/N	P-value
3'5' cAMP	330.0596	9.3	0.99	9.70E-01	6.9	3.40E-03
2',3' cAMP	330.0595	11.1	1.38	1.10E-02	1.5	7.00E-03
3'5' cGMP	346.0548	9.1	0.60	3.60E-01	5.4	4.40E-03
GMP	364.0647	8.9	0.82	4.50E-01	ND	ND

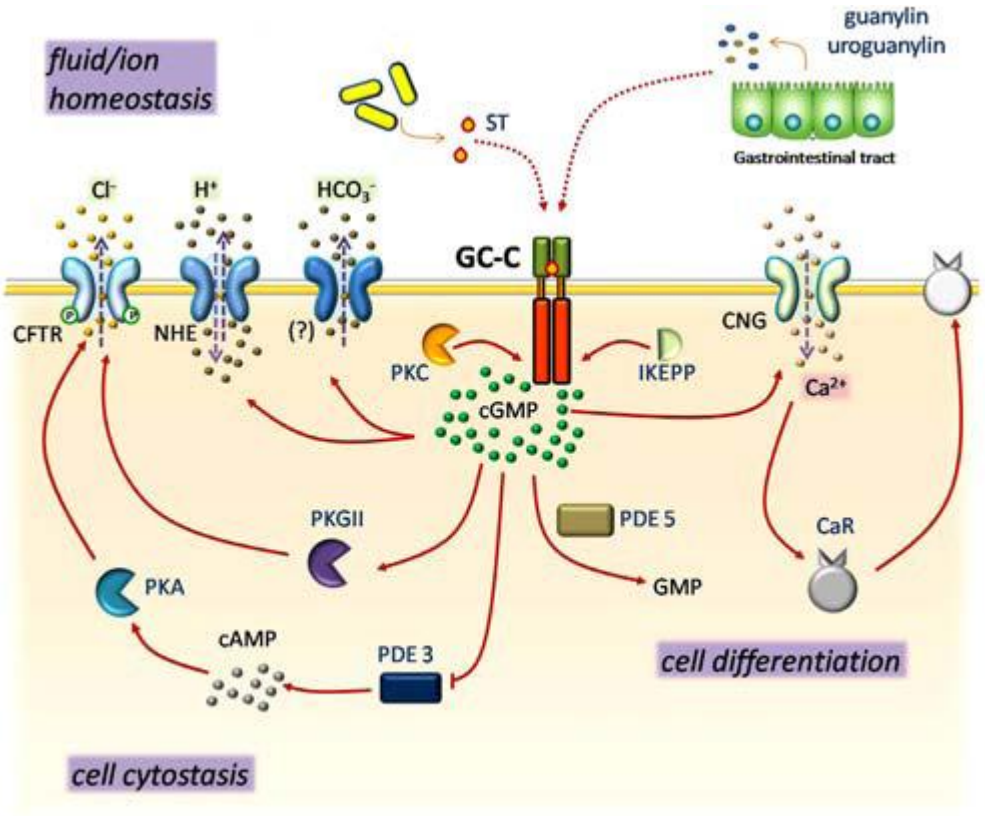

Figure 7-20 Pathways that are either directly regulated byguanylate cyclase C(GC-C) or modified by cGMP production (adapted from Radeff-Huang, Seasholtz et al. 2004).

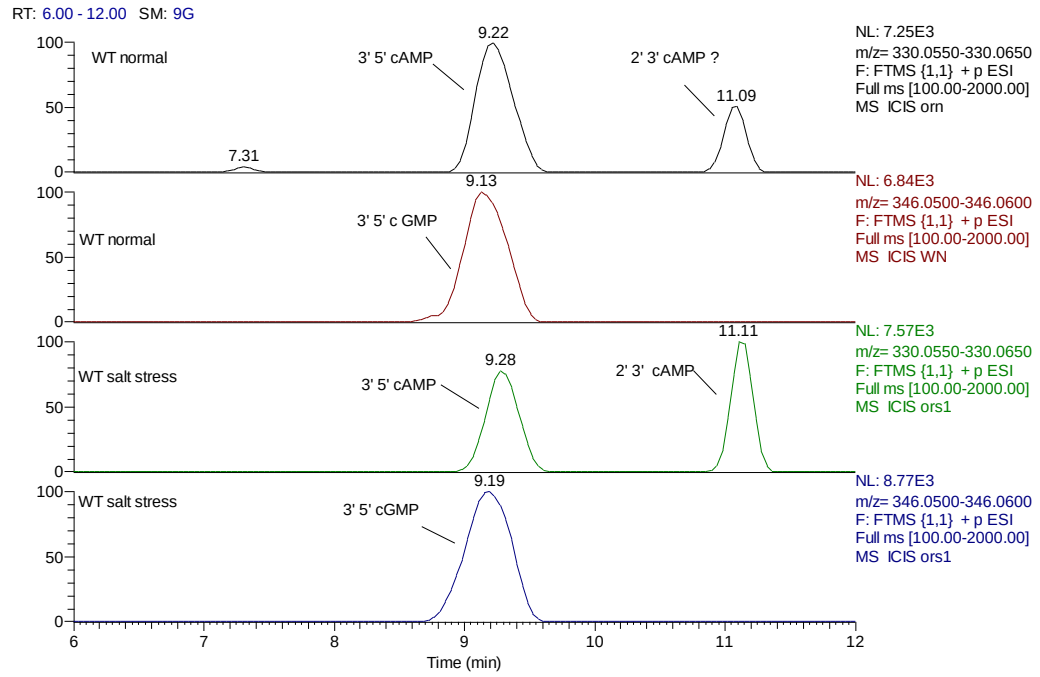

Figure 7-21. Effect of salt stress on cAMP and cGMP in WT flies. Chromatographic conditions as in 2.12.3.

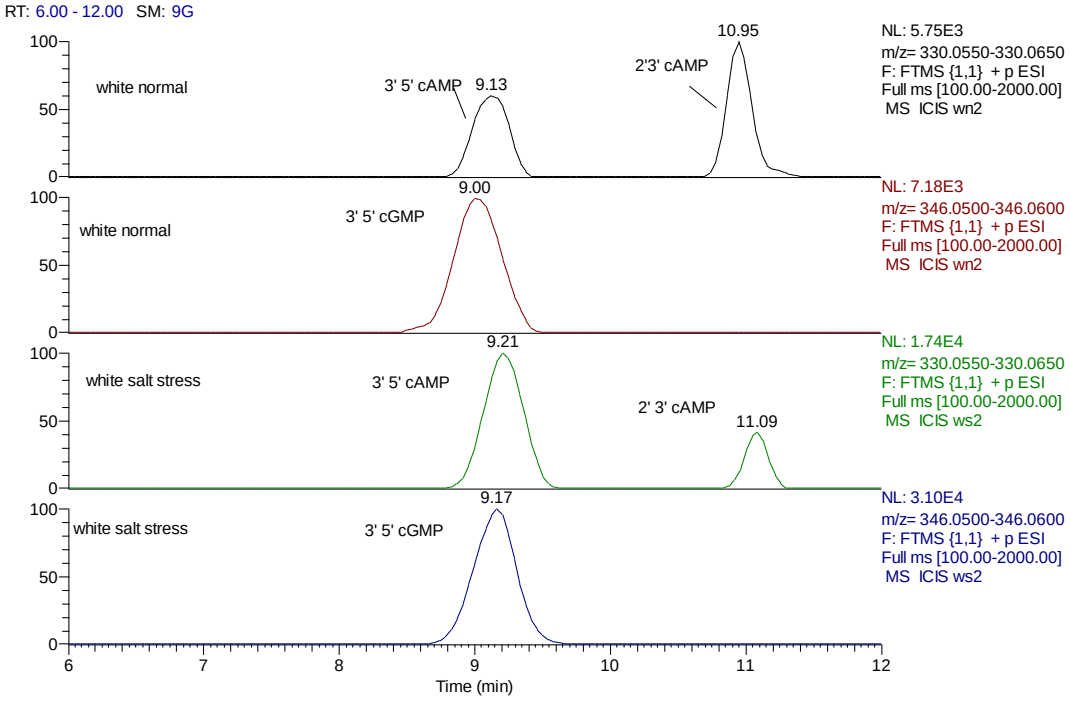

Figure 7-22. Effect of salt stress on cAMP and cGMP in *w.* Chromatographic conditions as in 2.12.3.

7.12 Overall Conclusion and Future Work

It was not possible within the timeframe of the thesis to fully explore many of the questions and hypotheses generated by the work within the thesis. Indeed there was much additional work carried out which could not be incorporated into the thesis without making it much longer. Some of the additional work is presented without comment in the appendices. In particular a lot of effort was devoted to making a lipid map of several tissues within Drosophila and the preliminary data on this is presented in appendix IX. The completion of the lipid map in publishable form will require a lot more processing and checking. The metabolic difference between male and female flies deserves a more thorough investigation and linked to this further exploration of the *w* mutation is required. Labelling studies will be required in order to understand a possible role for histone modification/turnover in relation to the compensation phenonmenon which occurs in male flies due to having only one X chromosome. The treatment of flies with allopurinol provided a proof of concept with regard using Drosophila as a test organism for drug treatment and two more treatments of this nature with paraquat and hydrazine were carried out but the data has not been fully processed. Thus there is enough work for several people to carry out but as a matter of priority I would like to propose the following studies as seen in chapter 8.

8. Chapter eight: Summary and future work

8.1 *Drosophila melanogaster* used as model for genetic lesions and environmental stimuli

Genetic experiments are best conducted with excellent genetic animal models such as *Drosophila melanogaster*. This has clear advantages for the study of some human disease genes, based on the information available for research. The strength of *Drosophila* as a model is underpinned by the availability of the complete *Drosophila* genome sequence(Adams and Sekelsky, 2002), the tens of thousands of available classical mutants in stock centres, RNAi stocks for nearly every gene(Dietzl et al., 2007).A transgenic fruit-fly line can be produced for approximately $500 in under four months and costs just $30 per year to maintain(Julian A.T, 2007). It is also one of the best and useful genetic animal models owing to its short life cycle, which allows multiple generations to be screened quickly. The small size of the insect makes it better than many other animal models in terms of lab space and food requirements. At the molecular level, balancers and P-elements provide ideal genetic tools for gene transformation and phenotype selection. Interfering RNA is also an important molecular genetic tool which helps in the field of functional genomics, specifically reverse genetics. These facts form the basis for applying metabonomics to unlock the mystery of *Drosophil*a mutants in captivity in stock centres. The *white* mutant was used for further metabolic investigation and the list could be expanded to other mutants in stock centres worldwide.

The current study has helped in addressing some scientific questions fairly quickly and easily. It costs few dollars to run the samples which take the technician less than 30 minutes in sample preparations and setting up the instruments. The analysis could be left overnight or up to a few days depending on the amount of data needed to finalize the results. *Drosophila*, as genetic model, has its limitations as it is not mammalian; however with new technologies and techniques continually emerging, the Orbitrap with great certainty will help in closing the phenotype gap between human and *Drosophila* models. The current study has also shown the usefulness of *Drosophila* in modelling of rare diseases of humans that might otherwise be considered too rare to attract research funding. The techniques developed in

the thesis could be used to integrate the wealth of *Drosophila* genetics and metabonomics in other branches of biology. For example measuring the changes in development, modes of drug action and testing new applications of existing drugs and also use in insecticide and detoxifications studies.

8.2 Optimisation of metabonomics studies

Although the LTQ-Orbitrap-MS is an important in sample analysis, the other aim was to improve sample selection and treatment. Mutant flies could provide a background for a genetic screen to identify modifiers of a disease – this is a very standard *Drosophila* technique. Secondly, the same background could be used to screen for compounds which improve survival. Although this is not a high-throughput screen, it is much less expensive than working with mice or humans. Thirdly work in *Drosophila* could allow us to build systems biology metabolic models that could predict the impact of mutations, and potentially predict possible therapies.

In addition it is possible to observe metabolites in different tissues and link this with gene expression level in those individual tissues (Chintapalli et al., 2007a), suggesting that it may ultimately be possible to build models linking transcriptome and metabolome. However, this is not as easy as it sounds, as metabonomic analysis consists of different stages. The hardest part is the data analysis; it requires up-to-date speedy computers as well as continuously cutting-edge computational skills along with very strong biochemistry background knowledge.

Metabonomics can be applied not only to mutants or specific tissues, but can also be used to follow and investigate the pharmacological effects of drug actions. The anti-gout drug allopurinol was used as it is considered to phenocopy the *rosy* mutant in humans and flies. Consequently, effects on purine pathway were observed, however interference with isomers was also observed and this is important in metabolic analysis. Unexpected levels of hypoxanthine and xanthine were found. However, these changes were as a result of the hypoxanthine and xanthine isomers, the original drug allopurinol

and its oxypurinol metabolite. Even less expected were effects of allopurinol on tryptophan metabolism which perhaps support its established, but not fully understood, activity in refractory schizophrenia and the treatment of stroke.

8.3 Future work

Metabonomic studies are very useful and a highly applicable method, along with what is available from the transcriptomic datasets, in the biological studies, in the normal as well as in the diseased states. There are tens of thousands of *Drosophila* mutants in stock centres world over. Many of these fly lines are kept for several years without their genetic makeup being determined or metabolomic profiling. Thus it can be argued that metabolic analysis along with the transcriptomic data would enable scientists unlock the genetic mystery of many of the lines and perhaps human genetic diseases. Furthermore, there is a huge pressure for cost-effective treatment programmes for rare but lethal genetic diseases (like IEMs) in the neonatal and perhaps the premarital periods especially in a society like the Kingdom of Saudi Arabia. For this purpose the Orbitrap analyzer is sensitive, fast; cost effective and high throughput enough to be applied in diagnostics as well as in screening.

9. Appendices

Appendix I: List of standards and their retention times on ZicHILIC under the conditions described in section 2.12.1. N.B. This column tends to lose retentivity with time and over around three months of usage retention times decrease by around 1.5 minutes thus these retention times are only approximate with regard to those reported elsewhere.

Compound Name	Formula	Polarity	Detected m/z	Delta (ppm)	RT
3-(2-Aminoethyl)-1H-indol-5-ol	C10H12N2O	+	177.1021	-0.98	15.79
Adenosine	C10H13N5O4	+	268.104	-0.1	12.93
AMP	C10H14N5O7P	+	348.0703	-0.31	17.7
GMP	C10H14N5O8P	+	364.0651	-0.41	17.7
5-Hydroxyindoleacetate	C10H9NO3	+	192.0654	-0.55	7.96
Antipyrine	C11H12N2O	+	189.1022	-0.35	7.56
5'-Methylthioadenosine	C11H15N5O3S	+	298.0967	-0.53	10.69
10-Phenanthroline	C12H8N2	+	181.0759	-0.54	14.4
Allantoin	C4H6N4O3	-	157.0369	1.26	12.83
β-alanine-methyl-ester	C4H9NO2	+	104.0706	-0.54	15.11
Betaine	C5H11NO2	+	118.0862	-0.75	15.95
2-Oxoglutarate	C5H6O5	-	145.0143	0.67	10.97
5-Oxoproline	C5H7NO3	+	130.0498	-0.38	8.07
5-Aminolevulinate	C5H9NO3	+	132.0654	-0.8	17.7
β-L-fucose	C6H12O5	-	163.0615	1.54	11.06
D-Glucose	C6H12O6	-	179.0563	1.17	14.04
Cis-Aconitate	C6H6O6	-	173.0095	1.82	7.99
Benzenesulfonate	C6H6O3S	-	156.9967	1.57	7.99
Citrate	C6H8O7	-	191.02	1.22	11.26
1-Phenylethylamine	C8H11N	+	122.0964	-0.3	12.66
Adenine	C5H5N5	+	136.0618	0.31	14.4
2-Phenylglycine	C8H9NO2	+	152.0706	0.08	13.09
Amphetamine	C9H13N	+	136.1122	0.78	12.29
CMP	C9H14N3O8P	-	322.045	1.17	19.34
4-Coumarate	C9H8O3	-	163.0403	1.42	6.04
Inosine	C10H12N4O5	+	269.088	-0.24	10.67
IMP	C10H13N4O8P	-	347.0404	1.68	15.87
Guanosine	C10H13N5O5	+	284.0989	-0.35	12.46
dAMP	C10H14N5O6P	-	330.0616	2.1	17.1
Glutathione	C10H17N3O6S	-	306.0772	2.22	14.84
glutethimide	C13H15NO2	+	218.1176	0.27	5.85
Glycine	C2H5NO2	+	76.03934	0.52	18
Ethanolamine phosphate	C2H8NO4P	-	140.012	0.93	19.21
L-Alanine	C3H7NO2	+	90.05499	0.42	16.34
Fumarate	C4H4O4	-	115.0037	0.43	7.25
Imidazole-4-acetate	C5H6N2O2	+	127.0501	-1.1	14.9
Homoserine lactone	C4H7NO2	+	102.055	0.59	17.16

L-Aspartate	C4H7NO4	+	134.0445	-2.39	17.58
D-Xylose	C5H10O5	-	149.0457	1.03	11.98
Hypoxanthine	C5H4N4O	+	137.0459	0.7	9.94
Isonicotinic acid-not isomers	C6H5NO2	+	124.0393	-0.17	9.43
Guanine	C5H5N5O	+	152.0567	0.1	12.44
Cis-4-Hydroxy-D-Proline	C5H9NO3	+	132.0653	-1.95	17
L-Glutamate	C5H9NO4	+	148.0604	-0.27	14.42
Creatinine	C4H7N3O	+	114.0662	-0.23	15.6
L-Cystine	C6H12N2O4S2	+	241.0307	-1.82	21.5
D-Fructose	C6H12O6	-	179.0564	1.42	12.71
L-Arginine	C6H14N4O2	+	175.119	0.12	25.88
D-Glucosamine 6-Phosphate	C6H14NO8P	+	260.0527	-0.94	21.5
D-Sorbitol	C6H14O6	+	183.0862	-0.64	14.86
Cytosine	C4H5N3O	+	112.0505	-0.01	17.18
Isocitrate	C6H8O7	-	191.0201	1.78	12.22
Cystathionine	C7H14N2O4S	+	223.0745	-1.08	22
Gallate	C7H6O5	-	169.0145	1.57	9.37
Dopamine	C8H11NO2	+	154.0862	-0.08	14.9
Homogentisate	C8H8O4	-	167.0351	0.77	7.96
4-Hydroxyphenylacetaldoxime	C8H9NO2	+	152.0706	-0.22	7.9
Cytidine	C9H13N3O5	+	244.0842	-35.17	18.98
L-Adrenaline	C9H13NO3	+	184.0968	-0.02	16.72
Aspirin	C9H8O4	+	181.0494	-0.62	5.59
L-Kynurenine	C10H12N2O3	+	209.0916	-2.1	10.49
O-Acetylcarnitine	C9H17NO4	+	204.1231	0.43	13.56
Pantothenate	C9H17NO5	+	220.1178	-0.62	7.92
L-Metanephrine	C10H15NO3	+	198.1121	-2.14	17.23
L-Tryptophan	C11H12N2O2	+	205.0899	-35.42	11.84
Maltose	C12H22O11	-	341.1098	2.63	15.18
NAD+	C21H27N7O14P2	+	664.1168	0.64	20.46
Oxalate	C2H2O4	-	88.99133	37.1	17.88
Pyruvate	C3H4O3	-	87.00871	-0.63	8.51
Malonate	C3H4O4	-	103.0037	-0.19	15.91
Phosphoenolpyruvate	C3H5O6P	-	166.9752	0.73	16.96
Maleic acid	C4H4O4	-	115.0037	0.29	13.18
Methylmalonate	C4H6O4	-	117.0192	-0.77	14.88
L-Homocysteine	C4H9NO2S	+	136.0425	-1.1	20.37
Alloxanthine	C5H4N4O2	-	151.0262	0.03	10.52
D-Glucuronate	C6H10O7	-	193.0354	0.13	16.45
D-Galactose	C6H12O6	-	179.0563	0.91	14.39
Nicotinate	C6H5NO2	+	124.0393	-0.11	8.31
L-Histidine	C6H9N3O2	+	156.0768	0.48	14.84
N(pi)-Methyl-L-histidine	C7H11N3O2	+	170.0965	24.16	12.48

Theophylline	C7H8N4O2	+	181.076	21.93	4.48
N-Acetyl-D-Glucosamine	C8H15NO6	+	222.0972	-0.27	11.82
N6-Acetyl-L-Lysine	C8H16N2O3	+	189.1233	-0.25	14.75
N-Acetyl-D-glucosamine 6-phosphate	C8H16NO9P	+	302.0635	-0.32	14.61
L-Phenylalanine	C9H11NO2	+	166.0862	-0.08	9.73
L-Tyrosine	C9H11NO3	+	182.0815	1.8	5.95
Biopterin	C9H11N5O3	+	238.0934	-0.34	14.1
D-Mannose	C6H12O6	-	179.0565	2.02	13.07
L-Arabinose	C5H10O5	-	149.0457	1.23	12.34
N-Acetyl-D-mannosamine	C8H15NO6	-	220.0832	2.34	11.97
Picolinic acid	C6H5NO2	+	124.0392	-0.79	6.23
Sarcosine	C3H7NO2	+	90.05494	-0.18	16.49
Sepiapterin	C9H11N5O3	+	238.0934	-0.34	11.13
Spermidine	C7H19N3	+	146.165	-1.34	20.25
Succinate	C4H6O4	-	117.0195	1.51	7.87
Sucrose	C12H22O11	+	343.1234	-0.22	13.11
Thymidine	C10H14N2O5	+	243.0974	-0.56	7.91
Triethanolamine	C6H15NO3	+	150.1125	0.32	18.29
UDP-N-acetyl-D-glucosamine	C17H27N3O17P2	+	608.0892	0.54	19.86
Biotin	C10H16N2O3S	+	245.0954	-0.36	7.89

Appendix II : Chromatogram of standards that helped in identifying some metabolites using ToxID software. These Chromatograms were generated by using Chromatographic conditions as in 2.12.1. This represents 1 of four standard test mixtures containing around 50 compounds each.

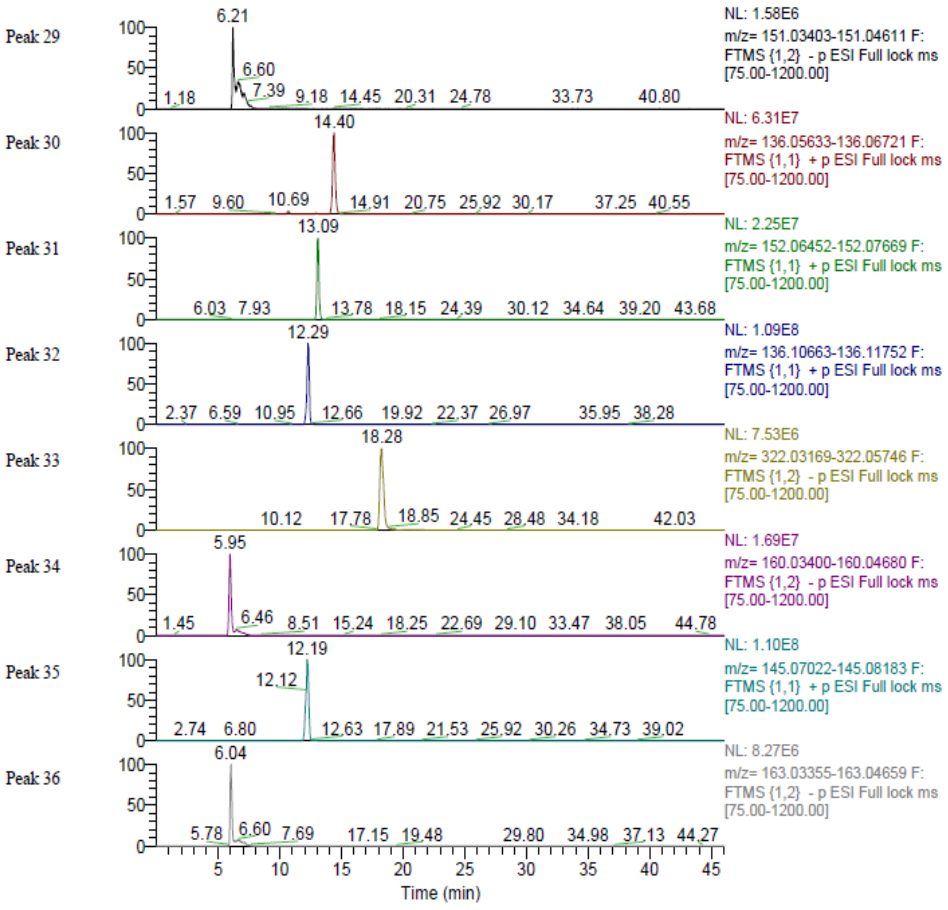

#	Comp. Index	Compound Name	Formula	Detected m/z	Delta (ppm)	Expected RT	Actual RT	Intensity	Adducts		
									H+	NH4+	Na+
29	41	4-hydroxylphenylacetate	C8H8O3	151.04034	1.8	6.59	6.21	1565043	Y*	-	-
30	42	Adenine	C5H5N5	136.06181	0.3	14.89	14.40	63051429	Y*	-	-
31	43	2-Phenylglycine	C8H9NO2	152.07062	0.1	13.50	13.09	22476041	Y*	-	-
32	44	Amphetamine	C9H13N	136.11218	0.8	12.42	12.29	108975224	Y*	-	-
33	45	CMP	C9H14N3O8P	322.04495	1.2	19.53	19.34	46665	Y*	-	-
34	46	2-Indolecarboxylicacid	C9H7NO2	160.04070	1.8	5.89	5.95	16847065	Y*	-	-
35	47	2-phenyl Imidazole	C9H8N2	145.07600	-0.1	12.34	12.19	109637033	Y*	-	-
36	48	4-Coumarate	C9H8O3	163.04030	1.4	6.01	6.04	8258940	Y*	-	-

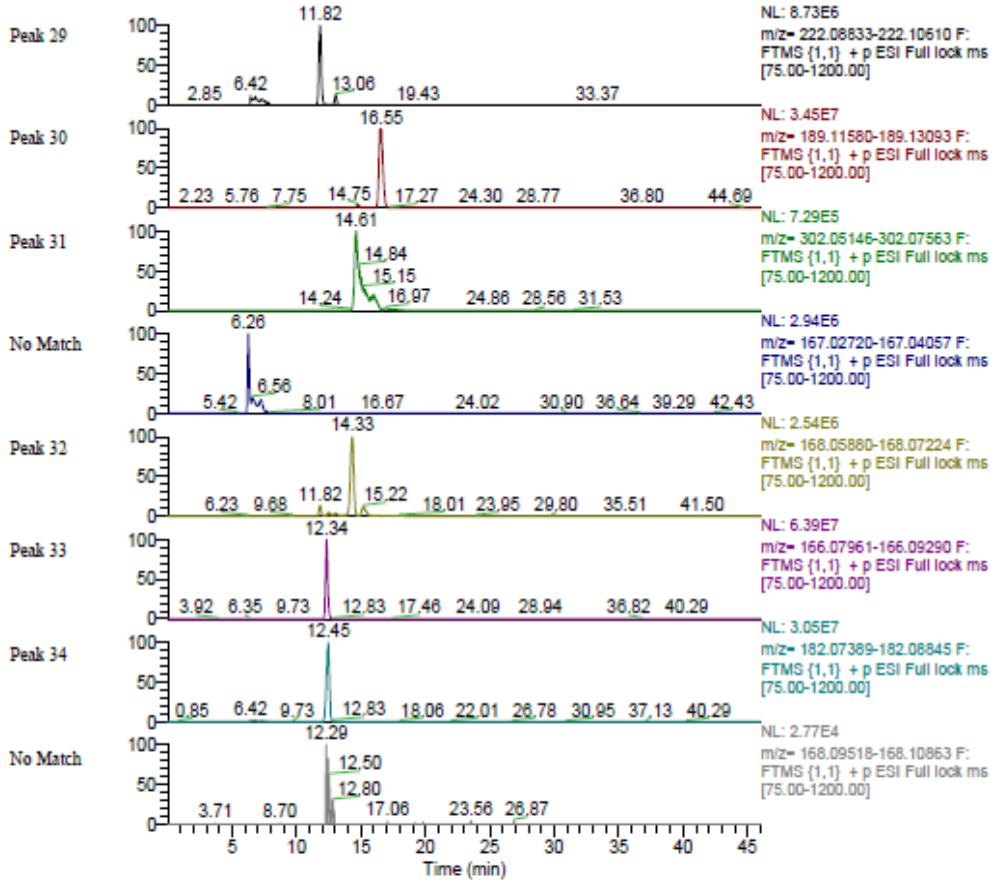

#	Comp. Index	Compound Name	Formula	Detected m/z	Delta (ppm)	Expected RT	Actual RT	Intensity	Adducts		
									H+	NH4+	Na+
29	49	N-Acetyl-D-Glucosamine	C8H15NO6	222.09715	-0.3	11.79	11.82	8721404	Y*	-	-
30	50	N6-Acetyl-L-Lysine	C8H16N2O3	189.12332	-0.3	14.94	14.75	1445219	Y*	-	-
31	51	N-Acetyl-D-glucosamine 6-phosphate	C8H16NO9P	302.06345	-0.3	15.02	14.61	696933	Y*	-	-
N	52	Phthalate	C8H6O4	-	-	13.94	-	-	N	-	-
32	53	Pyridoxal	C8H9NO3	168.06512	-2.4	8.36	7.92	4735	Y*	-	-
33	54	L-Phenylalanine	C9H11NO2	166.08624	-0.1	10.17	9.73	15799	Y*	-	-
34	55	L-Tyrosine	C9H11NO3	182.08150	1.8	5.80	5.95	7628	Y*	-	-
N	56	Phenylephrine	C9H13NO2	-	-	20.00	-	-	N	-	-

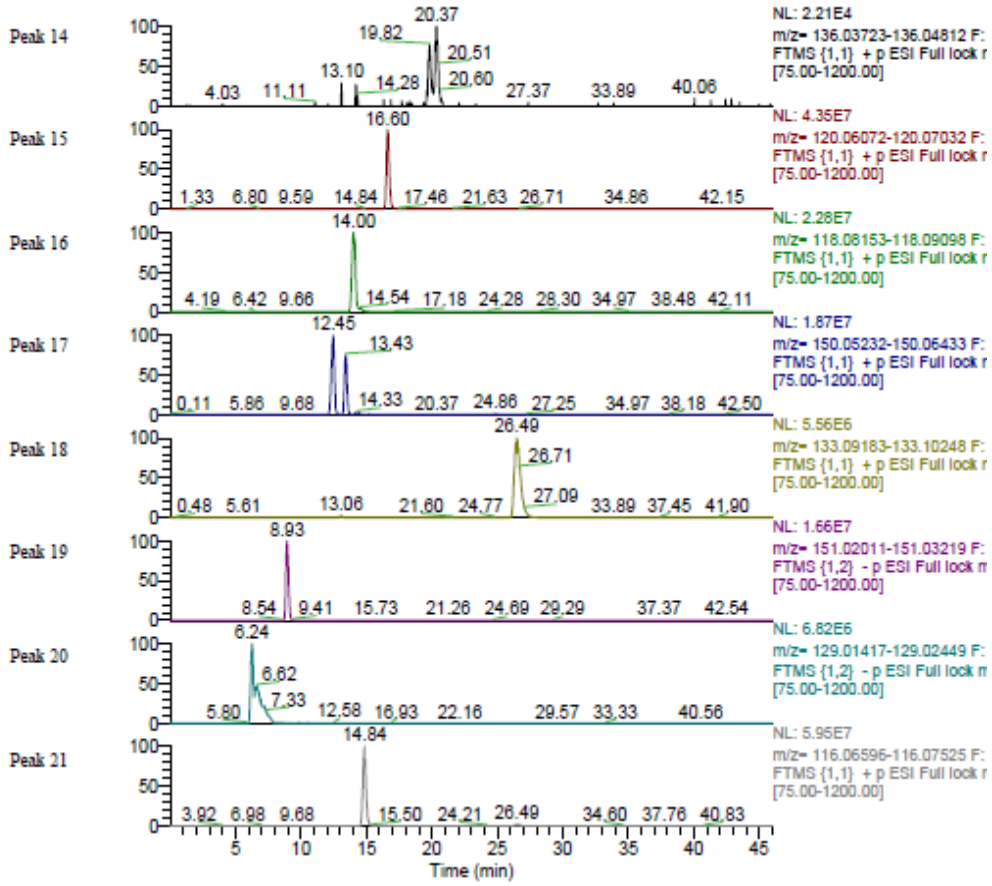

#	Comp. Index	Compound Name	Formula	Detected m/z	Delta (ppm)	Expected RT	Actual RT	Intensity	Adducts H+	Adducts NH4+
14	25	L-Homocysteine	C4H9NO2S	136.04253	-1.1	20.00	20.37	21298	Y*	-
15	26	L-Homoserine	C4H9NO3	120.06516	-3.0	14.90	14.84	33690	Y*	-
16	27	L-Valine	C5H11NO2	118.08626	0.0	12.53	12.61	8506	Y*	-
17	28	L-Methionine	C5H11NO2S	150.05843	0.7	11.52	11.89	4401	Y*	-
18	29	L-Ornithine	C5H12N2O2	133.09705	-0.8	22.10	21.60	3821	Y*	-
19	30	Alloxanthine	C5H4N4O2	151.02615	0.0	10.67	10.52	13490	Y*	-
20	31	Mesaconate	C5H6O4	129.01945	1.0	15.40	15.56	13491	Y*	-
21	32	L-Proline	C5H9NO2	116.07058	-0.2	12.80	12.54	17674	Y*	-

Appendix III: Some stable metabolites which do not vary between 8 weeks and 1 week for sample storage period. Four extracts of 10 wild type adult flies were prepared and stored over two month time period at -20^{o}C. "Ratio" is of 8: 1 signal

Formula	Compounds	MZ	Time	ratio 8/1	p-value
C4H6O2	butanedione	87.04404	15.548	0.82	0.445
C3H7NO2	Alanine	90.05487	19.234	0.87	0.113
H3PO4	Phosphoric acid	98.98415	19.672	1.04	0.743
H3PO4	Phosphoric acid	98.98418	17.903	1.00	0.976
C3H7NO3	L-Serine	106.0498	19.383	0.71	0.089
C5H9N3	1H-Imidazole-4-ethanamine	112.087	28.385	0.93	0.230
C6H8O2	cis-1,2-Dihydro benzene-1,2-diol	113.0597	7.905	0.76	0.325
C5H11NO2	valine	118.086	17.386	0.79	0.187
C4H9NO3	L-Threonine	120.0655	18.413	0.72	0.246
C7H6O2	Benzoate	123.0441	16	0.69	0.097
C6H6O3	1,2,3-Trihydroxybenzene	127.039	19.66	0.91	0.510
C5H7NO3	Pyrroline-4-hydroxy-2-carboxylate	130.0498	18.913	0.98	0.807
C5H7NO3	Pyrroline-4-hydroxy-2-carboxylate	130.0498	17.911	0.97	0.789
C6H11NO3	methylproline3	130.0863	25.083	0.66	0.124
C6H10O3	beta-Ketoisocaproate	131.0703	7.971	0.75	0.433
C5H5N5	Adenine1	136.0617	14.066	0.70	0.359
C5H5N5	Adenine2	136.0618	18.562	1.33	0.098
C5H4N4O	Hypoxanthine	137.0458	17.021	1.14	0.600
C7H7NO2	4-Aminobenzoate	138.0549	17.057	0.88	0.673
C6H6N2O2	Urocanate	139.0502	15.362	1.03	0.685
C2H8NO4P	Ethanolamine phosphate	142.0263	20.226	0.68	0.071
C7H16NO2+	acetylcholine 1+	146.1175	15.621	0.78	0.378
C5H10N2O3	diaminooxopentanoic acid(Msc)	147.0764	18.913	1.00	0.966
C5H9NO4	O-Acetyl-L-serine	148.0603	18.041	0.83	0.121
C6H7N5	Methyladenine	150.0774	16.956	0.72	0.257
C5H5N5O	Guanine1	152.0566	14.269	0.82	0.254
C5H5N5O	Guanine2	152.0567	13.032	0.93	0.685
C5H4N4O2	Xanthine	153.0406	10.599	0.70	0.204
C7H11N3O	N-acetylhistamine isomer	154.0974	17.578	1.14	0.256
C6H9N3O2	L-Histidine	156.0765	24.44	0.97	0.759
C6H10O3S	Dihydroxy-5-(methylthio)pent-1-en-3-one	163.0423	8.594	1.25	0.510
C9H8O3	Phenylpyruvate	165.0546	16.062	0.75	0.152
C5H11NO3S	L-Methionine S-oxide	166.053	18.873	1.19	0.601
C7H11N3O2	1-Methylhistidine	170.0924	24.57	1.05	0.744
C3H9O6P	Glycerolphosphate	173.0208	17.211	0.73	0.083
C6H14N4O2	L-Arginine	175.1186	25.067	0.95	0.729
C9H11NO3	L-Tyrosine	182.0809	16.062	0.76	0.141
C5H15NO4P+	Choline phosphate+	184.0734	23.837	0.99	0.934

C11H9NO2	Indole acrylic acid	188.0704	14.431	0.83	0.118
C7H11NO5	N-Acetyl-L-glutamate	190.0709	8.375	0.86	0.606
C10H9NO3	5-Hydroxyindoleacetate	192.0655	13.969	1.24	0.112
C11H12N2O2	L-Tryptophan	205.097	14.431	0.81	0.099
C10H12N2O3	L-Kynurenine	209.0917	13.994	1.33	0.067
C9H16N2O4	gamma-Glutamyl-gamma-aminobutyraldehyde	217.1182	7.916	1.24	0.373
C10H19NO4	Propionyl carnitine	218.1387	13.824	1.35	0.448
C9H17NO5	Pantothenate	220.1177	7.895	0.95	0.869
C9H17NO5	Pantothenate	220.1179	6.734	0.99	0.939
C14H31NO	Dodecyldimethylamine oxide	230.2479	11.053	0.89	0.320
C10H22N2O4	1,1,3-tris(ethoxymethyl)urea	235.1652	17.41	0.62	0.250
C11H12N2O4	N-Formylkynurenine	237.0869	14.25	1.28	0.225
C12H20N2O3	Pirbuterol	241.1547	16.095	0.95	0.877
C6H14NO8P	D-Glucosamine 6-phosphate	260.0531	18.464	0.78	0.143
C6H13O9P	Glucose phosphate1	261.0369	19.635	1.30	0.313
C10H13N5O4	Deoxyguanosine	268.1039	14.09	0.66	0.301
C10H13N5O5	Guanosine1	284.0989	14.286	0.83	0.182
C10H13N5O5	Guanosine2	284.099	15.293	0.82	0.578
C9H13N2O9P	uridine monophosphate	325.0433	16.509	1.26	0.516
C12H20O10	Difructose anhydride isomer	325.1128	17.643	0.66	0.121
C10H14N5O7P	AMP isomer 2	348.0702	18.566	1.29	0.166
C10H14N5O7P	AMP isomer 2	348.0703	19.576	1.25	0.262
C10H13N4O8P	IMP	349.0544	17.021	1.13	0.620
C19H34O5N	C19H34O5N	356.2427	5.238	0.75	0.252
C10H14N5O8P	GMP	364.065	18.837	0.84	0.116
C18H32O16	Raffinose	505.177	17.723	1.02	0.912
C21H28N7O14P2+	NAD+	664.1163	20.17	0.93	0.307
C24H42O21	Stachyose	667.2297	17.697	1.36	0.283

Appendix IV: The known lipids that are consistently enriched in midgut, number of lipids enriched (at least 2-fold) in adult or in both epithelia (p-value ≤0.05). Adult epithelia were compared against their respective whole animals to obtain the fold changes. Four extracts of 10 each individual epithelium and 10 adult whole fly were prepared to obtain the significantly differentially expressed (up regulated) (p-value ≤0.05). The main lipids enriched in the midgut were small triglycerides and ceramides. These were observed, using the chromatographic conditions in 2.12.3 as their ammonium adducts and sodium adducts respectively. Thus for example C40 H78 O6 N represents a triglyceride with acyl chains adding up to C37:1.

Metabolites	MZ	Time	FC midgut vs whole fly)
C31 H59 O3 N Na	516.477	2.767	70.56
C31 H61 O3 N Na	518.4928	2.767	9.67
C32 H65 O3 N Na	534.4876	2.767	29.85
C34 H69 O3 N Na	562.5187	2.744	23.15
C34 H71 O3 N Na	564.5348	2.982	58.34
C35 H67 O3 N Na	572.5395	2.744	10.98
C35 H71 O3 N Na	576.5344	2.676	40.35
C36 H65 O3 N Na	582.5452	2.744	13.87
C36 H69 O3 N Na	586.5169	3.035	12.50
C36 H73 O3 N Na	590.5503	2.676	20.40
C40 H78 O6 N	668.5813	2.609	71.78
C40 H80 O6 N	670.5977	2.515	18.92
C41 H78 O6 N	680.5813	2.606	45.86
C41 H80 O6 N	682.5971	2.515	31.69
C42 H82 O6 N	686.6199	2.515	4.81
C42 H76 O6 N	690.5717	2.734	10.32
C42 H82 O6 N	696.6126	2.609	47.18
C42 H84 O6 N	698.6291	2.702	14.63
C43 H80 O6 N	706.5972	2.606	51.57
C43 H88 O6 N	708.6127	2.515	27.39
C43 H84 O6 N	710.6287	2.515	5.08
C45 H84 O6 N	734.6286	2.515	20.89
C45 H86 O6 N	736.6082	2.793	12.79
C45 H88 O6 N	738.66	2.666	3.15
C46 H80 O6 N	742.5994	2.85	14.91

Appendix V: The known lipids that are consistently enriched in head, number of lipids enriched (at least 2-fold) in adult or in both epithelia (p-value ≤0.05). adult epithelia were compared against their respective whole animals to obtain the fold changes. Four extracts of 10 each individual epithelium and 10 adult whole fly were prepared to obtain the significantly differentially expressed (up regulated) (p-value ≤0.05). As in the midgut the enriched lipids are mainly triglycerides.

Metabolites	MZ	Time	FC head vs whole fly
C23 H49 O7 N P	482.3303	13.345	6.90
C30 H63 O3 N Na	508.4569	2.766	32.10
C31 H63 O3 N Na	520.5086	2.898	21.84
C32 H63 O3 N Na	532.4699	3.035	16.17
C32 H67 O3 N Na	536.5041	2.767	19.13
C33 H67 O3 N Na	548.5029	2.767	16.51
C34 H61 O3 N Na	554.5142	2.836	42.40
C34 H71 O3 N Na	564.5348	2.982	92.15
C35 H68 O5 N	582.5087	2.702	6.02
C36 H65 O3 N Na	582.5452	2.744	24.69
C35 H70 O5 N	584.525	2.707	6.04
C36 H75 O3 N Na	592.5661	2.982	37.41
C37 H74 O5 N	612.5567	2.702	10.15
C45 H86 O6 N	736.6082	2.793	8.28
C45 H88 O6 N	738.66	2.666	12.73
C45 H90 O6 N	740.6751	2.718	9.82
C46 H92 O6 N	754.6923	2.749	3.99
C47 H92 O6 N	766.6904	2.718	10.76
C48 H96 O6 N	782.7007	2.82	50.26
C49 H94 O6 N	792.7068	2.666	6.62
C49 H96 O6 N	794.7215	2.756	6.07
C50 H96 O6 N	806.7233	2.749	4.54
C51 H92 O6 N	814.6912	2.682	5.60
C51 H96 O6 N	818.7228	2.666	5.98
C51 H98 O6 N	820.7372	2.756	5.80
C52 H96 O6 N	830.7226	2.682	4.64
C53 H96 O6 N	842.7222	2.682	6.67
C53 H98 O6 N	844.7383	2.712	7.77
C53 H100 O6 N	846.7541	2.847	9.95

Appendix VI: The known lipids that are consistently enriched in hindgut, number of lipids enriched (at least 2-fold) in adult or in both epithelia (p-value ≤0.05). adult epithelia were compared against their respective whole animals to obtain the fold changes. Four extracts of 10 each individual epithelium and 10 adult whole fly were prepared to obtain the significantly differentially expressed (up regulated) (p-value ≤0.05). Again the main lipids enriched at triglycerides.

Metabolites	MZ	Time	FC hidgut vs whole fly
C30 H63 O3 N Na	508.4569	2.766	19.05
C33 H67 O3 N Na	548.5029	2.767	9.04
C34 H71 O3 N Na	564.5348	2.982	8.64
C45 H72 O6 N	722.5271	2.675	88.30
C45 H86 O6 N	736.6082	2.793	7.93
C45 H90 O6 N	740.6751	2.718	2.36
C46 H80 O6 N	742.5994	2.85	2.53
C46 H82 O6 N	744.6188	2.798	2.92
C48 H70 O6 N	756.5263	2.772	4.30
C47 H94 O6 N	768.6957	2.71	118.07
C48 H92 O6 N	778.6911	2.747	3.51
C48 H94 O6 N	780.7077	2.749	2.35
C48 H96 O6 N	782.7007	2.82	97.51
C49 H92 O6 N	790.6914	2.702	5.01
C49 H94 O6 N	792.7068	2.666	2.58
C49 H96 O6 N	794.7215	2.756	3.15
C50 H94 O6 N	804.7075	2.702	4.13
C50 H96 O6 N	806.7233	2.749	2.96
C51 H92 O6 N	814.6912	2.682	17.38
C51 H96 O6 N	818.7228	2.666	4.22
C51 H98 O6 N	820.7372	2.756	3.69
C52 H96 O6 N	830.7226	2.682	5.21
C53 H96 O6 N	842.7222	2.682	55.77
C53 H98 O6 N	844.7383	2.712	16.57
C53 H100 O6 N	846.7541	2.847	8.59
C54 H100 O6 N	858.7539	2.758	6.74
C54 H102 O6 N	860.7704	2.807	4.48

Appendix VII: The known lipids that are consistently enriched in tubule, number of lipids enriched (at least 2-fold) in adult or in both epithelia (p-value ≤0.05). Adult epithelia were compared against their respective whole animals to obtain the fold changes. Four extracts of 10 each individual epithelium and 10 adult whole fly were prepared to obtain the significantly differentially expressed (up regulated) (p-value ≤0.05).

Metabolites	MZ	Time	FC tubule vs whole fly
C30 H63 O3 N Na	508.4569	2.766	17.51
C31 H59 O3 N Na	516.477	2.767	2.48
C32 H63 O3 N Na	532.4699	3.035	7.94
C33 H67 O3 N Na	548.5029	2.767	29.95
C34 H71 O3 N Na	564.5348	2.982	4.98
C36 H69 O3 N Na	586.5169	3.035	3.94
C37 H73 O3 N Na	602.5116	2.782	4.96
C39 H76 O5 N	638.5736	2.702	2.18
C45 H72 O6 N	722.5271	2.675	187.90
C47 H94 O6 N	768.6957	2.71	7.35

Appendix VIII: The known lipids that are consistently enriched in ovary, number of lipids enriched (at least 2-fold) in adult or in both epithelia (p-value ≤0.05). adult epithelia were compared against their respective whole animals to obtain the fold changes. Four extracts of 10 each individual epithelium and 10 adult whole fly were prepared to obtain the significantly differentially expressed (up regulated) (p-value ≤0.05).

Metabolites	MZ	Time	FC ovary vs whole fly
C30 H63 O3 N Na	508.4569	2.8	41.57
C31 H61 O3 N Na	518.4928	2.8	8.16
C31 H63 O3 N Na	520.5086	2.9	179.30
C32 H63 O3 N Na	532.4699	3.0	529.80
C32 H67 O3 N Na	536.5041	2.767	6.81
C34 H67 O3 N Na	560.5012	2.893	49.36
C34 H71 O3 N Na	564.5348	2.982	77.53
C36 H69 O3 N Na	586.5169	3.035	12.90
C36 H71 O3 N Na	588.5327	2.761	8.29
C36 H75 O3 N Na	592.5661	2.982	64.19
C37 H68 O5 N	606.5087	2.702	5.01
C40 H78 O6 N	668.5813	2.609	7.01
C41 H78 O6 N	680.5813	2.606	14.31
C42 H76 O6 N	690.5717	2.734	8.25
C42 H82 O6 N	696.6126	2.609	8.45
C43 H80 O6 N	706.5972	2.606	30.76
C43 H88 O6 N	708.6127	2.515	6.21
C45 H84 O6 N	734.6286	2.515	9.74
C46 H80 O6 N	742.5994	2.85	17.74
C41 H79 O8 N P	744.5542	13.304	5.23
C46 H82 O6 N	744.6188	2.798	6.71

Appendix IX: Direct comparison of lipidom of each epithelium against their adult whole fly. Four extracts of 10 each individual epithelium and 10 adult whole fly were prepared to obtain the differentially expressed (up and down regulated), lipidom and absolute intesity (over adult tissue) are shown.

		Carbon Number *	Intensity of the peaks in each lipidome (v)							
Formula	MZ		Food#	MEDIA•	Whole	ovary	tubule	head	Hindgut	Midgut
Lysophosphoethanolamine										
C19 H39 O7 N P	424.2451	14:1	0	0	57223	0	0	1301	0	985
C19 H41 O7 N P	426.2614	14:0	7114	0	194632	1528	21	3637.5	349	6858
C20 H43 O7 N P	440.2774	15:0	1302	43	67738	177	0	1159	0	732
C21 H39 O7 N P	448.2427	16:3	81	107	9363	37	0	101	9	413
C21 H43 O7 N P	452.2766	16:1	249752	215	9919545	8004	280	327076	1384	27844
C21 H45 O7 N P	454.2928	16:0	246424	16670	678703	53968	12401	47853	19888	31268.5
C22 H47 O7 N P	468.3087	17:0	1011	0	51469	446	71	1615	29	499
C23 H41 O7 N P	474.2593	18:4	13316	0	358161	356	0	21745	0	1960
C23 H43 O7 N P	476.2773	18:3	26748	0	2910073	4432	67	132214	594	9112
C23 H45 O7 N P	478.2927	18:2	228948	136	10312379	8072	555	282763	1279	59011.5
C23 H49 O7 N P	482.3303	18:0	5131	0	1357	4963	184	9359	198.75	1385
C24 H49 O7 N P	494.3241	20:8	226	213	24748	0	0	142	586	3114
C25 H41 O7 N P	498.2589	20:6	6922	0	102386	659	0	8789	87	692
C25 H43 O7 N P	500.2747	20:5	12520	0	339304	446	0	18193	0	4369
C25 H45 O7 N P	502.2899	20:4	4808	76	400205	1520	26	32584	148	7624
C25 H47 O7 N P	504.297	20:3	0	0	13951	215	0	1396	0	173

C25 H49 O7 N P	506.3243	20:2	208	0	108761	0	0	174	0	0
C25 H53 O7 N P	510.3547	20:0	0	0	5134	2413	0	434	0	1505
C27 H41 O7 N P	522.2571	22:8	0	0	15201	0	0	3042	0	359
C27 H43 O7 N P	524.2712	22:7	297	0	18173	195	0	7489	0	1956
C41 H77 O8 N P	742.5386	---	0	108	835026.5	1637274	9928	926268	22981	610017
C41 H79 O8 N P	744.5542	---	0	0	292281	1528092	3925	149717.5	15123	239403
[PS (20:4)] 1-(5Z,8Z,11Z,14Z-eicosatetraenoyl)-sn-glycero-3-phosphoserine	544.2658	---	0	0	303945	65.	16.5	1782.	26.	3120
SM d18:0 16:1 or isomer	699.544	---	0	0	42836	3467	1365	11033	2031.25	8021
Lysophosphatidylcholine										
C21 H45 O7 N P	454.2929	---	4865	8114	48501	9279	7473.25	11393.75	9257.5	9380.75
C22 H47 O7 N P	468.3084	14:0	178	0	1142334	1650.5	15.25	17348	47.5	5916.5
C23 H49 O7 N P	482.3242	---	41	0	319878.5	101	131.5	4602.5	32.75	1479.75
C24 H47 O7 N P	492.3085	16:2	0	0	170811.8	0	15.25	4228	0	462.75
C24 H49 O7 N P	494.324	16:1	27548	1475	19058699	11363.25	111	398873	708.75	39595.5
C24 H51 O7 N P	496.34	16:0	47015	261	2232608	13341.25	23.5	59092.5	1336.25	14485
C25 H51 O7 N P	508.3404	17:1	49	0	455109.3	35.75	0	6405	0	4248.75
C25 H53 O7 N P	510.3564	17:0	0	0	236832.5	129	0	3559.5	7.25	793.25
C26 H47 O7 N P	516.3062	18:4	110	0	667685	55.75	0	7779.75	0	716
C26 H49 O7 N P	518.3241	18:3	2114	0	3871286	2372	454.5	106273	329.75	5852.75
C26 H51 O7 N P	520.3397	18:2	32932	3644	17728920	13010	4044.7	351779.8	5315.5	54555.25

							5			
C26 H53 O7 N P	522.3551	18:1	20052	665	12696785	10825	82.75	289630	1688	69671.75
C26 H55 O7 N P	524.3751	18:0	481	0	25115.75	1887.5	0	4300.25	88.5	1481
C27 H55 O7 N P	536.3715	20:8	0	0	28596.5	0	0	268.25	0	1542
18:2 lyso PC FA or isomer	564.3301	---	2324	405	6185355	5165	155.75	166615.5	787.75	26243.75
phosphoethanolamine										
C31 H63 O8 N P	608.4283	26:0	0	0	26149	74799.5	23.75	2221.25	959	18235
C32 H65 O8 N P	622.4449	27:0	0	0	3111	4588.25	13	71.5	0	2576.5
C33 H65 O8 N P	634.4431	28:1	9759	10302	40527.75	75339.25	13631	11559.5	14012.25	46658
C34 H69 O8 N P	650.4762	29:0	0	0	12005.5	6608.25	0	1042.5	888.75	5466.75
C35 H67 O8 N P	660.4601	30:2	0	0	21890	33979.25	0	2391.5	4693.5	37192.5
C35 H69 O8 N P	662.4752	30:1	207	0	371577.3	371988.5	2740	100869.3	51286.25	152206
C35 H71 O8 N P	664.4918	30:0	0	0	125162.8	107570	779.5	19353.25	4896.75	46631
C36 H71 O8 N P	676.4912	31:1	0	0	71024	45094.25	630.5	12906.25	7474.75	27063.75
C37 H69 O8 N P	686.4757	32:3	0	0	97590.5	72100.25	1910.25	40467	18331.75	37991.75
C37 H71 O8 N P	688.4908	32:2	7438	77	1031760	872235.8	33236	291005.5	167752.3	397192.3
C37 H73 O8 N P	690.5066	32:1	16846	310	2656083	3200073	87492.75	928245.3	387247.3	990917.8
C37 H75 O8 N P	692.5248	32:0	1630	0	11174.75	23163.25	811.25	16500.75	165.25	16795.25
C38 H69 O8 N P	698.5107	33:4	0	0	60033.5	39.25	0	306.25	514.75	0

C38 H71 O8 N P	700.5278	33:3	0	0	165868	1059.5	265.75	89511.5	10536	2122.25
C38 H73 O8 N P	702.5423	33:2	9154	10273	119915	19444.5	14421.25	21089.5	22082.75	26074
C38 H75 O8 N P	704.5592	33:1	0	0	158530.3	51839.25	439.5	34868.25	15055.25	51199.75
C38 H77 O8 N P	706.5405	33:0	0	0	18403.5	4982	484.25	7474.75	638.5	2197.75
C39 H69 O8 N P	710.4725	34:5	0	0	12461.5	16686.5	1878.75	13112.5	7566.75	9959
C39 H73 O8 N P	714.507	34:3	19284	423	3152113	1990044	215703.3	1628596	348266.8	1033754
C39 H75 O8 N P	716.5222	34:2	49717	941	4491589	5017569	624360.3	1920982	889553.8	3096505
C39 H77 O8 N P	718.5376	34:1	3988	667	3281629	4809424	461260.8	2080530	977991.8	1912350
C39 H79 O8 N P	720.5444	34:0	298	112	342275.3	491965.5	47474.75	202076.3	100977.8	204383.5
C40 H69 O8 N P	722.5485	35:6	0	0	12142.25	11538.5	187	3894.5	2248.25	9022
C40 H71 O8 N P	724.5273	35:5	0	69	11614.5	93.75	71.25	984.25	1328.25	6648
C40 H73 O8 N P	726.5062	35:4	0	0	13878.5	8951.75	739.25	7338.5	2077.25	6277.75
C40 H75 O8 N P	728.5228	35:3	0	0	82443	37125	6280.25	51283	8483	49343.5
C40 H77 O8 N P	730.5384	35:2	124	33	102702.3	86451.75	15397.25	33661.75	23352	119630
C40 H79 O8 N P	732.5541	35:1	1058	3068	129810.5	65364.75	12384.5	52626	29665	79517.75
C40 H81 O8 N P	734.5595	35:0	0	0	23556	5790	738	4725.5	4062.75	16248
C41 H71 O8 N P	736.4908	36:6	75	33	403268	50753	12996	762070	18423.75	26995.75
C41 H73 O8 N P	738.5067	36:5	843	237	1742783	289278.8	62502.25	1411424	96531.25	190669
C41 H75 O8 N P	740.522	36:4	8972	601	5206681	112228	244351	1989720	345422.8	923650.3

						3	.5			
C41 H81 O8 N P	746.5685	36:1	5596	6692	392885.5	529028.3	43461.5	447287.3	72409.25	242446.5
C41 H83 O8 N P	748.5742	36:0	0	0	33057	57486.25	3258.75	48996	4028	22085.25
C42 H73 O8 N P	750.5409	37:5	0	0	40385.75	0	39.25	87504.25	1389.5	1835.25
C42 H75 O8 N P	752.5577	37:4	0	0	27768.5	635	578.5	7818.5	1431.5	7342.75
C42 H79 O8 N P	756.5537	37:3	0	97	23693.75	4251.25	473.75	7519.25	1409.75	22789
C42 H81 O8 N P	758.5693	37:2	0	75	23179	9708.25	705.5	5541.75	4260.75	46894
C42 H83 O8 N P	760.585	37:1	0	1225	11865	2649.75	1125.75	7845.75	2337.25	24138.25
C43 H73 O8 N P	762.5037	38:7	135	0	41408.25	22276	20822	35897	21753.5	22669
C43 H75 O8 N P	764.5202	38:6	0	131	62683.5	44007	24698.25	71398	28916.25	52047.75
C43 H77 O8 N P	766.5364	38:5	0	806	24934	53711	14552.75	27701.75	27100.75	40196.5
C43 H81 O8 N P	770.5688	38:4	0	0	61399.25	24601.75	796.75	70685.75	6040.5	35121.25
C43 H83 O8 N P	772.585	38:3	0	0	54761.5	33249.25	1355.5	25249.5	11087.5	130280.3
C43 H85 O8 N P	774.5999	38:2	0	0	33502	31175	561.5	20594.25	7720	107092.5
C43 H87 O8 N P	776.6079	38:1	0	0	1293	1518	0	576	613.5	13557.25
C45 H87 O8 N P	800.6165	40:2	0	0	2900.5	0	0	105.25	0	1824.25
Phosphatidylcholine										
C38 H73 O8 N P	702.506	30:2	5270	8390	290459.8	419464	7001.5	28027.75	25387	216092.8
C38 H75 O8 N P	704.5223	30:1	144	450	2335624	1568469	1225.5	260598	64878.25	760881.5
C38 H79 O8 N P	708.5449	30:0	0	0	62504.25	11584.75	12.75	12438.5	1283.5	9346.25

C39 H75 O8 N P	716.5228	31:2	0	46	71236.75	50418.75	0	8824.25	3304.75	48011
C39 H77 O8 N P	718.5378	31:1	0	0	488949.3	163362.8	389	50736.75	13874.5	174777
C39 H79 O8 N P	720.5538	31:0	0	0	234935.5	28150.75	230.25	43120.5	4602.75	44716.5
C39 H81 O8 N P	722.5621	32:6	0	0	21490.5	2214.5	0	3039	248.5	4661
C40 H73 O8 N P	726.5035	32:4	0	0	52218.75	77770.25	0	6638	6326.75	28251.25
C40 H75 O8 N P	728.5229	32:3	0	0	685764.3	435481.3	742.5	147320.3	40105.5	194611
C40 H77 O8 N P	730.5375	32:2	868	73	7773459	7481884	12973	1308034	322488.3	2248176
C40 H79 O8 N P	732.5533	32:1	385	1915	10330622	6613685	20237.25	1671581	270302.5	1690063
C40 H81 O8 N P	734.5698	32:0	22	0	1165871	137809.3	2267	740557.8	16677.25	119092.8
C40 H83 O8 N P	736.5764	19.82	0	0	112799.3	9494	115.25	81175	652.25	2384.5
C41 H77 O8 N P	742.5389	33:3	0	0	126074	52872.75	344.75	34960.75	4726.5	46806.5
C41 H79 O8 N P	744.5533	33:2	0	0	587122.5	284719.5	2554.5	96074.5	22307	257296.3
C41 H81 O8 N P	746.569	33:1	1584	3373	751991.8	255431.8	5306.25	133211.5	25234.25	203414
C41 H83 O8 N P	748.5861	33:0	0	0	150480	10037.75	335	57762.75	1606.75	8078.25
C41 H85 O8 N P	750.5929	34:6	0	0	16465.5	749.75	0	5343	57.75	908
C42 H79 O8 N P	756.554	34:3	551	745	12920816	9064860	74231.25	4146777	525471.5	2926466
C42 H81 O8 N P	758.569	34:2	7468	1361	17958404	12989618	133786	5085207	689983.5	3818585
C42 H83 O8 N P	760.5843	34:1	656	697	7047684	603975	36812.	2727160	220896	1169439

						3	5			
C42 H85 O8 N P	762.6011	35:6	0	0	570956.5	184880.3	3283.5	283225.5	10947.75	104441.5
C42 H87 O8 N P	764.6076	35:5	0	0	31416.75	1548	16.5	27064.75	43.75	704.75
C43 H79 O8 N P	768.5521	35:4	0	0	56157	53784.5	431.75	21182	2333.75	17308.5
C43 H81 O8 N P	770.5696	35:3	871	0	392476.3	177056.5	3043.5	121258.8	12620	112611
C43 H83 O8 N P	772.5845	35:2	0	0	709002.3	213298.5	4605.75	156099.3	23571.5	238834.3
C43 H85 O8 N P	774.6003	35:1	0	0	335706.8	83687	1347.25	88716	8571.75	88584
C44 H75 O8 N P	776.5182	35:0	0	0	9996.5	36519	93.75	6922.5	2579.5	6896
C44 H77 O8 N P	778.538	36:6	0	39	606604	290662	2545.75	423064.8	15220	79816.25
C44 H79 O8 N P	780.5538	36:5	1409	118	3224927	1420662	26420.5	1020559	72020	365495.8
C44 H81 O8 N P	782.5693	36:4	5940	635	10241097	4483698	140126.5	2588646	274735.3	1659255
C44 H83 O8 N P	784.5842	36:3	2272	727	10163992	5466113	105026.3	3466580	383951.3	2370607
C44 H85 O8 N P	786.5992	36:2	1504	207	3765375	2564978	31578.75	1771697	167011	1480708
C44 H87 O8 N P	788.6158	36:1	90	64	1018361	459387	6700	564430	24307.25	279109
C44 H89 O8 N P	790.6227	36:0	0	0	117033	45963	666	70206.25	1701.25	29538.25
C45 H85 O8 N P	798.6012	37:3	0	0	62571.25	9073.25	291	8034.75	1728	50768.25
C45 H87 O8 N P	800.616	37:2	0	0	66141.25	4240.25	92.25	9359	1341.5	71960.5
C45 H89 O8 N P	802.6332	37:1	0	0	20573.75	136.25	0	3191	16.25	23692
C46 H85 O8 N P	810.6091	38:4	0	0	13953.25	7873.5	145.25	4296.75	2315.25	4567

C46 H87 O8 N P	812.6151	38:3	0	0	60918	23958	69	24003	2996.5	24919.25
C46 H89 O8 N P	814.6317	38:2	0	0	64908	22885	160.75	19300.25	3101.5	69641.25
C46 H91 O8 N P	816.6475	38:1	0	0	42030	8392	0	7773	868	52188.75
Triglycerides										
C40 H78 O6 N	668.5813	C40:1	0	0	2788.75	19562.75	144.75	13879.25	2703.25	200169.8
C40 H80 O6 N	670.5977	C40:0	0	0	23541.5	35276.25	168	47612.5	8547.5	445498.5
C41 H78 O6 N	680.5813	C41:2	0	0	8819	126227	0	28242.75	6165	404481.3
C41 H80 O6 N	682.5971	C41:1	89	191	201285.3	683915.8	3410.5	302493.8	77225.5	6378884
C42 H82 O6 N	686.6199	C42:5	0	0	35025.75	85866.5	327.25	174397	12746.5	168627
C42 H76 O6 N	690.5717	C42:3	0	0	4422.5	36478.25	140.75	45166	4211.25	45638.25
C42 H82 O6 N	696.6126	C42:1	0	0	9071.75	76681	723.75	64083.5	10823.25	428011.8
C42 H84 O6 N	698.6291	C42:0	0	0	13672	67502	1338.25	150619	26884.75	199963
C43 H80 O6 N	706.5972	C43:3	0	0	3677	113117	0	15468	6030.5	189620.8
C43 H88 O6 N	708.6127	C43:2	0	0	77337	479922.3	1899.75	158173.8	42024	2118305
C43 H84 O6 N	710.6287	C43:1	38	391	277073.8	1034290	7598.5	1258376	105048.8	1406937
C43 H88 O6 N	712.6444	C43:0	356	1292	257266.8	518740.5	15772.5	3234196	430547.5	416424.3
C44 H96 O6 N	718.5173	C44:4	0	0	341	39	0	0	83.75	270.25
C44 H88 O6 N	726.6606	C44:0	0	0	35156	48088.5	3048.25	231408.8	69275.75	57971.75
C45 H84 O6 N	734.6286	C45:3	0	125	20967.75	204172	812	57461.5	22841	438014.5
C45 H86 O6 N	736.6082	C45:2	0	0	723.25	3008.25	568.75	5986.5	5738	9251.25

C45 H88 O6 N	738.66	C45:1	336	620	205053.8	836132	20956.5	2610350	408219.8	645174.5
C45 H90 O6 N	740.6751	C45:0	627	1122	264419	284521	21084	2596102	624079.3	97895
C46 H80 O6 N	742.5994	C46:5	0	99	1411.5	25037.5	624.5	10185	3573.25	21046.75
C46 H82 O6 N	744.6188	C46:4	0	0	5372.25	36043.25	1450.25	40394	15674.75	13851.25
C46 H86 O6 N	748.6447	C46:3	0	0	3742.75	19064.7	54.5	14810.	5448.5	39306.
C46 H88 O6 N	750.6592	C46:2	0	0	9402	53808	1472.75	66634.25	18879	121675.3
C46 H90 O6 N	752.6758	C46:1	255	449	26398.25	67452.75	4050	185512.5	60756.5	97612
C46 H92 O6 N	754.6923	C46:0	247	361	38419.75	24133.5	3640	153135.3	73196.75	15149.75
C48 H70 O6 N	756.5263	---	0	0	262	0	0	226	1127.75	5728.5
C48 H74 O6 N	760.556	---	0	0	18672.25	0	0	93.5	182	383
C47 H90 O6 N	764.6757	---	364	436	107312	694767.5	19019.25	1246172	289272.5	598230
C47 H92 O6 N	766.6904	C47:1	1701	2617	320515.3	597240	37078.5	3449017	903698.8	240611.8
C47 H94 O6 N	768.6957	C47:0	133	153	274.75	43841	2018.25	237031.5	32440	24125
C48 H84 O6 N	770.5775	C48:6	54	104	5033.25	2927.25	0	898.5	65.5	1603.25
C48 H90 O6 N	776.676	C48:3	0	0	7303.5	27333.25	1137.75	32028.25	11682.5	60154.25
C48 H92 O6 N	778.6911	C48:2	286	681	13087	54889	4315	111725.8	45941	88379.25
C48 H94 O6 N	780.7077	C48:1	2095	2809	46124.75	50062	8629.5	214022.3	108595.5	44661.5
C48 H96 O6 N	782.7007	C48:0	0	0	21.5	3892	0	1080.5	2096.5	2970
C50 H74 O6 N	784.5579	---	569	0	378.25	121.25	0	0	430	2992

C49 H92 O6 N	790.6914	---	36	273	44670.25	650400.3	20728.75	555164.5	223830.5	379456.8
C49 H94 O6 N	792.7068	---	2530	3546	346817.8	955980.8	53539.5	2297328	893330.3	315862.8
C49 H96 O6 N	794.7215	---	5658	6370	462787.5	557379.3	50240.75	2807688	1458363	161581.3
C50 H94 O6 N	804.7075	---	0	190	7911.5	42063.25	4737.75	61418	32671.5	54927
C50 H96 O6 N	806.7233	---	2426	3154	34980.25	65035	12702	158688.8	103447.3	61259
C51 H92 O6 N	814.6912	---	585	578	6573.25	143432.3	2798.25	36842.75	114247.8	26500.5
C51 H96 O6 N	818.7228	---	1566	2312	169857.5	741647	63779.5	1016544	716976	349887
C51 H98 O6 N	820.7372	---	5474	6851	335363	820572.5	77507.5	1946017	1237540	264676.5
C52 H96 O6 N	830.7226	---	894	761	5649.5	21056.75	4561.75	26222.75	29416	22509.75
C53 H96 O6 N	842.7222	---	379	133	10263.75	176883.3	14546.75	68493.5	572363.8	46433.75
C53 H98 O6 N	844.7383	---	253	333	33544.75	431179	55173.25	260780.5	555692.8	116804.8
C53 H100 O6 N	846.7541	---	2123	2901	61057.75	653843.3	75144	607696	524660	314092.8
C54 H100 O6 N	858.7539	---	82	163	3770.25	16781	5039.75	20388.75	25425.25	19875.25
C54 H102 O6 N	860.7704	---	376	658	9631.25	25126.25	9264.5	42089.75	43112.25	38153
Diglycerides										
C35 H68 O5 N	582.5087	C30:2	0	0	470.5	403	0	2834	0	627.25
C35 H70 O5 N	584.525	C30:1	0	0	374.5	45.5	0	2261.75	0	186
C37 H68 O5 N	606.5087	C37:4	0	0	386	1934	0	1463	117	501
C37 H72 O5 N	610.5406	C37:3	747	280	880	2988.2	115.25	4211.25	389.75	1800.5

						5				
C37 H74 O5 N	612.5567	C37:2	0	48	197.75	0	0	2006.25	0	418
C39 H68 O5 N	630.5085	C39:6	44	141	0	80.75	149.75	8753	15.75	820
C39 H70 O5 N	632.5241	C39:5	631	0	1065.5	1752.25	0	8045.75	1628.5	7612.5
C39 H74 O5 N	636.5571	C39:4	498	0	791.5	1393	24.25	3409.25	485.75	5471.75
C39 H76 O5 N	638.5736	C39:3	126	0	56.25	100.75	122.5	32.75	0	1294
Ceramides										
C30 H57 O3 N Na	502.4468	C30::2	0	0	0	0	0	352.75	0	0
C30 H59 O3 N Na	504.4769	C30::1	0	0	0	115.25	86.25	177.25	0	2263.25
C31 H59 O3 N Na	516.477	---	0	0	99	0	246	265.5	109.5	6985
C31 H61 O3 N Na	518.4928	---	0	0	9325.25	76131.5	6908.5	39162.25	10951.5	90177.25
C31 H63 O3 N Na	520.5086	---	0	50	1962.5	351875.8	540	42851.75	3333.5	4863.25
C31 H65 O3 N Na	522.5153	---	0	0	0	22337.5	0	1568	40.25	111.5
C32 H63 O3 N Na	532.4699	C32:1	0	0	17.5	9271.5	139	283	0	212.75
C32 H65 O3 N Na	534.4876	C32:0	658	0	3007.75	2189	5681.5	4309.25	4855	89795
C33 H63 O3 N Na	544.5081	---	0	0	262.5	0	473.75	671.75	21.75	10137.25
C33 H65 O3 N Na	546.5239	---	0	0	14952.5	54126	9302	61550	12500	75305
C33 H67 O3 N Na	548.5029	---	5653	12822	276	3385.5	8267.5	4557.25	2494	19290.75
C33 H69 O3 N Na	550.5465	---	110	0	0	11625.25	0	3846	37.5	0
C34 H61 O3 N Na	554.5142	---	0	194	477.5	765.25	367.25	20245.25	215.5	3393.25
C34 H63 O3 N Na	556.5294	---	1075	1538	2056.5	9913	531.5	15160.75	1835.75	16902.5
C34 H65 O3 N Na	558.4854	---	0	0	2464.75	7379.5	1887.75	1718.75	617.25	6813
C34 H67 O3 N Na	560.5012	---	0	0	2508.25	123810	619.25	7882.25	809.25	1535.75

C34 H69 O3 N Na	562.5187	---	178	201	6913.25	2812.25	8388.5	8393.25	6741.5	160060.8
C34 H71 O3 N Na	564.5348	---	0	67	98	7598	488.25	9031	846.25	5717.5
C35 H67 O3 N Na	572.5395	---	0	0	323.75	69.75	0	768.5	0	3556.25
C35 H69 O3 N Na	574.5551	---	0	0	2935.5	8471	476.5	10881.75	1187	12119
C35 H71 O3 N Na	576.5344	---	0	0	670.5	0	212.75	447.5	159.75	27052.25
C35 H73 O3 N Na	578.5508	---	131	409	0	106	20.5	2101.5	0	13.75
C36 H63 O3 N Na	580.5301	---	0	47	683	424.5	142	3404.25	46.75	3814.75
C36 H65 O3 N Na	582.5452	---	83	87	446.5	527.75	412.75	11023.5	147.75	6191.25
C36 H69 O3 N Na	586.5169	---	0	0	395.75	5107	1560.25	3416.25	626.25	4948.25
C36 H71 O3 N Na	588.5327	---	0	0	7287	60430.5	1353.75	16084	985.25	2811.75
C36 H73 O3 N Na	590.5503	---	191	143	2755.25	380.75	981.75	1966	2009.75	56214.75
C36 H75 O3 N Na	592.5661	---	0	65	120.25	7718.5	41.75	4498.5	38	791
C37 H73 O3 N Na	602.5116	---	0	0	288.75	0	1433	1374.25	100.5	8986.5
C39 H65 O3 N Na	618.5174	---	92	0	801.5	133	0	90	0	545
C39 H72 O13 P	779.4708	30:1	5183	0	21173	24663.25	98.75	5867	2068.5	24831.75
C41 H74 O13 P	805.4858	32:2	58605	0	126302	131822.3	1426.75	32440	12272.5	47105
C41 H76 O13 P	807.5013	32:1	155387	40	159998	134581.8	4203.75	57709.5	9973.75	38330
C42 H76 O13 P	809.5082	33:3	19108	204	19357.25	16222	389.5	7400.75	1055	4522
C42 H76 O13 P	819.5018	33:2	8682	40	17949.25	10733	171	1881	854.5	11889.75
C43 H74 O13 P	829.486	34:4	0	0	85174.5	161636.5	3073.5	24090.25	26735.75	36857
C43 H76 O13 P	831.5013	34:3	291557	57	433965.5	625537	27942.5	120628.8	46266.5	155677
C43 H78 O13 P	833.517	34:2	1716413	1441	696522.5	102602	65365	194020.3	59363.25	254816

						8				
C43 H80 O13 P	835.5322	34:1	388058	133	174720	193233.5	13222	57716.75	13795.75	51385.5
C43 H82O13 P	837.5399	34:0	46325	0	19499.25	22977.5	1380.5	8456	1502	5868.75
C44 H80 O13 P	847.5336	35:2	13405	0	30020.75	15484.75	1783.5	6393.25	2972.5	17437.75
C45 H74 O13 P	853.4865	36:6	5330	0	248929.5	16633.5	548	265700.5	741.75	4816.75
C45 H76 O13 P	855.5016	36:5	85394	0	502303.3	182688.5	12890.25	273930.5	11070.5	63468
C45 H78 O13 P	857.5173	36:4	291300	113	1336635	723137	54158.5	748260.8	74662.75	259433.3
C45 H80 O13 P	859.5325	36:3	155322	47	654948.5	779710.8	53945	255597.8	67223	277511.8
C45 H82 O13 P	861.548	36:2	222694	101	260045.3	414187.3	39075.5	58186.75	29483.75	133225.3
C45 H84 O13 P	863.5637	36:1	85723	38	60585.5	64209.25	7283.25	8110	5433.75	27809.5
Lysophosphoinositol										
C25 H46 O12 P	569.2732	16:1	17941	0	3673416	5656.5	214.25	89407.75	1154.5	6122
C25 H48 O12 P	571.2773	16:0	419	0	159314.8	9.5	0	2614.75	7.25	15.25
C27 H46 O12 P	593.2731	18:3	0	0	266758.5	15689.75	1199.5	133299.5	7702.75	15403.75
C27 H48 O12 P	595.2886	18:2	27542	0	5328383	21760.75	1063	179599.3	6389	20212.5
C27 H50 O12 P	597.3048	18:1	12413	0	1395474	12489.25	847	35485.75	1979.5	17541.25
C27 H52 O12 P	599.321	18:0	274	0	20584.5	3546.5	617.5	1954.75	212	1575
Phosphoglycerides										
16:0 lyso PG	483.273	---	0	0	186576	799.25	0	428.5	17	1957

PG 16:1 16:1 or isomer	717.4709	---	0	0	215334.8	96499.25	722.5	16120.75	4383	13005
Sphingomyelin										
SM d18:0 16:1 or isomer	699.544	---	0	0	42836.75	3467.75	1365.75	11033	2031.25	8021
Miscellaneous										
[PS (20:4)] 1-(5Z,8Z,11Z,14Z-eicosatetraenoyl)-sn-glycero-3-phosphoserine	544.2658	---	0	0	303945	654.75	16.5	17822.75	26.75	3120.5
PC (21:4)] 1-(6Z,9Z,12Z,15Z-heneicosatetraenoyl)-sn-glycero-3-phosphocholine	556.3391	---	0	0	164960	16577	193.75	10036	11287	2875.5
SP (18:0)] N-(9Z-octadecenoyl)-sphing-4-enine	562.52	---	0	0	2795.25	227.75	50	391.25	57.5	798.25
N-Palmitoylsphingosine ,Ceramide (d18:1/16:0) [FA-]	582.51	---	0	0	170878.5	403928.8	1158.5	33563.5	5538.5	7325.5
Dipalmitoylphosphatidic acid [FA-]	693.4709	---	0	0	71990	6147	0	4404.25	376.25	1235.5
Dipalmitoylphosphatidic acid [FA-]	693.4709	---	0	0	39609	2874.5	0	1863.5	165	598.5
SP (16:0)] N-(hexadecanoyl)-1-beta-glucosyl-sphing-4-enine	698.5567	---	0	0	7028.25	4732.5	0	7045	0	264.75
MG 14:0	301.2383	---	2560	4624	95308.5	4625.25	7647.5	6679.75	7045	8522.5

MG 16:1	327.254	---	13029	5125	171191	2846.75	4705.25	7131.25	5363	14764
MG 16:0	329.2695	---	64	2873	20601.75	3986.75	4444.25	4484.75	4338	5881
Myristic acid	227.2017	---	471	4890	90810.75	4056.5	9603.75	8499.25	8601.25	28021.75
Gamma-Linolenic acid	277.2171	---	83043	10287	705299	896.75	510.5	24206.75	1403.5	15775.75
Stearic acid	283.2643	---	27075	26399	38651.25	24337.25	30994	22336.5	27700.5	29087.75
hydroxylinolenic acid or isomer	295.228	---	468319	4041	26082	3036.5	9620.25	3526	5098	8415.75
hydroxylinoleic acid or isomer	297.2435	---	30229	11850	49939	14689	14223	14034.75	14143.75	22255
hydroxyoctadecanoic acid	299.2592	---	3025	5913	14223.75	5963.5	7942.5	6634	8732	15006.5
Eicosenoic acid	309.2799	---	7220	408	68360.5	200.5	831	4344.25	908.75	2663
(9Z,12Z)-(11S)-11-Hydroperoxyoctadeca-9,12-dienoic acid	311.2229	---	175223	4699	18096	5502.5	4964.25	7309	7315.5	8095.25
Phytanic acid	311.2957	---	0	1452	66507.25	1614	1633.25	3970.25	2110.75	6882.5
FA (20:2)] 15S-hydroperoxy-11Z,13E-eicosadienoic acid	339.2541	---	1184	237	3625.5	441.75	750.25	637	712.25	960.75
Behenic Acid ,calcifediol ,Isobehenic acid [FA-]	385.3323	---	0	0	8291.25	0	0	1957.75	86.25	2005.5
Hexacosanoic acid	395.3895	---	0	807	225004	13889.75	2007.25	16828.5	9721	68239.5

[FA (28:0)] octacosanoic acid	423.4205	---	0	99	57212	7623.75	423.75	2830	4132	9916.75
Cerotic acid ,3,13,19-trimethyl-tricosanoic acid ,Isocerotic acid [FA-]	441.3951	---	0	0	19700	1110.5	20.25	152.25	833.5	8833.75
1-Oleoyl-lysophosphatidic acid [FA-]	481.257	---	0	0	90477.5	0	0	5241.25	0	0
18:1 Lysophosphatidic acid FA	481.2571	---	0	0	699235.3	76.25	0	14187.75	0	101.25
hentriacontanoic acid ,D-Mycoceranic acid ,(+)-28-methyl-triacontanoic acid [FA-]	511.4733	---	0	0	12772.75	0	0	231	0	0
Dipalmitoylphosphatidic acid [FA-]	693.4709	---	0	0	71990	6147	0	4404.25	376.25	1235.5
Dipalmitoylphosphatidic acid [FA-]	693.4709	---	0	0	39609	2874.5	0	1863.5	165	598.5

* Chain length: saturation state. • Media is Schneider's medium which can be used for tissues dissection in it, more detalies in appenidix X.

Food is a fly food which can be used for fly diet regime, more detalies in appendix XI.

Appendix X: *Drosophila* Schneider's media according to manufacturer's protocol (Invitrogen, UK).

COMPONENTS	Concentration (mg/L)
Glycine	250
L-Arginine	400
L-Aspartic acid	400
L-Cysteine	60
L-Cystine	100
L-Glutamic Acid	800
L-Glutamine	1800
L-Histidine	400
L-Isoleucine	150
L-Leucine	150
L-Lysine hydrochloride	1650
L-Methionine	800
L-Phenylalanine	150
L-Proline	1700
L-Serine	250
L-Threonine	350
L-Tryptophan	100
L-Tyrosine	500
L-Valine	300
beta-Alanine	500
Calcium Chloride (CaCl2-2H2O)	794
Magnesium Sulfate (MgSO4-7H2O)	3700
Potassium Chloride (KCl)	1600
Potassium Phosphate monobasic (KH2PO4)	450
Sodium Bicarbonate (NaHCO3)	400
Sodium Chloride (NaCl)	2100
Sodium Phosphate monobasic (NaH2PO4-2H2O)	1321
Alpha-Ketoglutaric acid	200
D-Glucose (Dextrose)	2000
Fumaric acid	100
Malic acid	100
Succinic acid	100
Trehalose	2000

Appendix XI: Fly food recipe according to the members of media preparation room at university of Glasgow.

Reagent composition
Standard fly food Per 1 litre of water
10 g agar
15 g sucrose
33 g glucose
35 g dried yeast
15 g maize meal
10 g wheat germ
30 g treacle
5 ml Propionic acid
10 g soya flour

10. References

ADAMS, M. D. & SEKELSKY, J. J. 2002. From sequence to phenotype: reverse genetics in drosophila melanogaster. *Nat Rev Genet,* 3**,** 189-198.

ADAMSON, A. L., CHOHAN, K., SWENSON, J. & LAJEUNESSE, D. 2011. A Drosophila Model for Genetic Analysis of Influenza Viral/Host Interactions. *Genetics,* 189**,** 495-506.

AMBEGAOKAR, S. S. & JACKSON, G. R. 2010. Interaction Between Eye Pigment Genes and Tau-Induced Neurodegeneration in Drosophila melanogaster. *Genetics,* 186**,** 435-442.

AMERICA, A. H. P. & CORDEWENER, J. H. G. 2008. Comparative LCMS: A landscape of peaks and valleys. *Proteomics,* 8**,** 731-749.

ANAKA, M., MACDONALD, C. D., BARKOVA, E., SIMON, K., ROSTOM, R., GODOY, R. A., HAIGH, A. J., MEINERTZHAGEN, I. A. & LLOYD, V. 2008. The white gene of Drosophila melanogaster encodes a protein with a role in courtship behavior. *Journal of neurogenetics,* 22**,** 243-276.

ARTSCIENCE. 2011. *Drosophila life cycle* [Online]. Available: http://invitero.tumblr.com/drosophila [Accessed 12th December 2012].

ASHBURNER, M. 1990. Puffs, genes, and hormones revisited. *Cell,* 61**,** 1-3.

ATACK, J. R., BROUGHTON, H. B. & POLLACK, S. J. 1995. Structure and mechanism of inositol monophosphatase. *FEBS Letters,* 361**,** 1-7.

BARRY, S., CLARKE, G., SCULLY, P. & DINAN, T. G. 2009. Kynurenine pathway in psychosis: evidence of increased tryptophan degradation. *Journal of Psychopharmacology,* 23**,** 287-294.

BATABYAL, D. & YEH, S.-R. 2007. Human Tryptophan Dioxygenase:?A Comparison to Indoleamine 2,3-Dioxygenase. *Journal of the American Chemical Society,* 129**,** 15690-15701.

BECK, F.-X., NEUHOFER, W. & MÜLLER, E. 2000. Molecular chaperones in the kidney: distribution, putative roles, and regulation. *American Journal of Physiology - Renal Physiology,* 279**,** F203-F215.

BHOJWANI, J., SINGH, A., MISQUITTA, L., MISHRA, A. & SINHA, P. 1995. Search for Drosophila genes based on patterned expression of mini-white reporter gene of a P lacW vector in adult eyes. *Development Genes and Evolution,* 205**,** 114-121.

BIER, E. 2005. Drosophila, the golden bug, emerges as a tool for human genetics. *Nat Rev Genet,* 6**,** 9-23.

BILEN, J. & BONINI, N. M. 2005. Drosophila as a model for human neurodegenerative disease. *Annual Review of Genetics.* Palo Alto: Annual Reviews.

BLAU, N., DE KLERK, J. B. C., THONY, B., HEIZMANN, C. W., KIERAT, L., SMEITINK, J. A. M. & DURAN, M. 1996. Tetrahydrobiopterin Loading Test in Xanthine Dehydrogenase and Molybdenum Cofactor Deficiencies. *Biochemical and Molecular Medicine,* 58**,** 199-203.

BLOM, T., SOMERHARJU, P. & IKONEN, E. 2011. Synthesis and Biosynthetic Trafficking of Membrane Lipids. *Cold Spring Harbor Perspectives in Biology.*

BOLTSHAUSER, E., NIEDERWIESER, A., KIERAT, L., HAENGGELI, C. A., OPITZ, J. M. & REYNOLDS, J. F. 1986. Pterins in patients with Rett syndrome. *American Journal of Medical Genetics,* 25**,** 317-321.

BOTTING, N. P. 1995. Chemistry and neurochemistry of the kynurenine pathway of tryptophan metabolism. *Chemical Society Reviews,* 24**,** 401-412.

BOY, A. L., ZHAI, Z., HABRING-MÜLLER, A., KUSSLER-SCHNEIDER, Y., KASPAR, P. & LOHMANN, I. 2010. Vectors for efficient and high-throughput construction of fluorescent drosophila reporters using the PhiC31 site-specific integration system. *genesis,* 48**,** 452-456.

BRAND, A. H. & PERRIMON, N. 1993. Targeted gene expression as a means of altering cell fates and generating dominant phenotypes. *Development,* 118**,** 401-415.

BROSNAN, J. T. & BROSNAN, M. E. 2006. The Sulfur-Containing Amino Acids: An Overview. *The Journal of Nutrition,* 136**,** 1636S-1640S.

BUIE, L. W., OERTEL, M. D. & CALA, S. O. 2006. Allopurinol as Adjuvant Therapy in Poorly Responsive or Treatment Refractory Schizophrenia. *The Annals of Pharmacotherapy,* 40**,** 2200-2204.

BURNS, K. E., BAUMGART, S., DORRESTEIN, P. C., ZHAI, H., MCLAFFERTY, F. W. & BEGLEY, T. P. 2005. Reconstitution of a New Cysteine Biosynthetic Pathway in Mycobacterium t uberculosis. *Journal of the American Chemical Society,* 127**,** 11602-11603.

CAKOUROS, D., MILLS, K., DENTON, D., PATERSON, A., DAISH, T. & KUMAR, S. 2008. dLKR/SDH regulates hormone-mediated histone arginine methylation and transcription of cell death genes. *J Cell Biol,* 182**,** 481-95.

CHAPMAN, R. F. 1998. *The insects: structure and function*, Cambridge Univ Pr.

CHESTER, T. L. 2012. Recent Developments in High-Performance Liquid Chromatography Stationary Phases. *Analytical Chemistry*.

CHIEN, S., REITER, L. T., BIER, E. & GRIBSKOV, M. 2002. Homophila: human disease gene cognates in Drosophila. *Nucleic Acids Research,* 30**,** 149-151.

CHINTAPALLI, V. R., TERHZAZ, S., WANG, J., AL BRATTY, M., WATSON, D. G., HERZYK, P., DAVIES, S. A. & DOW, J. A. T. 2012. Functional Correlates of Positional and Gender-Specific Renal Asymmetry in <italic>Drosophila</italic>. *PLoS ONE,* 7**,** e32577.

CHINTAPALLI, V. R., WANG, J. & DOW, J. A. 2007a. Using FlyAtlas to identify better Drosophila melanogaster models of human disease. *Nat Genet,* 39**,** 715-20.

CHINTAPALLI, V. R., WANG, J. & DOW, J. A. T. 2007b. Using FlyAtlas to identify better Drosophila melanogaster models of human disease. *Nat Genet,* 39**,** 715-720.

CHUNG, H. Y., BAEK, B. S., SONG, S. H., KIM, M. S., HUH, J. I., SHIM, K. H., KIM, K. W. & LEE, K. H. 1997. Xanthine dehydrogenase/xanthine oxidase and oxidative stress. *AGE,* 20**,** 127-140.

COAST, G. M., CUSINATO, O., KAY, I. & GOLDSWORTHY, G. J. 1991. An evaluation of the role of cyclic AMP as an intracellular second

messenger in Malpighian tubules of the house cricket, Acheta domesticus. *Journal of Insect Physiology,* 37**,** 563-573.
COHEN, D. M. 1999. SIGNALLING AND GENE REGULATION BY UREA AND NaCl IN THE RENAL MEDULLA. *Clinical and Experimental Pharmacology and Physiology,* 26**,** 69-73.
COLEMAN, C. M. & NECKAMEYER, W. S. 2005. Serotonin synthesis by two distinct enzymes in Drosophila melanogaster. *Archives of insect biochemistry and physiology,* 59**,** 12-31.
COLLINS, J. F., DUKE, E. J. & GLASSMAN, E. 1970. Nutritional control of xanthine dehydrogenase I. The effect in adult Drosophila melanogaster of feeding a high protein diet to larvae. *Biochimica et Biophysica Acta (BBA)-General Subjects,* 208**,** 294-303.
CORPORATION, W. 2010. *Hydrophilic interaction chromatography* [Online]. Available: http://www.sepscience.com/Techniques/LC/Articles/501-/Hydrophilic-interaction-chromatography-HILIC [Accessed 12th December 2012].
COSSINS, E. A. & SINHA, S. K. 1966. The interconversion of glycine and serine by plant tissue extracts. *Biochemical Journal,* 101**,** 542-549.
COUTELIS, J. B., PETZOLDT, A. G., SPÉDER, P., SUZANNE, M. & NOSELLI, S. 2008. Left–right asymmetry in Drosophila. *Seminars in Cell & Developmental Biology,* 19**,** 252-262.
CREEK, D. J., JANKEVICS, A., BREITLING, R., WATSON, D. G., BARRETT, M. P. & BURGESS, K. E. V. 2011. Toward Global Metabolomics Analysis with Hydrophilic Interaction Liquid Chromatography Mass Spectrometry: Improved Metabolite Identification by Retention Time Prediction. *Analytical Chemistry,* 83**,** 8703-8710.
DARLINGTON, L. G., MACKAY, G. M., FORREST, C. M., STOY, N., GEORGE, C. & STONE, T. W. 2007. Altered kynurenine metabolism correlates with infarct volume in stroke. *European Journal of Neuroscience,* 26**,** 2211-2221.
DEAN, M., HAMON, Y. & CHIMINI, G. 2001. The human ATP-binding cassette (ABC) transporter superfamily. *Journal of Lipid Research,* 42**,** 1007-1017.
DENT, C. E. & PHILPOT, G. R. 1954. Xanthinuria, an inborn error (or deviation) of metabolism. *Lancet,* 266**,** 182.
DETTMER, K., ARONOV, P. A. & HAMMOCK, B. D. 2007. Mass spectrometry-based metabolomics. *Mass Spectrometry Reviews,* 26**,** 51-78.
DICHTL, B., STEVENS, A. & TOLLERVEY, D. 1997. Lithium toxicity in yeast is due to the inhibition of RNA processing enzymes. *The EMBO journal,* 16**,** 7184-7195.
DICKERSON, F. B., STALLINGS, C. R., ORIGONI, A. E., SULLENS, A., KHUSHALANI, S., SANDSON, N. & YOLKEN, R. H. 2009. A double-blind trial of adjunctive allopurinol for schizophrenia. *Schizophrenia Research,* 109**,** 66-69.
DIETZL, G., CHEN, D., SCHNORRER, F., SU, K.-C., BARINOVA, Y., FELLNER, M., GASSER, B., KINSEY, K., OPPEL, S., SCHEIBLAUER, S., COUTO, A., MARRA, V., KELEMAN, K. & DICKSON, B. J. 2007. A genome-wide

transgenic RNAi library for conditional gene inactivation in Drosophila. *Nature,* 448**,** 151-156.
DOW, J. A. T. 2003. The Drosophila phenotype gap — and how to close it. *Briefings in Functional Genomics & Proteomics,* 2**,** 121-127.
DOW, J. A. T. 2009. Insights into the Malpighian tubule from functional genomics. *Journal of Experimental Biology,* 212**,** 435-445.
DOW, J. A. T., DAVIES, S. A. & SOOZEN, M. A. 1998. Fluid Secretion by the Drosophila Malpighian Tubule. *American Zoologist,* 38**,** 450-460.
DOW, J. A. T. & ROMERO, M. F. 2010. Drosophila provides rapid modeling of renal development, function, and disease. *American Journal of Physiology - Renal Physiology,* 299**,** F1237-F1244.
DRAPEAU, M. D. 2003a. A novel hypothesis on the biochemical role of the Drosophila Yellow protein. *Biochem Biophys Res Commun,* 311**,** 1-3.
DRAPEAU, M. D. 2003b. A novel hypothesis on the biochemical role of the Drosophila Yellow protein. *Biochemical and Biophysical Research Communications,* 311**,** 1-3.
DRAPEAU, M. D., CYRAN, S. A., VIERING, M. M., GEYER, P. K. & LONG, A. D. 2006. A cis-regulatory sequence within the yellow locus of Drosophila melanogaster required for normal male mating success. *Genetics,* 172**,** 1009-30.
DUDAI, Y. 1977. Properties of learning and memory in<i>Drosophila melanogaster</i&gt. *Journal of Comparative Physiology A: Neuroethology, Sensory, Neural, and Behavioral Physiology,* 114**,** 69-89.
DUNN, W. B. 2008. Current trends and future requirements for the mass spectrometric investigation of microbial, mammalian and plant metabolomes. *Physical Biology,* 5**,** 011001.
ELLAWAY, C. J., WILCKEN, B. & CHRISTODOULOU, J. 2002. Clinical approach to inborn errors of metabolism presenting in the newborn period. *Journal of Paediatrics and Child Health,* 38**,** 511-517.
ENRICO, P., ESPOSITO, G., MURA, M. A., MIGHELI, R., SERRA, P. A., DESOLE, M. S., MIELE, E., DE NATALE, G. & MIELE, M. 1997. EFFECTS OF ALLOPURINOL ON STRIATAL DOPAMINE, ASCORBATE AND URIC ACID DURING AN ACUTE MORPHINE CHALLENGE: EX VIVO AND IN VIVO STUDIES. *Pharmacological Research,* 35**,** 577-585.
EVANS, J. M., DAY, J. P., CABRERO, P., DOW, J. A. T. & DAVIES, S.-A. 2008. A new role for a classical gene: White transports cyclic GMP. *Journal of Experimental Biology,* 211**,** 890-899.
FERGUSON, L. C., GREEN, J., SURRIDGE, A. & JIGGINS, C. D. 2011. Evolution of the insect yellow gene family. *Mol Biol Evol,* 28**,** 257-72.
FIEHN, O. 2001. Combining Genomics, Metabolome Analysis, and Biochemical Modelling to Understand Metabolic Networks. *Comparative and Functional Genomics,* 2**,** 155-168.
FOLCH, J., LEES, M. & SLOANE-STANLEY, G. H. 1957. A simple method for the isolation and purification of total lipids from animal tissues. *J. biol. Chem,* 226**,** 497-509.

FORET, S., KUCHARSKI, R., PITTELKOW, Y., LOCKETT, G. A. & MALESZKA, R. 2009. Epigenetic regulation of the honey bee transcriptome: unravelling the nature of methylated genes. *BMC Genomics,* 10**,** 472.

FRIEDMAN, T. B. & JOHNSON, D. H. 1977. Temporal control of urate oxidase activity in Drosophila: evidence of an autonomous timer in malpighian tubules. *Science,* 197**,** 477-479.

GALINSKI, E. A. & TRÜPER, H. G. 1994. Microbial behaviour in salt-stressed ecosystems. *FEMS Microbiology Reviews,* 15**,** 95-108.

GEORGE EP. BOX, N. R. D. 1987. *Empirical Model-Building and Response Surfaces*, Wiley.

GILFILLAN, G. D., DAHLSVEEN, I. K. & BECKER, P. B. 2004. Lifting a chromosome: dosage compensation in< i> Drosophila melanogaster</i>. *FEBS Letters,* 567**,** 8-14.

GIRTON, J. R. & JOHANSEN, K. M. 2008. Chromatin structure and the regulation of gene expression: the lessons of PEV in Drosophila. *Advances in genetics,* 61**,** 1-43.

GLANTZOUNIS, G. K., TSIMOYIANNIS, E. C., KAPPAS, A. M. & GALARIS, D. A. 2005. Uric Acid and Oxidative Stress. *Current Pharmaceutical Design,* 11**,** 4145-4151.

GLASSMAN, E. 1965. Genetic regulation of xanthine dehydrogenase in *Drosophila melanogaster*. *Fed. Proc.,* 24**,** 1243-1251.

GOH, K.-I., CUSICK, M. E., VALLE, D., CHILDS, B., VIDAL, M. & BARABÁSI, A.-L. 2007. The human disease network. *Proceedings of the National Academy of Sciences,* 104**,** 8685-8690.

HADORN, E. 1956. Patterns of Biochemical and Developmental Pleiotropy. *Cold Spring Harbor Symposia on Quantitative Biology,* 21**,** 363-373.

HALLACLI, E. & AKHTAR, A. 2009. X chromosomal regulation in flies: when less is more. *Chromosome Research,* 17**,** 603-619.

HAMMAD, L. A., COOPER, B. S., FISHER, N. P., MONTOOTH, K. L. & KARTY, J. A. 2011. Profiling and quantification of Drosophila melanogaster lipids using liquid chromatography/mass spectrometry. *Rapid Communications in Mass Spectrometry,* 25**,** 2959-2968.

HAN, Q., FANG, J., DING, H., JOHNSON, J. K., CHRISTENSEN, B. M. & LI, J. 2002. Identification of Drosophila melanogaster yellow-f and yellow-f2 proteins as dopachrome-conversion enzymes. *Biochemical Journal,* 368**,** 333-40.

HANSEN, S., ANDERSEN, M., BIRKEDAL, H., CORNETT, C. & WIBRAND, F. 2006. The important role of taurine in oxidative metabolism. *Taurine 6,* 129-135.

HILLE, R. & NISHINO, T. 1995. Flavoprotein structure and mechanism. 4. Xanthine oxidase and xanthine dehydrogenase. *The FASEB Journal,* 9**,** 995-1003.

HILLIKER, A. J., DUYF, B., EVANS, D. & PHILLIPS, J. P. 1992. Urate-null rosy mutants of Drosophila melanogaster are hypersensitive to oxygen stress. *Proceedings of the National Academy of Sciences,* 89**,** 4343-4347.

HOBANI, Y. H. 2012. *Metabolomic analyses of Drosophila models for human renal disease* [Online]. [Accessed].

HOLČAPEK, M., JIRÁSKO, R. & LÍSA, M. 2012. Recent developments in liquid chromatography–mass spectrometry and related techniques. *Journal of Chromatography A,* 1259**,** 3-15.

HOLTZMAN, S., MILLER, D., EISMAN, R., KUWAYAMA, H., NIIMI, T. & KAUFMAN, T. 2010. Transgenic tools for members of the genus Drosophila with sequenced genomes. *Fly,* 4**,** 349.

HOUTEN, S. M. 2009. Metabolomics: Unraveling the chemical individuality of common human diseases. *Annals of Medicine,* 41**,** 402-407.

IMLER, J.-L. & HOFFMANN, J. A. 2000. Signaling mechanisms in the antimicrobial host defense of Drosophila. *Current Opinion in Microbiology,* 3**,** 16-22.

INESTROSA, N. C., SUNKEL, C. E., ARRIAGADA, J., GARRIDO, J. & GODOY-HERRERA, R. 1996. Abnormal development of the locomotor activity in yellow larvae of Drosophila: a cuticular defect? *Genetica,* 97**,** 205-10.

JANDERA, P. 2008. Stationary phases for hydrophilic interaction chromatography, their characterization and implementation into multidimensional chromatography concepts. *Journal of Separation Science,* 31**,** 1421-1437.

JESSOP, C. E., CHAKRAVARTHI, S., WATKINS, R. H. & BULLEID, N. J. 2004. Oxidative protein folding in the mammalian endoplasmic reticulum. *Biochemical Society Transactions,* 32**,** 655.

JOHNSEN, E., WILSON, S. R., ODSBU, I., KRAPP, A., MALEROD, H., SKARSTAD, K. & LUNDANES, E. 2011. Hydrophilic interaction chromatography of nucleoside triphosphates with temperature as a separation parameter. *Journal of Chromatography A,* 1218**,** 5981-5986.

JULES A, H. 1995. Innate immunity of insects. *Current Opinion in Immunology,* 7**,** 4-10.

JULIAN A.T, D. 2007. Model organisms and molecular genetics for endocrinology. *General and Comparative Endocrinology,* 153**,** 3-12.

KAMAKURA, M. 2011. Royalactin induces queen differentiation in honeybees. *Nature,* 473**,** 478-83.

KAMLEH, A., BARRETT, M. P., WILDRIDGE, D., BURCHMORE, R. J. S., SCHELTEMA, R. A. & WATSON, D. G. 2008a. Metabolomic profiling using Orbitrap Fourier transform mass spectrometry with hydrophilic interaction chromatography: a method with wide applicability to analysis of biomolecules. *Rapid Communications in Mass Spectrometry,* 22**,** 1912-1918.

KAMLEH, M. A., DOW, J. A. T. & WATSON, D. G. 2009a. Applications of mass spectrometry in metabolomic studies of animal model and invertebrate systems. *Briefings in Functional Genomics & Proteomics,* 8**,** 28-48.

KAMLEH, M. A., HOBANI, Y., DOW, J. A. & WATSON, D. G. 2008b. Metabolomic profiling of Drosophila using liquid chromatography Fourier transform mass spectrometry. *FEBS Lett,* 582**,** 2916-22.

KAMLEH, M. A., HOBANI, Y., DOW, J. A., ZHENG, L. & WATSON, D. G. 2009b. Towards a platform for the metabonomic profiling of

different strains of Drosophila melanogaster using liquid chromatography-Fourier transform mass spectrometry. *FEBS J,* 276**,** 6798-809.

KAMLEH, M. A., HOBANI, Y., DOW, J. A. T. & WATSON, D. G. 2008c. Metabolomic profiling of Drosophila using liquid chromatography Fourier transform mass spectrometry. *FEBS Letters,* 582**,** 2916-2922.

KAMLEH, M. A., HOBANI, Y., DOW, J. A. T., ZHENG, L. & WATSON, D. G. 2009c. Towards a platform for the metabonomic profiling of different strains of Drosophila melanogaster using liquid chromatography-fourier transform mass spectrometry. *FEBS Journal,* 276**,** 6798-6809.

KAMLEH, M. A., HOBANI, Y., DOW, J. A. T., ZHENG, L. & WATSON, D. G. 2009d. Towards a platform for the metabonomic profiling of different strains of Drosophila melanogaster using liquid chromatography–Fourier transform mass spectrometry. *FEBS Journal,* 276**,** 6798-6809.

KATAJAMAA, M., MIETTINEN, J. & ORESIC, M. 2006. MZmine: toolbox for processing and visualization of mass spectrometry based molecular profile data. *Bioinformatics,* 22**,** 634-636.

KATAJAMAA, M. & ORESIC, M. 2005. Processing methods for differential analysis of LC/MS profile data. *BMC bioinformatics,* 6**,** 179.

KATAJAMAA, M. & ORESIC, M. 2007. Data processing for mass spectrometry-based metabolomics. *Journal of Chromatography A,* 1158**,** 318-328.

KIM, J., SUH, H., KIM, S., KIM, K., AHN, C. & YIM, J. 2006. Identification and characteristics of the structural gene for the Drosophila eye colour mutant sepia, encoding PDA synthase, a member of the Omega class glutathione S-transferases. *Biochemical Journal,* 398**,** 451.

KIM, Y., NAM, H., CHUNG, H., KIM, N., RYU, J., LEE, W., ARKING, R. & YOO, M. 2001. Role of xanthine dehydrogenase and aging on the innate immune response of <i>Drosophila</i&gt. *AGE,* 24**,** 187-193.

KING, N. J. C. & THOMAS, S. R. 2007. Molecules in focus: Indoleamine 2,3-dioxygenase. *The International Journal of Biochemistry & Cell Biology,* 39**,** 2167-2172.

KLEINJAN, D. J. & VAN HEYNINGEN, V. 1998. Position effect in human genetic disease. *Human molecular genetics,* 7**,** 1611-1618.

KLUCKEN, J., BÜCHLER, C., ORSÓ, E., KAMINSKI, W. E., PORSCH-ÖZCÜRÜMEZ, M., LIEBISCH, G., KAPINSKY, M., DIEDERICH, W., DROBNIK, W., DEAN, M., ALLIKMETS, R. & SCHMITZ, G. 2000. ABCG1 (ABC8), the human homolog of the Drosophila white gene, is a regulator of macrophage cholesterol and phospholipid transport. *Proceedings of the National Academy of Sciences,* 97**,** 817-822.

KÔMOTO, N., QUAN, G. X., SEZUTSU, H. & TAMURA, T. 2009. A single-base deletion in an ABC transporter gene causes white eyes, white eggs, and translucent larval skin in the silkworm w-3oe mutant. *Insect Biochemistry and Molecular Biology,* 39**,** 152-156.

KONIG, R., STERTZ, S., ZHOU, Y., INOUE, A., HOFFMANN, H. H., BHATTACHARYYA, S., ALAMARES, J. G., TSCHERNE, D. M., ORTIGOZA, M. B., LIANG, Y., GAO, Q., ANDREWS, S. E., BANDYOPADHYAY, S., DE JESUS, P., TU, B. P., PACHE, L., SHIH, C., ORTH, A., BONAMY, G., MIRAGLIA, L., IDEKER, T., GARCIA-SASTRE, A., YOUNG, J. A. T., PALESE, P., SHAW, M. L. & CHANDA, S. K. 2010. Human host factors required for influenza virus replication. *Nature,* 463**,** 813-817.

KONOPKA, R. J. & BENZER, S. 1971. Clock Mutants of Drosophila melanogaster. *Proceedings of the National Academy of Sciences,* 68**,** 2112-2116.

KOPF, T., PEER, M. & SCHMITZ, G. 2012. Genetic and Metabolic Determinants of Fatty Acid Chain Length and Desaturation, Their Incorporation into Lipid Classes and Their Effects on Risk of Vascular and Metabolic Disease. *Genetics Meets Metabolomics***,** 191-231.

KRAL, L. G., JOHNSON, D. H., BURNETT, J. B. & FRIEDMAN, T. B. 1986. Cloning a cDNA for *Drosophila melanogaster* urate oxidase. *Gene,* 45**,** 131-137.

KRASTANOV, A. 2010. Metabolomics the State of Art. *Biotechnology & Biotechnological Equipment,* 24**,** 1537-1543.

KRIAUCIONIS, S. & HEINTZ, N. 2009. The nuclear DNA base 5-hydroxymethylcytosine is present in Purkinje neurons and the brain. *Science,* 324**,** 929-30.

KUCHARSKI, R., MALESZKA, J., FORET, S. & MALESZKA, R. 2008. Nutritional Control of Reproductive Status in Honeybees via DNA Methylation. *Science,* 319**,** 1827-1830.

KUHARA, T. 2005. Gas chromatographic–mass spectrometric urinary metabolome analysis to study mutations of inborn errors of metabolism. *Mass Spectrometry Reviews,* 24**,** 814-827.

LASKO, P. 2002. Diabetic flies? Using Drosophila melanogaster to understand the causes of monogenic and genetically complex diseases. *Clinical Genetics,* 62**,** 358-367.

LE ROES-HILL, M., GOODWIN, C. & BURTON, S. 2009. Phenoxazinone synthase: what's in a name? *Trends in biotechnology,* 27**,** 248-258.

LEGAN, S. K., REBRIN, I., MOCKETT, R. J., RADYUK, S. N., KLICHKO, V. I., SOHAL, R. S. & ORR, W. C. 2008. Overexpression of Glucose-6-phosphate Dehydrogenase Extends the Life Span of Drosophila melanogaster. *Journal of Biological Chemistry,* 283**,** 32492-32499.

LI, J., BEERNTSEN, B. T. & JAMES, A. A. 1999. Oxidation of 3-hydroxykynurenine to produce xanthommatin for eye pigmentation: a major branch pathway of tryptophan catabolism during pupal development in the yellow fever mosquito, Aedes aegypti. *Insect Biochemistry and Molecular Biology,* 29**,** 329-338.

LIM, H.-Y., WANG, W., WESSELLS, R. J., OCORR, K. & BODMER, R. 2011. Phospholipid homeostasis regulates lipid metabolism and cardiac function through SREBP signaling in Drosophila. *Genes & Development,* 25**,** 189-200.

LINDSLEY, D. L., GRELL, E.H. 1968. Genetic variations of Drosophila melanogaster. *Carnegie Institution of Washington Publication*.

LONGO, N. 2009. Disorders of biopterin metabolism. *Journal of inherited metabolic disease,* 32**,** 333-342.

LOTITO, S. B. & FREI, B. 2004. The increase in human plasma antioxidant capacity after apple consumption is due to the metabolic effect of fructose on urate, not apple-derived antioxidant flavonoids. *Free Radical Biology and Medicine,* 37**,** 251-258.

MACCHIARULO, A., CAMAIONI, E., NUTI, R. & PELLICCIARI, R. 2009. Highlights at the gate of tryptophan catabolism: a review on the mechanisms of activation and regulation of indoleamine 2,3-dioxygenase (IDO), a novel target in cancer disease. *Amino Acids,* 37**,** 219-229.

MACKENZIE, S. M., BROOKER, M. R., GILL, T. R., COX, G. B., HOWELLS, A. J. & EWART, G. D. 1999. Mutations in the white gene of Drosophila melanogaster affecting ABC transporters that determine eye colouration. *Biochimica et Biophysica Acta (BBA) - Biomembranes,* 1419**,** 173-185.

MAKAROV, A. 2000. Electrostatic Axially Harmonic Orbital Trapping: A High-Performance Technique of Mass Analysis. *Analytical Chemistry,* 72**,** 1156-1162.

MAKAROV, A., DENISOV, E., KHOLOMEEV, A., BALSCHUN, W., LANGE, O., STRUPAT, K. & HORNING, S. 2006. Performance Evaluation of a Hybrid Linear Ion Trap/Orbitrap Mass Spectrometer. *Analytical Chemistry,* 78**,** 2113-2120.

MALESZKA, R. & KUCHARSKI, R. 2000. Analysis of Drosophila yellow-B cDNA reveals a new family of proteins related to the royal jelly proteins in the honeybee and to an orphan protein in an unusual bacterium Deinococcus radiodurans. *Biochem Biophys Res Commun,* 270**,** 773-6.

MARTINS, A. M. 1999. Inborn errors of metabolism: a clinical overview. *Sao Paulo Medical Journal,* 117**,** 251-265.

MASSIE, H. R., SHUMWAY, M. E. & WHITNEY, S. J. P. 1991. Uric acid content of Drosophila decreases with aging. *Experimental gerontology,* 26**,** 609-614.

MCGETTIGAN, J., MCLENNAN, R. K. J., BRODERICK, K. E., KEAN, L., ALLAN, A. K., CABRERO, P., REGULSKI, M. R., POLLOCK, V. P., GOULD, G. W., DAVIES, S. A. & DOW, J. A. T. 2005. Insect renal tubules constitute a cell-autonomous immune system that protects the organism against bacterial infection. *Insect Biochemistry and Molecular Biology,* 35**,** 741-754.

MENESHIAN, A. & BULKLEY, G. B. 2002. The physiology of endothelial xanthine oxidase: from urate catabolism to reperfusion injury to inflammatory signal transduction. *Microcirculation,* 9**,** 161-175.

MERZENDORFER, H. & ZIMOCH, L. 2003. Chitin metabolism in insects: structure, function and regulation of chitin synthases and chitinases. *Journal of Experimental Biology,* 206**,** 4393-4412.

MEYER ZU HERINGDORF, D. & JAKOBS, K. H. 2007. Lysophospholipid receptors: Signalling, pharmacology and regulation by

lysophospholipid metabolism. *Biochimica et Biophysica Acta (BBA) - Biomembranes,* 1768**,** 923-940.

MICHAEL, P., RENHUA, L. & BRIAN, O. 2011. Lipid profiles of female and male Drosophila. *BMC Research Notes,* 4.

MOHAMEDALI, K. A., GUICHERIT, O. M., KELLEMS, R. E. & RUDOLPH, F. B. 1993. The highest levels of purine catabolic enzymes in mice are present in the proximal small intestine. *Journal of Biological Chemistry,* 268**,** 23728-33.

MONTELL, I., RASMUSON, A., RASMUSON, B. & HOLMGREN, P. 1992. Uptake and incorporation in pteridines of externally supplied GTP in normal and pigment-deficient eyes ofDrosophila melanogaster. *Biochemical Genetics,* 30**,** 61-75.

MOOLENAAR, S. H., ENGELKE, U. F. H. & WEVERS, R. A. 2003. Proton nuclear magnetic resonance spectroscopy of body fluids in the field of inborn errors of metabolism. *Annals of Clinical Biochemistry,* 40**,** 16-24.

MORRIS JR, S. M. 2002. Regulation of enzymes of the urea cycle and arginine metabolism. *Annual review of nutrition,* 22**,** 87-105.

MUIR, S. W., HARROW, C., DAWSON, J., LEES, K. R., WEIR, C. J., SATTAR, N. & WALTERS, M. R. 2008. Allopurinol Use Yields Potentially Beneficial Effects on Inflammatory Indices in Those With Recent Ischemic Stroke. *Stroke,* 39**,** 3303-3307.

NAIKKHWAH, W. & O'DONNELL, M. J. 2011. Salt stress alters fluid and ion transport by Malpighian tubules of Drosophila melanogaster: evidence for phenotypic plasticity. *The Journal of Experimental Biology,* 214**,** 3443-3454.

NICHOLSON, J. K., LINDON, J. C. & HOLMES, E. 1999. 'Metabonomics': understanding the metabolic responses of living systems to pathophysiological stimuli via multivariate statistical analysis of biological NMR spectroscopic data. *Xenobiotica,* 29**,** 1181-1189.

NICHOLSON, J. K. & WILSON, I. D. 2003. Understanding 'Global' Systems Biology: Metabonomics and the Continuum of Metabolism. *Nat Rev Drug Discov,* 2**,** 668-676.

NORDSTROM, A., WANT, E., NORTHEN, T., LEHTIO, J. & SIUZDAK, G. 2007. Multiple Ionization Mass Spectrometry Strategy Used To Reveal the Complexity of Metabolomics. *Analytical Chemistry,* 80**,** 421-429.

O'DONNELL, M. J. & MADDRELL, S. H. 1995. Fluid reabsorption and ion transport by the lower Malpighian tubules of adult female Drosophila. *Journal of Experimental Biology,* 198**,** 1647-53.

OLDIGES, M., LÜTZ, S., PFLUG, S., SCHROER, K., STEIN, N. & WIENDAHL, C. 2007. Metabolomics: current state and evolving methodologies and tools. *Applied microbiology and biotechnology,* 76**,** 495-511.

OLIVER, S. G., WINSON, M. K., KELL, D. B. & BAGANZ, F. 1998. Systematic functional analysis of the yeast genome. *Trends in biotechnology,* 16**,** 373-378.

PACHER, P., NIVOROZHKIN, A. & SZABO, C. 2006. Therapeutic effects of xanthine oxidase inhibitors: renaissance half a century after the discovery of allopurinol. *Pharmacological reviews,* 58**,** 87-114.

PARISI, G., CARFAGNA, M. & D'AMORA, D. 1976. A proposed biosynthesis pathway of drosopterins in Drosophila melanogaster. *Journal of Insect Physiology,* 22**,** 415-423.

PASIKANTI, K. K., HO, P. C. & CHAN, E. C. Y. 2008. Gas chromatography/mass spectrometry in metabolic profiling of biological fluids. *Journal of Chromatography B,* 871**,** 202-211.

PATEL, J., PATHAK, R. R. & MUJTABA, S. 2011. The biology of lysine acetylation integrates transcriptional programming and metabolism. *Nutr Metab (Lond),* 8**,** 12.

PEA, F. 2005. Pharmacology of Drugs for Hyperuricemia.

PLUSKAL, T., CASTILLO, S., VILLAR-BRIONES, A. & ORESIC, M. 2010. MZmine 2: Modular framework for processing, visualizing, and analyzing mass spectrometry-based molecular profile data. *BMC bioinformatics,* 11**,** 395.

POTTER, C. J., TURENCHALK, G. S. & XU, T. 2000. Drosophila in cancer research: an expanding role. *Trends in Genetics,* 16**,** 33-39.

RADEFF-HUANG, J., SEASHOLTZ, T. M., MATTEO, R. G. & BROWN, J. H. 2004. G protein mediated signaling pathways in lysophospholipid induced cell proliferation and survival. *Journal of Cellular Biochemistry,* 92**,** 949-966.

RAHMAN, I., MARWICK, J. & KIRKHAM, P. 2004. Redox modulation of chromatin remodeling: impact on histone acetylation and deacetylation, NF-kappaB and pro-inflammatory gene expression. *Biochem Pharmacol,* 68**,** 1255-67.

REAUME, A. G., CLARK, S. H. & CHOVNICK, A. 1989. Xanthine dehydrogenase is transported to the Drosophila eye. *Genetics,* 123**,** 503-509.

REITER, L. T., POTOCKI, L., CHIEN, S., GRIBSKOV, M. & BIER, E. 2001. A Systematic Analysis of Human Disease-Associated Gene Sequences In Drosophila melanogaster. *Genome Research,* 11**,** 1114-1125.

RIEDEL, F., VORKEL, D. & EATON, S. 2011. Megalin-dependent yellow endocytosis restricts melanization in the Drosophila cuticle. *Development,* 138**,** 149-58.

ROBERTS, M. F. 2000. Osmoadaptation and osmoregulation in archaea. *Frontiers in Bioscience,* 5**,** 796-812.

RYDER, E. & RUSSELL, S. 2003. Transposable elements as tools for genomics and genetics in Drosophila. *Briefings in Functional Genomics & Proteomics,* 2**,** 57-71.

SAGER, G. 2004. Cyclic GMP transporters. *Neurochemistry International,* 45**,** 865-873.

SAMBROOK, J., FRITSCH, E. F. & MANIATIS, T. 1989. *Molecular cloning: a laboratory manual*, Cold Spring Harbor Laboratory Press.

SCALBERT, A., BRENNAN, L., FIEHN, O., HANKEMEIER, T., KRISTAL, B. S., VAN OMMEN, B., PUJOS-GUILLOT, E., VERHEIJ, E., WISHART, D. & WOPEREIS, S. 2009. Mass-spectrometry-based metabolomics: limitations and recommendations for future progress with particular focus on nutrition research. *Metabolomics,* 5**,** 435-458.

SERRANO, R., MULET, J. M., RIOS, G., MARQUEZ, J. A., LEUBE, M. P., MENDIZABAL, I., PASCUAL-AHUIR, A., PROFT, M., ROS, R. & MONTESINOS, C. 1999. A glimpse of the mechanisms of ion homeostasis during salt stress. *Journal of Experimental Botany,* 50**,** 1023.

SERRANO, R. & RODRIGUEZ-NAVARRO, A. 2001. Ion homeostasis during salt stress in plants. *Current opinion in cell biology,* 13**,** 399-404.

SEVANIAN, A., DAVIES, K. J. & HOCHSTEIN, P. 1991. Serum urate as an antioxidant for ascorbic acid. *The American Journal of Clinical Nutrition,* 54**,** 1129S-1134S.

SHAHJEE, H. M., BANERJEE, K. & AHMAD, F. 2002. Comparative analysis of naturally occurring L-amino acid osmolytes and their D-isomers on protection ofEscherichia coli against environmental stresses. *Journal of biosciences,* 27**,** 515-520.

SHILATIFARD, A. 2008. Molecular implementation and physiological roles for histone H3 lysine 4 (H3K4) methylation. *Current opinion in cell biology,* 20**,** 341-348.

SÖZEN, M. A., ARMSTRONG, J. D., YANG, M., KAISER, K. & DOW, J. A. T. 1997. Functional domains are specified to single-cell resolution in a Drosophila epithelium. *Proceedings of the National Academy of Sciences,* 94**,** 5207-5212.

ST JOHNSTON, D. 2002. The art and design of genetic screens: Drosophila melanogaster. *Nat Rev Genet,* 3**,** 176-188.

STERGIOPOULOS, K., CABRERO, P., DAVIES, S. A. & DOW, J. A. T. 2009. Salty dog, an SLC5 symporter, modulates Drosophila response to salt stress. *Physiological genomics,* 37**,** 1-11.

STRAHL, B. D., OHBA, R., COOK, R. G. & ALLIS, C. D. 1999. Methylation of histone H3 at lysine 4 is highly conserved and correlates with transcriptionally active nuclei in Tetrahymena. *Proceedings of the National Academy of Sciences,* 96**,** 14967-14972.

SULLIVAN, D. T., BELL, L. A., PATON, D. R. & SULLIVAN, M. C. 1979. Purine transport by Malpighian tubules of pteridine-deficient eye color mutants of <i>Drosophila melanogaster</i&gt. *Biochemical Genetics,* 17**,** 565-573.

SULLIVAN, D. T., BELL, L. A., PATON, D. R. & SULLIVAN, M. C. 1980. Genetic and functional analysis of tryptophan transport in Malpighian tubules of Drosophila. *Biochemical Genetics,* 18**,** 1109-1130.

SUMMERS, K. M., HOWELLS, A. J. & PYLIOTIS, N. A. 1982. Biology of eye pigmentation in insects. *Adv. Insect Physiol,* 16**,** 166.

SUN, Y. H., TSAI, C. J., GREEN, M. M., CHAO, J. L., YU, C. T., JAW, T. J., YEH, J. Y. & BOLSHAKOV, V. N. 1995. white as a Reporter Gene to Detect Transcriptional Silencers Specifying Position-Specific Gene Expression During Drosophila melanogaster Eye Development. *Genetics,* 141**,** 1075-1086.

TAVAZZI, B., LAZZARINO, G., LEONE, P., AMORINI, A. M., BELLIA, F., JANSON, C. G., DI PIETRO, V., CECCARELLI, L., DONZELLI, S., FRANCIS, J. S. & GIARDINA, B. 2005. Simultaneous high performance liquid chromatographic separation of purines, pyrimidines, N-

acetylated amino acids, and dicarboxylic acids for the chemical diagnosis of inborn errors of metabolism. *Clinical Biochemistry,* 38**,** 997-1008.

TEARLE, R. 1991. Tissue specific effects of ommochrome pathway mutations in Drosophila melanogaster. *Genet Res,* 57**,** 257-66.

THÖNY, B., AUERBACH, G. & BLAU, N. 2000. Tetrahydrobiopterin biosynthesis, regeneration and functions. *Biochem. J.,* 347**,** 1-16.

TRYGG, J., HOLMES, E. & LUNDSTEDT, T. 2007. Chemometrics in metabonomics. *Journal of Proteome Research,* 6**,** 469-479.

VAZ, F. M. & WANDERS, R. J. 2002. Carnitine biosynthesis in mammals. *Biochem J,* 361**,** 417-29.

VOET, D. & VOET, J. G. 2006. *Bioquimica,* Media Panamericana.

VOGELS, G. D. & VAN DER DRIFT, C. 1976. Degradation of purines and pyrimidines by microorganisms. *Bacteriological reviews,* 40**,** 403.

VORBACH, C., HARRISON, R. & CAPECCHI, M. R. 2003. Xanthine oxidoreductase is central to the evolution and function of the innate immune system. *Trends in immunology,* 24**,** 512-517.

WANG, J., KEAN, L., YANG, J., ALLAN, A., DAVIES, S., HERZYK, P. & DOW, J. 2004. Function-informed transcriptome analysis of Drosophila renal tubule. *Genome Biology,* 5**,** R69.

WERNER, E., HEILIER, J.-F., DUCRUIX, C., EZAN, E., JUNOT, C. & TABET, J.-C. 2008. Mass spectrometry for the identification of the discriminating signals from metabolomics: Current status and future trends. *Journal of Chromatography B,* 871**,** 143-163.

WIGGLESWORTH, V. B. 1939. *The principles of insect physiology,* London, Methuen.

WILCOXEN, K. M., UEHARA, T., MYINT, K. T., SATO, Y. & ODA, Y. 2010. Practical metabolomics in drug discovery. *Expert Opinion on Drug Discovery,* 5**,** 249-263.

WILLIAM, G. 1999. The FlyBase Database of the Drosophila Genome Projects and community literature. *Nucleic Acids Research,* 27**,** 85-88.

WITTKOPP, P. J. & BELDADE, P. Year. Development and evolution of insect pigmentation: genetic mechanisms and the potential consequences of pleiotropy. *In,* 2009. Elsevier, 65-71.

WOODWARD, O. M., KOTTGEN, A., CORESH, J., BOERWINKLE, E., GUGGINO, W. B. & KOTTGEN, M. 2009. Identification of a urate transporter, ABCG2, with a common functional polymorphism causing gout. *Proceedings of the National Academy of Sciences,* 106**,** 10338.

XU, Y. 2002. Sphingosylphosphorylcholine and lysophosphatidylcholine: G protein-coupled receptors and receptor-mediated signal transduction. *Biochimica et Biophysica Acta (BBA) - Molecular and Cell Biology of Lipids,* 1582**,** 81-88.

YAMAMOTO, T., MORIWAKI, Y., TAKAHASHI, S., TSUTSUMI, Z., YAMAKITA, J., NASAKO, Y., HIROISHI, K. & HIGASHINO, K. 1996. Determination of human plasma xanthine oxidase activity by high-performance liquid chromatography. *Journal of Chromatography B: Biomedical Sciences and Applications,* 681**,** 395-400.

YAO, Q., ZHANG, D., TANG, B., CHEN, J., LU, L. & ZHANG, W. 2010. Identification of 20-hydroxyecdysone late-response genes in the chitin biosynthesis pathway. *PLoS ONE,* 5**,** e14058.

YARFITZ, S., PROVOST, N. M. & HURLEY, J. B. 1988. Cloning of a Drosophila melanogaster guanine nucleotide regulatory protein beta-subunit gene and characterization of its expression during development. *Proceedings of the National Academy of Sciences,* 85**,** 7134-7138.

ZEE, B. M., LEVIN, R. S., DIMAGGIO, P. A. & GARCIA, B. A. 2010. Global turnover of histone post-translational modifications and variants in human cells. *Epigenetics Chromatin,* 3**,** 22.

ZHANG, T., CREEK, D. J., BARRETT, M. P., BLACKBURN, G. & WATSON, D. G. 2012. Evaluation of Coupling Reversed Phase, Aqueous Normal Phase, and Hydrophilic Interaction Liquid Chromatography with Orbitrap Mass Spectrometry for Metabolomic Studies of Human Urine. *Analytical Chemistry,* 84**,** 1994-2001.

ZHANG, Y. & OLIVER, B. 2010. An evolutionary consequence of dosage compensation on Drosophila melanogaster female X-chromatin structure? *BMC Genomics,* 11**,** 6.

ZHANG, Y. & REINBERG, D. 2001. Transcription regulation by histone methylation: interplay between different covalent modifications of the core histone tails. *Genes & Development,* 15**,** 2343-2360.

ZHOU, H. & CLAPHAM, D. E. 2009. Mammalian MagT1 and TUSC3 are required for cellular magnesium uptake and vertebrate embryonic development. *Proceedings of the National Academy of Sciences,* 106**,** 15750-15755.

ZHU, W., SMITH, J. W. & HUANG, C. M. 2009. Mass spectrometry-based label-free quantitative proteomics. *J Biomed Biotechnol,* 2010**,** 840518.